A THERMODYNAMIC SIMULATION MODEL FOR STORAGE OF CORN

by

Chung-Teh Sheng

Thesis submitted to the Faculty of the
Virginia Polytechnic Institute and State University
in partial fulfillment of the requirements for the degree of
MASTER OF SCIENCE
in
Agricultural Engineering

APPROVED:

Jerry J. Baker, Chairman

David H. Vaughan

J. Philip Mason

John S. Cundiff

August, 1982
Blacksburg, Virginia

ACKNOWLEDGEMENT

The auther wishes to express his gratitude and apreciation to Drs. J. P. Mason, J. S. Cundiff, and D. H. Vaughan for serving on his graduate committee. Special appreciation is expressed to his major professor, Dr. J. L. Baker, for serving as chairman of the auther's graduate committee. His encouragement and unselfish guidance were important and worthy throughout this graduate program. A special thanks is given to Mr. Steve Spadlin for his aid in the construction of the storage bins. The auther would also like to thank Mr. Jan Carr for his guidance regarding the use of the computer. Gratitude is given to his fellow graduate students, especially Mr. Joseph Harner, Ms. Deborah Cook, and Mr. and Mrs. John Reid.

Finally the auther would like to express his sincere appreciation to his parents, Mr. and Mrs. P. Sheng, who have given their encouragement and expressions of confidence in all of the auther's decisions.

TABLE OF CONTENTS

Appendix

LIST OF TABLES

LIST OF FIGURES

Chapter I

INTRODUCTION

There are two major classifications of mathematical simulations of grain drying and storage: one uses thin layer drying theory, and the other is based on the theory of transport phenomena. Neither is more reliable than the other based on environmental, boundary or executing conditions, but thin-layer drying models seem to be more applicable than transport phenomena models.

It is well known that temperature and moisture distributions within a mass grain are basic conditions to the establishment of a drying and storage model, but to accurately predict moisture distributions of grains during the period of drying is very difficult. In 1961, Henderson and Pabis experimentally examined the temperature relationship between air and grain during the drying process. In 1968, Thompson ascertained that if changes in the properties of grain occurred in the process of drying, that there were simultaneous respondent changes in the properties of the drying air. In other words, the properties of grain could be predicted using the measured properties of the drying air. Using Thompson's suggestion, it is possible to construct a grain drying model via the drying air, whose properties can be

determined much easiler and more precisely with instruments than the properties of grain. The basic approach for building a thin layer drying model is the continuous process of a deep bed dryer, divided into many small processes and simulating each of these by successively calculating the changes that occur during a short time increment. Finally, to combine all the thin layers and add all the time increments would form a complete and practical thin-layer grain drying model.

Since thin-layer drying theory is easily applied to a deep bed grain dryer, many thin layer grain drying models have been developed in the past 15 years, such as: Mathematical Simulation of Corn Drying(Thompson et al. 1968), Near Equilibrium Simulation of Shelled Corn Drying(Bloome and Shove, 1971), Mathematical Description of the Drying Rate of Fully Exposed Corn(Troeger and Hukill, 1971), Simulation of a Natural-Air Corn Drying System(Flood et al. 1979), A Model for Low-Temperature Corn Drying Systems(Van Ea and Kline, 1979), Simulation of Low Temperature Drying of Corn for Ontario Conditions (Mittal and Otten, 1980), and Thin-Layer Drying and Rewetting Equations for Shelled Yellow Corn(Misra and Brooker, 1980). The concept of a thin-layer drying model for grain has already been proven to be very practical; however, it is only available in situations where the flow rate and the properties of air can be determined.

For the above limitations, the thin layer drying model can not be used for all drying and storage cases, especially grain storage without ventilation or drying using natural air. When the situation of insufficient data for the thin layer model is met, an alternative approach, a mathematical simulation based on transport phenomena theory for hygroscopic porous bodies, can be used to replace the thin layer model. Using Crank's(1979) equations, Aldis and Foster (1980) presented a model to simulate the moisture changes in grain from exposure to ambient air where velocity was constant.

The simplest transport phenomena for drying or storage of a hygroscopic porous body can be described using the basic theories of heat and mass trasnfer: the basic heat transfer theory is Fourier's heat diffusion law, and the basic mass transfer theory is Fick's mass diffusion law. The drying theory based on transport phenomena for a moist body was developed much earlier than the thin layer drying theory; however, it has not been applied widely for actual drying cases of agricultural products since it is difficult to accurately determine the physical coefficients relted to heat and mass transfer. Now, modern scientific techniques and instruments for testing the transfer coefficients have been improved significantly; hence, mathematical simulations based on the

theory of transport phenomena to predict the drying process are more applicable than before. But a model based on the simple heat and mass transfer for a porous hygroscopic body, which are independent of each other, can only be applied to a few actual cases where the coupled effects of heat transfer and mass transfer can be neglected. In 1961, Luikov experimentally verified the coupled heat and mass transfer of capillary-porous bodies through Onsager's reciprocal principle for irreversible thermodynamic processes. Since Luikov's investigation, mathematical simulations based on the theory of transport phenomena have been a powerful tool to solve current drying and storage problems.

1.1 OBJECTIVES

The primary goal of this research was to develop a mathematical model based on Luikov's theory to simulate the storage performance of a bulk of corn. Specific objectives are:

1. To choose a suitable mixing model to determine the bulk properties in a bed of corn, which are based on the physical properties of air and a kernel of corn during the storage period.
2. To develop a mathematical simulation using the differential equations of coupled heat and mass transfer in a porous hygroscopic body.

3. To verify the model with experimental data collected during storage experiments.

Chapter II

LITERATURE REVIEW

2.1 BASIC GRAIN STORAGE PRINCIPLES

The amount of moisture contained in grain is one of the important factors which affect processes such as storage, germination, etc. The reason for concern over the moisture content of grain is that molds, yeasts, and other microorganisms require a certain level of moisture for their growth, which for most grains is greater than 13% moisture content wet basis. However, the critical moisture amount which causes damage also depends on temperature, the kind of grain, and the nature of the organism. Normally, the amount of moisture in grain is higher than the critical moisture content when it is harvested, thus drying becomes a necessary processing procedure to prevent spoliage of grain.

Henderson and Perry(1980) defined drying as the removal of moisture from a hygroscopic material to a certain level that is in equilibrium with atmosphere air or to a level which eliminates the spoilage or reduction in quality from molds, enzymatic action, and insects. There is no doubt that the chief objective in a drying process of grain is to reduce the moisture content to a certain level so that spoi-

lage can be avoided before organisms can utilize the water. It must be emphasized that dried grain with a safe moisture amount still has a potential to be spoiled due to the temperature and moisture variations during the storage period. Successful grain storage means preventing grain spoilage by keeping temperature and moisture content of grain within safe ranges.

2.2 MECHANISMS OF HEAT AND MASS TRANSFER

The grain can gain or lose moisture as well as increase or decrease temperature in the process of storage. Understanding the mechanism of moisture and heat transfer will further help people optimize the quality of grain during the drying and storage period. The basic mechanisms for heat transfer are:

1. conductive heat flow within the interior of body;
2. convective heat flow on the surface of body;
3. radiative heat flow on the surface of body.

The effect of heat radiation can be neglected when the experiment is executed under controlled conditions. The free convective heat transfer of air is considered in this study.

Van Arsdel(1973) emphasized two major modes of moisture migration inside a moist porous body: one is molecular diffusion for vapor moisture and the other is capillary flow

for liquid moisture. Molecular diffusion is defined as the molecular motion of translation which causes the distribution of the molecules. Capillary flow means molecular attraction between the liquid through the interstices and over the surface of a solid. Marshall and Friedman(1950) pointed out five distinct mechanisms for moisture movement:

1. liquid movement by capillary forces;
2. diffusion of moisture caused by a difference in concentration;
3. moisture flow caused by pressure gradients and shrinkage;
4. moisture flow caused by gravity;
5. moisture flow caused by a vaporization-condensation sequence.

Goring(1958) added another three mechanisms for moisture removal:

1. surface diffusion in liquid layers adsorbed at solid interfaces;
2. water vapor diffusion in air-filled pores, caused by a difference in partial pressure;
3. water vapor flow under differences in total pressure.

So the moisture of a moist solid body may flow by a number of methods, such as by diffusion, by capillary, by gravity, by external pressure, or by convection and a sequence of va-

porization-condensation phenomenon where temperature gradients are present.

A drying curve can be divided into the constant rate period and the falling rate period. It is an acceptable assumption that only the falling rate period exists during the storage period for grains. In 1939, Houghen et al. reported the mass transfer by diffusion could not occur during the constant rate period in drying. The flow of moisture during this period might better be attributed to by capillary force. The diffusion flow of moisture which was associated with capillary flow occurred and took an important place in the last stage-the falling rate period. The resultant distribution of moisture in the falling rate period depended on the value of moisture diffusivity decreasing with decreasing moisture content of moist bodies. Houghen et al. also made the following conclusions:

1. The moisture diffusion in drying or storage of hygroscopic solids was restricted to the equilibrium mositure content below the saturation point of environmental air.
2. The diffusivity of a hygroscopic solid decreased with temperature, moisture content and pressure.
3. Vapor diffusion might occur through the solid provided a temperature gradient existed, which created a vapor pressure gradient toward the surface.

2.2.1 Soret Effect and Dufour Effect

Onsager(1931) developed the principle of reciprocal relations in coupled irreversible thermodynamic processes and pointed out that when two or more irreversible transport processes, such as heat conduction and mass diffusion, took place simultaneously in a thermodynamic system, the processes might interfer with each other. According to Onsager's theory, the molecular transfer of heat and mass were related with each other and described by a system of linear equations, which were the combinations of generalized thermodynamic motive forces:

$$J_m = L_{mm} F_m + L_{mT} F_T \qquad (1)$$

and

$$J_q = L_{Tm} F_m + L_{TT} F_T \qquad (2)$$

where

L : Onsager's kinetic coefficients,

J : flux of energy or mass, and

F : thermodynamic motive forces

The thermodynamic force of heat is proportional to the gradient of temperature:

$$F_T = - \frac{1}{T} \text{grad}(T) \qquad (3)$$

where

T : temperature, °F, and

grad : mathematical operator-gradient.

The thermodynamic force of mass corresponds to the gradient of chemical potential divided by the temperature:

$$F_m = - T \, \text{grad}\left(\frac{U}{T}\right) \qquad (4)$$

where

U : chemical potential.

In 1957, Philip and De Veries observed the moisture migration in porous materials under temperature gradients. Luikov(1966) experimentally investigated the Soret effect, which is thermal mass diffusivity, and the Dufour effect, which is diffusional thermal conduction, occurring in a drying process of a hygroscopic material.

1. Soret Dffect:

> "In gas mixtures and in solutions, heat transfer by conduction is combined with mass transfer, when there is a temperature gradient in such systems, thermal diffusion(the Soret effect) occurs."

2. Dufour Effect

> "Mass diffusion causes heat transfer which is referred to as diffusion heat conduction or diffusion thermal conductivity (the Defour effect)."

2.3 SIMPLE HEAT AND MASS DIFFUSION LAWS

It is recognized that any drying or storage process can be analyzed using the theory of heat and mass transfer described in terms of potentials that determine the extent of change. The potential for heat transfer is clearly defined as the degree of hotness or temperature, but the potential for mass transfer is so ambiguous that the application of mass transfer is restricted.

Luikov(1961) found that the partial pressure of water vapor could not be considered as a potential for mass transfer in a boundary layer, but mass transfer was a function of the differences of mass concentration and temperature for a hygroscopic porous solid. A scale of moisture, which was found by analogy with that of temperature, was constructed by Luikov(1966).

The scale of moisture, a scale of moisture potential, was chosen as a percent of moistness at the maximum hygroscopic moisture content, always 100M, and the mass capacity was taken as one-hundredth of the maximum sorption moisture content M_{max}

$$W = \frac{M}{C_m} = \frac{M}{M_{max}} \cdot 100 \qquad (5)$$

where

W : moistness,

M : moisture content,

lbs of water/lb of dried matter,

C_m : moisture capacity, lbs/lbs-moistness.

The method of finding mass capacity is similar to the simple calorimetric method of estimating specific heat.

Fortes and Okos(1981) proposed that the driving forces for heat and mass transport are the gradients of equilibrium moisture content and temperature. The gradient of equilibrium moisture content is the difference between grain moisture content and the equilibrium grain moisture content that surrounding air would provide. They pointed out two cases that could cause moisture migration from a region of lower to higher moisture content

1. The region of lower moisture content could get moisture due to a higher equilibrium moisture content of the surrounding air.
2. The effect of the temperature gradient which favored the moisture movement was greater than the effect of the equilibrium moisture content.

Luikov(1966) also verified that the direction of heat transfer was dependent on the potential of temperature, and was independent of the specific heat. Figure 1 contains analogies for heat transfer and mass transfer. In the example of heat transfer, the flow of heat is from the high

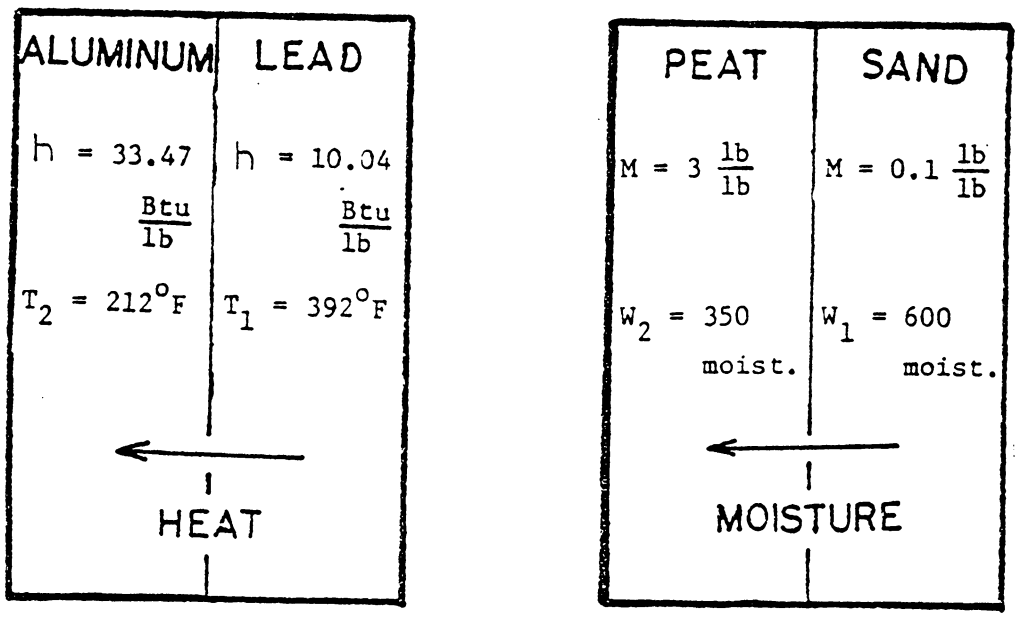

Figure 1 : Analogies for the transfer of moisture and heat from an area of high temperature or moistness to an area of low temperature or moistness. This transfer occurs regardless of heat or moisture content. Symbols are
h - heat content, Btu/lb,
M - moisture content, lb H2O/lb dry material,
T - temperature, °F, and
W - moistness.

temperature body to the low temperature body, regardless of the heat content of the two bodies. By analogy, moisture flow is from a body of high moistness to a body of low moistness, regardless of moisture content.

2.3.1 Heat and Mass Diffusion Laws

When the moisture contents of hygroscopic bodies in the drying or storage process are below the maximum absorption moisture, it has been verified that the basic mechanism of heat transfer is heat diffusion, and one of the mechanisms for mass transfer is mass diffusion, which are represented by Fourier's law of heat diffusion and Fick's law of mass diffusion respectively.

2.3.1.1 Fourier's Law of Heat Diffusion

Heat diffusion is primarily a molecular phenomenon requiring a temperature gradient as a driving force. In other words, the heat flux is proportional to the negative of the temperature gradient

$$J_q = \frac{Q'}{A} = -K \, \mathrm{grad}(T) \qquad (6)$$

where

J_q : heat flux , Btu/hr-ft^2,

Q' : heat flow, Btu/hr,

A : area normal to the direction of heat flow, ft^2,

K : thermal conductivity, Btu/hr-ft-°F, and

grad(T) : temperature gradient, °F/ft.

2.3.1.2 Fick's Law of Mass Diffusion

Mass diffusion flux is proportional to the negative of the moisture concentration gradient of which there are two cases.

1. The ingredients of two bodies in contact are different.

For body 1,

$$J_{m2} = - \rho_1 C_{m2} D_{21} \text{ grad}(W_2) \quad (7)$$

and for body 2,

$$J_{m1} = - \rho_2 C_{m1} D_{12} \text{ grad}(W_1) \quad (8)$$

where

J : mass flux, lb/hr-ft^2,

ρ : specific density, lb/ft^3, and

D : molecular diffusivity, ft^2/hr.

The mass fluxes for bodies 1 and 2 must obey the law of conservation; then,

$$J_{m1} + J_{m2} = 0 \quad (9)$$

The moisture diffusivities are also equivalent by the theory of thermodynamic molecular diffusion:

$$D_{12} = D_{21} = D \quad (10)$$

2. The ingredients of two contacting bodies are the same.

These two bodies should have the same properties, such as

$$C_{m1} = C_{m2} = C_m \qquad (11)$$

and

$$\rho_1 = \rho_2 = \rho \qquad (12)$$

The substitution of equations (5), (9), (10), (11) and (12) into equations (7) and (8) yields

$$J_m = J_{m1} = -J_{m2} = - D \text{ grad}(M) \qquad (13)$$

2.3.2 The Law of Conservation

The expression of conservation for a property (X) in the differential form is:

$$v \frac{dX}{dt} = v \frac{\partial X}{\partial t} + X \frac{\partial v}{\partial t} \qquad (14)$$

where

v : velocity, ft/hr, and

t : time, hr.

The law of conservation indicates that

net the out of control volume	rate of fluxes	+ rate of accumulation or diminishment in control volume	= net amount created or destroyed in control volume	

1. The law of mass conservation is expressed as:

$$\rho \frac{\partial M}{\partial t} = -\text{div}(J_m) + I_m \qquad (15)$$

where

ρ : density, lb/ft^3,

I_m : mass source or sink, lb/hr-ft^3,

J_m : mass flux, lb/hr-ft^2, and

div : mathematical operator-divergence.

Since mass is neither created nor destroyed, the equation can be reduced to

$$\rho \frac{\partial M}{\partial t} = -\text{div}(J_m) \qquad (16)$$

2. The law of heat conservation is written in the form

$$C_p \rho \frac{\partial T}{\partial t} = -\text{div}(J_q) - h J_m - I_q \qquad (17)$$

where

C_p : specific heat, Btu/lb-°F,

h : latent heat for phase conversion, Btu/hr,

I_q : heat source or sink, Btu/hr-ft^3, and

J_q : heat flux, Btu/hr-ft^2.

Combining the laws of conservation with the laws of heat and mass transfer yields

1. The equation of heat transfer without mass flux is

$$C_p \rho \frac{\partial T}{\partial t} = K \nabla^2 T \qquad (18)$$

or

$$\frac{\partial T}{\partial t} = \alpha \nabla^2 T \qquad (19)$$

where

K : thermal conductivity, Btu/hr-ft-°F,

α : thermal diffusivity, ft^2/hr, and

∇^2 : Laplacian operator.

$$\nabla^2 = \frac{\partial}{r\partial r} + \frac{\partial^2}{\partial r^2} + \frac{\partial^2}{\partial z^2}$$

Equation (19) can be used to describe the thermal behavior in the process of storage.

2. The equation of isothermal mass transfer is

$$\frac{\partial M}{\partial t} = D_m \nabla^2 M \qquad (20)$$

Equation (20) can be applied to predict the moisture distribution during the storage period.

The two equations (19 and 20) above are also the phenomenological equations of heat and mass transfers. Sherwood(1936) was the first to use the phenomenological mass diffusion equation to analyze the phenomenon of moisture mi-

gration in moist bodies. Brooker(1973) mentioned that the practical temperature gradient of cereal grain was too small to be considered during the drying period. In other words, the Soret effect was significant only at temperatures well above the normal drying temperature ranges of cereal grains; thus, the simple phenomenological mass transfer equation still can be applied to illustrate the moisture migration of cereal grains during the drying period. Becker(1959) derived and drew the theoretical drying curve for wheat using the simple mass diffusion equation. Hustrulid and Flikke(1959) also developed and pictured the drying curve of corn from the diffusion equation. In 1961, Henderson and Pabis applied the three dimensional mass diffusion equation to shelled maize, whose shape was assumed to be a brick, and calculated the mass diffusivity which is a function of temperature only.

A modified mass diffusion equation to describe the fact that the net mass change in a differential element of a body by diffusion was equal to the sum of the changes of vapor concentration and moisture content of the body was presented by Whitney and Porterfield(1968). The modified mass diffusion equation was written as:

$$D \nabla^2 C = f \frac{\partial C}{\partial t} + (1 - f) \rho \frac{\partial M}{\partial t} \qquad (21)$$

where

C : concentration of water vapor, lb/ft^3, and

f : void fraction of the body, decimal

The modified equation has been further proved by Young(1969). Whitaker et al.(1969) also presented the mass diffusivity of corn, which is a function of temperature and concentration, from the radial phenomenological mass diffusion equation

$$\frac{\partial C}{\partial t} = \frac{\partial}{\partial r}\left(D \frac{\partial C}{\partial r}\right) + \frac{2}{r} D \frac{\partial C}{\partial r} \qquad (22)$$

2.4 LUIKOV'S COUPLED HEAT AND MASS TRANSFER EQUATIONS

Nordon and David(1967) developed coupled differential equations of heat and mass transfer for a hygroscopic textile-wood, which included a simplified mass diffusion equation (24) without the term of temperature and a heat diffusion equation (25) with the coupled effect of mass diffusion. The equations are

$$\frac{\partial C'_w}{\partial t} + f \frac{\partial C_{vc}}{\partial t} = D \frac{\partial^2 C_{vc}}{\partial x^2} \qquad (23)$$

and

$$\alpha \frac{\partial^2 T}{\partial x^2} = \frac{\partial T}{\partial t} - \frac{h}{C_p} \frac{\partial C'_w}{\partial t} \qquad (24)$$

where

C'_w : concentration of water vapor in an

absorbed state, lb/ft^3, and

C_{vc} : concentration in air filling the interfiber void space, lb/ft^3.

They also pointed out that the thermal mass diffusion in a moist textile body was important only for high temperature drying. Whitney and Porterfield(1973) used similar equations as Nordon and David's equations to describe the drying process for corn meal. The equations are

$$\frac{1}{r^2}\frac{\partial}{\partial r}\left(r^2 D \frac{\partial C}{\partial r}\right) = f\frac{\partial C}{\partial t} + (1 - f)\rho\frac{\partial M}{\partial t} \qquad (25)$$

and

$$\frac{1}{r^2}\frac{\partial}{\partial r}\left(r^2 K \frac{\partial T}{\partial r}\right) = C_d (1 - f)\rho\frac{\partial T}{\partial t} + C_w (1 - f)\rho\frac{\partial T}{\partial t} - h (1 - f)\rho\frac{\partial M}{\partial t} + Q \qquad (26)$$

where

C_w : specific heat of water, Btu/lb-°F,

C_d : specific heat of solid, Btu/lb-°F,

Q : internal generated heat, Btu/hr-ft^3,

f : porosity, decimal,

ρ : density of solid material, lb/ft^3, and

D : mass diffusivity, ft^2/hr

Based on Whitney and Porterfield's coupled equations, Young(1969) defined a modified Lewis number to evaluate the significance of the coupled effect of heat transfer in the drying and storage process:

$$L_{em} = \frac{K\,(f + (1 - f)\,\rho\,C_1)}{(D\,(1 - f)\,\rho\,(C_d + C_w\,M + h\,C_2))} \qquad (27)$$

where

K : thermal conductivity, Btu/hr-ft-°F,

M : moisture content, decimal,

h : latent heat of vaporization, Btu/lb, and

C_1, C_2 : constant coefficients, determined by experiment

$$M = C_o + C_1\,C + C_2\,T' \qquad (28)$$

where T' is thermodynamic temperature, °R and C is the concentration of vapor moisture, lb/ft^3.

He found that the mass transfer equation alone was sufficient to describe the drying process, and the temperature gradient due to evaporization cooling was very small when the modified Lewis number was greater than or equal to 60. Fortes and Okos(1981) also applied the theory of coupled heat and mass transfer to agricultural grains, and derived equations which were similar as Norden and David's equations

$$\rho \frac{\partial M}{\partial t} = -\text{div}(J_w + J_v) \tag{29}$$

and

$$C_p \rho \frac{\partial T}{\partial t} - \rho h'_w \frac{\partial M}{\partial t} = -\text{div}(J_q) - h_v \, \text{div}(J_v) \tag{30}$$

where

J_w : liquid moisture flux, lb/hr,

J_v : vapor moisture flux, lb/hr,

h' : enthalpy of liquid moisture, Btu/lb, and

h_v : latent heat for water vaporization in a kernel of grain, Btu/lb.

Due to the shortage of knowledge about the above coupled heat and mass transfer models, none of the above systems can be accepted as a powerful means for analysis of a drying or storage process of grain.

Luikov(1934) was the first one to apply the principle of non-equilibrium thermodynamic to drying of a hygroscopic capillary-porous solid. Luikov derived the simultaneous coupled heat and mass transfer equations for hyproscopic capillary solids, based on Onsager's reciprocal principle for irreversible thermodynamic process, the law of conservation, Fourier's law of heat diffusion and Fick's law of mass diffusion. The equations are

$$\frac{\partial M}{\partial t} = D_m \nabla^2 M + D_m \delta \nabla^2 T + D_p \nabla^2 P \qquad (31)$$

where

D_m : moisture diffusivity, ft^2/hr,

δ : thermal gradient coefficient, $1/°F$,

D_p : molecular vapor transfer coefficient, ft^2/hr, and

P : vapor pressure, $moles/ft^3$.

and

$$\frac{\partial T}{\partial t} = \alpha \nabla^2 T + \frac{\varepsilon h}{C_p} \frac{\partial M}{\partial t} \qquad (32)$$

where

ε : phase conversion factor,

which is defined as

$$\varepsilon = \frac{J_v}{J_w + J_v} \qquad (33)$$

whose variables are

J_v : moisture flow in vapor, and

J_w : moisture flow in liquid.

At $\varepsilon = 0$, the total mass of moisture is in the phase of liquid, and at $\varepsilon = 1$, the moisture is only in the vapor phase.

Substituting equation (31) into equation (32) yields

$$\frac{\partial T}{\partial t} = K_1 \nabla^2 M + K_2 \nabla^2 T + K_3 \nabla^2 P \qquad (34)$$

where

$$K_1 = \frac{\varepsilon h D_m}{C_p}$$

$$K_2 = \alpha + \frac{h D_m \varepsilon \delta}{C_p}$$

$$K_3 = \frac{\varepsilon h D_p}{C_p}$$

The system of differential equations for heat and mass transfer in a porous-capillary moist body consists of equations (31) and (34).

The coupled equations were investigated by Luikov(1966) using experiments to verify that increases in the difference of temperature, moisture concentration or vapor pressure within the interior of a moist body caused an adequate respondent increase in the rate of drying. Luikov proposed that a moist body heated above 212°F would appear to have a vapor pressure gradient and that might also take place at temperature below 212°F due to effusion of the humid air through micro-capillaries inside the body. This mode of moisture migration was described by Darcy's Law:

$$J_p = - D_p \ \text{grad}(P) \qquad (35)$$

where

D_p : total filtration coefficient, $ft^2/hr.$

In 1961, Lebedev conducted several experiments based on Luikov's(1961) equations, and concluded that the gradient of excessive vapor pressure was a significant driving force for moisture migration only at temperatures exceeding 100°C within the interior of moist materials. On the other hand, if the internal temperature of the material was less than 100°C, Luikov's coupled equations could be simplified to

$$\frac{\partial M}{\partial t} = D_m \nabla^2 M + D_m \delta \nabla^2 T \qquad (36)$$

and

$$\frac{\partial T}{\partial t} = \frac{\varepsilon h D_m \delta}{C_p} \nabla^2 M + \left(\alpha + \frac{\varepsilon h D_m \delta}{C_p}\right) \nabla^2 T \qquad (37)$$

Equations (36) and (37), recognized as the fundamental system of coupled heat and mass transfer for a porous moist body, are applied to this work.

Because few of the coefficients of basic physical phenomenological transport equations and coupled mass and heat transfer equations for grain drying and storage are determined, Brooker et al.(1974) stated that Luikov's coupled equations for hygroscopic porous-capillary bodies were not applicable to most grain drying cases. Husain et al.(1970, 1972 and 1973) presented an analytic method, developed from non-equilibrium thermodynamics, to evaluate the thermodynam-

ic parameters for coupled heat and mass diffusion equations, which included the thermal gradient coefficients and isothermal mass capacities of rough rice, shelled corn and potato. He found out that these parameters were highly sensitive to the moisture contents and temperatures. Husain et al.(1970) also proposed a mathematical model of coupled heat and mass transfer for a porous moist body, derived from Onsager's principle for irreversible thermodynamic processes and Luikov's coupled equations. Finally, he emphasized that it was very difficult to draw any general conclusion as to the behavior of these thermodynamic parameters for biological materials.

Experiments conducted by Eckert and Faghri(1980) expressed the transport properties of a porous body as functions of moisture content, temperature, and its structure. They also pointed out that a detailed study of the transport process occurring within an unsaturated porous body was complicated even for a regularly shaped solid matrix, and was almost impossible for the irregular void configurations in general for most porous media; therefore, the normal approach in the analysis was to consider the media involved as a continua.

2.5 MIXING PROPERTIES OF HEAT AND MASS DIFFUSION FOR GRANULAR MATERIALS

The thermal physical properties of a kernel of corn or a bed of corn have been determined by many researchers: Kazarian and Hall(1965) measured the thermal properties of wheat and corn; Brooker et al.(1974) summarized specific heats, specific weights and thermal diffusivities of grains and vegetables; Vemuganti and Pfost(1980) experimentally determined the specific heats and test weights of 20 grains. Unfortunately, few experiments have been conducted to define the moisture diffusivities of grains and vegetables. In 1961, Henderson and Pabis evaluated the moisture diffusivity for a kernel of corn and suggested the diffusivity is a function of the absolute temperature only. Chu and Hustrulid(1968) studied and obtained the mass diffusivity of a kernel of corn as a function of moisture content and temperature. Husain et al.(1970) conducted experiments to determine the thermal gradient coefficient and specific mass capacity of a kernel of corn.

Since the mechanisms of moisture movement in bulk grain are unclear, it is very difficult to develop a rational theory to predict the effective properties of granular materials found in conjuction with various fluids. At the present, there are no effective mathematical models based on

the theory of transport phenomena to be able to predict the drying or storage behavior accurately for a bed of corn.

Fick's equation for moisture diffusion obeys the same mathematical laws that Fourier used to derive the conductivity for heat transfer, therefore the diffusivity coefficient has the same mathematical meaning in mass transfer as heat conductivity in heat transfer. This suggests that if there is a method to determine the thermal conductivity for a mixture of solids and liquids, a similar method should be available to calculate the mass diffusivity of the mixture.

Several formulae have been presented to relate the thermal conductivity of fractional volumes of component phases in granular materials; such as sand and ice mixtures (McGaw 1968); soils and sands (Von Rooyen and Winterkon, 1957); or unconsolidated sands (Woodside and Messmer, 1961). These equations will be discussed later and applied to evaluate the mass diffusivity of a mixture with dried matter, liquid moisture, vapor moisture, and air.

Most of the porous hygroscopic granular materials have more than two phases. Since the evaluation of the combined thermal properties of a mixture including more than two phases is very complicated, the simplified case considers a porous material in two phases: one is a solid component, and the other is a single phase fluid that occupies the pore

space. The following five methods have been developed for this simplified case:

2.5.1 Parallel Model (Woodside and Messmer, 1961)

Solids and fluids within the interior of the system construct two independent paths for the heat fluxes respectively. Figure 2 is a schematic that illustrates the paths of heat fluxes. Total heat flux is the sum of heat flow through the solid path and heat flow through the fluid path

$$Q = Q_d + Q_f \qquad (38)$$

where

Q : net heat flux, Btu/hr,

Q_d : heat flow through the solid component only, Btu/hr, and

Q_f : heat flow through the fluid component only, Btu/hr.

The parallel arrangement has the maximum effective conductivity, and the minimum thermal resistance to heat flow. The resulant thermal conductivity of a mixture is written as:

$$K = (1 - f)\, K_d + f\, K_f \qquad (39)$$

where

K : thermal conductivity of the mixture, Btu/hr-ft-°F,

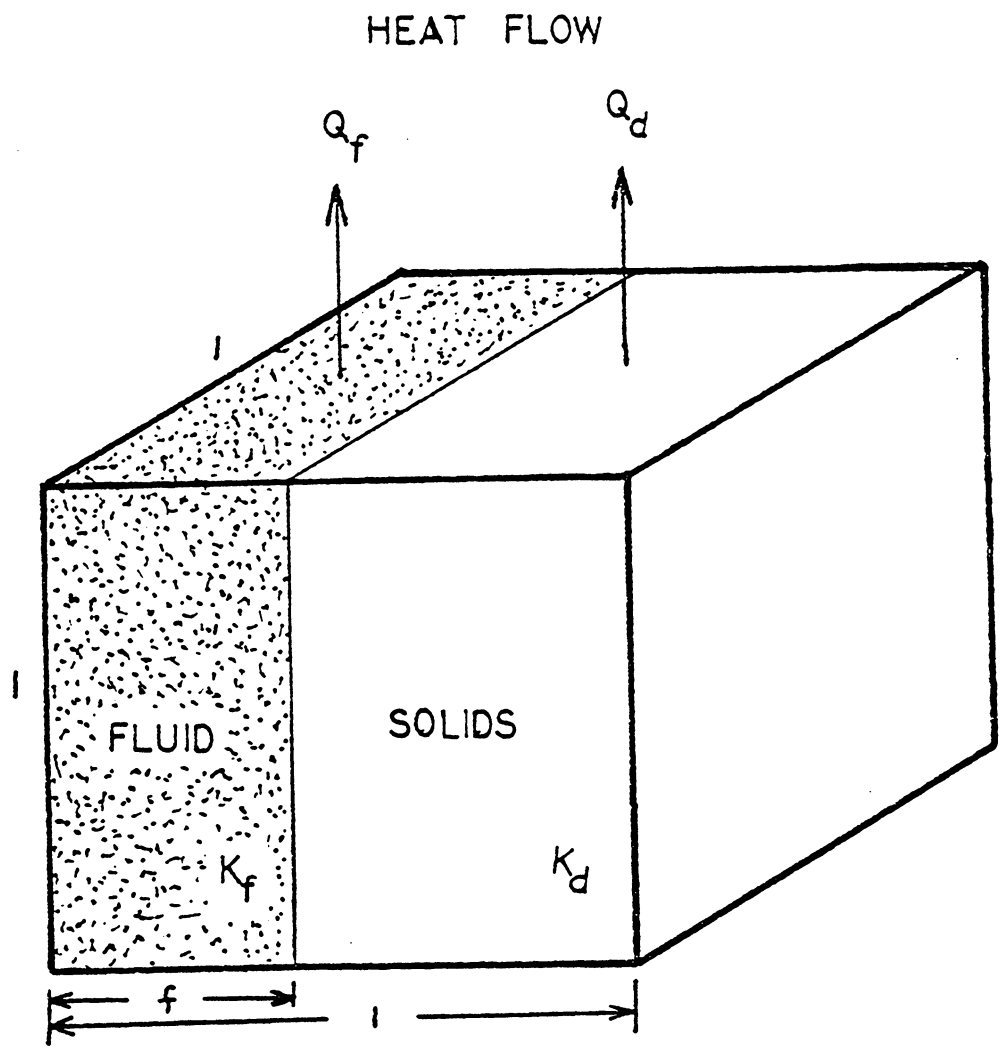

Figure 2 : A schematic model for parallel heat and mass flow. The distributions of the components are parallel. The total flow is the summation of two independent continuous flows: Qf(only through fluid portion) and Qd(only through solid portion)

K_d : thermal conductivity of the solid component Btu/hr-ft-°F,

K_f : thermal conductivity of the fluid component Btu/hr-ft-°F, and

f : porosity, decimal.

2.5.2 Series Model (Woodside and Messmer, 1961)

Solid and fluid, when arranged in series, form a heat flow path; then, heat flux flows through solid and fluid sequentially(Fig 3). The series arrangement has the minimum effective conductivity

$$\frac{1}{K} = \frac{(1 - f)}{K_d} + \frac{f}{K_f} \qquad (40)$$

Equation (40) can be further rearranged as

$$K = \frac{K_d K_f}{(1 - f) K_f + f K_d} \qquad (41)$$

2.5.3 Geometric Mean Model (Lichtenecker, 1926)

The geometric mean equation applied to a random distribution of the phases is expressed as

$$K = K_d^{(1 - f)} K_f^f \qquad (42)$$

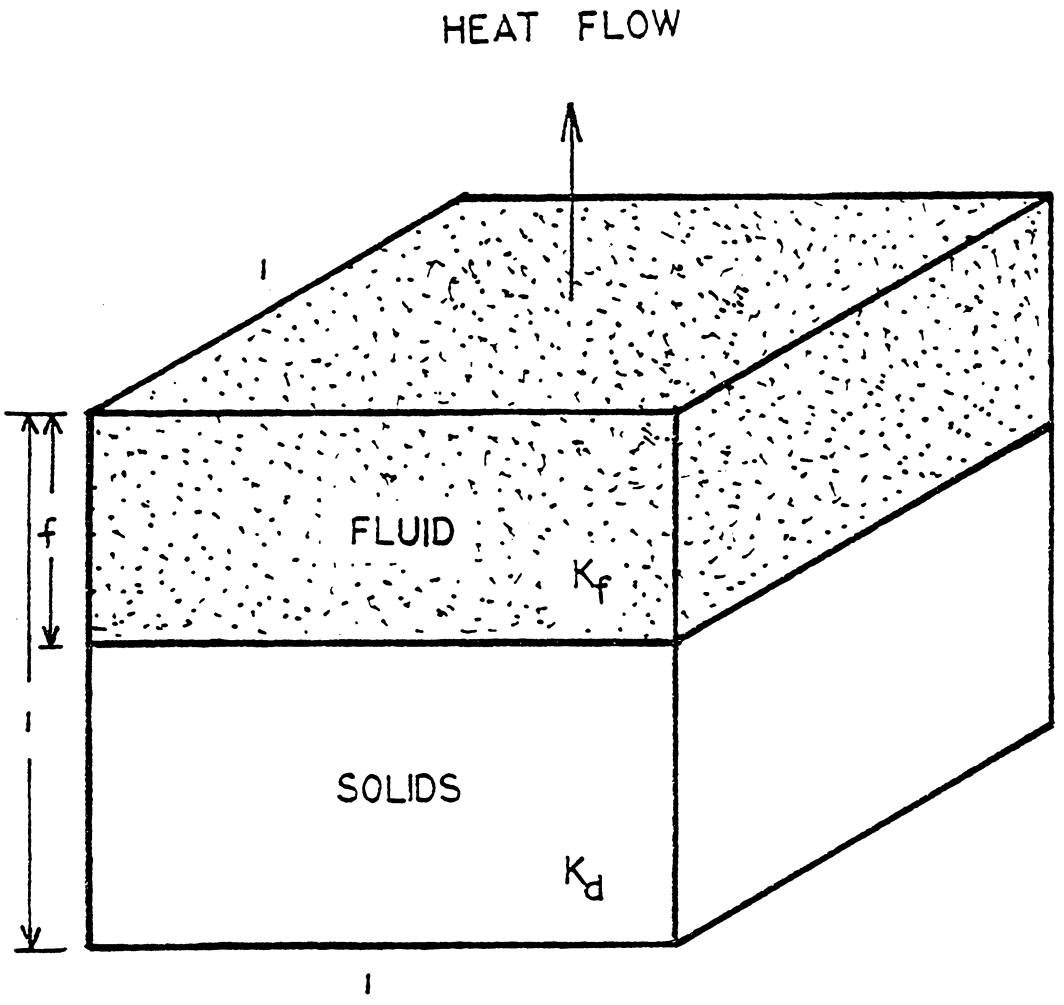

Figure 3 : A schematic model for series heat and mass flow. The distributions of the components are series. The flow passes through the different components sequentially. The magnitude of the flow is determined by the component which has the lowest thermal conductivity or mass diffusivity.

Woodside and Messmer(1961) stated that the geometric mean model is only applicable when K_d/K_f is less than 20.

2.5.4 Equivalent Resistor Model (Wyllie and Southwick, 1954)

Wyllie and Southwick(1954) recognized at least two distinct paths existing for heat fluxes: a continuous path through the major portion of the fluid, and a series path through the solid particles that are bridged by a small portion of the liquid (Fig 4). The model which combines the series and parallel distributions is

$$K = \frac{a\, K_d\, K_f}{(1 - d)\, K_d + d\, K_f} + b\, K_d + c\, K_f \qquad (43)$$

where the coefficients are

$$a + b + c = 1$$

$$b + a\, d = 1 - f$$

For porosity from 20% to 60%, Woodside(1961) suggested

$$b = 0$$

$$c = f - 0.03$$

$$a = 1 - c$$

$$d = (1-f) / a$$

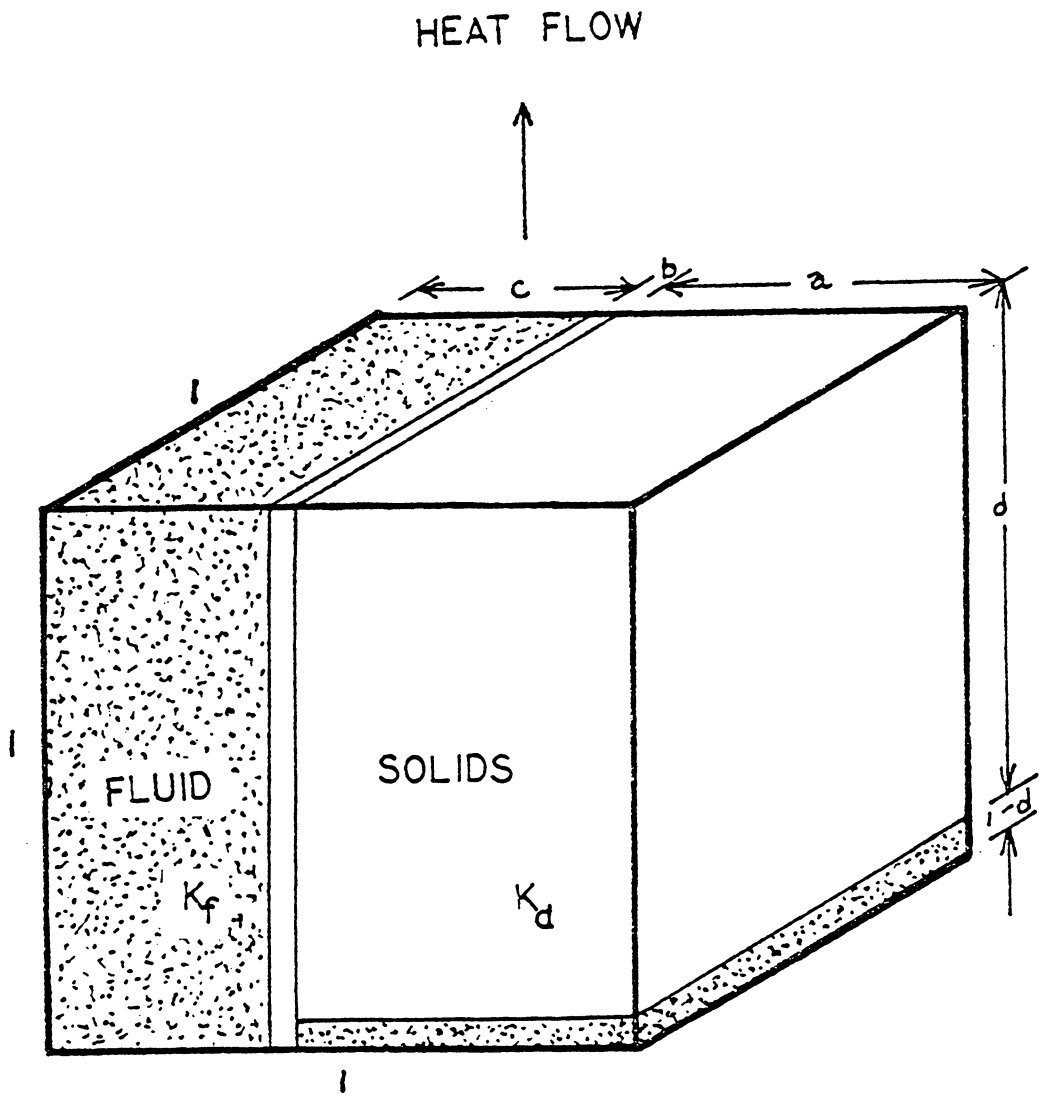

Figure 4 : A schematic equivalent resistor model for heat and mass flow. This model combines series and parallel distributions. The model incorporates continuous(parallel) paths through solid and fluid respectively in addition to the series path.

2.5.5 Modified Maxwell Model (Brailsford and Major, 1964)

Brailsford and Major obtained the formula using Maxwell (1954) result for the average conductivity, K, of a random distribution of solid spheres of conductivity, K_d, in a continuous medium of conductivity, K_f,

$$K = K_f \frac{1 - (1 - a K_d / K_f) f}{1 + (a - 1) f} \qquad (44)$$

where $$a = \frac{3 K_f}{2 K_f + K_d} .$$

McGaw(1969) suggested that the modified Maxwell model was directly applicable only when porosity is well below 50%.

McGaw(1969) investigated these five mixing models for calculating the conductivity of granular materials and compared them with experimental data. He found none of the equations was established to have a truly rational basis; although, each equation could predict the data to a fair degree for a few cases. If a storage bin with grain is assumed to be a system with granular materials, then the above equations can be used to calculate the mixture properties of heat and mass transfer for the storage bin.

2.6 MATHEMATICAL APPROACH

The analytical solutions of the isothermal mass diffusion equation and the simple heat diffusion equation with constant diffusion coefficients were supplied by Crank(1979) for a plane sheet, a cylinder, and a sphere. The analytical solution for Whitney and Porterfield's(1968) modified differential equations was also offered by Crank. In 1966, Luikov obtained the analytical solution for his coupled equations with constant coefficients, which is given in the Appendix B. It is recognized that an analytical mathematical method to solve the practical heat and mass transfer problems is only available for constant coefficients cases and few select special diffusional problems with variable coefficients. Thus, with the disadvantage of getting an analytical solution and the advantage of a high speed digital computer, a numerical method is suggested as a means to solve the coupled heat and mass transfer differential equations with variable coefficents.

Numerical methods include the iteration method, the finite element method and the finite difference method. All of these can be applied to the system of coupled differential equations of heat and mass transfer. The iteration method is suitable for solving a steady state diffusion problems, but requires much more time for a time-series

problem than the other methods. The finite element method is also a potential way to solve the equations. Comni and Lewis(1976) obtained a solution for a two-dimensional problem including coupled effects of heat and mass transfer for moist bodies using the finite element method. However, the finite difference method is still applied more often than any other one for solving a diffusion problem.

Usually, the finite difference method includes the implicit method and explicit method. The explicit finite difference method can be applied more easily than the implicit method. The explicit method avoids the need for iteration or matrix inversion, since future nodal properties can be individually calculated for a time increment, delta(t), from current nodal properties. With the imposition of a stability limit on $\text{delta}(t)/(\text{delta}(r))^2$, the explicit finite difference method for the diffusion equation can give a useful approximate solution. The explicit finite difference method has been applied to the drying of cereal grains by many researchers: Wang and Hall(1961), Kass and O'keeffe(1966), Chu and Hustrulid(1968), Whitaker et al.(1969), Young(1969), Husain et al.(1970) and Ingram(1979).

Consistency, stability, and convergence are critical criteria for the numerical method, and the applicability of the explicit method is restricted by them. Although the im-

plicit method can reduce the above restrictions, it always requires more computer time than the explicit method. Since the solution from the implicit method is more reliable, the implicit method was chosen for this work.

Chapter III

EXPERIMENTAL PROCEDURES

The objective of this research was to describe the temperature and moisture content distributions in the interior of a storage bin. Experimental data will be used to validate Luikov's coupled equations of heat and mass transfer for porous-capillary moist bodies, which were discussed previously.

Three laboratory bins and eight grain columns were designed and constructed, and three experiments were conducted in the processing laboratory. Windows were kept closed to reduce the effects of the variations in the environmental conditions. The bins were placed on a table, 31 inches high, to lessen the interference of the ground. Considering the natural convective heat transfer occurring on the wall of a bin, an interval of six inches was maintained between the bins. No moisture flux could flow through the metal wall of the bin. The measuring instruments were arranged close to the bins so that the measured data represented the actual state of the experimental environment. The temperatures and relative humidities of the surrounding air were recorded and calculated with a hygro-thermograph, a psychrometer and a dry bulb and wet bulb thermocouple measurement unit.

A computer model based on Luikov's coupled equations was developed to simulate the storage process. The theory of control volume, the law of conservation, the law of natural convective heat and mass transfer, Fourier's heat diffusion law and Fick's mass diffusion law were used to determine the boundary conditions.

3.1 LABORATORY STORAGE BINS

An overall view of the bin, 22 inches in diameter and 11 inches in depth, is presented in Figure 5. Considering the natural convective heat and mass transfer between corn and surrounding air, an interval should exist between the floor of a bin and the surface of the table. Three pieces of 1.27 cm angle iron, 120° apart from each other, were riveted on a bin whose floor was eight inches above the table surface. The floors of bins were made of the perforated metal screen with 37% hole area through which moisture flux could flow. 56 pairs of thermocouple were placed in Bin 1 to determine the temperature distribution during the storage period. As illuatrated in Figure 6, thermocouples were installed at seven depth levels, 1, 2, 3.5, 5, 6.5, 8 and 9 inches, and at nine radial intervals from the wall, 0, 1, 2, 3, 4.5, 6,, 8, 9.5 and 11 inches(center). Because the temperature distribution was assumed to be axisymetric, the thermocouples

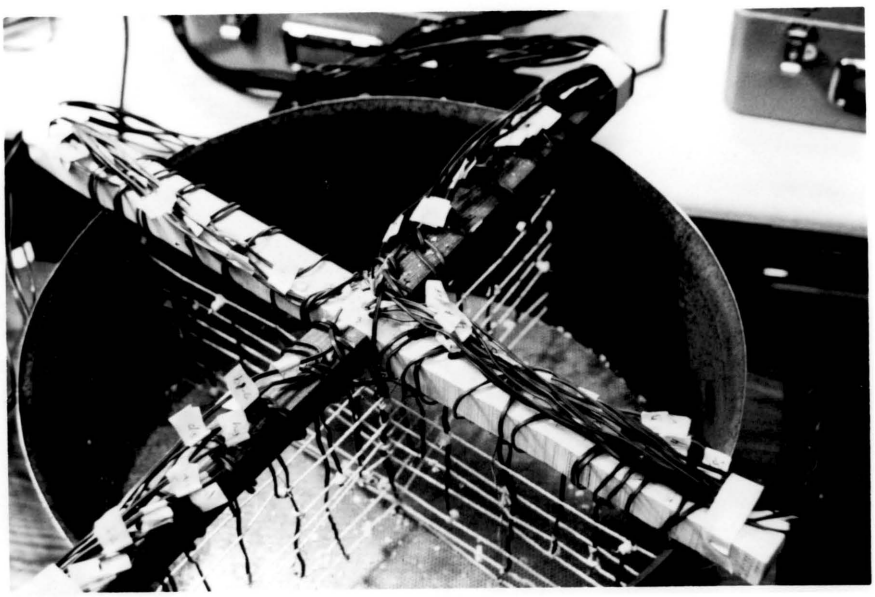

Figure 5 : A view of the laboratory storage bin, 22 inches in diameter and 10 inches in length. The floor has a hole area of 37%. The thermocouples are placed inside the bin to determine the temperature distributions.

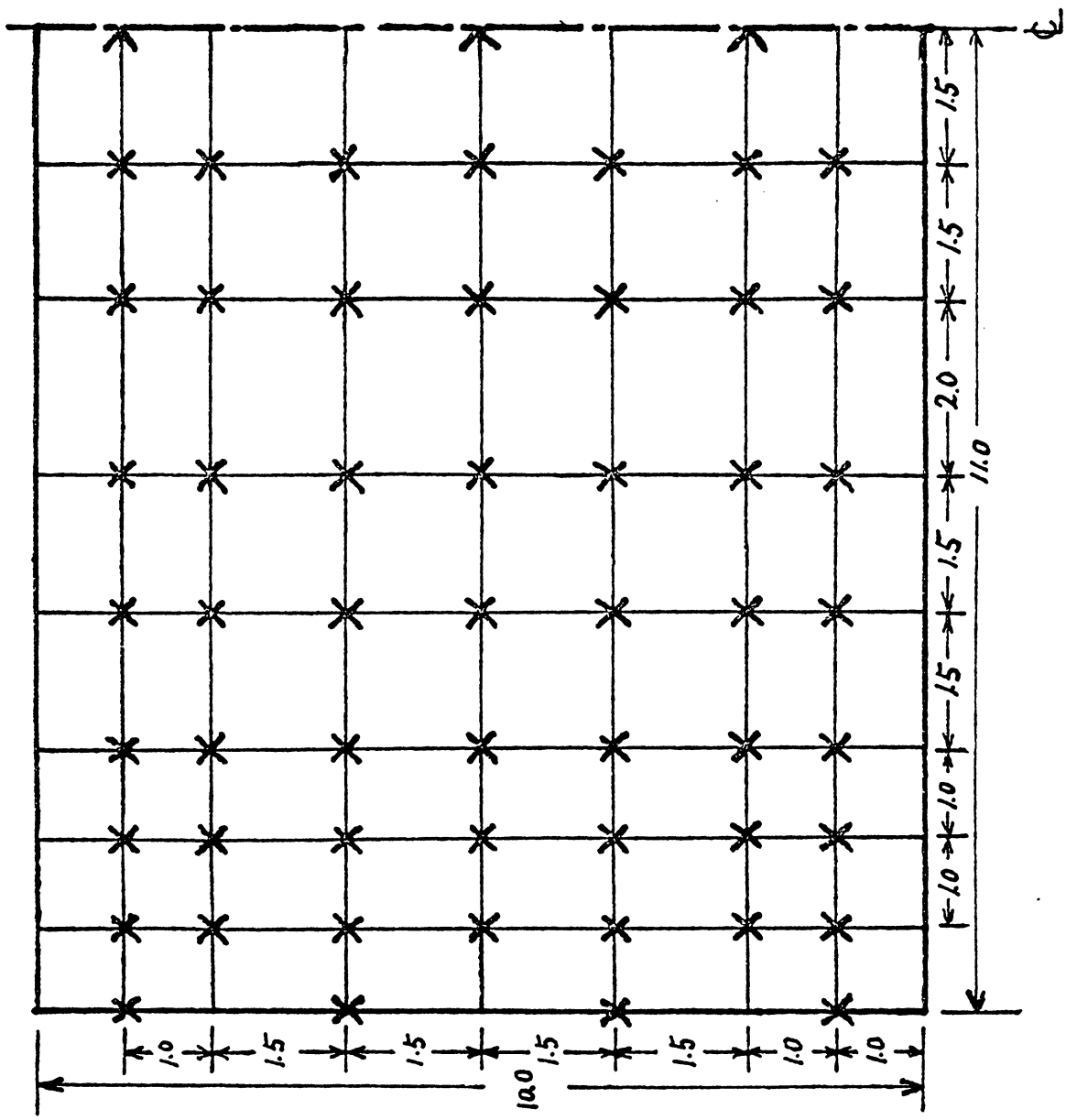

Figure 6 : A schematic illustrating the positions of the the thermocouples placed in storage bin.

were located in 4 radial directions, which were 90° apart with each other to reduce unnecessary thermal interference between the thermocouples. The thermocouples were fastened in radial direction using a 1/12 inch rope with low thermal conductivity and fixed in the axial direction using 1/32 inch iron wire, a low mass diffusivity material.

Since both the values of moisture diffusivity and thermal diffusivity are low, there is no doubt that any disturbance caused by temperature or moisture measurement inside the bin will heavily affect the precision of an experiment. No method was identified to directly determine the moisture content but avoid all external disturbances during the storage period. To face this restriction, there are two possible ways to further improve the precision of an experiment, to extend the time interval between two measurements or to reduce the number of disturbances. Thus, Bin 2 and Bin 3 were constructed without thermocouples and were used to determine the moisture content only.

3.2 GRAIN SAMPLE COLUMN

Since the moisture determinations at some specific positions inside of the bin are needed to validate the mathematical computer model, the grain sample columns are designed and used to determine the values of moisture content at the specified positions. Figure 7 is a schematic of the grain cylinder, 1.5 inches in diameter and 9.6 inches in length, and made of 1/4"x1/4" wire screen mesh. This was done to minimize interference with heat and moisture fluxes. The bottoms of the sample columns were woven from sewing thread to avoid the loss of grain from the cylinder when samples were taken. The fluxes of heat and moisture were admitted to penetrate the floor with 1/4"x1/4" holes. The eight columns were distributed in the three bins, two columns for Bin 1, three columns for Bin 2, and three for Bin 3.

3.3 SAMPLE PREPARATION

It is inevitable that the steady state conditions of an experiment will be altered when sample cylinders are removed. Bin 1 with thermocouples was used to determine the temperature distributions inside the bin; meanwhile, it also was used to measure the terminal moisture content. In other words, there were no samples to be taken from Bin 1 during the process except at the termination of the experiment.

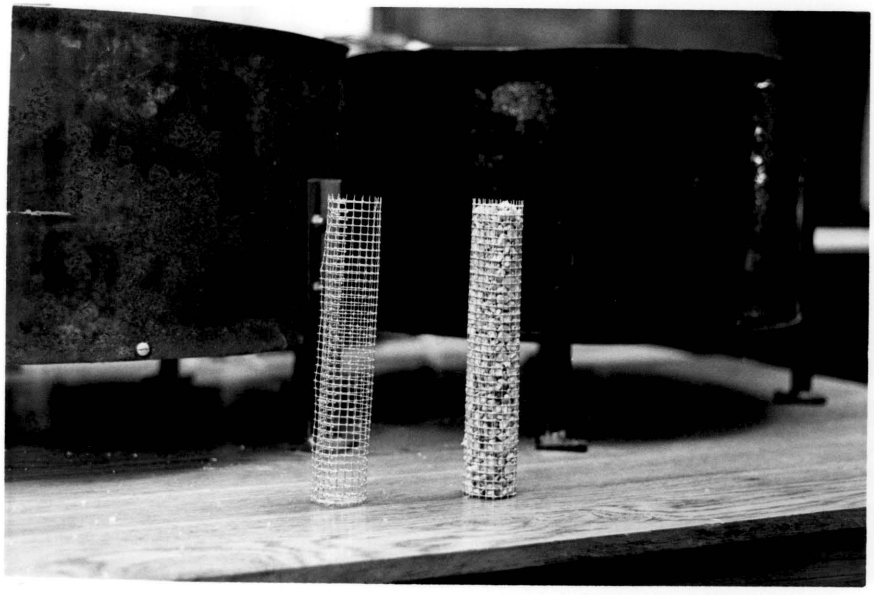

Figure 7 : A grain sample column, 1.5 inches in diameter and 9.6 inches in length, is made of 1/4"x1/4" wire screen mesh.

Bins 2 and 3 were sampled one after the other during the experimental period. The sample columns were placed at 2 and 6 inch radial intervals from the wall for the first experiment, and the remaining two tests at 3 and 8 inch intervals. Using an ice bath, the recorders(A.D. Data System ML-20A) were calibrated and the results are contained in Table 1. The deviations of the recorder measurements, ranged from +1.5°F to -1.0°F, which were within the level of precision of the experiments. Comparisons between the moisture measurements using the direct oven method and a Steinlite Electronic Moisture Tester Model 90(Fred Stein Labortories) are included in Table 2. Since the moisture determinations at specified positions were desired, the sample weight was limited less than 50 grams. Thus, the direct oven method must be used to replace the convenient electronic method which requires 250 grams per sample. Although the average value from the oven method is 0.21% higher than the average value from the Steinlite tester, the oven method is still considered as a stable and reliable way to determine the moisture content.

Table 1 : Calibration of A. D. Data Systems
(ML-20A Minilogger)
Using an ice bath.

System 1 : Channel 1 - Channel 20
System 2 : Channel 21 - Channel 40
System 3 : Channel 41 - Channel 56
(CHAN. : Channel; DEV. : Deviation)

CHAN.	DEV.	CHAN.	DEV.	CHAN.	DEV.	CHAN.	DEV.
1	0.1	2	0.1	3	-0.1	4	0.0
5	0.2	6	0.1	7	0.0	8	0.1
9	0.1	10	0.4	11	0.9	12	0.8
13	1.2	14	1.2	15	1.5	16	1.2
17	1.0	18	1.2	19	1.4	20	1.0
21	-0.3	22	0.2	23	0.1	24	-0.3
25	-0.1	26	0.0	27	-0.1	28	-0.1
29	-0.1	30	0.1	31	0.2	32	0.0
33	0.1	34	0.2	35	0.4	36	0.4
37	0.1	38	0.3	39	0.3	40	0.1
41	-0.9	42	-1.0	43	-0.8	44	-0.8
45	-1.0	46	-1.0	47	-0.6	48	-0.8
49	-0.9	50	-0.7	51	0.0	52	0.4
53	0.3	54	0.3	55	0.2	56	0.1

Table 2 : Moisture contents of samples from the 3 experiments using a moisture tester and a drying oven.

Exp.	Steinlite	D. Oven	Deviation
Exp. 1	13.50	13.89	0.39
		13.55	0.05
	13.20	13.45	0.25
		13.60	0.30
	13.69	13.83	0.14
		13.92	0.23
	13.17	13.30	0.13
		13.45	0.28
	13.23	13.13	-0.10
		13.45	0.22
	13.37	13.59	0.22
		13.80	0.43
Exp. 2	12.71	12.98	0.27
		12.75	0.04
	12.44	12.80	0.36
		12.74	0.30
	13.00	12.99	-0.01
		13.40	0.40
	12.17	12.42	0.25
		12.60	0.43
	12.65	13.01	0.36
		12.95	0.30
	12.60	12.76	0.16
		12.68	0.08
Exp. 3	12.255	12.57	0.315
		12.56	0.305
	12.425	12.53	0.105
		12.73	0.305
	12.305	12.47	0.165
		12.43	0.125
	12.33	12.70	0.37
		12.37	0.04
	12.20	12.50	0.30
		12.47	0.27
	12.015	12.10	0.085
		12.02	0.005
Average			0.212

the unit of the moisture content: %, dry basis

3.3.1 Moisture Content Determination

1. Five sets of moisture measurements were determined initially, after 4, 8, and 11 days and at termination for the first and second experiments, and initially, after 2, 4, and 6 days and at termination in the third test.
2. Two columns at different locations were selected for every set.
3. Every sample column was divided into five subsamples as: top surface to 2 inches, 2 to 4 inches, 4 to 6 inches, 6 to 8 inches, and 8 inches to bottom.
4. Subsamples were weighed and put into an evaporation disk and placed in an oven(Testlib Scientific Equipment Model TG3 .008) at 103°C for 72 hours or at 130°C for 24 hours(ASAE S352).

Moisture contents were calculated on dry basis. The formula for moisture content is

$$M = \frac{(W_i - W_d) - (W_f - W_d)}{(W_f - W_d)} \qquad (45)$$

where

W_d : weight of an evaporation disk only, lb,

W_i : initial weight including moist corn and an evaporation disk, lb,

W_f : final weight including total dried corn

and an evaporation disk, lb, and

M : moisture content dry basis, decimal.

3.3.2 Temperature Measurement

1. Figure 6 is a schematic identifying the locations of the thermocouples, ASNI Type T, used to find the temperature distribution within the interior of the bin.
2. The data were collected hourly in the first two tests and at one half-hour interval in the last test.
3. The data were recorded and stored on a magnetic tape using A. D. Data System ML-20A Data Loggers and subsequently placed into the digital computer.

3.4 TEMPERATURE AND RELATIVE HUMIDITY OF THE SURROUNDING AIR

The temperatures and relative humidities of the surrounding air were recorded with a hygro-thermograph. Simultaneously, wet and dry bulb temperatures were measured with a motorized psychrometer and a thermocouple measurement unit. Data at one hour interval from the Charts (No.-207-WB) used in the hygro-thermograph were digitized and subsequently printed and stored on a magnetic tape for use in the computer analysis. Data collected using a motorized psychrometer

in the first test were also entered into a data file. The results of the dry bulb and wet bulb unit were recorded using the A.D. Data System. Comparisons between the values of these three resources for the first experiment are given in Table 3. The data of the dry bulb and wet bulb measurement unit were questionable, however the results of the psychrometer verified the accuracy of the hygro-thermograph. The hygro-thermograph data were utilized for all three tests.

Table 3 : Temperature and relative humidity measurements of the ambient air during Test 1.

Psy : Psychrometer
H-Ther : Hygro-thermograph
D,W-Bu : Dry and wet bulbs measurement unit

Time	Psy		H-Ther		D,W-Bu	
	TEMP. °F	R.H. %	TEMP. °F	R.H. %	TEMP. °F	R.H. %
March 10						
11:00	73	25	72.7	30.6	72.5	49.4
March 11						
9:00	71	30	71.3	32.8	70.8	49.9
12:00	72.5	33	71.5	35.2	72.3	50.1
16:00	78	35	77.1	38.2	77.3	50.0
19:00	79	35	79.0	39.5	79.4	51.3
March 12						
11:00	77	37.5	77.9	40.1	76.4	57.3
14:00	79.5	42.5	80.4	40.1	78.6	49.5
15:00	79	35	78.8	40.0	78.2	50.1
22:00	79	36	80.2	38.9	79.4	52.4
March 13						
13:00	79.8	46	80.1	43.2	79.5	53.5
15:00	81.2	36	80.9	42.7	80.4	53.5
17:00	80	35.5	80.6	35.1	81.1	53.0
20:00	80.5	35.5	80.6	35.5	81.1	53.2
March 14						
15:00	76.5	29	76.4	26.6	77.1	48.2
18:00	77	29	77.6	26.6	77.7	48.1
22:00	76	27	77.7	29.6	77.8	48.3
March 15						
13:00	74	36	74.7	34.6	74.4	48.0
15:00	73	34	74.6	35.5	74.4	48.1
17:00	74	34	74.4	35.0	74.3	48.3
20:00	73.5	30	73.6	34.4	74.4	50.3
March 16						
15:00	73	36.5	73.1	38.0	73.6	51.3
18:00	76	35	76.1	37.2	75.4	52.4
22:00	77.5	30.5	77.2	37.6	77.1	53.2
March 17						
11:00	81.5	38	80.1	43.5	80.7	50.2
March 18						
8:00	80.5	35	78.5	40.5	79.4	55.3
10:00	75.5	44	77.9	43.3	76.6	50.3
12:00	77.5	40	78.9	41.6	76.3	51.2
March 19						
8:00	78	40	78.1	42.1	78.2	51.7
16:00	81.5	45	81.6	47.0	81.8	51.4
March 20						
13:00	75.5	40	74.8	44.7	76.4	53.1
March 21						
11:00	76	45	77.0	46.7	77.5	61.0
19:00	79	35	79.4	40.2	79.4	61.3
March 22						
10:00	73.5	32	72.3	33.8	73.1	50.4
15:00	74	33.5	73.7	33.9	72.8	50.2
17:00	75.5	33	74.8	31.7	75.1	50.9
March 23						
10:00	77	32	76.5	31.6	76.8	50.1
12:00	77	32	78.1	31.1	77.7	50.7

Chapter IV

MODEL DEVELOPMENT

The overall objective in this research was to develop a mathematical model based on the theory of coupled heat and mass transfer for a porous hygroscopic body to simulate the temperature and moisture distributions of grain in a storage bin during the period of storage. Luikov's(1966) coupled differential equations are applied in this model. The variables in the model(thermal properties of the grain, diffusional properties of grain, initial temperature distribution, initial moisture distribution, and temperature and relative humidity of ambient air) are discussed in this chapter.

The numerical method(implicit finite difference method), which could eliminate the restrictions of time and space increments, was chosen to formulate the coupled partial differential equations. The required boundary conditions for the system were derived from the law of conservation, the law of convective heat and mass transfer, Fourier's heat diffusion law and Fick's mass diffusion law.

Some of the information needed was not available. It was not practical to structure the model without some simplying assumptions. In addition, it was necessary to keep computer

execution time within resonable limits. The following assumptions were made:

1. Shrinkage or expansion due to desorption or adsorption were small and negligible;
2. The potential, moisture concentration difference, produces moisture diffusion;
3. Diffusion is the only mechanism controlling the mass transfer rate;
4. The moisture content of the corn is always less than equilibrium moisture content of grain that corresponds to saturated atmospheric air;
5. The latent heat for moisture evaporization is equal to the value for vapor condensation;
6. Temperature and moisture distributions are independent of vapor pressure;
7. The temperature of the water vapor is equal to the associated temperature of the solid material;
8. The solid matrix is fixed and rigid in an inertial frame;
9. The multi-phase porous system is in thermodynamic equilibrium;
10. Water vapor, air, and their mixture are ideal gases;
11. The moisture content in the vapor phase is negligible in comparison with the moisture content in liquid phase;

12. The properties of corn in the storage bin were isotropic.

4.1 EQUATIONS SYSTEM AND VARIABLE COEFFICIENTS

The model is based on Luikov's coupled heat and mass transfer equations for porous-capillary bodies,

$$\frac{\partial M}{\partial t} = K_1 \nabla^2 M + K_2 \nabla^2 T$$

and

$$\frac{\partial T}{\partial t} = K_3 \nabla^2 M + K_4 \nabla^2 T$$

where

$$K_1 = D_m$$

$$K_2 = D_m \delta$$

$$K_3 = \frac{\varepsilon h D_m}{C_p}$$

$$K_4 = \alpha + \frac{\varepsilon h D_m \delta}{C_p}$$

The precision of a computer model to describe the transport phenomena about heat and mass transfer in a drying or storage process is dependent upon accurate measurements of physical properties. If the coefficents are constant, the system of equations (36) and (37) is linear. Some linear systems can be solved using the analytical method, but not

all linear systems have analytical solutions. Although Luikov(1965) had derived an analytical solution for a one-dimensional flat plate, none analytical solution is presented for a two-dimensional cylinder with finite length and diameter. Furthermore, it is difficult to get an analytical solution for a non-linear system. Unfortunately, most of the coupled differential equation systems are nonlinear because the phenomenological transfer coefficients and coupled transfer coefficients are functions of temperature or moisture content. Even if all the transfer coefficients are variables, they may be assumed as constant values using the principle of local thermodynamic equilibrium within short ranges of moisture change and temperature change during a short period. Thus, the nonlinear solution can be treated as a quasi-linear system, and an analytical solution is still available. Luikov(1966) presented an analytical solution(Appendix B) for a one-dimensional flat plate, which is so complicated that the utility is limited. Even if an analytical solution of equations (36) and (37) exists for a cylinder with a definite length, the solution is still too complicated to apply to an actual case. The only possible approach which seems likely is a numerical solution of the system. The coefficients are assumed as constant during a time increment, one hour; then, the terminal conditions are

calculated for the 1-hour period. The conditions at the end of each 1-hour period serve as initial conditions for the next 1-hour period, and the values of coefficients are updated for every 1-hour period.

4.1.1 Coefficient Variables

4.1.1.1 Bulk Density

Kazarian and Hall(1965) conducted density measurements for yellow dent corn and found the results to be approximately a constant of 46.8 lbs/ft^3 for moisture contents between 0% to 15% wet basis. In 1980, Vemuganti and Pfost evaluated the bulk density of shelled corn and developed a formula to represent the relationship between the bulk density and moisture content as:

$$\rho = 51.32 - 40.82 \frac{M}{1 - M} \qquad (46)$$

where

M : moisture content dry basis, decimal, and

ρ : bulk density, lb / ft^3.

The predicted bulk densities from equation (46) in the moisture range of 10% to 15% dry basis are from 47.61b/ft^3 to 45.981b/ft^3.

A comparison between these two results indicaties a deviation of less than 2%. Kazarian and Hall(1965) concluded that a constant bulk density at moisture from 10% to 15% dry basis was reliable.

4.1.1.2 Specific Heat

Kazarian and Hall(1965) also presented the equation of specific heat as

$$C_p = 0.350 + 0.851 \frac{M}{1 - M} \qquad (47)$$

There is another specific heat equation derived experimentally by Vemuganti and Pfost(1980) as

$$C_p = 0.1856 + 0.12 \frac{M}{1 - M} \qquad (48)$$

Both equations show the specific heat is related to moisture only. Since a significant difference exists between the predicted values of these two models, a selection must be done based on correctness. In fact, Kazarian and Hall's equation(1965) was used in most drying models, and was chosen for this work.

4.1.1.3 Latent Heat

Strohman and Troeger(1967) developed the following equation to describe the latent heat of vaporization of water in moist corn:

$$h = h_w (1 + a\, e^{b\, M}) \qquad (49)$$

where

a : 0.8953,

b : -12.32, and

h_w : the latent heat of vaporization of water from a free surface, Btu/lb.

$$h_w = 1075.9 - 0.56953\ (T - 32)$$

Thompson(1969) also experimentally established a latent heat model for shelled corn, which has the same form as Strohman's equation, Eq. (49), but has different coefficients:

a : 4.35, and

b : -28.5.

Both models yield similar results. Thompson's model was elected for this work.

4.1.1.4 Thermal Conductivity

Kazarian and Hall(1965) obtained the thermal conductivity of a bulk of corn,which was a function of moisture only

$$K = 0.0814 + 0.0646 \frac{M}{1 + M} \qquad (50)$$

where k : thermal conductivity, Btu/hr-ft-°F.

In 1980, Fortes and Okos evaluated Kazarian and Hall's data and expressed the model as

$$Ln(K) = C\ (-1.1738 - 3.696\ M + 0.0475\ T + 0.843\ M^2 - 0.0001499\ T^2 + 0.0006272\ M\ T) \qquad (51)$$

where

K : thermal conductivity, Btu/hr-ft-°F,

T : dried bulb temperature, °C,

C : 1.738, conversion factor from metric to english,

M : moisture content, decimal, and

Ln : natural logarithm.

This model which includes both temperature and moisture effects on thermal diffusivity was used in this study.

4.1.1.5 Thermal Diffusivity

Thermal diffusivity is defined as

$$\alpha = \frac{K}{\rho C_p} \qquad (52)$$

where

K : thermal conductivity, Btu/hr-ft-°F,

ρ : bulk density, lb/ft^3,

C_p : specific heat, Btu/lb-°F, and

α : thermal diffusivity, ft^2/hr.

4.1.1.6 Thermal Gradient Coefficient

The thermal gradient coefficient is related to the Soret effect and can be determined experimentally, but the determining method is somewhat tedious and requires sophisticated

instrumentation. Husain(1970) investigated the coefficient for a kernel of corn using the analytical method. Data from Husain's study is suitable for moisture constents of 4%(w.b.) to 20%(w.b.) and temperatures of 86°F to 140°F, and a linear relationship between the coefficient and the temperature exists. If the method of linear extrapolation is applied to derive the thermal gradient coefficient, the equation is

$$\delta = C\,(1.37625 + 2.56649\,M - 1.78362\,M^2 + 0.56685\,(86 - T)) \qquad (53)$$

where

δ : thermal gradient coefficient, $°F^{-1}$

C : 0.00005556

The experiments were conducted inside an area where the environmental conditions were under control, and the region of the experimental temperature was 63°F to 82°F which was below 86°F. Since the storage temperature of a bed of corn is lower than 86°F, the availability of the data from Husain is questionable for corn storage. By checking Husain's data(Table C.1), the thermal gradient coefficient is almost constant at the experimental temperature of 86°F. Even though the coefficient is independent of the moisture content, the relationship between the coefficient and the temp-

erature is still ambiguous. There are two possible ways to estimate the value of the coefficient: one is the coefficient to be assumed as a constant, the other is the coefficient which is a function of temperature only derived based on the method of linear extrapolation. In this work, the thermal gradient coefficient was assumed to be constant, 0.0000767 $^{\circ}F^{-1}$.

4.1.1.7 Bulk Moisture Diffusivity

A porous body can be divided into a solid portion including solid material and absorbed moisture, and a fluid portion including air and vapor. It is recognized that the mechanism of mass diffusion for the solid part is different from for the fluid part.

4.1.1.7.1. Air and Vapor

Since air and vapor occupy porous region of the storage bin, the mass diffusivity in the porous region can be treated as the molecular diffusivity of a binary gas. The molecular diffusivity of an ideal binary gas can be determined by Fuller's model(1966) or Sherwood's model(1952).

Sherwood recommended the following expression at pressures below 20 atm:

$$D_{ab} = \frac{0.0018583\ T^{3/2}}{P\ (A^{0})^{2}\ C_{i}} \left(\frac{1}{M\rho_{1}} + \frac{1}{M\rho_{2}} \right)^{1/2} \qquad (54)$$

where

T : thermodynamic temperature, °K,

P : pressure, atm,

A^0 : Lennard-Jones force constant, angstron,

C_i : collision integral,

$M\rho$: molecular weight, gm/mole, and

D : diffusivity, cm^2/sec.

The caculated values from Sherwood's equation are 0.835087 ft^2/hr at 80°F and 0.775595 ft^2/hr at 59°F; therefore, it is an acceptable assumption that the diffusivity of air and vapor is a constant, 0.80 ft^2/hr. The error between diffusivity calculated from the above equation and measured value at various temperature was 7.5%.

4.1.1.7.2. Diffusivity of A Kernel of Shelled Corn

Henderson and Pabis(1961) evaluated the diffusivity of a kernel of corn as

$$D_m = 0.000107639\ e^{(T - 114.8)\ 0.01953} \qquad (55)$$

where T is temperature °F.

The diffusivity from the above equation is related to temperature only.

It is recognized that moisture diffusivity is related to both the moisture and temperature. Chu and Hustrulid(1968)

experimentally evaluated the diffusivity of a kernel of corn in the neighborhood of R=0.50 as:

$$D_m = C\,(1.5134\, e^{(0.00045\,T - 0.05485)\,M - \frac{2513}{T}}) \quad (56)$$

where

T : temperature, °K,

M : moisture content, % dry basis,

C : 0.001076, and

D_m : diffusivity, ft^2/hr.

The surface moisture ratio(R) is

$$R = \frac{M - M_s}{M_i - M_s}$$

where

M_s : surface moisture content, and

M_i : initial moisture content

Since the value of R was indeterminate in this study, Henderson and Pabis's model was used.

4.1.1.7.3. Diffusivity of A Mixture of Corn and Air

The five models(geometric mean model, equivalent resistor model, modified Maxwell model, parallel model and series model) were chosen to calculate the moisture diffusivity of the mixture. The predicted moisture and temperature distributions of these five models are compared with the actual experimental results.

4.1.1.8 Porosity

Using an air-comparison pycnometer, Chung and Converse(1971) measured and calculated the porosity to be a function of bulk density only

$$f = 1.01 - 0.0125\,\rho \qquad (57)$$

where

f : the porosity, decimal.

Because the bulk density of corn has already been assumed to be constant in this work, the porosity is also taken as a constant of 0.425.

4.1.1.9 Phase Conversion Factor

The phase conversion factor is defined as the ratio of the amount of moisture flow in the vapor phase to the net amount of moisture flux. The phase conversion factor is an indication of the phase of moisture in the diffusive moisture flow. The domain of the factor is from zero to one. When the factor is zero, the total mass of moisture is transferred in the liquid phase. If the factor is equal to one, the mass is only in the vapor state.

Since the mechanisms of moisture movement are uncertain, it was hard to determine a proper phase conversion factor in this research. Five values(0.0, 0.25, 0.5, 0.75 and 1.0)

were chosen to determine the theoretical results which best compare with the experimental data.

4.2 BOUNDARY CONDITIONS

Space boundary conditions reflect the law of interaction between a body surface and the surrounding medium. This interaction implies the transfer of energy and mass. A general set of boundary conditions for the system of equations (36) and (37) is discussed below.

4.2.1 Heat Transfer

4.2.1.1 Boundary with constant temperature

Convective heat transfer can not occur through a boundary with a constant temperature which is equal to ambient air temperature

$$T_s = T_a \qquad (58)$$

where

T_s : body surface temperature, °F, and

T_a : ambient air temperature, °F.

4.2.1.2 Boundary subjected to heat fluxes

The boundary conditions are based on the law of energy conservation and the law of convective heat transfer

$$-K \, \mathrm{grad}(T) - (1 - \varepsilon) \, h \, J_m + J_q = 0 \qquad (59)$$

Equation (59) indicates that the amount of heat supplied to the body surface is equal to the heat flow which penetrates a body and heat flow which is spent for liquid evaporation.

1. When a moist body contacts heated air, Jq is heat flow supplied to the body surface by convective heat exchange. The heat flow is given by

$$J_q = h_q (T_a - T_s) \qquad (60)$$

where

J_q : heat flow, Btu/hr-ft^2, and

h_q : film heat transfer coefficient, Btu/hr-ft^2-°F.

McAdams(1954) recommended the relationship between the coefficient and the temperature for the simplified free heat convection of air(Table C.2)

2. The conductive heat flow, -K grad(T), occurs within the inside of the body. Although the conductive heat flux can occur between the moist body and the surrounding air, the effect of the interface minimizes it and it can be neglected.
3. The amount of heat required to evaporate the liquid moisture flow into the vapor phase is (1-ε) h Jm.

4.2.2 Mass Transfer

4.2.2.1 Boundary with constant moisture

At any moment, the moisture content at the boundary surface is equal to the equilibrium moisture content corresponding to the relative humidity of the surrounding air

$$M_s = M_e \tag{61}$$

where M_e is determined by Thompson(1969)

$$1 - RH = e^{C (T_a + 50) M_e^2} \tag{62}$$

where

RH : relative humidity, decimal,

C : -0.0000382,

T : temperature, °F, and

M_e : equilibrium moisture content of the grain, decimal dry basis.

4.2.2.2 Boundary subjected to mass fluxes

According to the law of convective mass transfer, Fick's law of mass transfer and the law of mass conservation, the boundary condition for mass is

$$-D_m \text{ grad}(M) + D_m \text{ grad}(T) + J_m = 0 \tag{63}$$

1. The term, Dm grad(M), is the internal moisture movement as a result of thermodynamic force grad(U).
2. The term, Dm δ grad(T), is the moisture flux due to the thermodynamic force grad(T).
3. The term, Jm, is a result of the interaction between the moist body and the surrounding air. In 1981, Fortes and Okos obtained

$$H_m = \frac{D_v \; P}{R_v \; T_a D_p \; P_{bm}} (2.0 + 0.6 \; Re^{1/2} \; Sc^{1/3}) \qquad (64)$$

where

H_m : molecular diffusivity coefficient of water vapor in air, M^2/s,

P : total pressure, N/m^2,

R_v : universal gas constant,

T : thermodynamic temperature, ^oK,

D_p : equivalent diameter, m,

P_{bm} : logarithmic mean of pressure at surface and at medium, N/m^2,

ν : kinematic viscosity, m^2/hr,

Re : Reynolds number

$$Re = \frac{V \; D_p}{\nu}$$

Sc : Schmidt number

$$Sc = \frac{\nu}{D}$$

and

$$J_m = H_m (P_{vd} - P_{va})$$

where

P_{va} : partial vapor pressure of air, N/m^2, and

P_{vd} : partial vapor pressure of solid skeleton, N/m^2.

Since Eq. (64) includes many undetermined variables and complicated coefficients, the applicability of the equation is limited. Based on the theory of free mass convective transfer, Luikov(1965) developed the convective moisture flow(Jm) is expressed as:

$$J_m = h_m (M_e - M_s) \qquad (66)$$

where

h_m : mass transfer film coefficient, $lb/hr\text{-}ft^2$.

Due to the difficulty of evaluating the moisture film coefficient in equation (66), the equation is not applicable in this study. The moisture content of corn which contacts the surrounding air is better determined using the drying equation. Sabbah's(1979) drying equation is

$$\frac{M - M_e}{M_i - M_e} = e^{-N\, t^{0.664}} \qquad (67)$$

where

t : time, hours, and

$$N = e^{-z\, t^{y}}$$

in which the variables are

$$y = 0.1245 - 0.0022\ RH - 0.000023\ RH\ T_a - 0.000058\ T_a$$

and

$$z = (6.0142 + 1.43\ RH^2)^{1/2} - 0.01\ T_a\ (3.353 + 3.0\ RH^2)^{1/2}$$

Convective mass transfer only happens on the surface of the corn where there is direct contact with the environmental air. The size of the corn kernel is contained in Table C.3. The one inch thickness of the top and bottom boundary elements is 5.66 times the average thickness of a kernel of shelled corn, and convective moisture transfer occurs on the surface layer and a portion of the next layer. As a result, the moisture flux on the top surface and the bottom surface are given as:

1. for the top surface was open to the atmosphere

$$J_{mt} = \frac{M_t - M_{t+\Delta t}}{5} \qquad (68)$$

where:

M_t : moisture at time t, and

$M_{t+\Delta t}$: obtained moisture from drying equation at time $t + \Delta t$.

2. for the bottom surface which was restricted by perforated metal which had a 37% hole area

$$J_{mb} = \frac{M_t - M_{t+\Delta t}}{12} \qquad (69)$$

4.3 NUMERICAL METHOD FORMULATION

Via the use of Taylor's expansion, Hornbeck(1975) pointed out that the relation of the finite difference expression to the differential equation could be understood by deriving the latter from the former. The implicit formulation is obtained by using the forward difference expression for the first derivative in place of the time derivative on the right side of equations (36) and (37). The central difference for the second derivative is used for the left side. The calculated moleculars for the implicit numerical method(Ames, 1977) are given by:

1. for the first time derivative

$$\left.\frac{\partial X}{\partial t}\right|_{ijk} = \frac{X_{ijk+1} - X_{ijk}}{\Delta t} \qquad (70)$$

2. for the first radial derivative

$$\left.\frac{\partial X}{r\partial r}\right|_{ijk} = \frac{X_{i+1jk+1} - X_{i-1jk+1}}{i\ \Delta r\ 2\ \Delta r} \qquad (71)$$

3. for the second radial derivative

$$\left.\frac{\partial^2 X}{\partial r^2}\right|_{ijk} = \frac{X_{i+1jk+1} + X_{i-1jk+1} - 2X_{ijk+1}}{(\Delta r)^2} \qquad (72)$$

4. for the second axial derivative

$$\left.\frac{\partial^2 X}{\partial z^2}\right|_{ijk} = \frac{X_{ij+1k+1} + X_{ij-1k+1} - 2X_{ijk+1}}{(\Delta z)^2} \qquad (73)$$

where

i : subscript used to denote the number of time increments,

j : subscript used to denote an interior spatial element in radial direction,

k : subscript used to denote an interior spatial element in axial direction,

Δr : a spatial increment in radial direction, ft,

Δz : a spatial increment in axial direction, ft, and

Δt : a time increment, hr.

All terms in equations (36) and (37) are replaced by the moleculars and the equations are further rearranged to yield

$$C_{i+1jk} M_{i+1jk+1} + C_{ijk} M_{ijk+1} + C_{i-1jk} M_{i-1jk+1}$$
$$+ C_{ij+1k} M_{ij+1k+1} + C_{ij-1k} M_{ij-1k+1}$$
$$+ C'_{i+1jk} T_{i+1jk+1} + C'_{ijk} T_{ijk+1} + C'_{i-1jk} T_{i-1jk+1}$$
$$+ C'_{ij+1k} T_{ij+1k+1} + C'_{ij-1k} T_{ij-1k+1}$$
$$= B_{ijk} \qquad (74)$$

The exact forms of the coefficients(C, C' and B) for the heat and mass transfer equations are presented in Appendix D.

To utilize the implicit technique, the grain bin was divided into 6 layers from bottom to top, and each layers was further divided into 6 annuli from wall to center as illustrated in Figure 8. Each element was called a numerical calculation element and the average temperature and moisture content of the element were determined. For comparative purpose, there were five layers defined from the experimental data. The top layer was from the surface down 2 inches. The middle layer was the layer from 4 to 6 inches down from the top surface and the bottom layer was 2 inches up from the bottom surface. Each numerical calculation element has

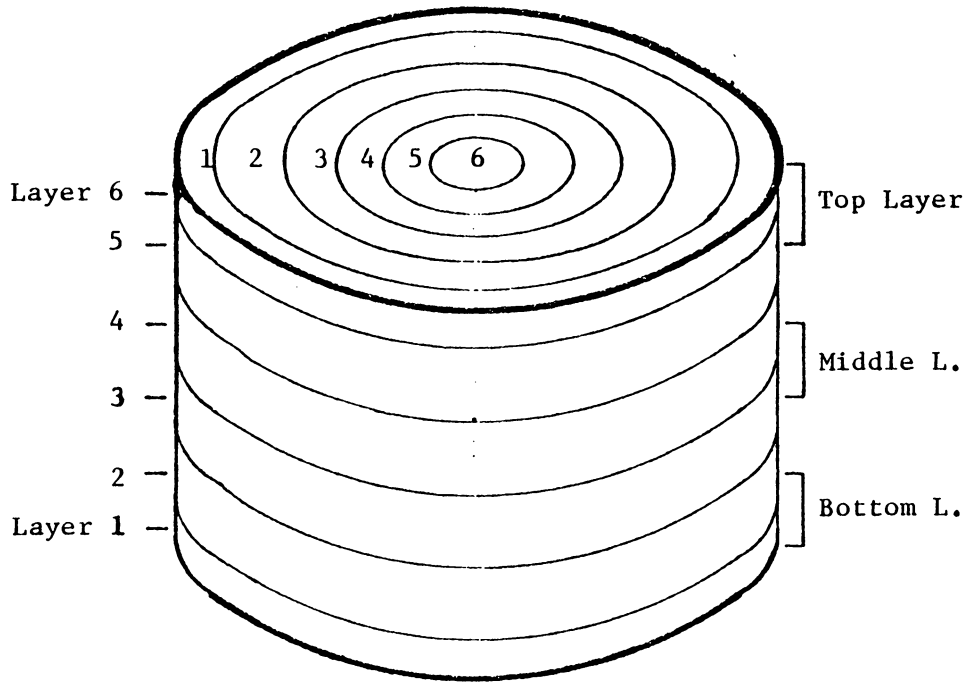

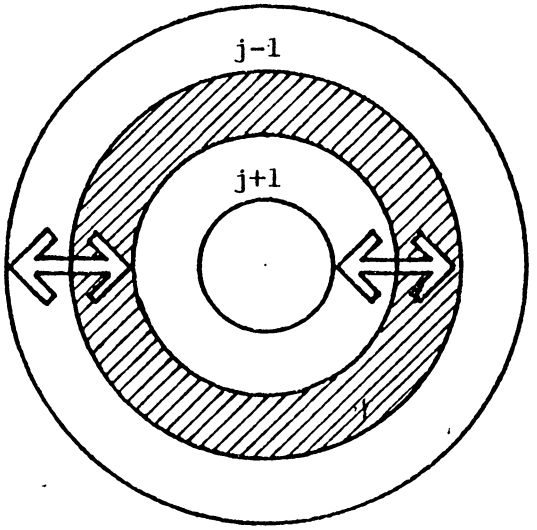

Heat and mass flow in radial direction

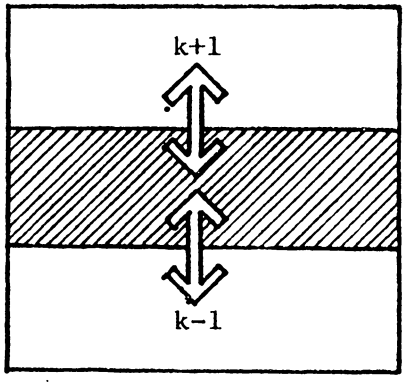

Heat and mass flow in axial direction

Figure 8 : Annular element of the storage bin for the implicit finite difference method. The bin was split into 36 elements(6 layers, 6 elements for per layer). Properties were determined on the average of the element.

two equations: one for mass and the other for heat. The implicit technique reduces to the solution of a set of simultaneous algebraic equations, which consist of the equations for all elements, at each time increment. The set of simultaneous equations can be solved by iteration , by relaxation, or by matrix inversion. With the efficiency and utility of a digital computer, the matrix inversion method was chosen. A program for matrix inversion was supplied by Hornbeck(1975).

Chapter V

MODEL VERIFICATION

The mathematical model derived previously illustrates the application of the theory of transport phenomenon and the reciprocal principle of irreversible thermodynamic processes to a porous-capillary hygroscopic body. To obtain a reliable model, the data of a bed of shelled corn collected during three storage experiments were used to validate the applicability of the above development.

The distributions of ambient air temperatures are expressed in Figure 9 and the equilibrium moisture contents are shown in figure 10 for all three experiments. The three tests had both heating and cooling phases, but only experiment 3 had both moisture absorption and desorption. The data from experiment 3 were used to verify the model. Data of the first two tests are presented in Appendices E and F. A flow chart which shows the complete procedure is outlined in Appendix G. The simulation program is also contained in Appendix G. Other data relative to test 3 are contained in Appendix H.

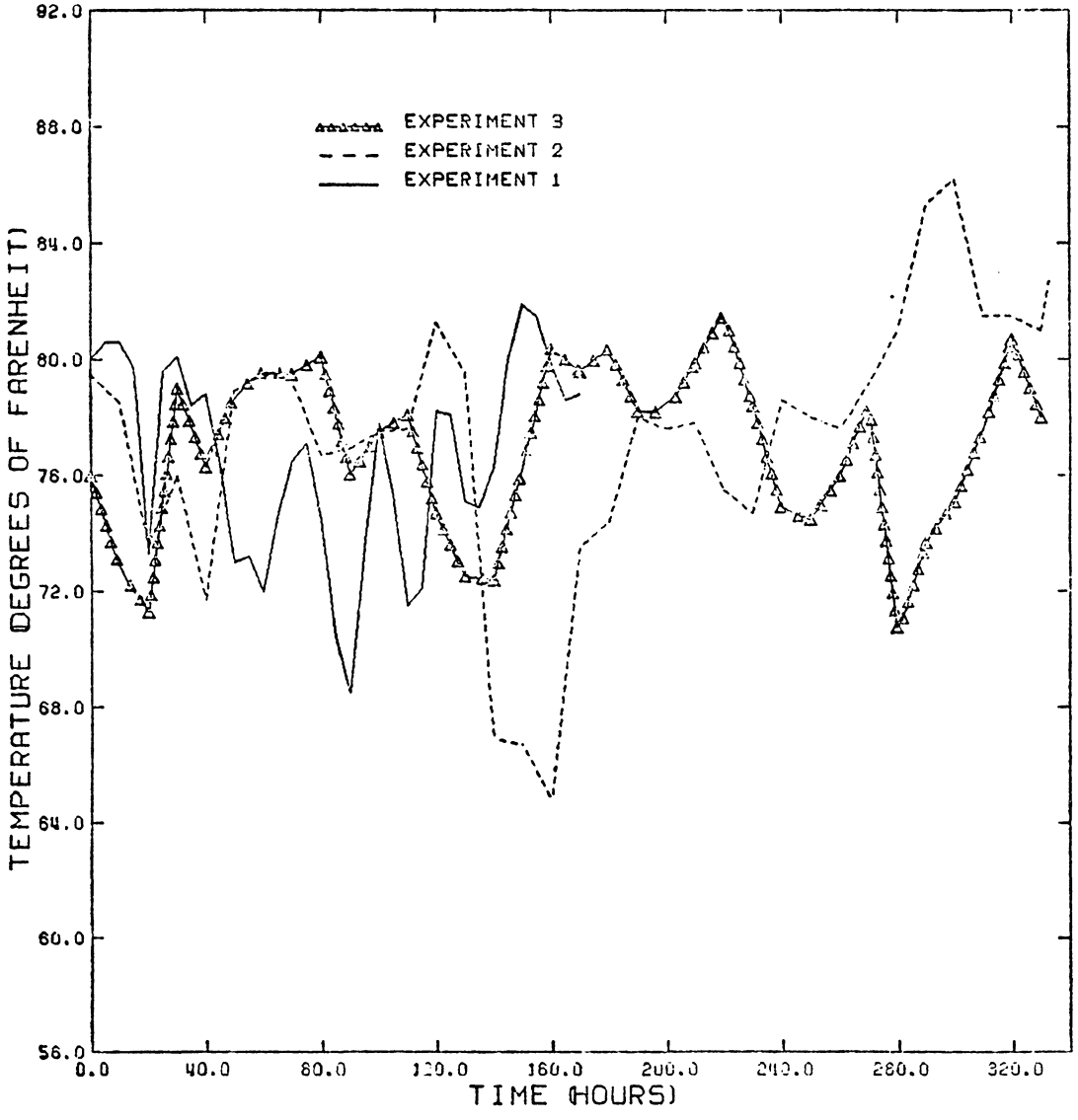

Figure 9 : Ambient air temperatures during the three tests. Illustrated are the unstable conditions of the environment.

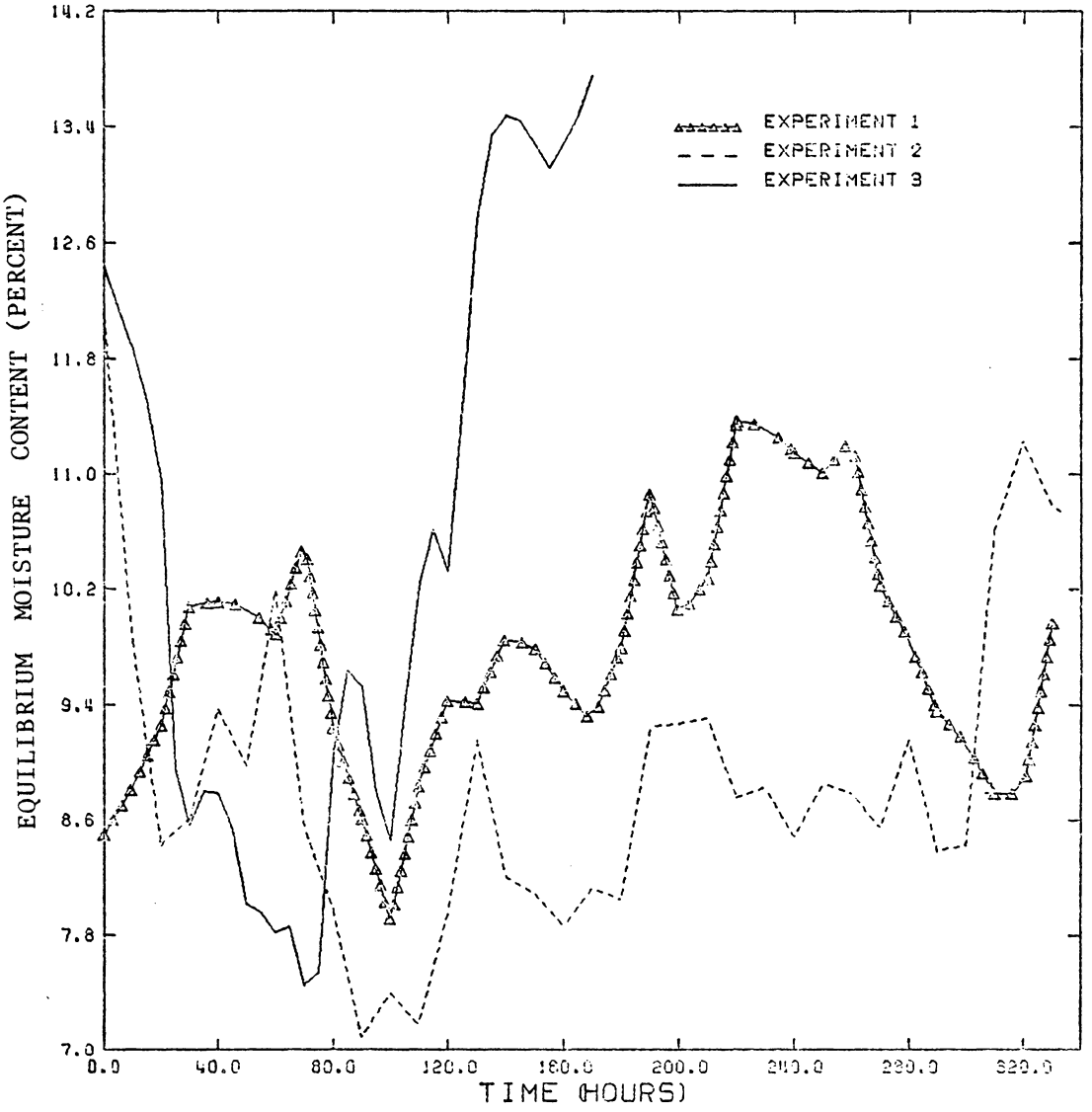

Figure 10 : Equilibrium moisture contents based on the ambient air conditions during the three tests. In test 3 both absorption and desorption occur.

5.1 TEMPERATURE DISTRIBUTION

Figures 11 and 12 illustrate the predicted temperatures at wall distances of 3 and 8 inches respectively using a geometric mean model with a phase conversion factor of zero. Ambient air temperature is ploted as a reference. Although the ambient air temperature is unstable during the whole process, the figures strongly reveal the existence of a positive relationship between the grain temperature and air temperature. Based on the temperature distribution curves, the experimental period can be divided into 3 stages: 0-80 hours, 80-125 hours and 125-170 hours. In the first and third periods, the change of temperature is influenced largely by moisture transfer, and the second stage of the curve illustrates the second law of thermodynamics (which states the direction of heat flux from high temperature to low temperature) and Fourier's law of heat diffusion. In the first period(0-80 hours), the corn temperature is always lower than the ambient air temperature, no matter how low the air temperature is. Even with the rapid decrease in air temperature between 15 and 20 hours, it is still higher than the corn temperature; thus, the temperature of corn should continue to increase. However, the experimental results reveal that the change in corn temperature has a positive relationship to the change in ambient air temperature, which

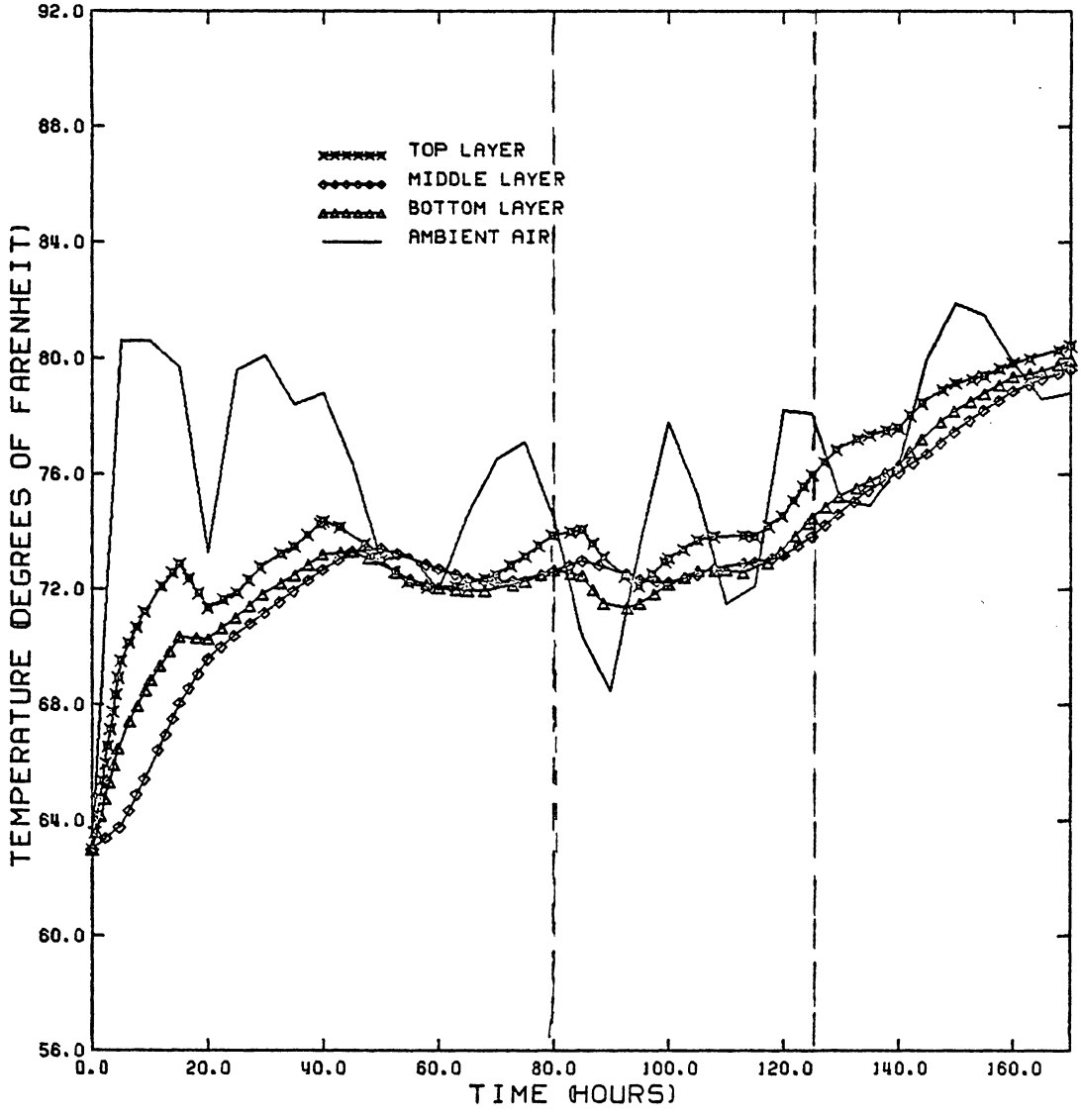

Figure 11 : Ambient and predicted temperatures from use of the geometric mean model with a phase conversion factor of zero for a wall distance of 3 inches in Test 3. During the time of 0-80 hours : a desorption process occurs, 80-125 hours : a thermodynamic equilibrium phase occurs, and 125-170 hours : a absorption process occurs.

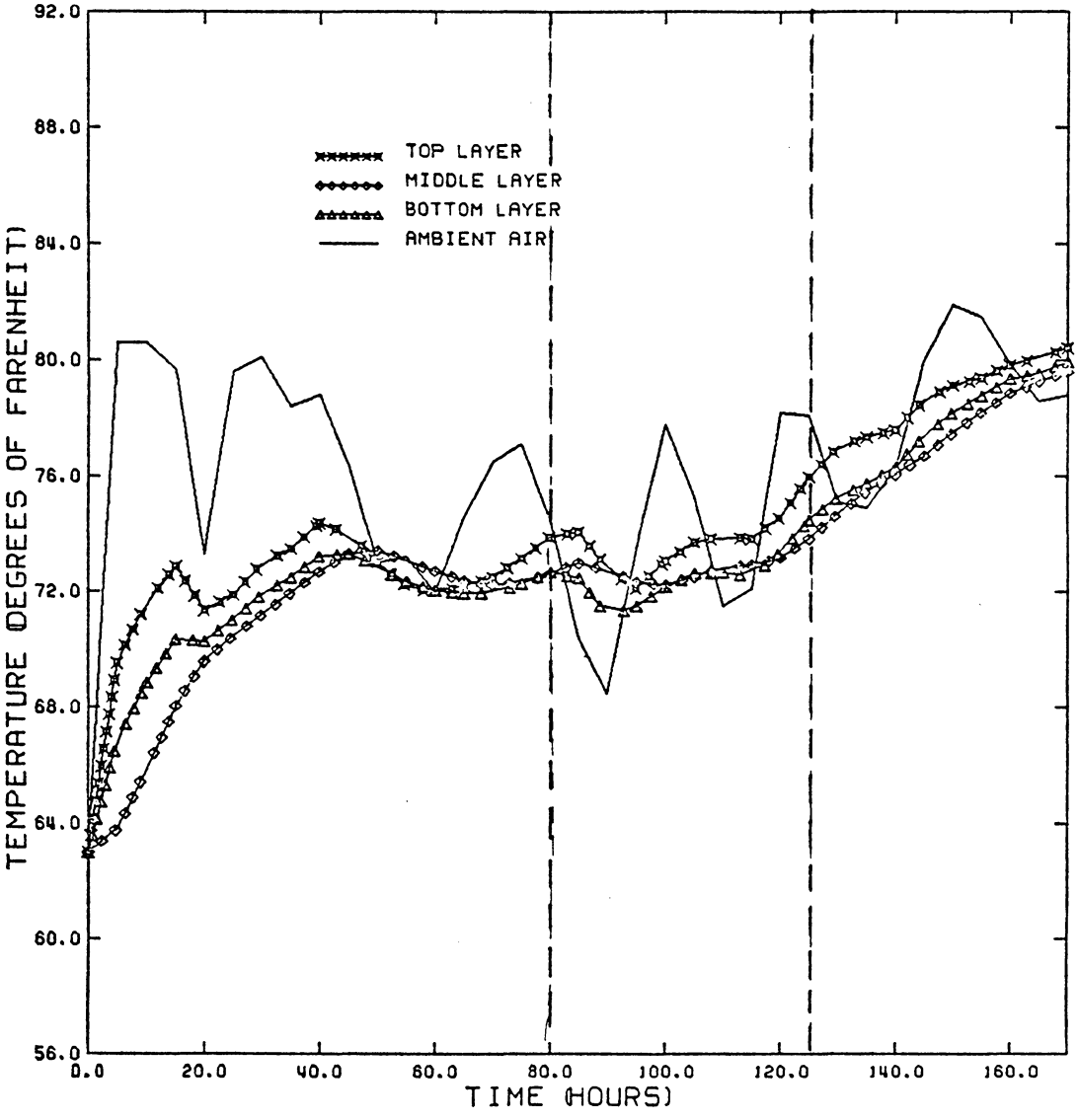

Figure 12 : Ambient and predicted temperatures from use of the geometric mean model with a phase conversion factor of zero for a wall distance of 8 inches in Test 3. During the time of 0-80 hours : a desorption process occurs, 80-125 hours : a thermodynamic equilibrium phase occurs, and 125-170 hours : a absorption process occurs.

conflicts with the second law of thermodynamics. One possible reason for this phenomenon is that corn is always cooler than the surrounding air due to the process of desorption which requires heat energy to evaporate liquid moisture. In the third period, corn gets extra heat which is released due to the process of absorption. This extra heat would raise the corn temperature, even if the ambient air temperature has already been lower than the corn temperature.

By observing the temperature distributions of three layers, the top layer and bottom layer are more sensitive to the changes of ambient air temperatures. It is proposed that the temperature of the middle layer is lower than the temperatures of the top and bottom layers in the heating process, and higher than the values in the cooling process. The temperature of the middle layer could be between the temperatures of the top and bottom layers in a transition period from absorption to desorption or from absorption to desorption.

5.2 MOISTURE DISTRIBUTION

The moisture content measurements for experiment 3 are presented in Table 4, and Figures 13 and 14. Figures 15 and 16 illustrate the predicted moisture distributions from a geometric mean model with a phase conversion factor of zero at wall distances of 3 and 8 inches. The figures reveal that the direction of moisture migration in corn is toward the equilibrium moisture content. Thus, the curves in Figures 15 and 16 can be divided into at least four significant periods:

1. Starting point to 20 hours

   The internal moisture is almost uniform throughout the bin during this period. The amount of external moisture flow is negligible, and the internal moisture migration does not occur in this stage. In 1939, Henry suggested that the only moisture migration of a moist air was in the vapor phase. As corn is moved into the room, the initial vapor pressure is close to the air vapor pressure; thus, the potential field of moisture migration does not exist. During this time period, a potential field is been creating for later internal moisture migration. Because the initial temperature is far below the surrounding air temperature, heat can be transported from the ambient

Table 4 : Moisture contents in five layers at wall distances of 3 and 8 inchrs for Test 3.

Time (hr)	M.C. (top)	M.C. (n.t.)	M.C. (mid)	M.C. (n.b.)	M.C. (bot)
R=3.0					
0	12.450	12.450	12.450	12.450	12.450
48	10.850	11.210	11.760	11.340	11.100
96	10.310	10.530	10.730	10.460	10.420
144	11.370	10.820	10.740	10.830	10.740
170	11.260	11.340	11.110	11.230	11.350
R=8.0					
0	12.450	12.450	12.450	12.450	12.450
48	10.910	11.320	12.010	11.510	11.270
96	10.370	10.690	10.910	10.820	10.670
144	11.150	10.910	10.860	10.900	11.103
170	11.150	11.310	11.160	11.370	11.350

top : layer at the top surface
n.t. : layer next to the top layer
mid : layer at the middle
n.b. : layer next to the bottom layer
bot. : layer at the bottom surface
R : the interval from the wall

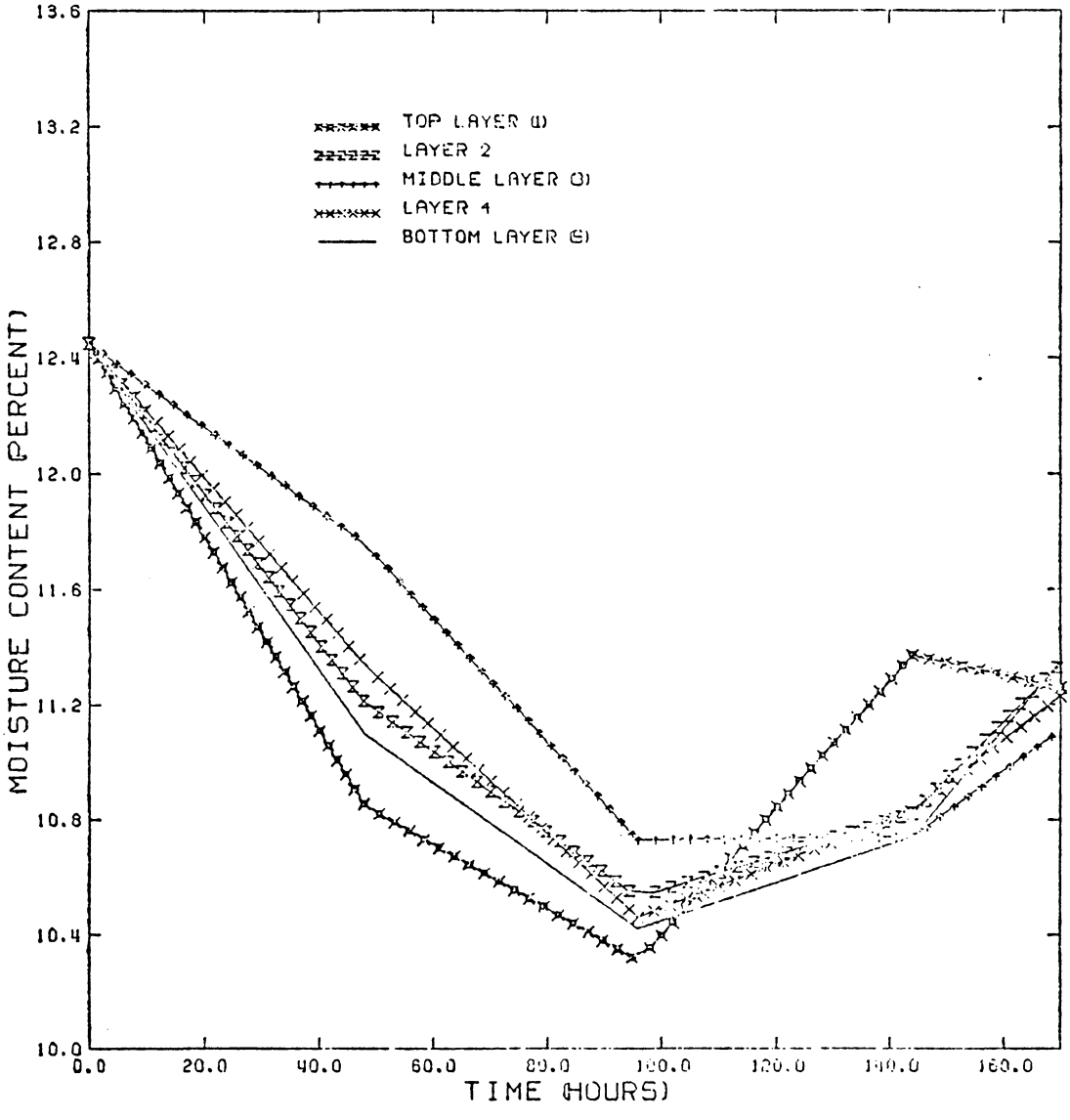

Figure 13 : Experimental moisture contents in the five layers during Test 3 at a wall distance of 3 inches. The curves indicates that the moisture contents in the surface layers are lower in desorption and higher in absorption than the values of the internal layers.

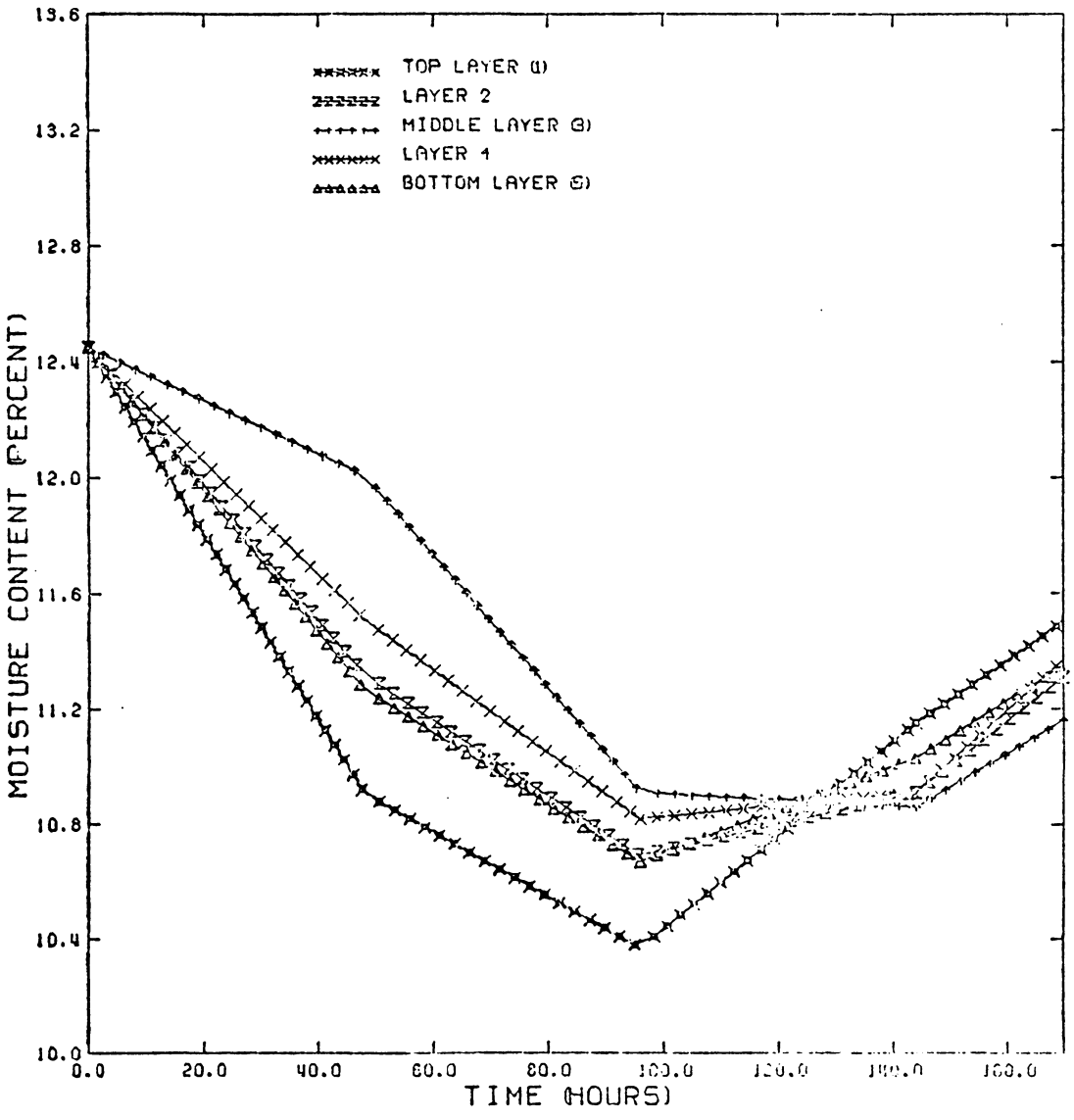

Figure 14 : Experimental moisture contents in the five layers during Test 3 at a wall distance of 8 inches. The curves indicates that the moisture contents in the surface layers are lower in desorption and higher in absorption than the values of the internal layers.

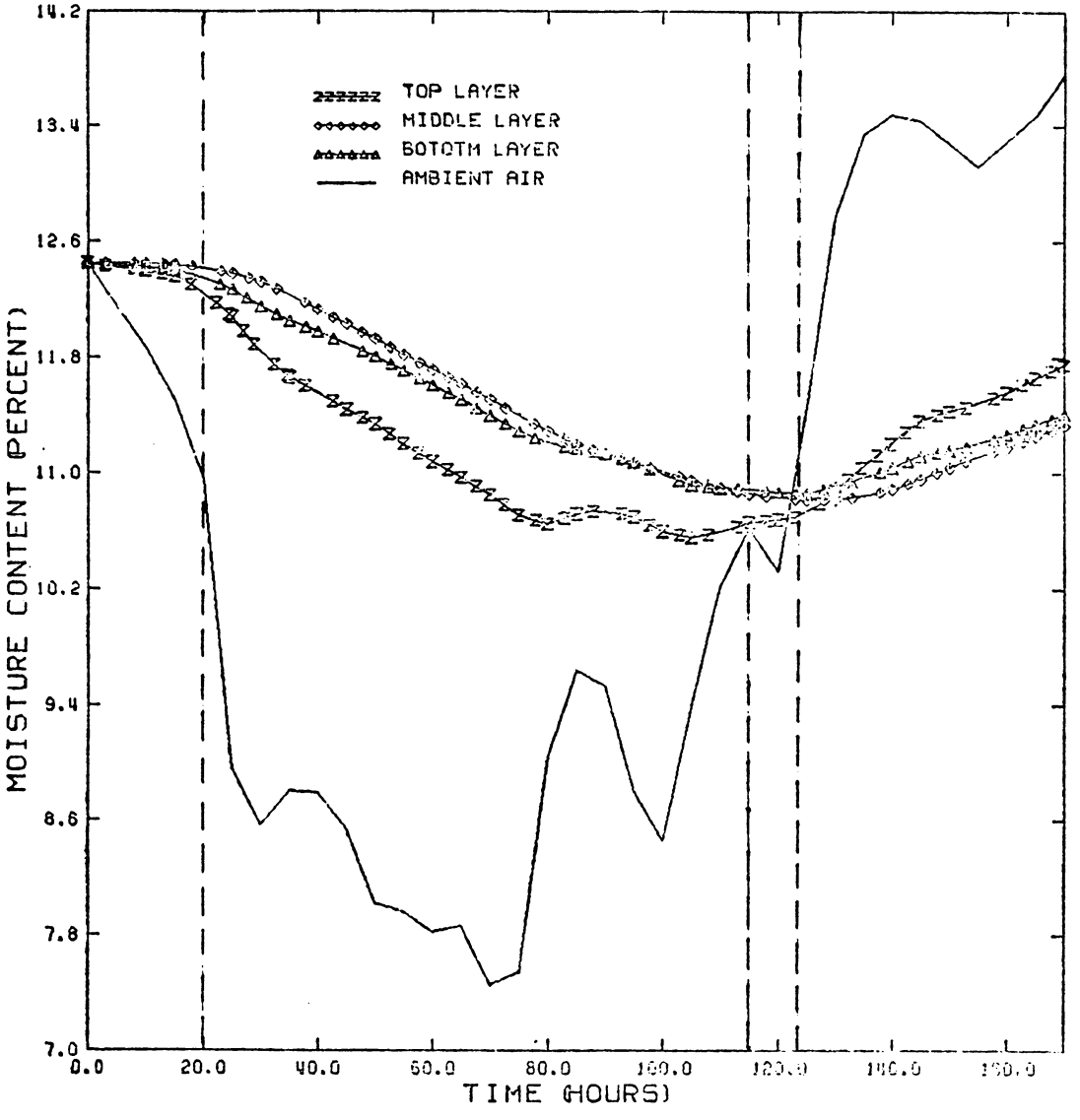

Figure 15 : Equilibrium moisture content and predicted moisture contents for the geometric mean model with a phase conversion factor of zero for a wall distance of 3 inches during Test 3. During the time of 0-20 hours : no change in in internal moisture occurs, 20-115 hours : the process of desorption occurs, 115-125 hours : moisture content is equal or near the equilibrium moisture content, and 125-170 hours : the process of absorption occurs.

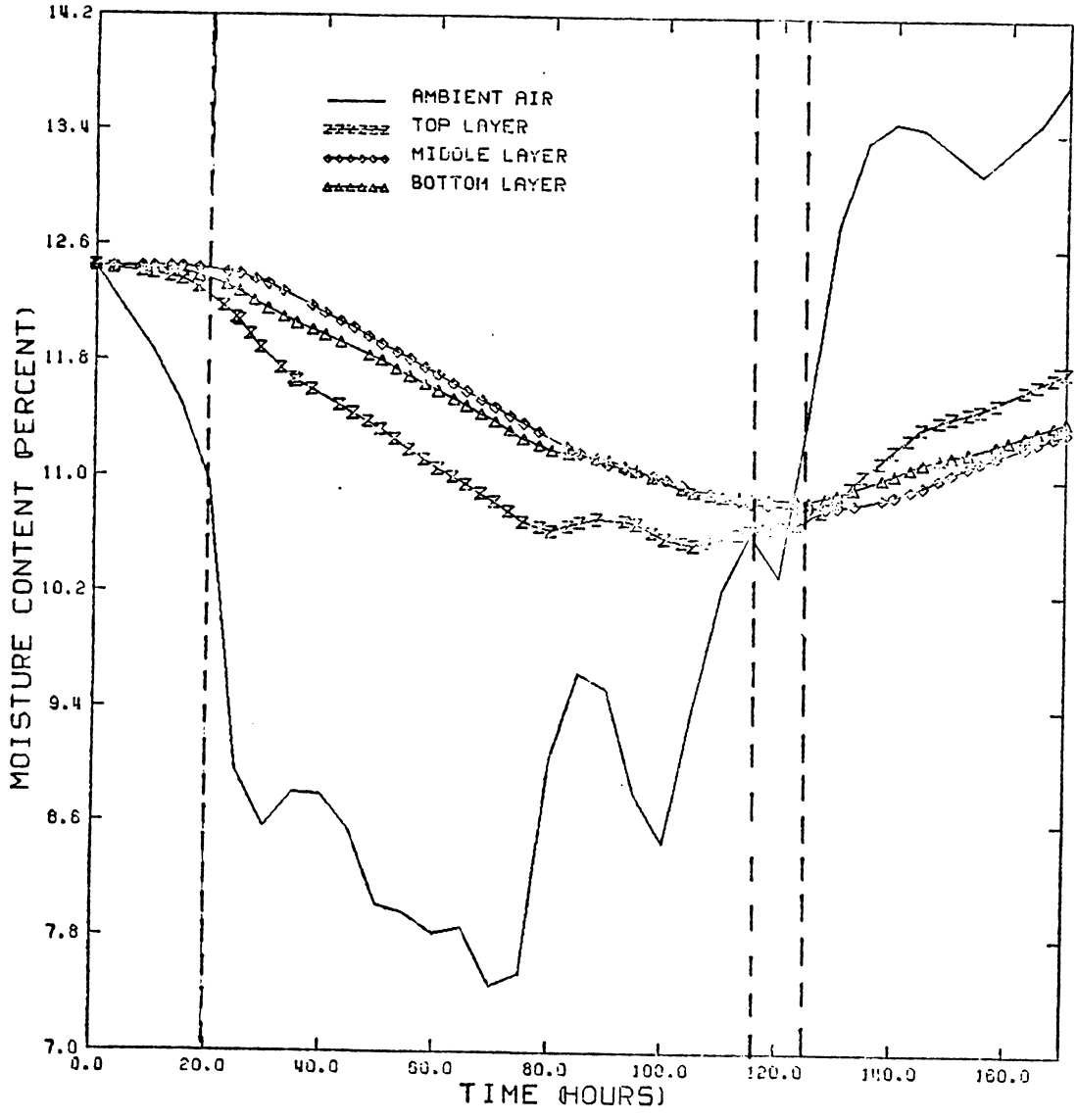

Figure 16 : Equilibrium moisture content and predicted moisture contents for the geometric mean model with a phase conversion factor of zero for a wall distance of 8 inches during Test 3. During the time of 0-20 hours : no change in in internal moisture occurs, 20-115 hours : the process of desorption occurs, 115-125 hours : moisture content is equal or near the equilibrium moisture content, and 125-170 hours : the process of absorption occurs.

air into the bin via convective heat transfer; then, the heat is spent to build a potential field for moisture migration by vaporizing the internal liquid moisture. Before the potential field has been constructed, the internal moisture flux is negligible.

2. 20 to 115 hours

It is known that vapor pressure is the chief driving force for moisture diffusion in the porous portion of the bin and the internal moisture gradient is the major motivation for the moisture migration in the solid portion of the bin. The internal moisture diffusion becomes important in the stored corn during this period. Corn loses moisture into the surrounding air during this time. This period will end when the corn moisture is equal or close to the equilibrium relative humidity of the surrounding air.

3. 115 to 125 hours

Although the moisture content of corn is almost equal to the equilibrium relative humidity of the ambient air during this period, this does not mean that internal moisture flux does not occur during this period. An observtion of the moisture curve indicates that the slope of the curve is still not equal to zero in this time interval; thus, the net moisture

change in the corn is still significant. The moisture transport phenomena illustrates that the driving forces of moisture migration are the moisture gradient and the temperature gradient. The gradient of vapor pressure, as a result of the temperature gradient, is another driving force for moisture migration. This phenomenon can not be described using the simple moisture diffusion theory; hence, the theory of coupled heat and mass transfer is adapted.

4. 125 hours to Termination

Due to rain, the equilibrium relative humidity of the environmental air is increased to break the equilibrium state. The equilibrium moisture gradient is again a significant driving force for moisture migration. Corn absorbs moisture from the ambient air due to the vapor pressure gradient and the equilibrium moisture gradient. Moisture condenses from vapor to liquid and releases the latent heat to increase the temperature of whole system.

By observing the relationships among the top, middle and bottom layers, one may conclude that the moisture content of the middle layer is higher than the moisture levels of the other layers in desorption, and lower than the other layers during the absorption period. If the moisture content of

middle layer is between the other layers (in Fig. 15 and 16), the process is in a transition period from absorption to desorption, or from desorption to absorption.

5.3 PARAMETER COMPARISON

Since the model is used to describe the storage behavior in a bulk of corn, the bulk properties of corn are needed. All physical properties except the moisture diffusivity and phase conversion factor were available for a bulk of corn in this study. Although a bulk moisture diffusivity has not been determined until now, a parametric value can be determined based on the moisture diffusivity of a kernel of corn, the molecular vapor diffusivity of an air and water vapor mixture, and the porosity in a bed of grain. The phase conversion factor can be determined experimentally or by a patameter study.

5.3.1 Moisture Diffusivity

The moisture diffusivity is one of the mechanisms which controls moisture migration. A high moisture diffusivity allows internal moisture flow to occur within the bin easily and fast, but the internal moisture gradient in the storage bin is lowered at the same time. A small internal moisture gradient can reduce the rate of internal moisture flow. The

favorable effect of increasing moisture diffusion due to the high moisture diffusivity always exceeds the negative influence of a reduced moisture flow rate which is caused by the low internal moisture gradient. Low moisture diffusivity generates a small internal moisture flow, but it amplifies the internal moisture gradient which can accelerate the rate of moisture migration inside the bin. However, a low moisture diffusivity is always accompanied by a low moisture flow. A possible bulk moisture diffusivity of the storage bin can be determined from the moisture diffusivity of a kernel of corn and the molecular diffusivity of air and vapor by using the appropriate mixing models which were discussed in the review of literature. The moisture diffusivity of a kernel of corn and the molecular diffusivity of the air and vapor mixture were determined by experiments.

5.3.2 Parallel Model

In the theory of parallel models, two paths for moisture movement are formed inside the bin: one is through air completely, and the other is through corn only. The calculated value of moisture diffusivity of the mixture is approximated as 0.34 ft^2/hr which is almost one half of the moisture diffusivity for a mixture of air and water vapor and significantly higher than the moisture diffusivity of a kernel of

corn, 0.00004 ft^2/hr. The mixing model yields a high bulk moisture diffusivity. High bulk moisture diffusivity indicates that most moisture fluxes flow through the air path. Since the state of moisture occupying the porous regions of the bin is vapor, it is concluded that the value of the phase conversion factor should be close or equal to one, but Figure 17 illustrates that the moisture distributions are independent of the phase conversion factors. The high moisture diffusivity reduces the resistance for internal moisture removal. Figure 18 illustrates the dependence of the predicted moisture distributions on the relative humidity of the ambient air. Uniform moisture distribution is a result of the high bulk moisture diffusivity in Fig. 18. In other words, almost no moisture gradient exists inside the bin. Figure 18 also shows that the predicted moisture contents in the surface layers are usually higher, and the internal predicted results are lower than the experimental values in a desorption process. For an absorption process, a reverse transport phenomenon exists when the predicted data are compared with the experimental results. Figure 19 illustrates that the temperature distributions in the top layer at a wall distance of 8 inches are influenced by the phase conversion factors. A lower phase conversion factor(ε) is accompanied by a more accurate predicted temperature distribu-

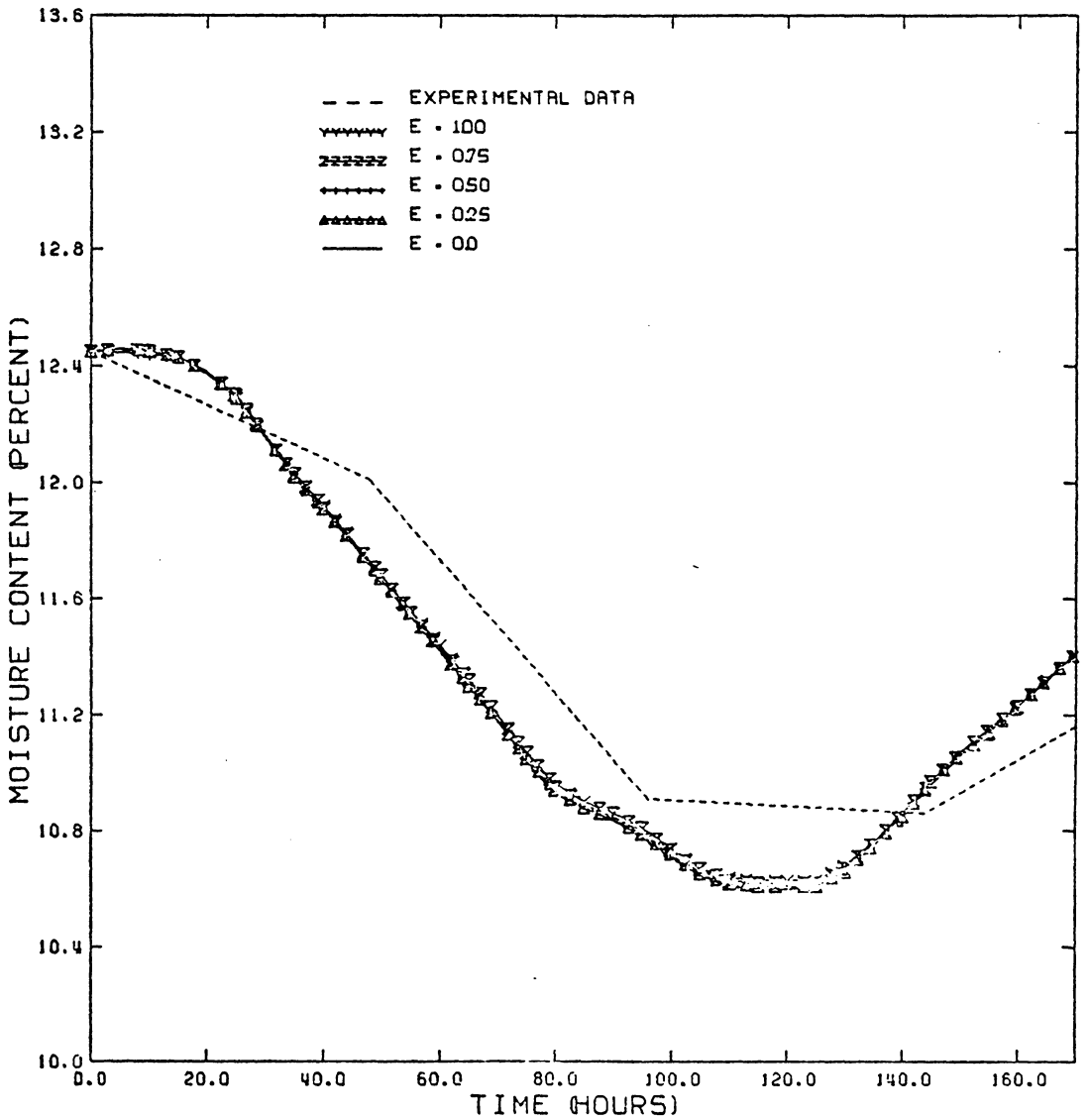

Figure 17 : Experimental and predicted moisture contents in the middle layer at a wall distance of 8 inches using the parallel model and five phase conversion factors for Test 3. It is obvious from this figure that moisture content is independent of the phase conversion factor.

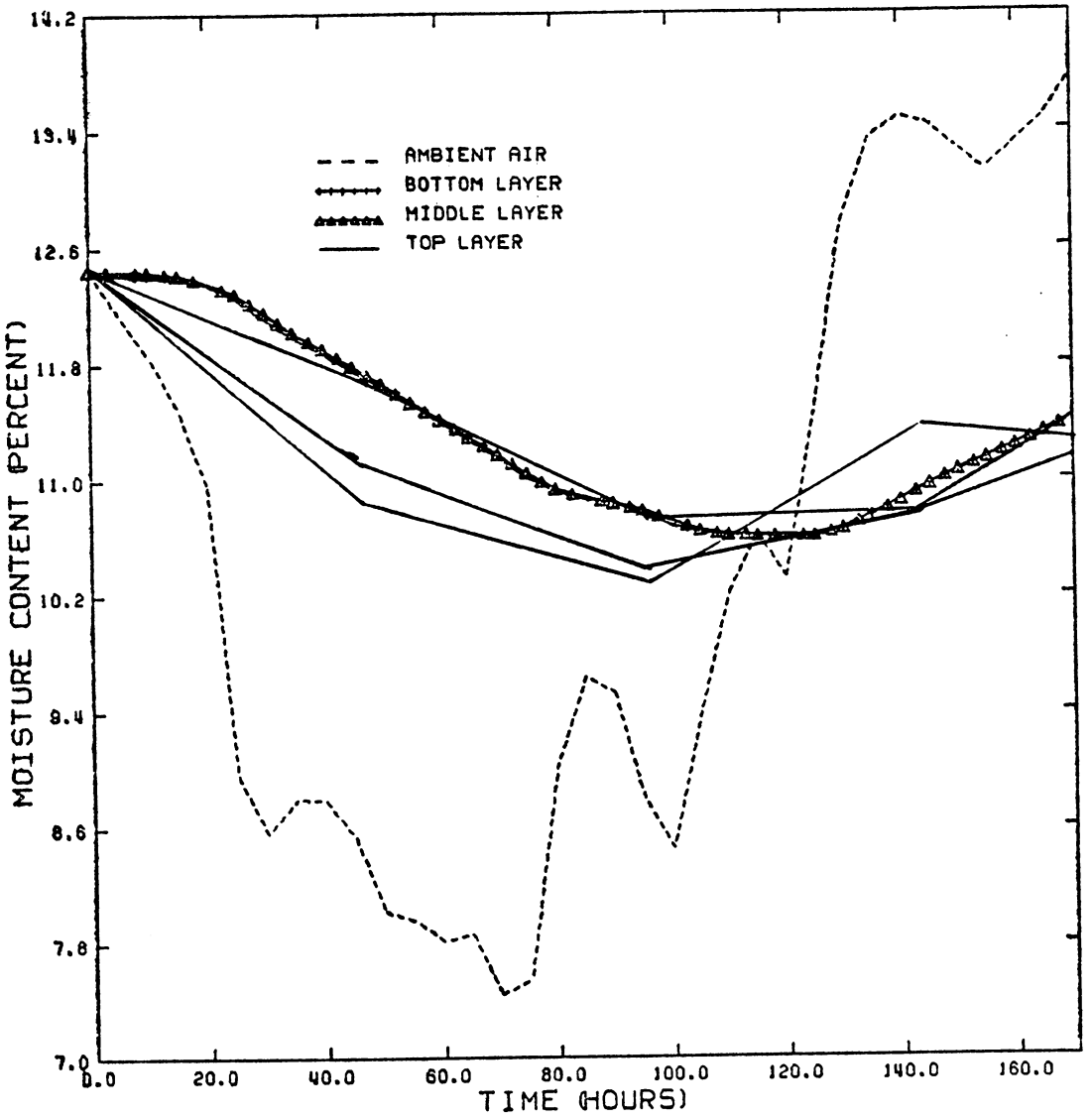

Figure 18 : Equilibrium moisture content and predicted moisture contents for the parallel model with a phase conversion factor of 0.25 for a wall distance of 3 inches during Test 3. The figure indicates that the predicted moisture distributions are homogeneous throughout the bin.

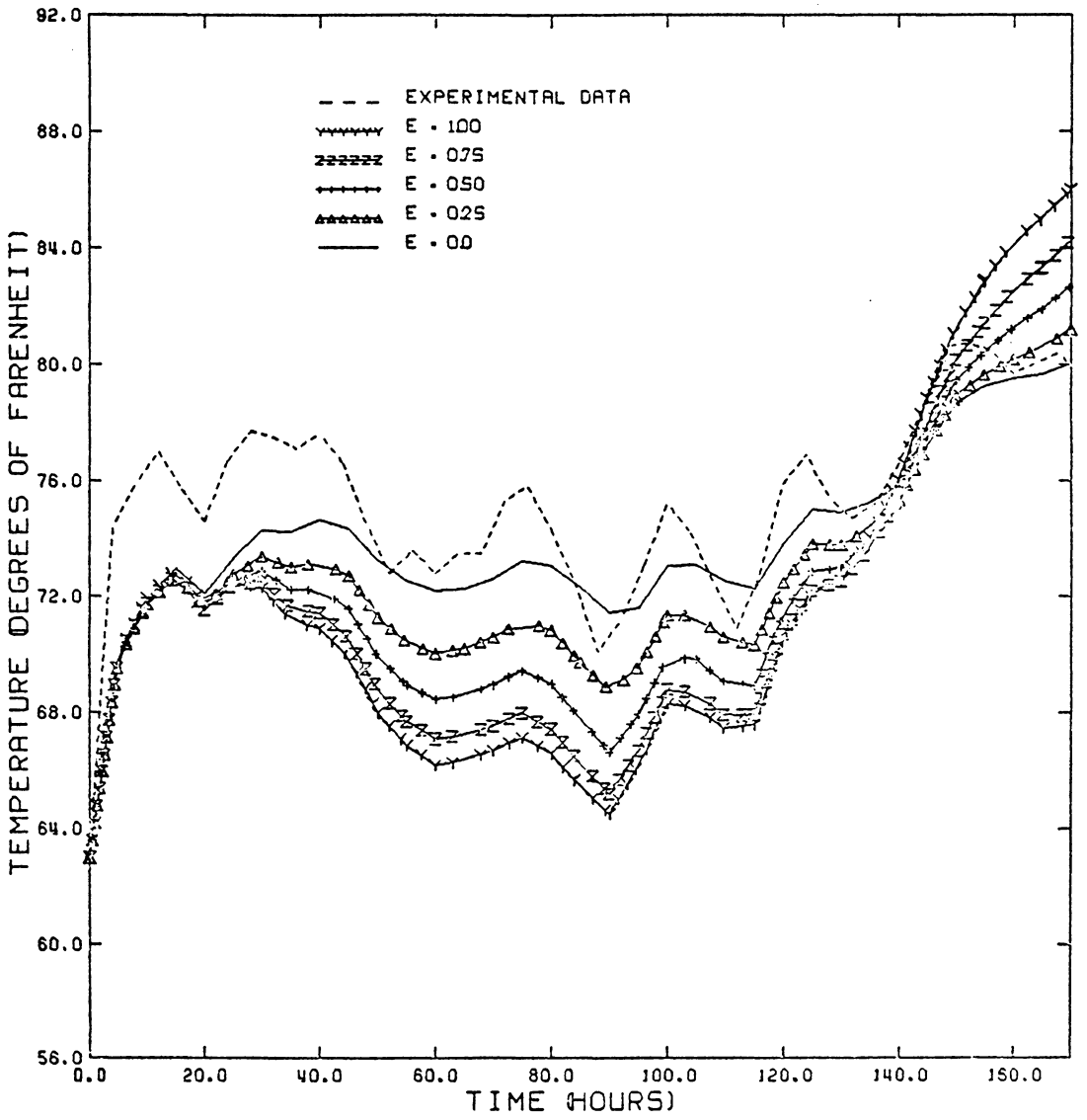

Figure 19 : Experimental and predicted temperatures in the top layer at a wall distance of 8 inches using the parallel model and five phase conversion factors for Test 3. It is obvious from this figure that temperature is highly related to the phase conversion factor.

tion. Figure 20 indicates that the change in the predicted temperature coincides with the changes in the ambient air temperature. Figure 21 to 24 illustrate that most of the predicted temperatures are lower in desorption and higher in absorption when compared to the actual data and may have been caused by: (1) underestimating the convective heat transfer coefficient, or (2) improperly neglecting conductive heat flow on the interface between the wall of the bin and the surrounding air.

5.3.3 Series Model

A series model has a relatively low value for the moisture diffusivity of the system, 0.0004 ft^2/hr, which is ten times the moisture diffusivity of corn and a one-thousandth of the molecular diffusivity of a air and vapor mixture. By the mechanism of moisture convection, the surface corn releases its moisture to the surrounding air, and a portion of the moisture loss in the surface corn should be supplied from the interior corn. A low bulk moisture diffusivity increases the internal resistance for moisture movement. From Figures 25 to 30, it is suggested that the rates of moisture migration on the surface elements are higher for the series model than for the other models because of the shortage of the internal moisture flow. The internal moisture content

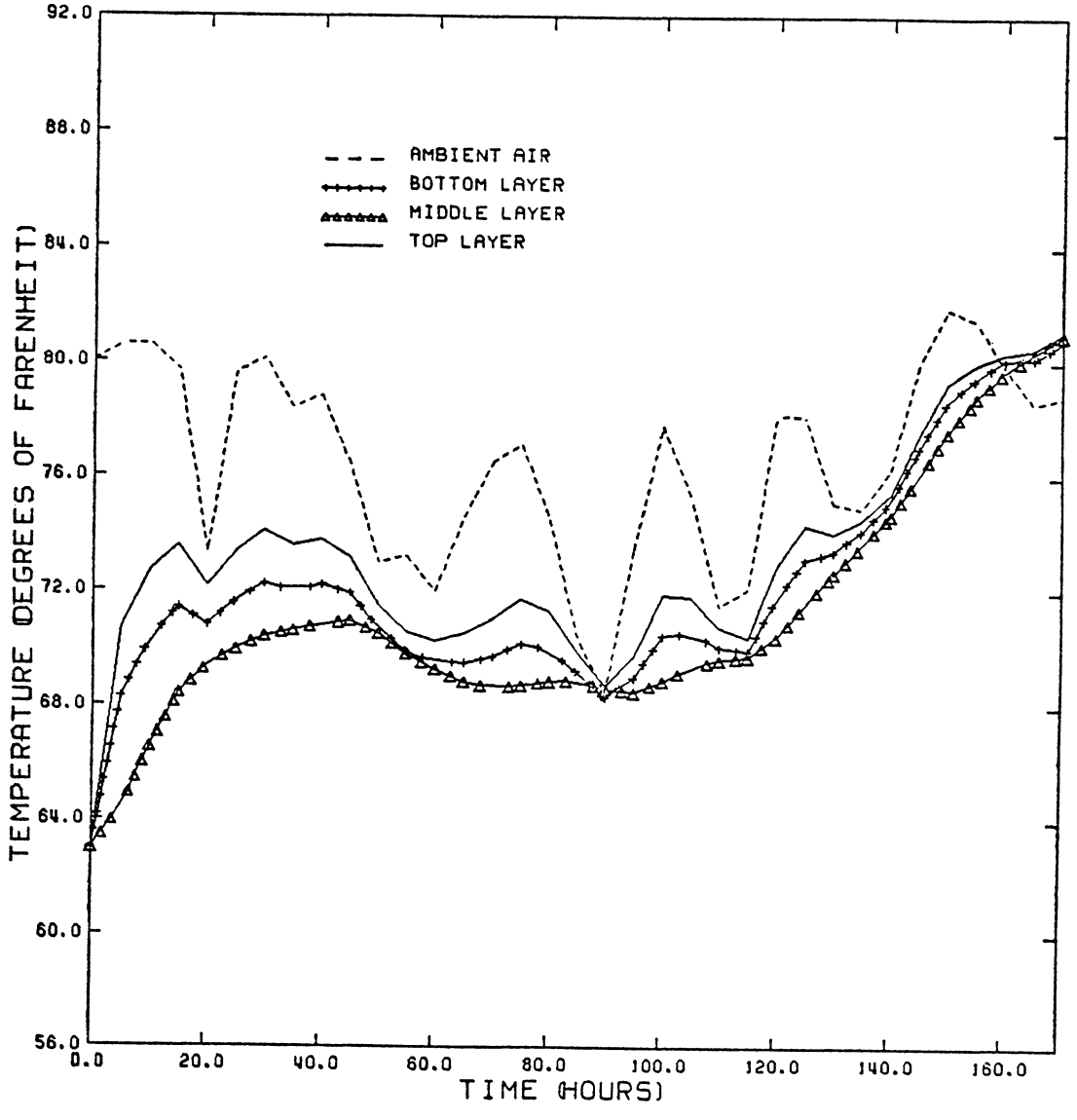

Figure 20 : Ambient and predicted temperatures at a wall distance of 3 inches using the parallel model with a phase conversion factor of 0.25 for Test 3. The figure indicates that the change of the predicted temperature is coincident with the change of ambient ait temperature.

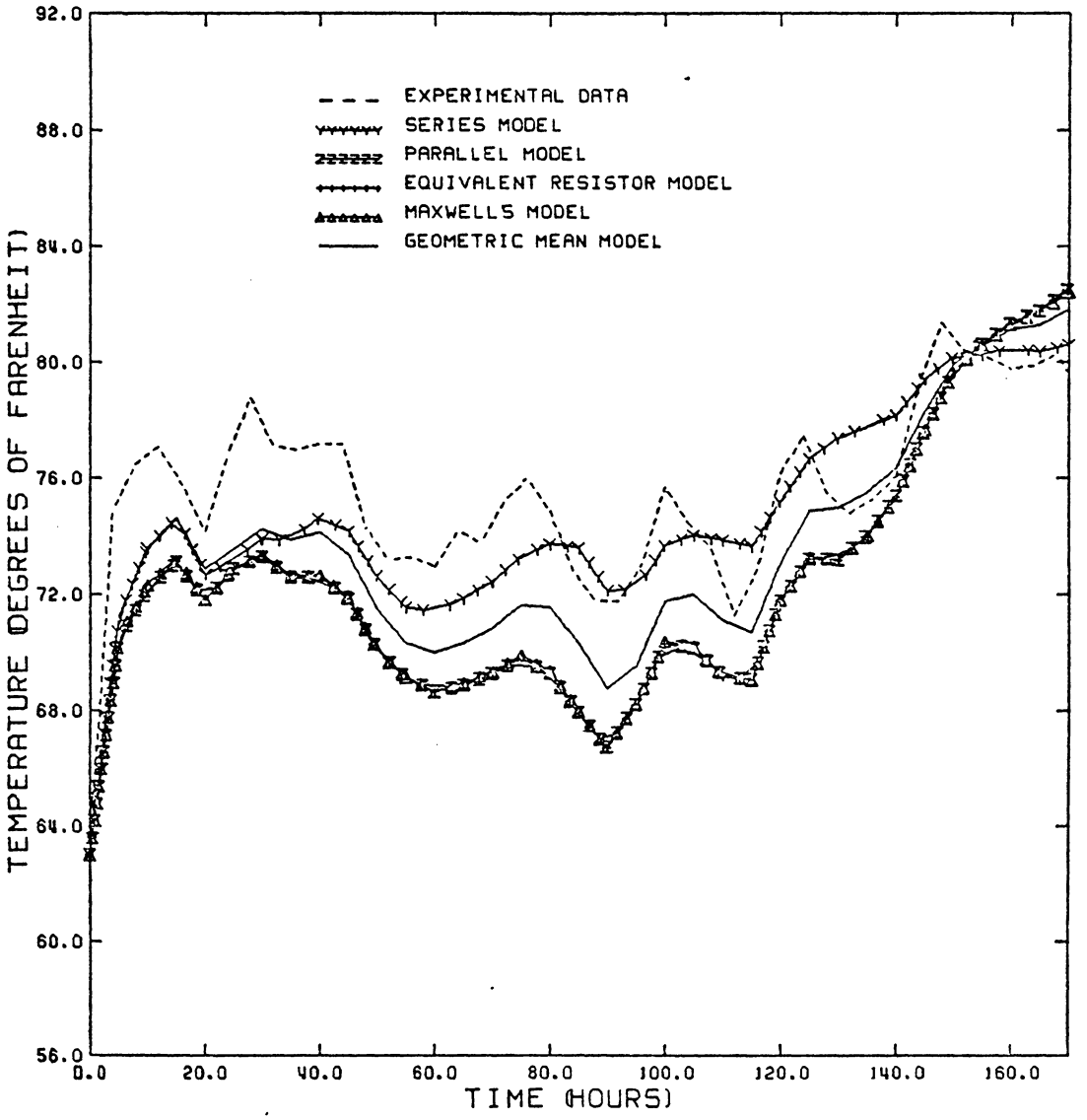

Figure 21 : Experimental and predicted temperatures in the top layer at a wall distance of 3 inches using five mixing models with a phase conversion factor of 0.50. The series model has the best predicted temperature when compared with the actual temperature.

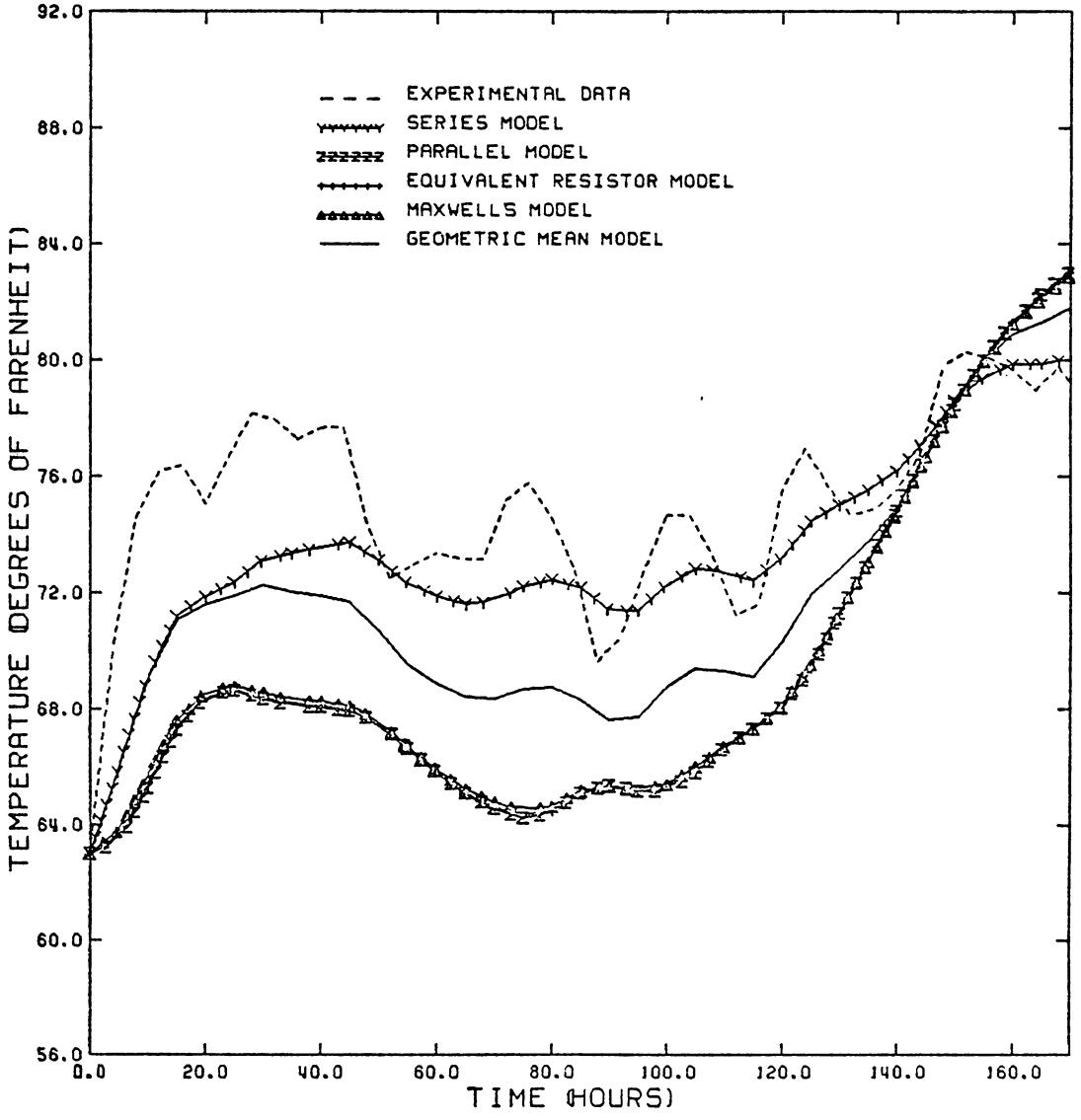

Figure 22 : Experimental and predicted temperatures in the middle layer at a wall distance of 3 inches using five mixing models with a phase conversion factor of 0.50. The series model has the best predicted temperature when compared with the actual temperature.

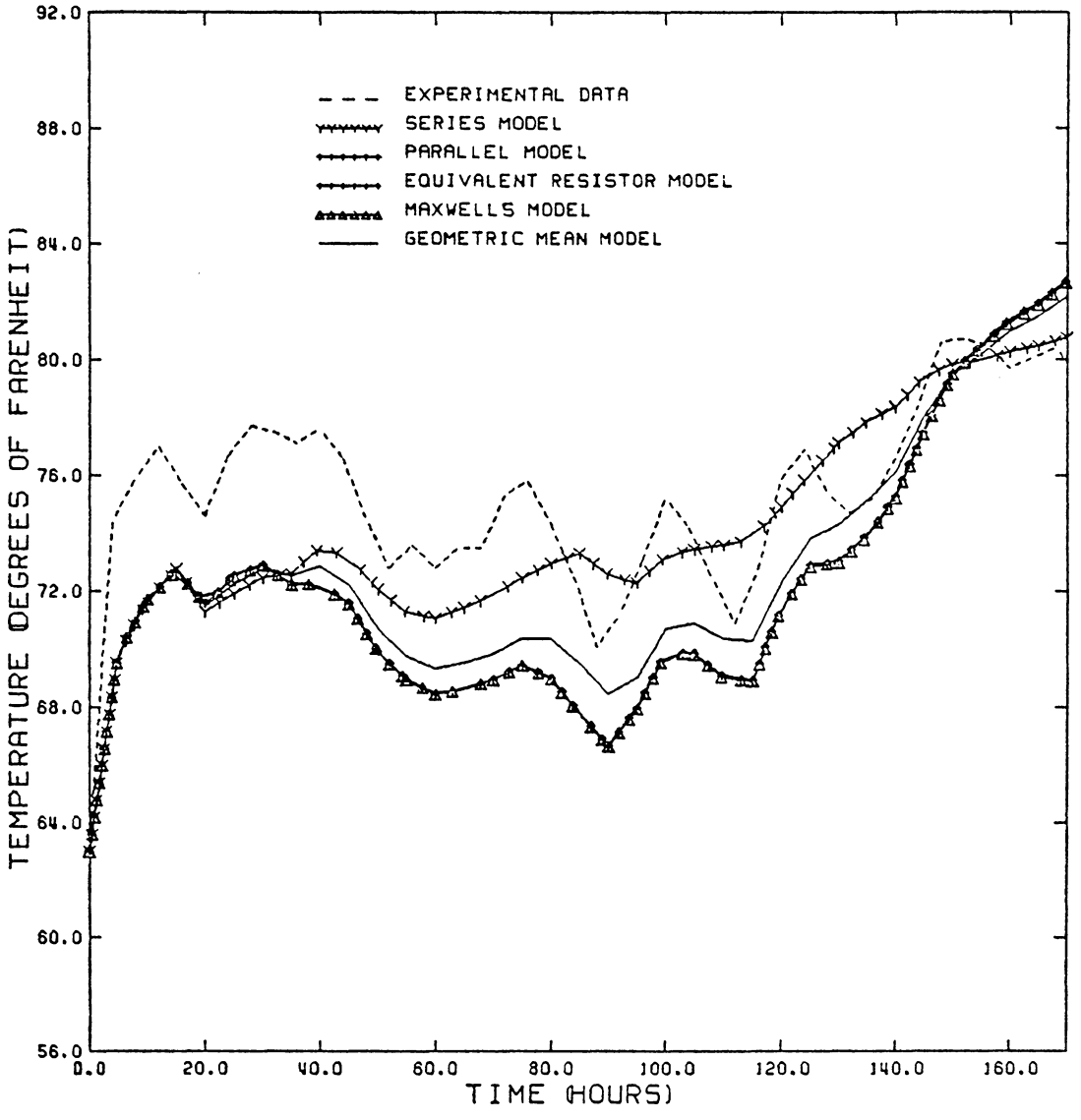

Figure 23 : Experimental and predicted temperatures in the top layer at a wall distance of 8 inches using five mixing models with a phase conversion factor of 0.50. The series model has the best predicted temperature when compared with the actual temperature.

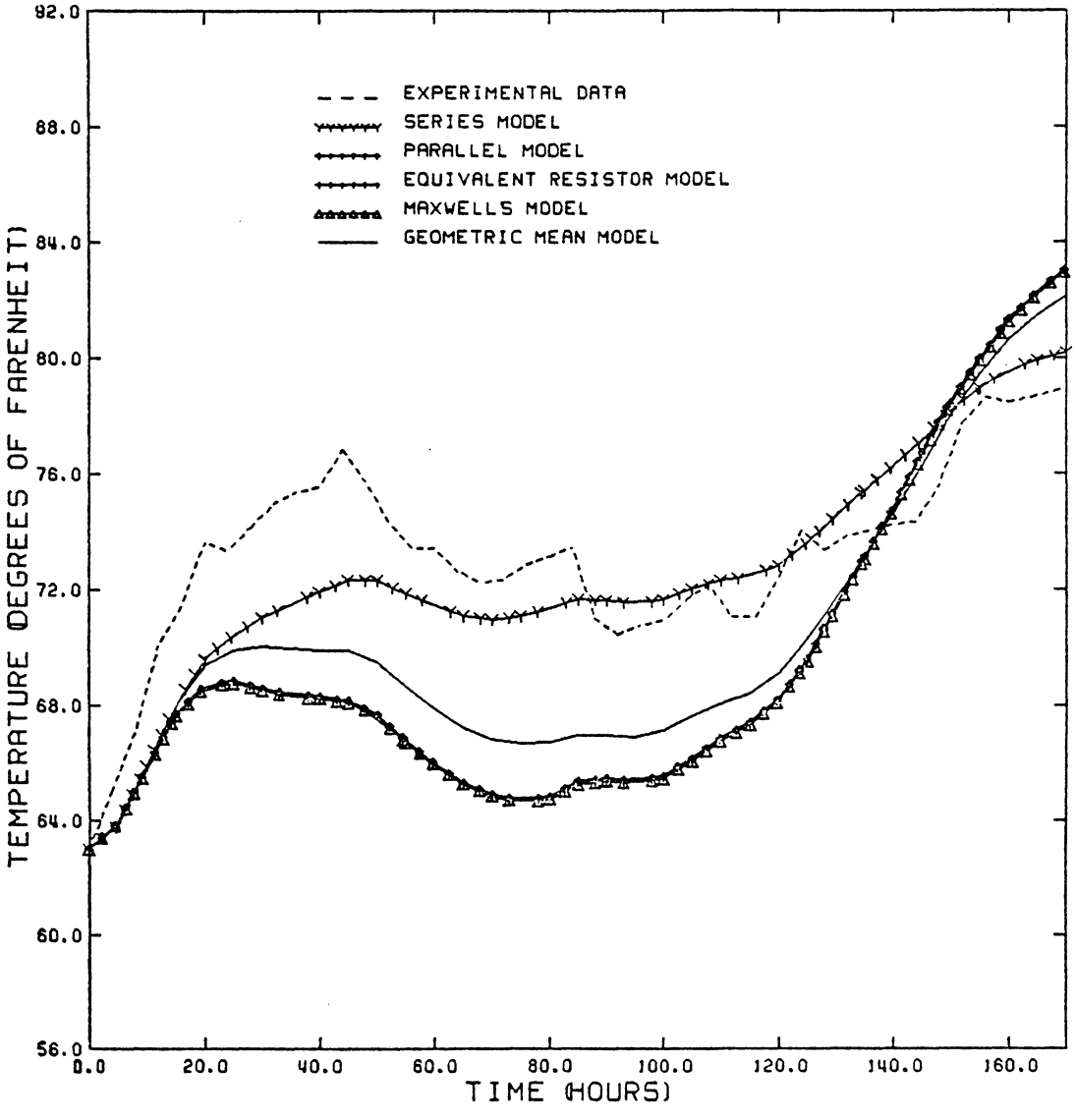

Figure 24 : Experimental and predicted temperatures in the middle layer at a wall distance of 8 inches using five mixing models with a phase conversion factor of 0.50. The series model has the best predicted temperature when compared with the actual temperature.

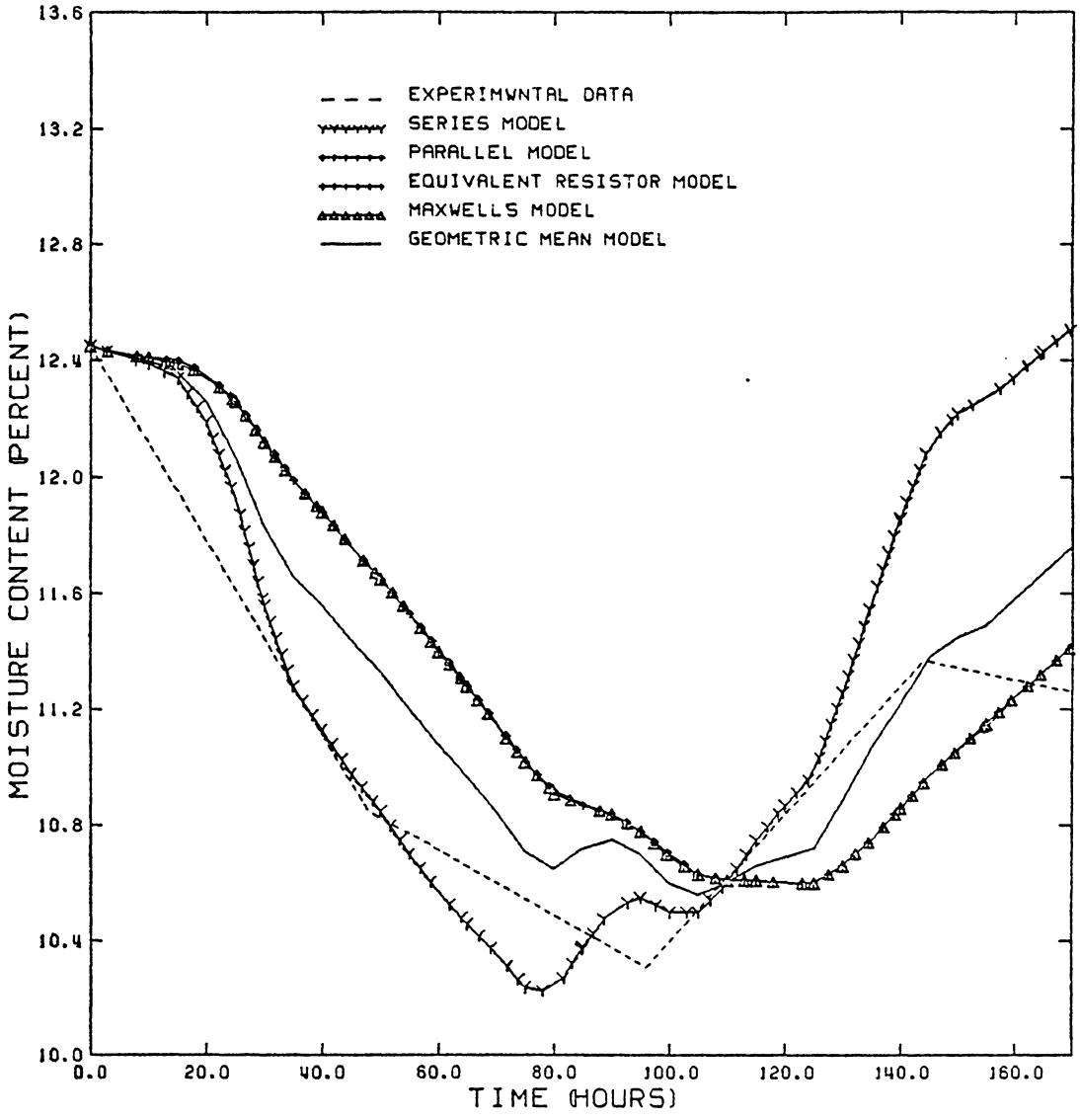

Figure 25 : Experimental and predicted moisture contents in the top layer at a wall distance of 3 inches using five mixing models with a phase conversion factor of 0.50. The series model has the best predicted moisture content in desorption and the geometric mean model has the best predicted moisture content in absorption.

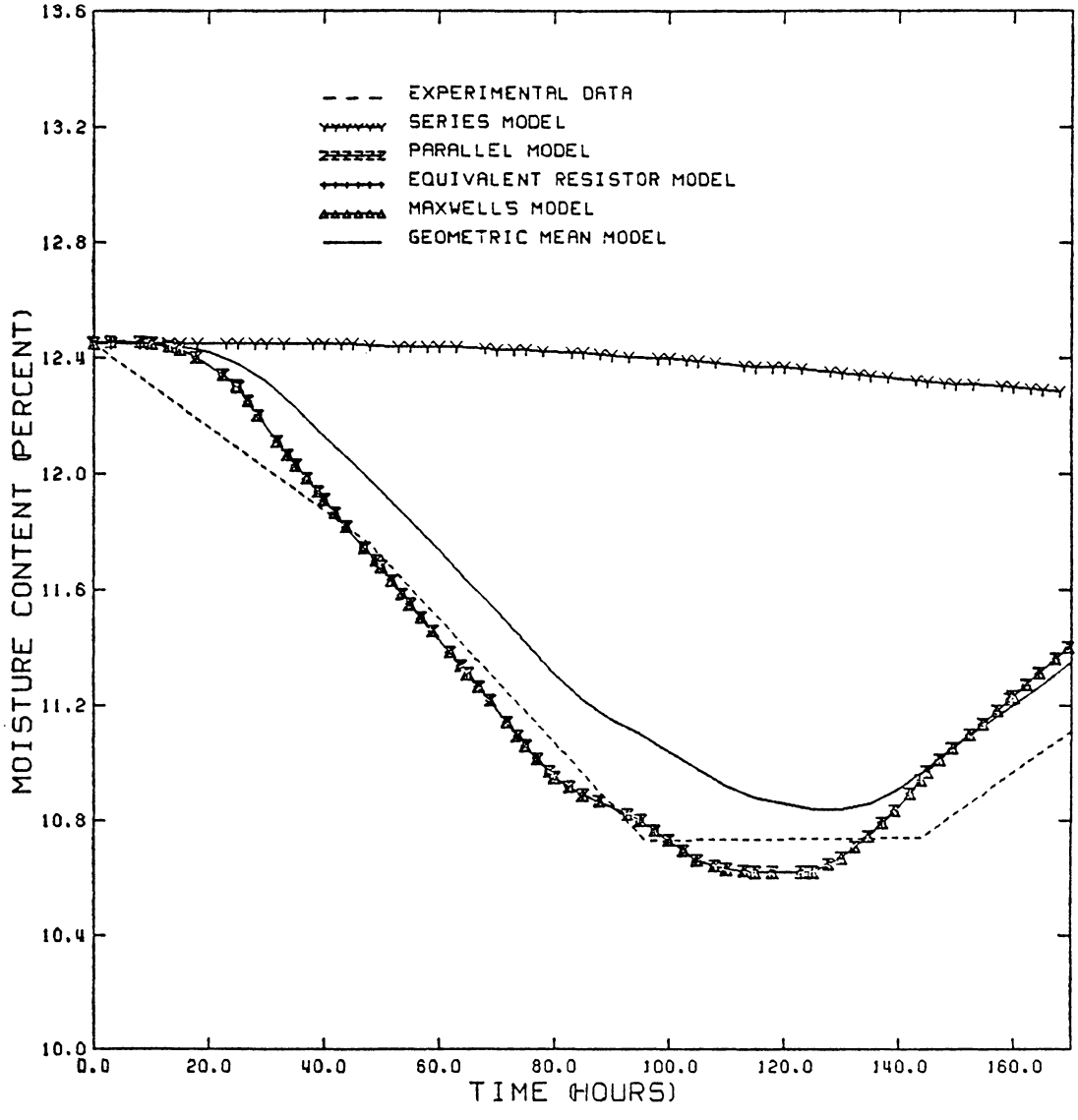

Figure 26 : Experimental and predicted moisture contents in the middle layer at a wall distance of 3 inches using five mixing models with a phase conversion factor of 0.50. The parallel model has the best predicted moisture content when compared with the actual moisture content.

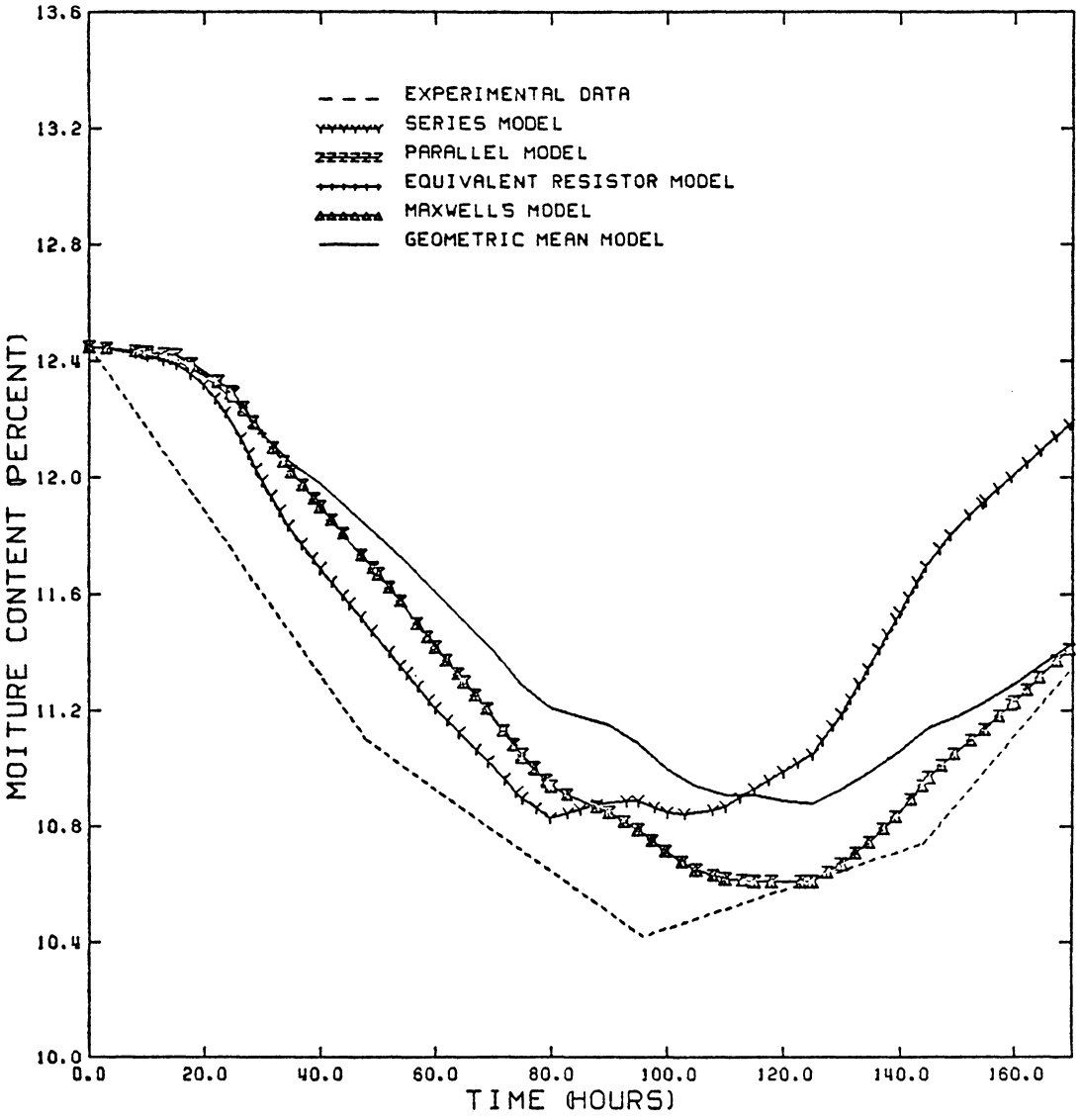

Figure 27 : Experimental and predicted moisture contents in the bottom layer at a wall distance of 3 inches using five mixing models with a phase conversion factor of 0.50. The series model has the best predicted moisture content during desorption and the parallel model has the best predicted moisture content during absorption.

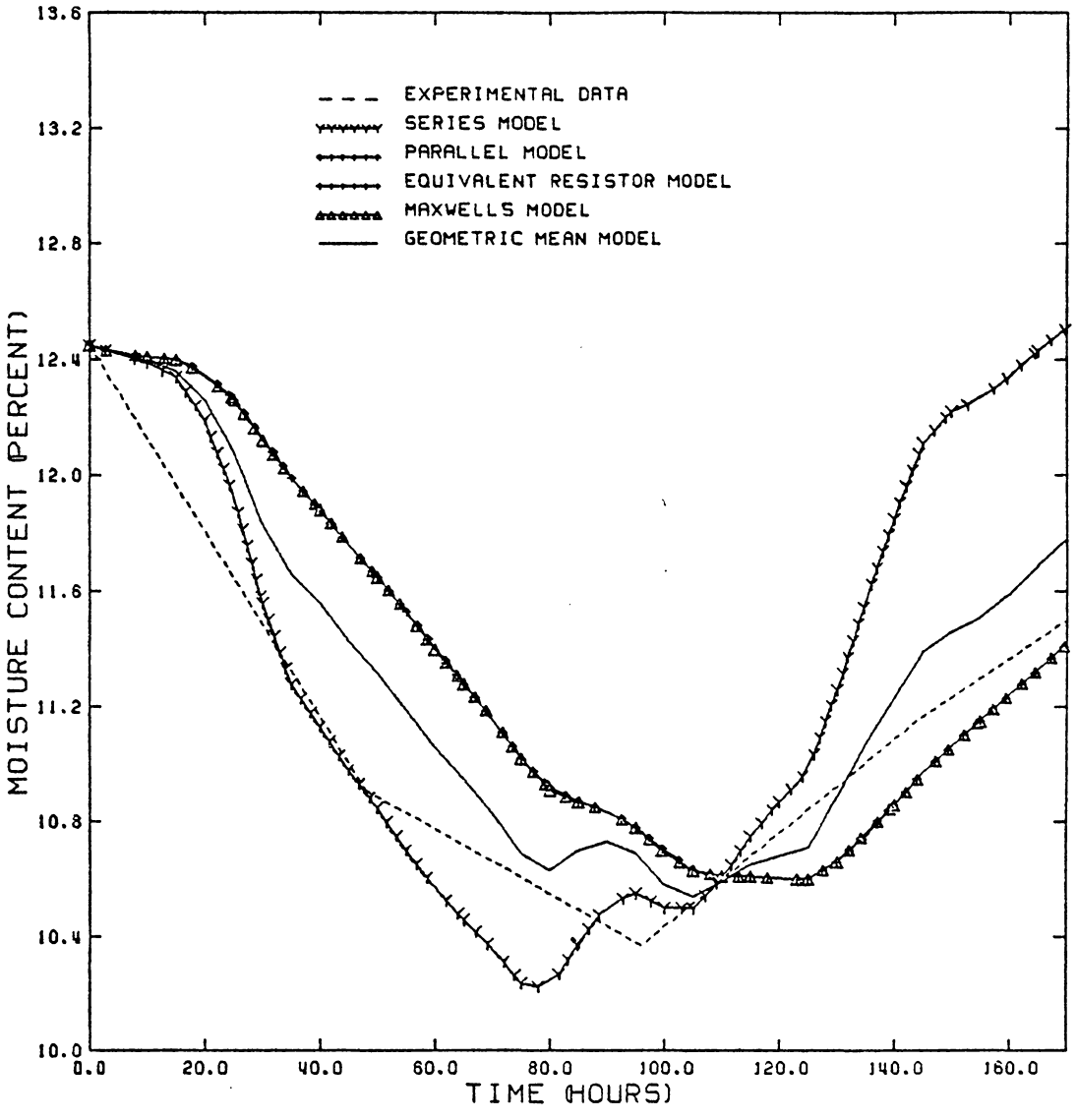

Figure 28 : Experimental and predicted moisture contents in the top layer at a wall distance of 8 inches using five mixing models with a phase conversion factor of 0.50. The geometric mean model has the best predicted moisture content when compared with the actual moisture content.

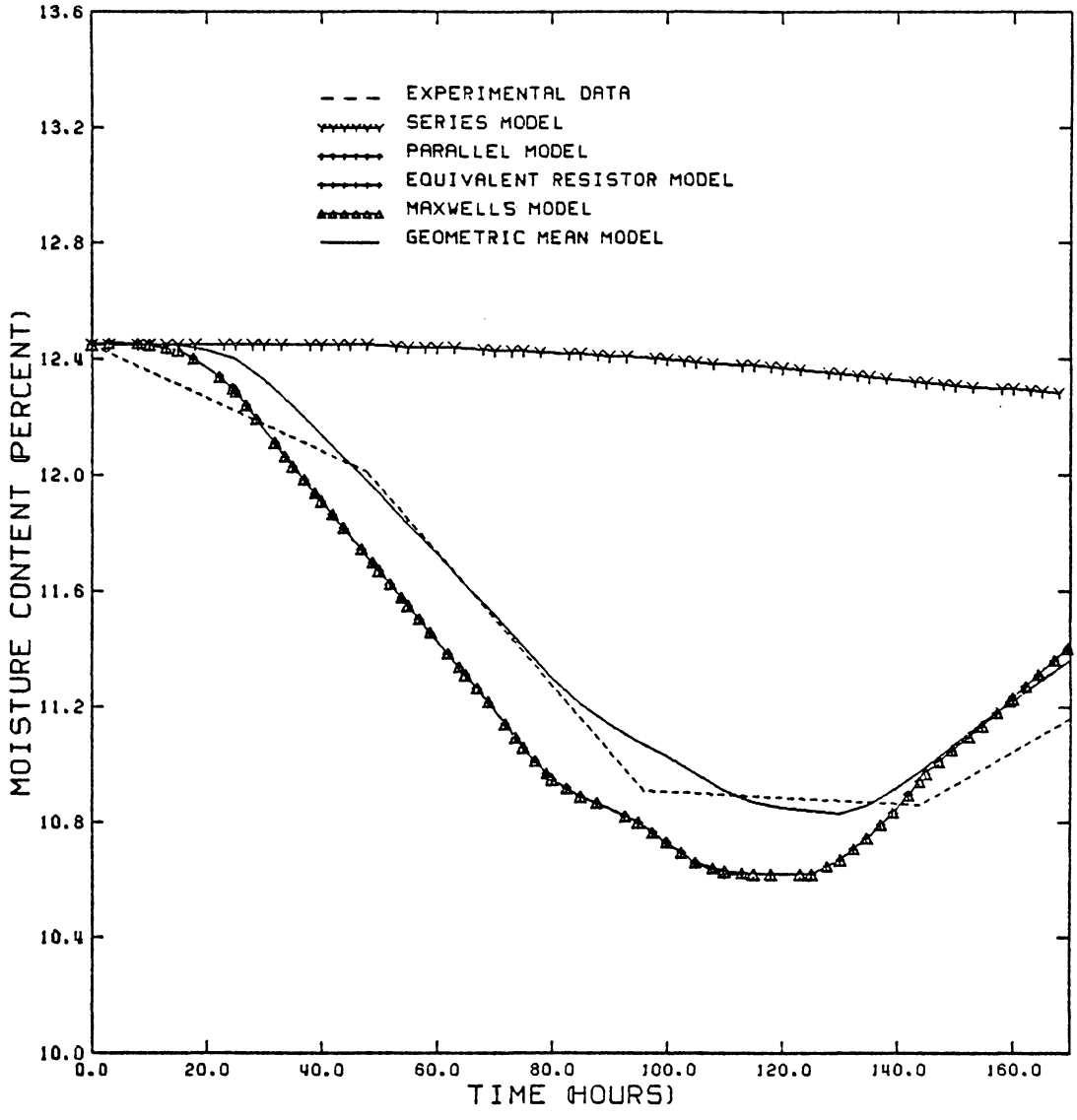

Figure 29 : Experimental and predicted moisture contents in the middle layer at a wall distance of 8 inches using five mixing models with a phase conversion factor of 0.50. The geometric mean model has the best predicted moisture content when compared with the actual moisture content.

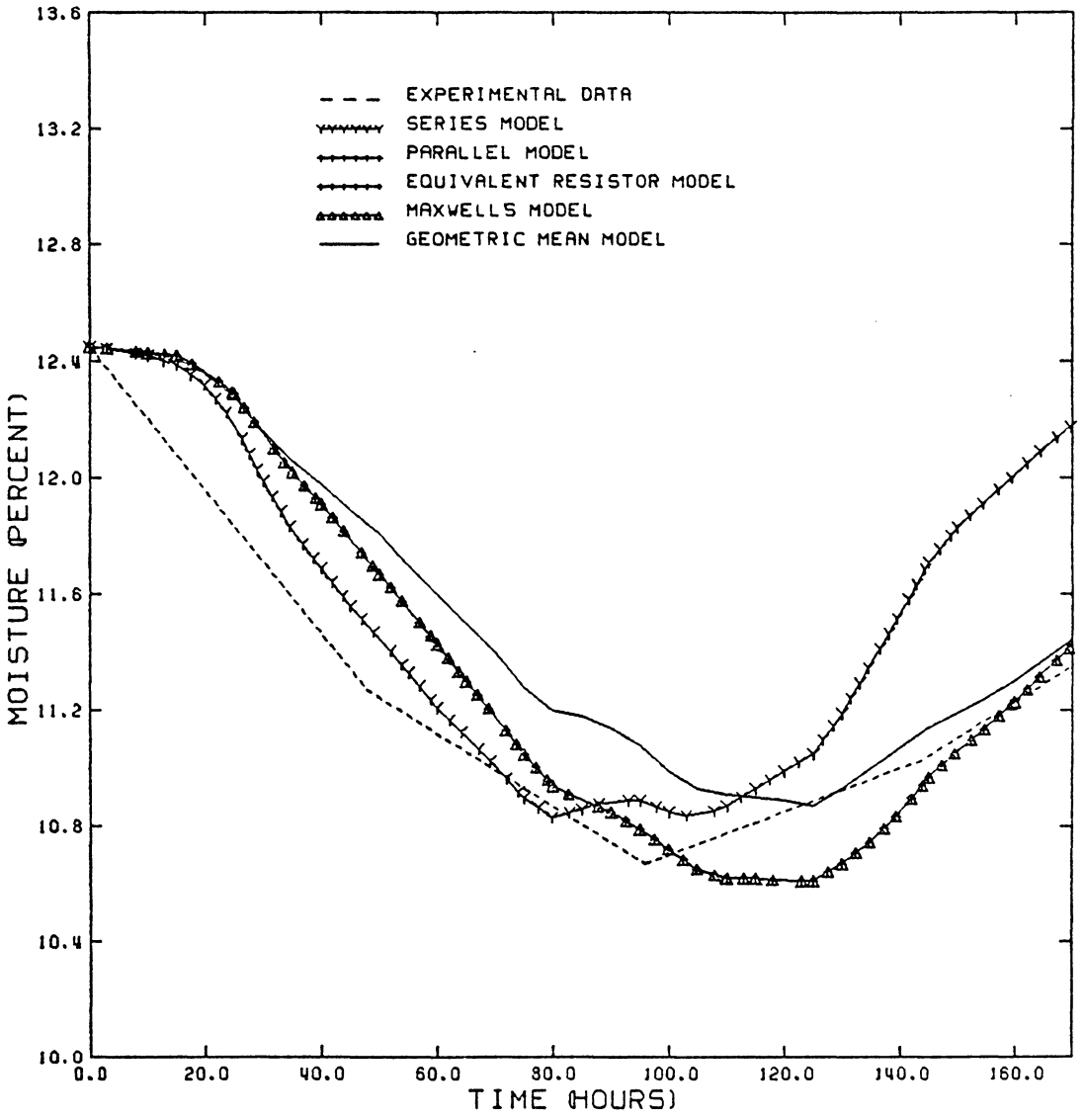

Figure 30 : Experimental and predicted moisture contents in the bottom layer at a wall distance of 8 inches using five mixing models with a phase conversion factor of 0.50. The series model has the best predicted moisture content during desorption and the geometric mean model has the best predicted values during absorption.

for the series model is stable regardless of what happens at the surface. The figures also show that the predicted moisture contents in the surface elements are higher in a absorption and lower in a desorption when compared to the actual data and the moisture of the interior layer is always much higher than the experimental results. Figure 31 indicates the predicted moisture contents of the top and bottom layers at a wall distance of 3 inches are very sensitive to the equilibrium moisture content. Figure 32 points out that the net simulated moisture changes in the middle layer at a wall distance of 8 inches is less than 0.2% through the whole process. Due to the stable moisture content within the interior of the bin, the predicted temperature distribution inside the bin can be explained using Fourier's heat diffusion law and the second law of thermodynamics. The predicted temperature distribution at a wall distance of 3 inches(Fig. 33) is rather uniform because the thermal diffusivity is almost a hundred times the bulk moisture diffusivity. It is realized that moisture change is accompanied with temperature change. The temperature changes in the surface elements are more fluctuant than the changes within the interior layers of the bin, because the surface moisture flux is much larger than the internal moisture flux for the series model. A high phase conversion factor is proposed

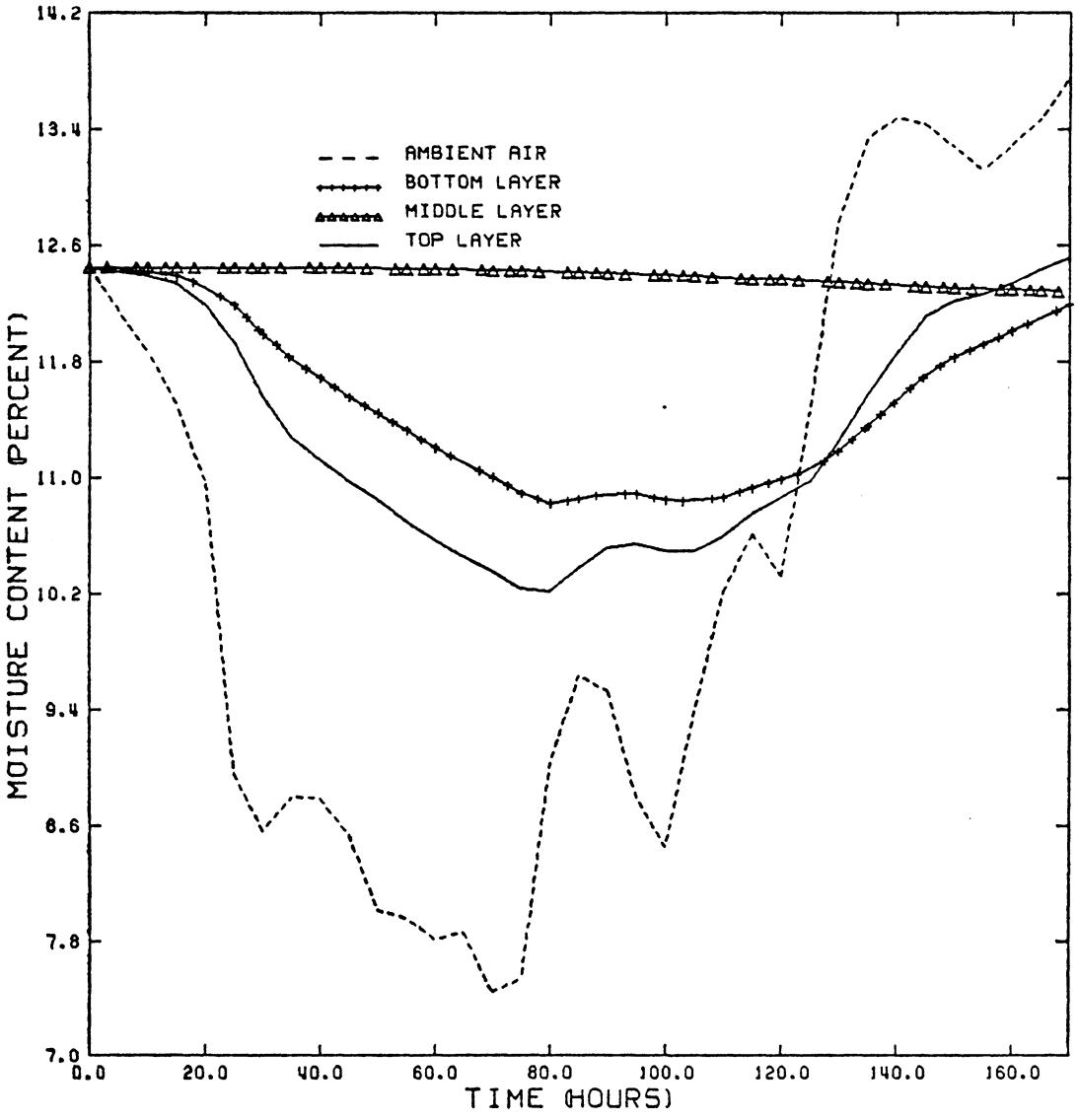

Figure 31 : Equilibrium moisture content and predicted moisture contents for the series model with a phase conversion factor of 0.25 for a wall distance of 3 inches during Test 3. Illustrated are the moisture contents in the surface layers are sensitive to the equilibrium moisture content of ambient air.

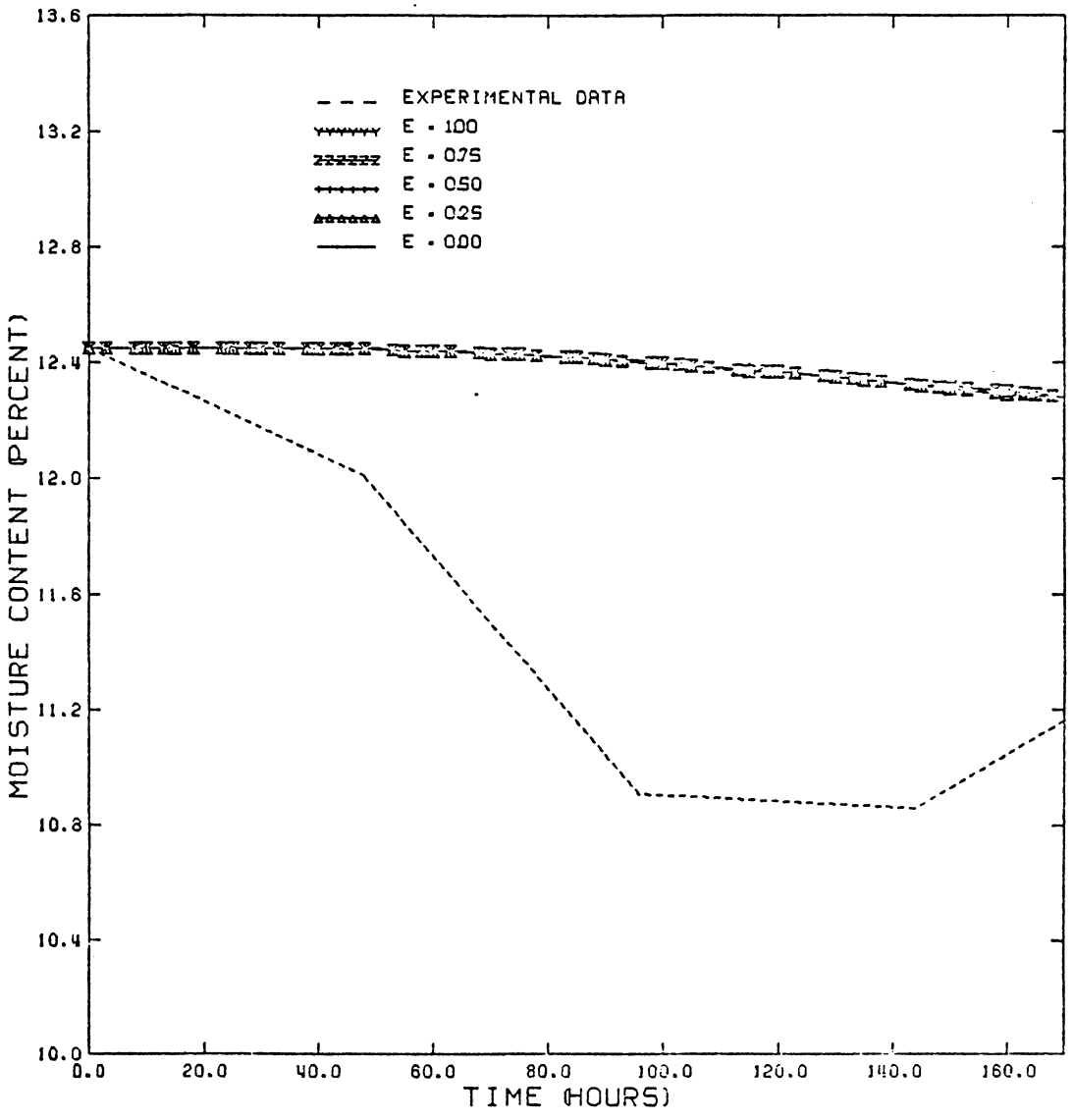

Figure 32 : Experimental and predicted moisture contents in the middle layer at a wall distance of 8 inches using the series model and five phase conversion factors for Test 3. It is obvious from this figure that moisture content is independent of the phase conversion factor, and internal moisture content is constant.

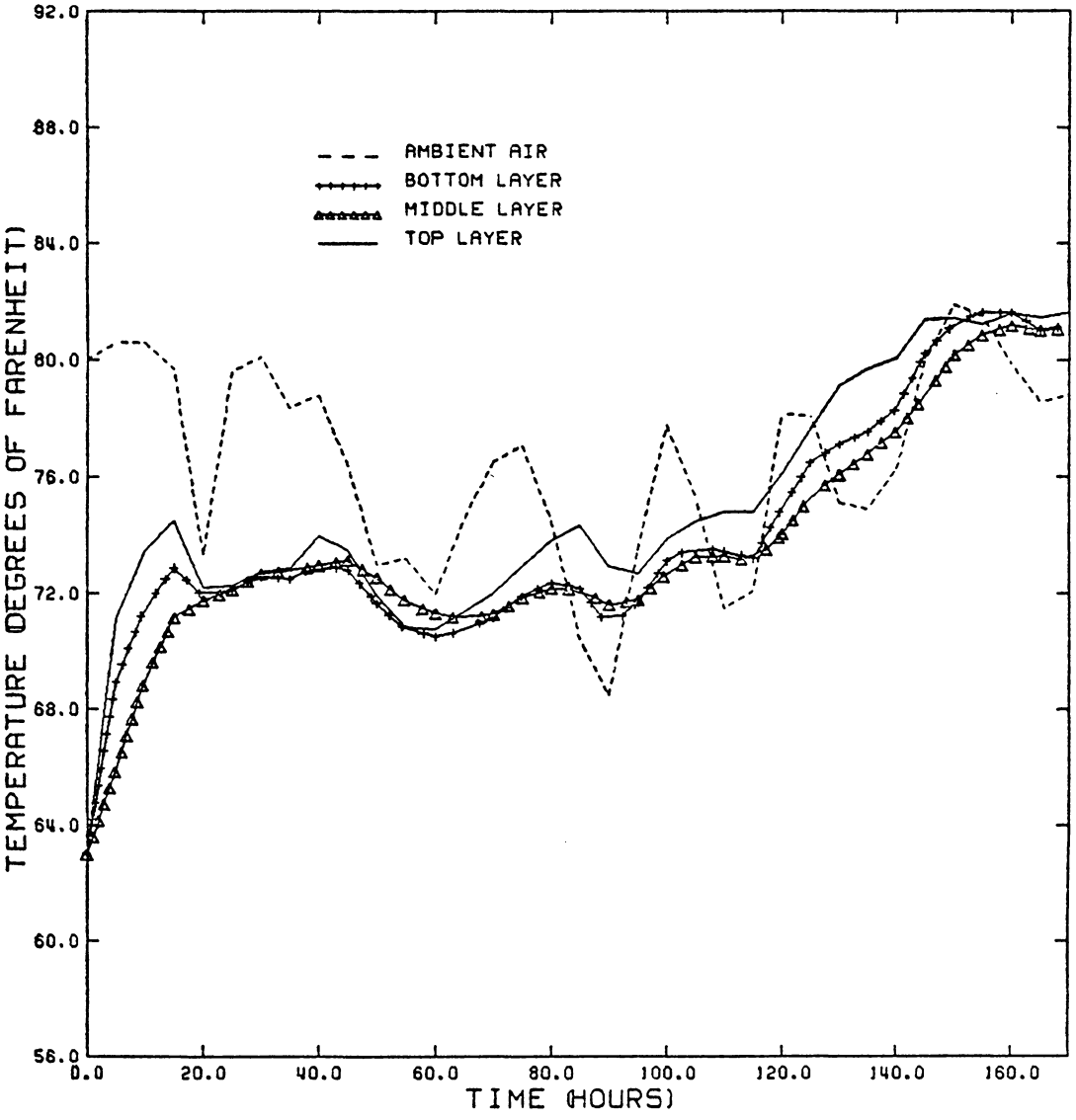

Figure 33 : Ambient and predicted temperatures at a wall distance of 3 inches using the series model with a phase conversion factor of 0.25 for Test 3. The figure indicates that the change of the predicted temperature is coincident with the change of ambient air temperature.

due to the low moisture diffusivity. Figure 34 illustrates that the predicted moisture contents of the surface layers at a wall distance of 8 inches are dependent only on convective moisture transfer, are not related to the phase conversion factor because the amount of the internal moisture flow is insignificant. Figure 35 indicates that the predicted temperature distributions of the middle layer at a wall distance of 3 inches are changed very little with different phase conversion factors. It is still concluded that a high phase conversion factor is acceptable for the series model is illustrated in Figure 35.

5.3.4 Modified Maxwell Model

The moisture diffusivity used for this model is approximately 0.26 ft^2/hr, which is close to the bulk moisture diffusivity in the parallel model. As a consequence, the transport behavior for a modified Maxwell model is almost identical to that of the the parallel model. Figures 36 to 38 illustrate the same predicted moisture distributions at a wall distance of 3 inches for the top, middle and bottom layers respectively as in the parallel model, and Figures 39 and 40 exhibit that a small variance exists between the predicted temperatures at a wall distance of 3 inches for the top and middle layers when comparing the modified Max-

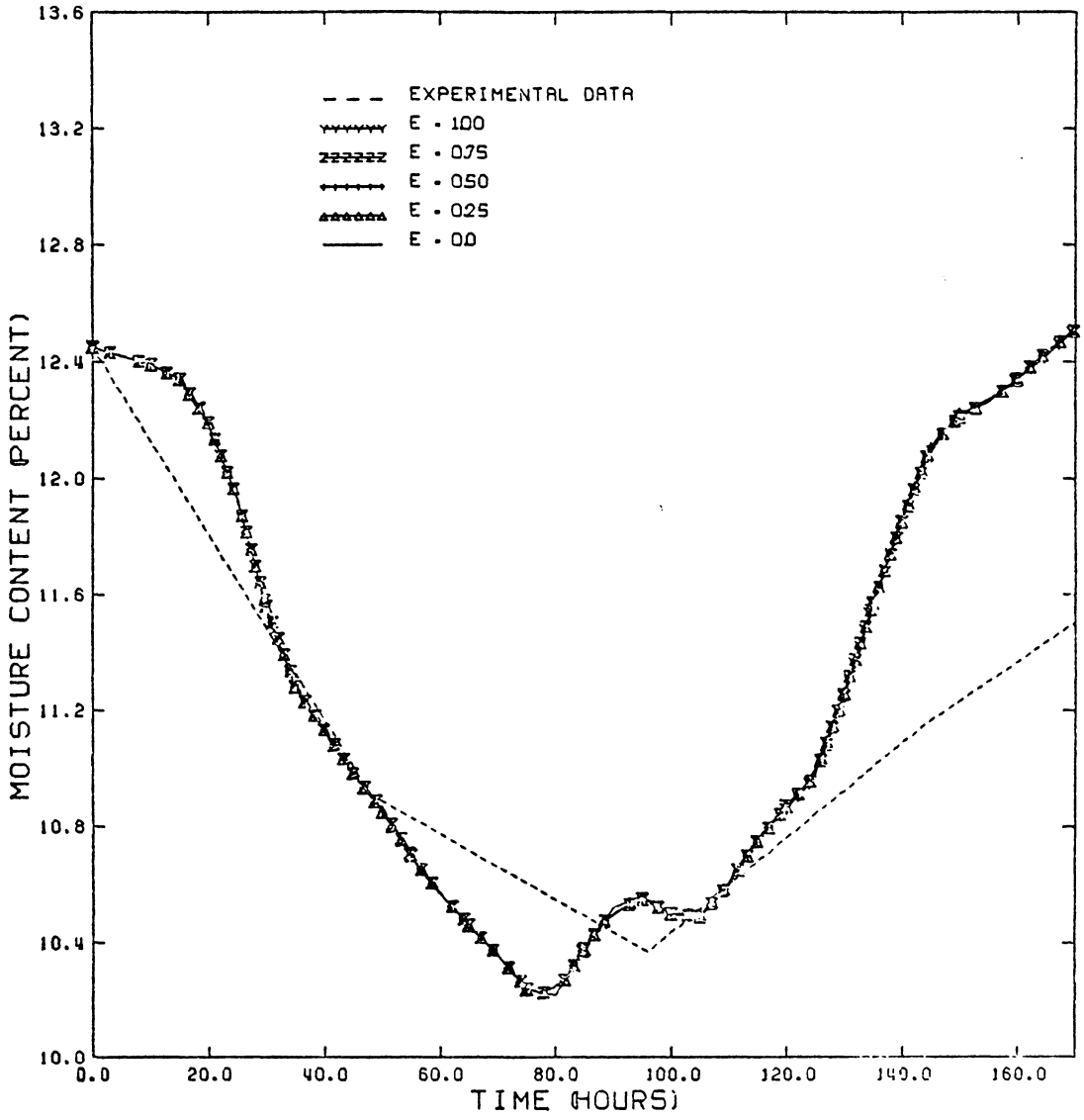

Figure 34 : Experimental and predicted moisture contents in the top layer at a wall distance of 8 inches using the series model and five phase conversion factors for Test 3. It is obvious from this figure that moisture content is independent of the phase conversion factor.

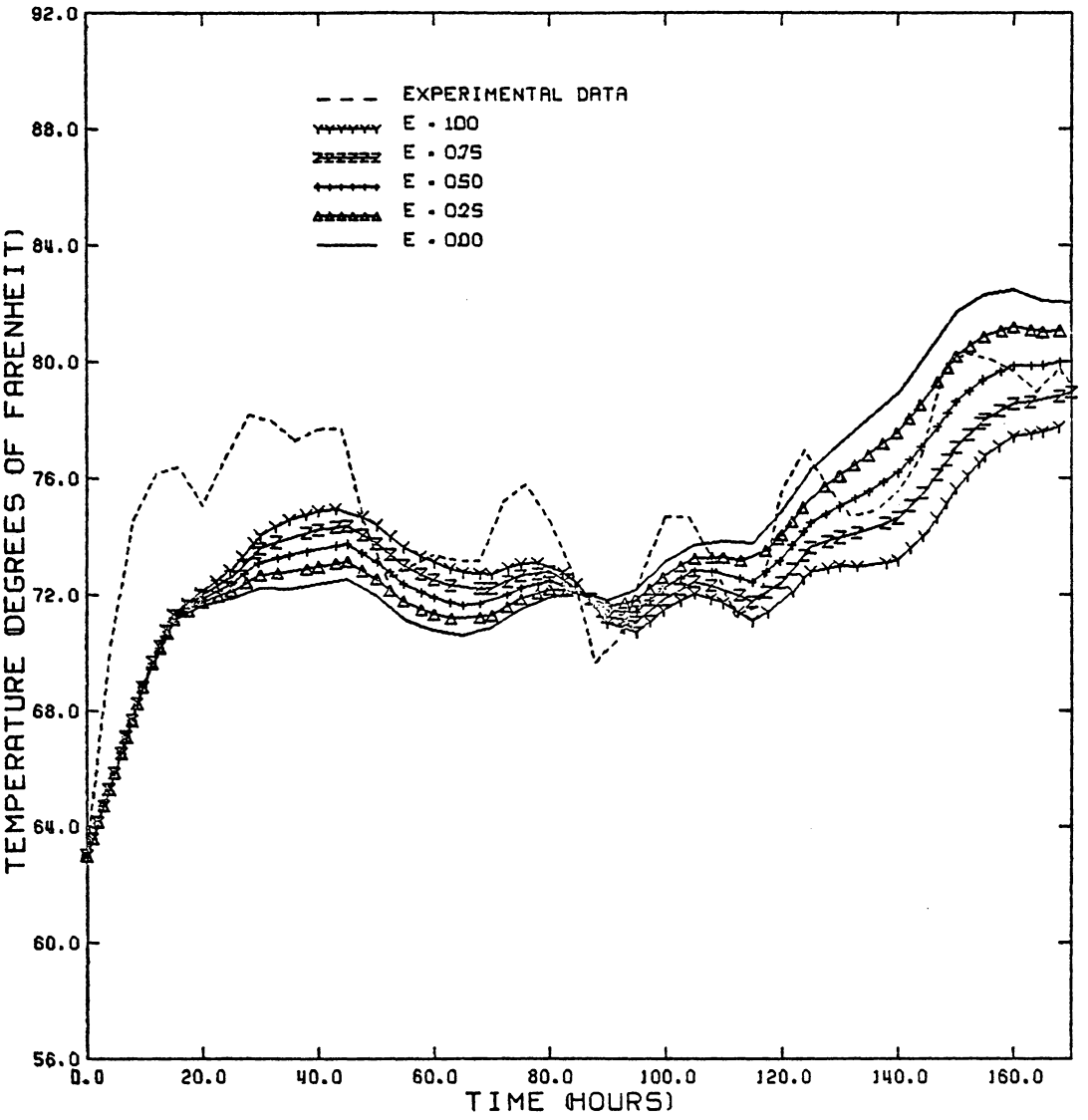

Figure 35 : Experimental and predicted temperatures in the middle layer at a wall distance of 8 inches using the parallel model and five phase conversion factors for Test 3. It is obvious from this figure that temperature is related to the phase conversion factor.

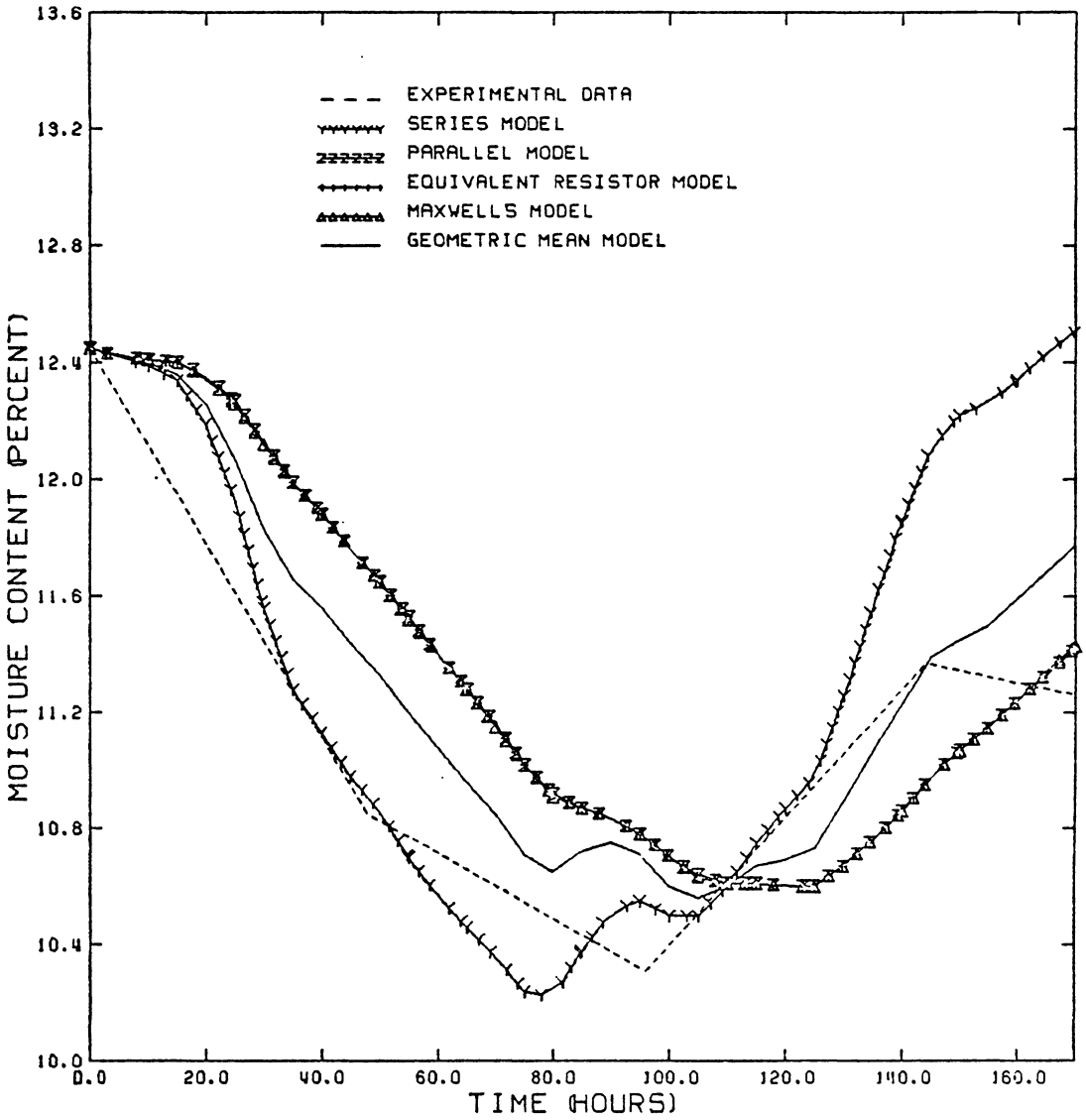

Figure 36 : Experimental and predicted moisture contents in the top layer at a wall distance of 3 inches using five mixing models with a phase conversion factor of 0.75. The series model has the best predicted moisture content during desorption and the geometirc mean model has the best predicted moisture content in absorption.

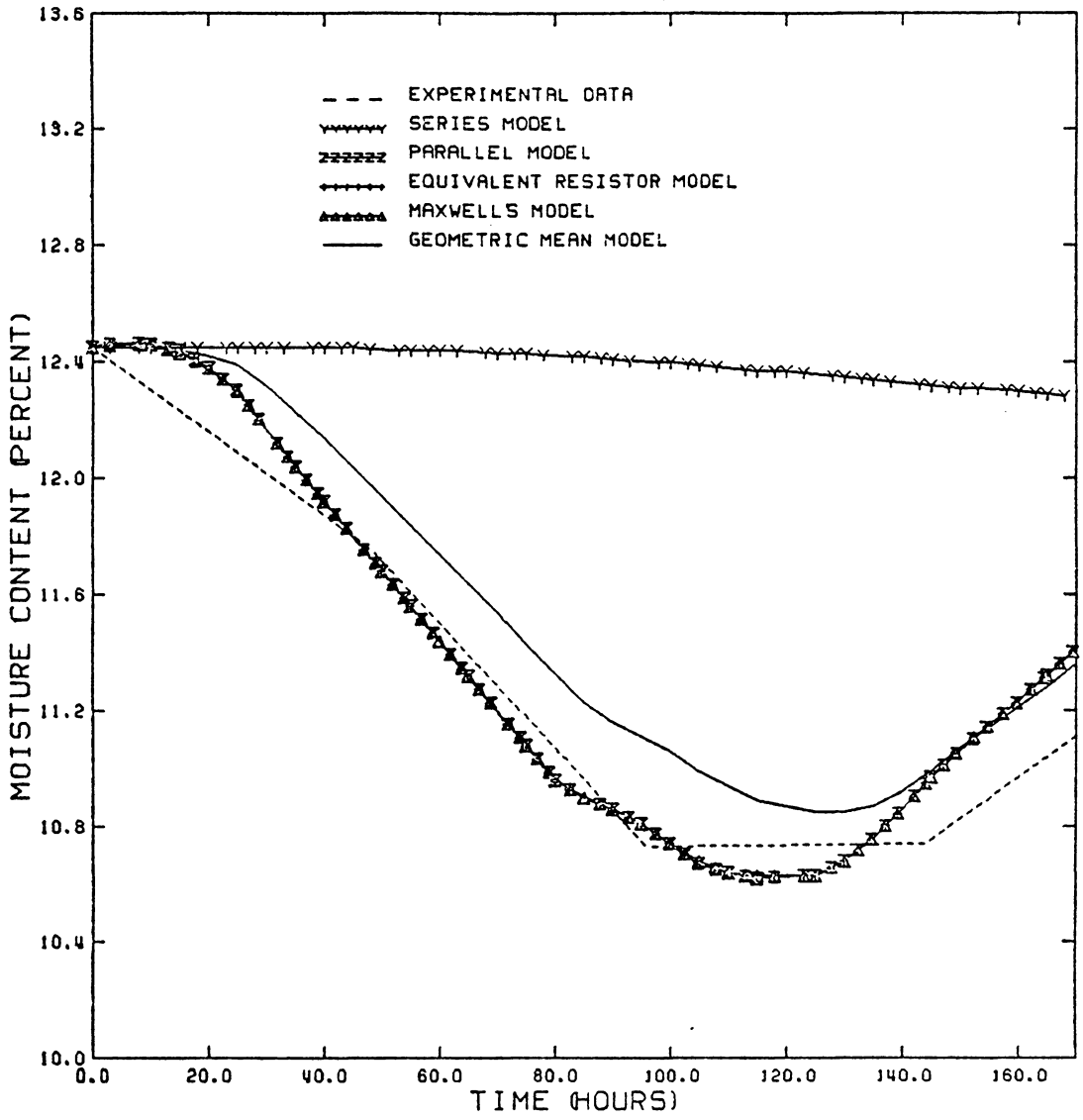

Figure 37 : Experimental and predicted moisture contents in the middle layer at a wall distance of 3 inches using five mixing models with a phase conversion factor of 0.75. The high bulk moisture diffusivity models(parallel model, equivalent resistor model and modified Maxwell model) have the best predicted moisture content when compared with the actual moisture content.

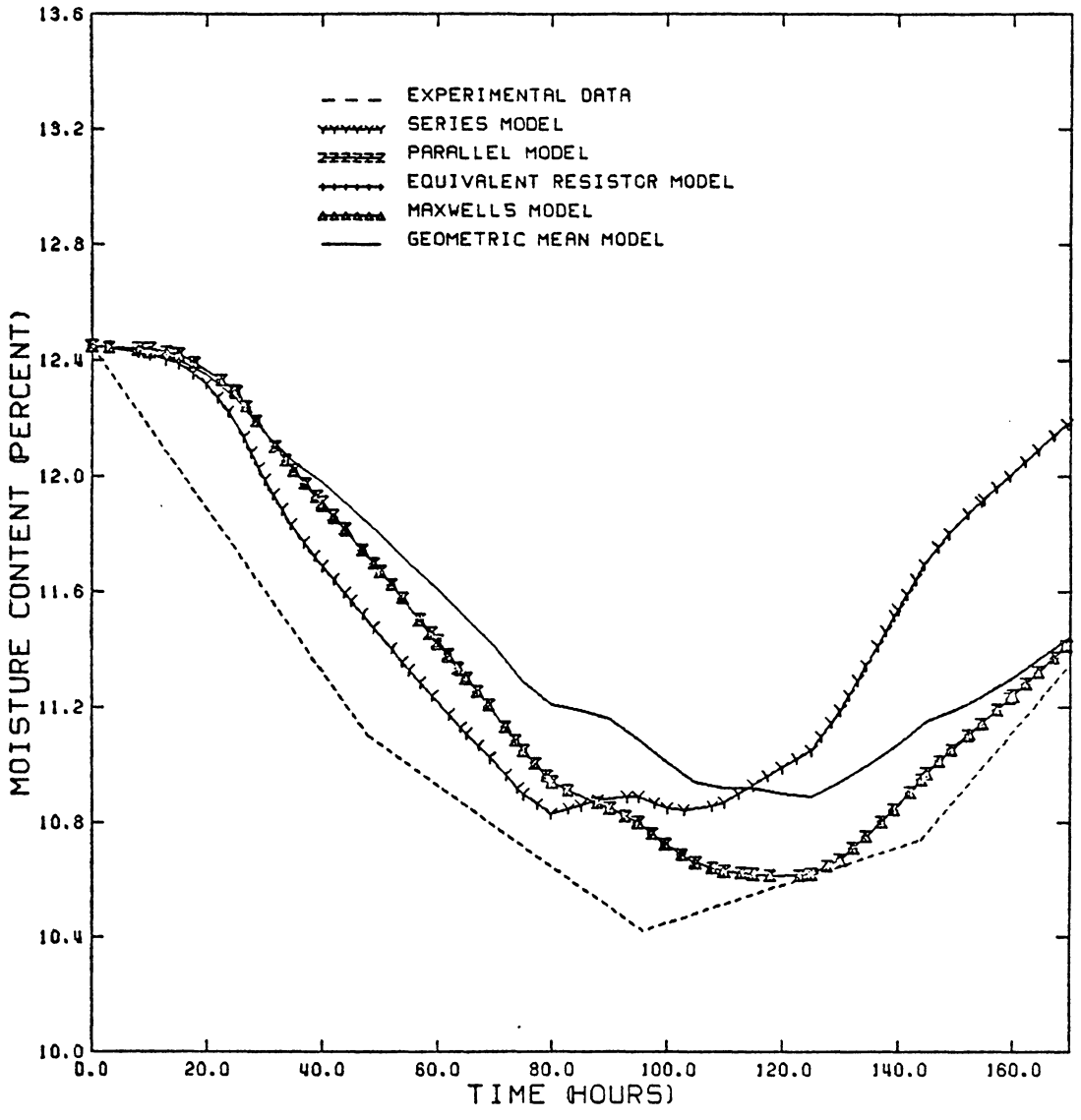

Figure 38 : Experimental and predicted moisture contents in the bottom layer at a wall distance of 3 inches using five mixing models with a phase conversion factor of 0.75. The high bulk moisture diffusivity models(parallel model, equivalent resistor model and modified Maxwell model) have the best predicted moisture content in absorption, and the series model has the best predicted moisture content in desorption.

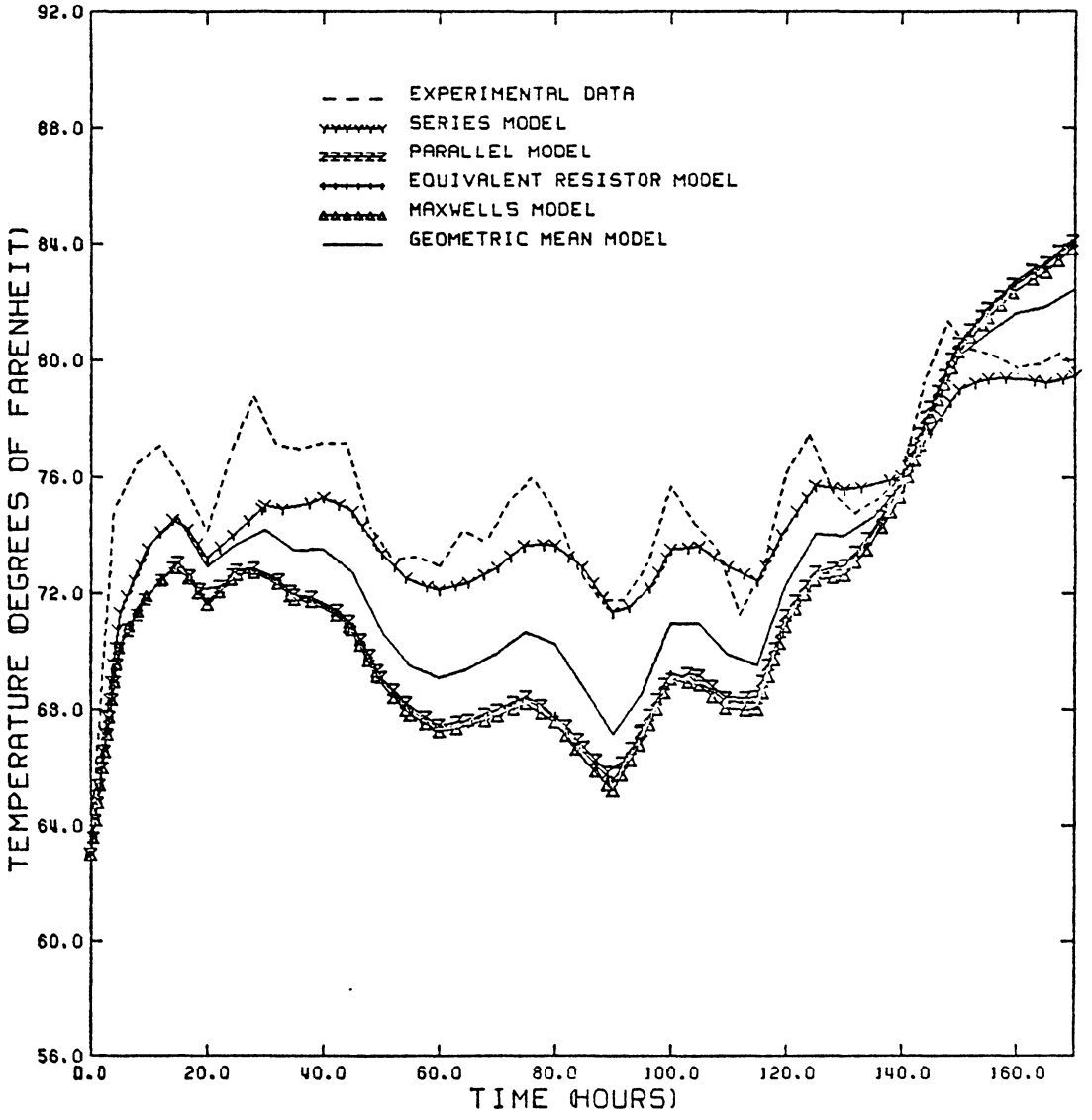

Figure 39 : Experimental and predicted temperatures in the top layer at a wall distance of 3 inches using five mixing models with a phase conversion factor of 0.75. The series model has the best predicted temperature when compared with the actual temperature.

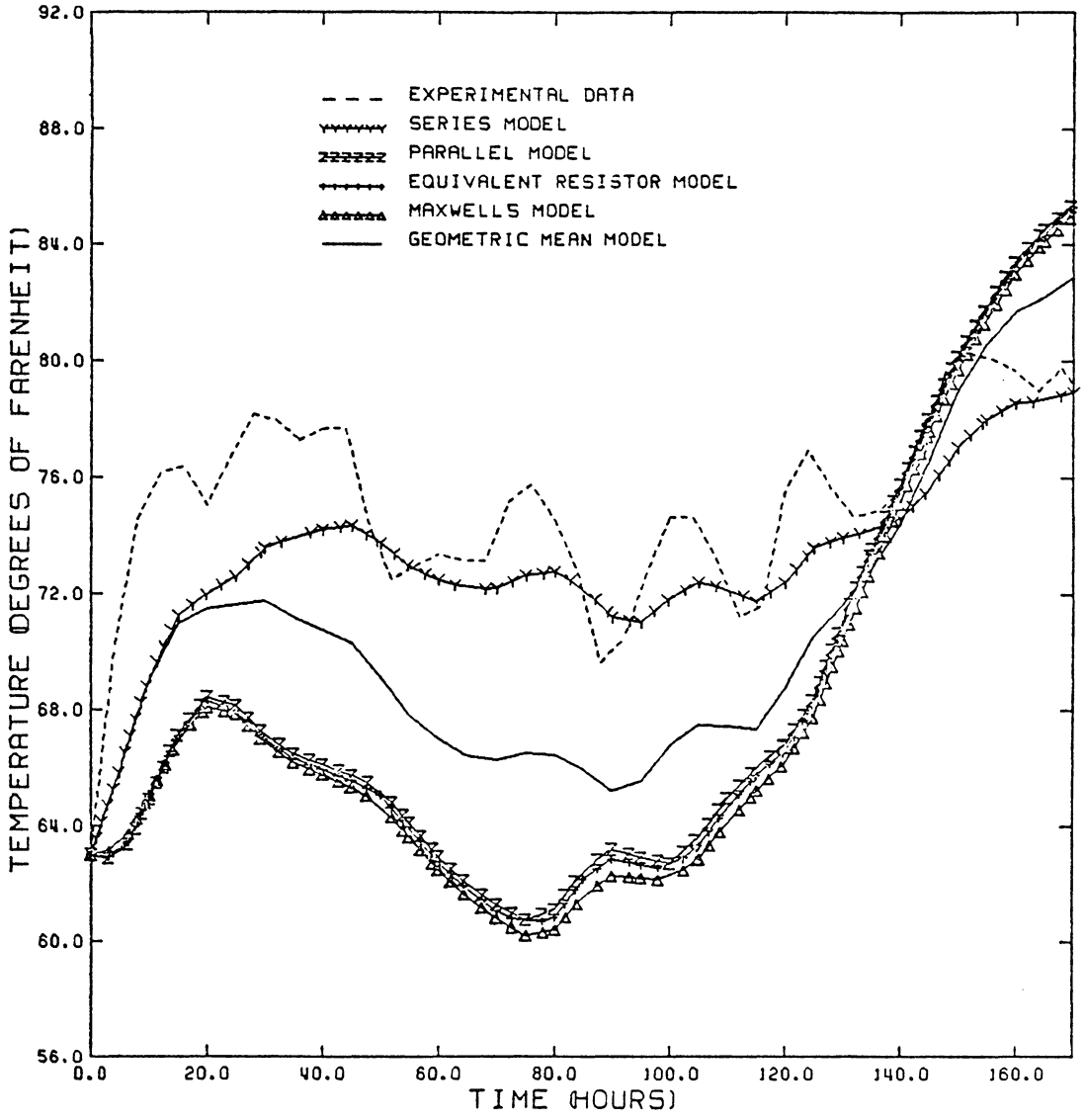

Figure 40 : Experimental and predicted temperatures in the middle layer at a wall distance of 3 inches using five mixing models with a phase conversion factor of 0.75. The series model has the best predicted temperature when compared with the actual temperature.

well model and the parallel model. Figure 41 presents a uniform predicted moisture distribution at a wall distance of 3 inches throughout the bin during the process, and Figure 42 illustrates the relationships among the temperature distributions of different layers at a wall distance of 3 inches inside the bin. Figure 43 again indicates the predicted moisture is independent of the phase conversion factor, but Figure 44 reveals that the predicted temperature is highly related to the phase conversion factor.

5.3.5 Equivalent Resistor Model

The bulk moisture diffusivity calculated using the equivalent resistor model is 0.31 ft^2/hr. In a comparison of the bulk moisture diffusivities of the equivalent resistor model, the parallel model and the modified Maxwell model, one may conclude that the predicted moisture distributions of these three models at a wall distance of 8 inches and a phase conversion factor of 0.75 for the top, middle and bottom layers (Fig. 45, 46 and 47) are almost identical and the predicted temperature distributions at the same wall distance and phase conversion factor as before (Fig. 48 and 49) are similar. Figure 50 presents the predicted moisture distribution for a phase conversion factor of zero and at a wall distance of 3 inches in the equivalent resistor model,

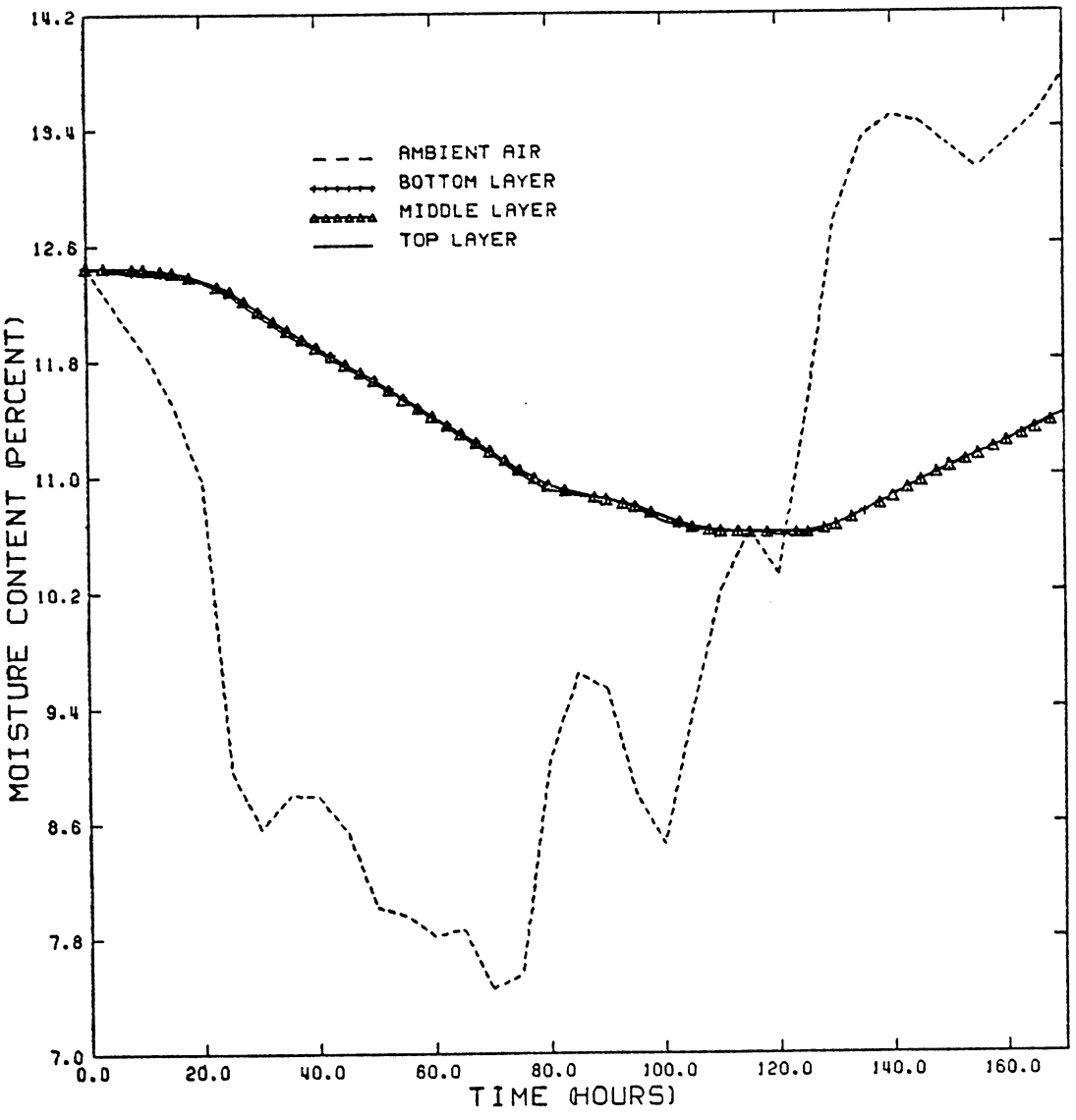

Figure 41 : Equilibrium moisture content and predicted moisture contents for the modified Maxwell model with a phase conversion factor of 0.25 for a wall distance of 3 inches during Test 3. The figure indicates that the predicted moisture content distributions are homogeneous throughout the bin.

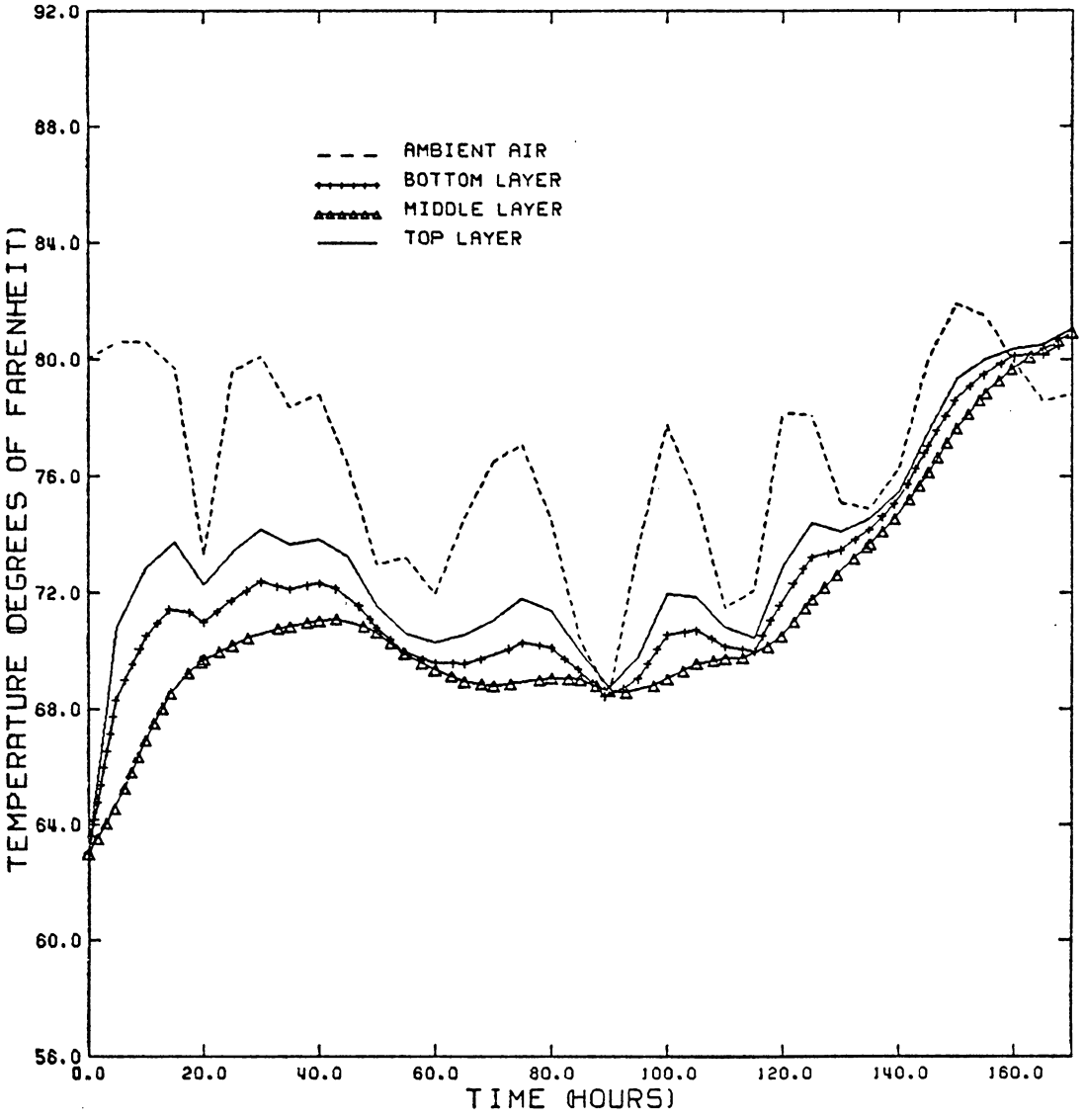

Figure 42 : Ambient and predicted temperatures at a wall distance of 3 inches using the modified Maxwell model with a phase conversion factor of 0.25 for Test 3. The figure indicates that the change of the predicted temperature is coincident with the change of ambient air temperature.

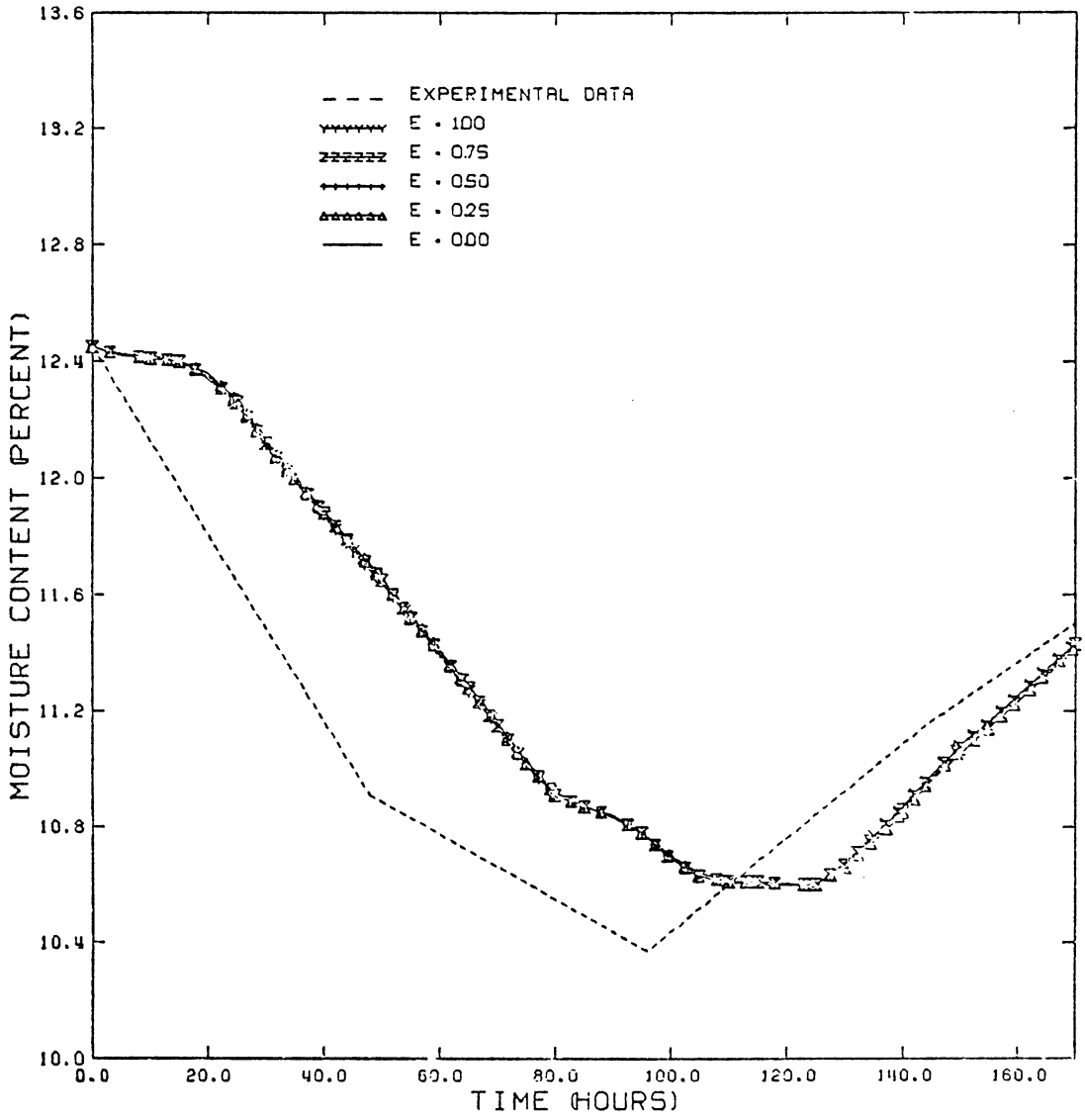

Figure 43 : Experimental and predicted moisture contents in the top layer at a wall distance of 8 inches using the modified Maxwell model and five phase conversion factors for Test 3. The moisture content is independent of the phase conversion factor.

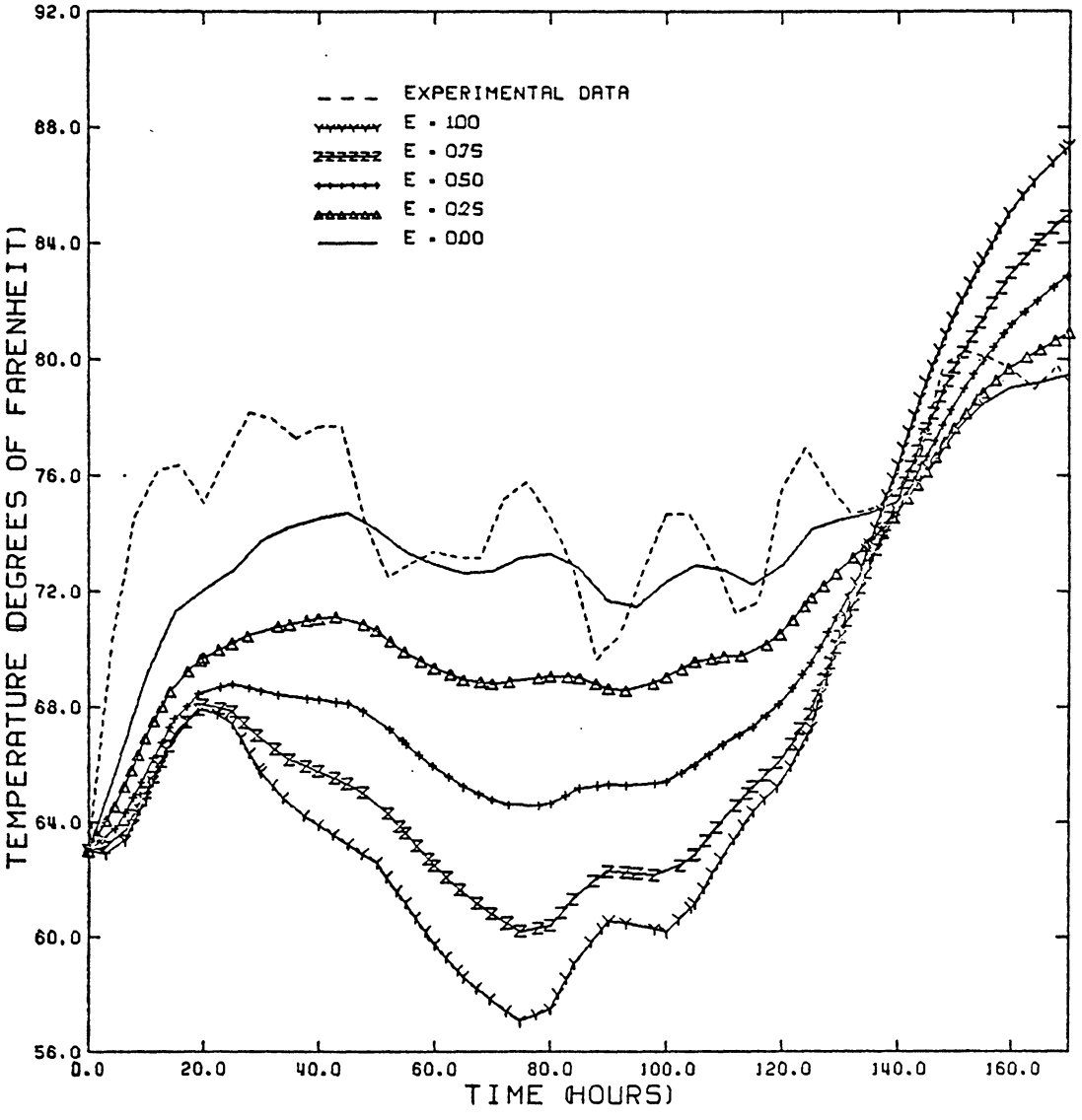

Figure 44 : Experimental and predicted temperatures in the middle layer at a wall distance of 3 inches using the modified Maxwell model and five phase conversion factors for Test 3. It is obvious from this figure that temperature is related to the phase conversion factor.

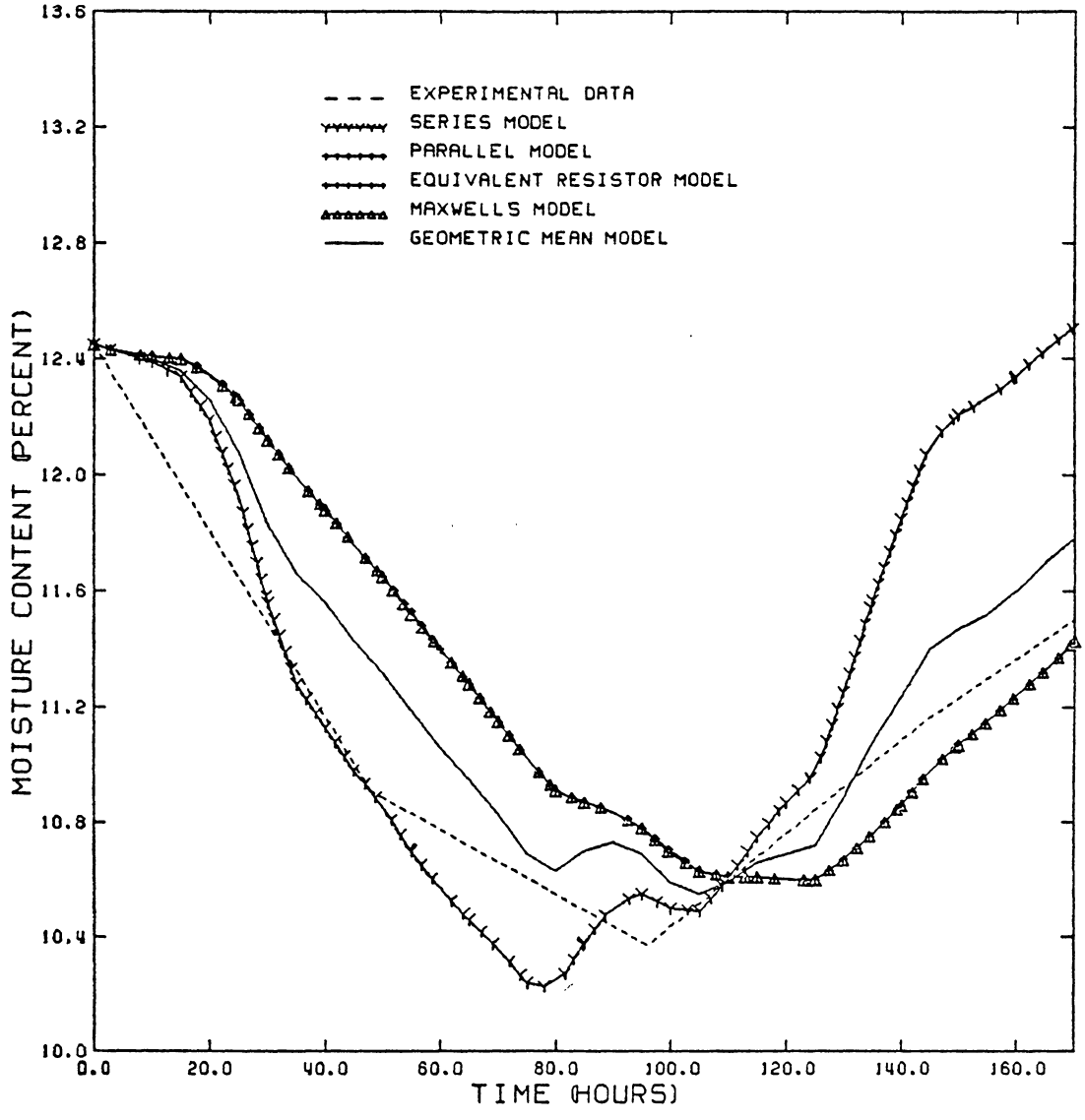

Figure 45 : Experimental and predicted moisture contents in the top layer at a wall distance of 8 inches using five mixing models with a phase conversion factor of 0.75. The geometric mean model has the best predicted moisture content when compared with the actual moisture content.

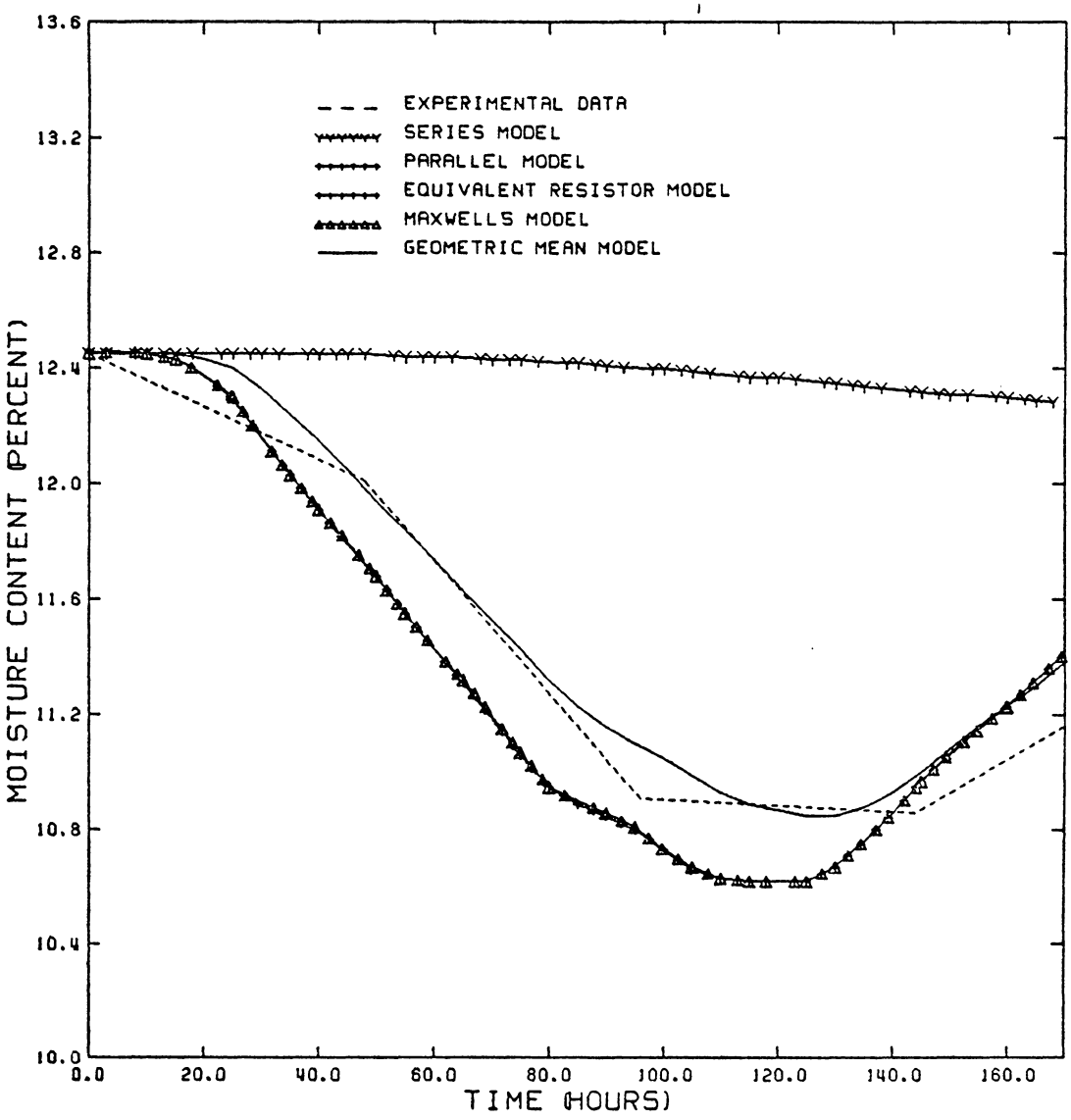

Figure 46 : Experimental and predicted moisture contents in the middle layer at a wall distance of 8 inches using five mixing models with a phase conversion factor of 0.75. The geometric mean model has the best predicted moisture content when compared with the actual moisture content.

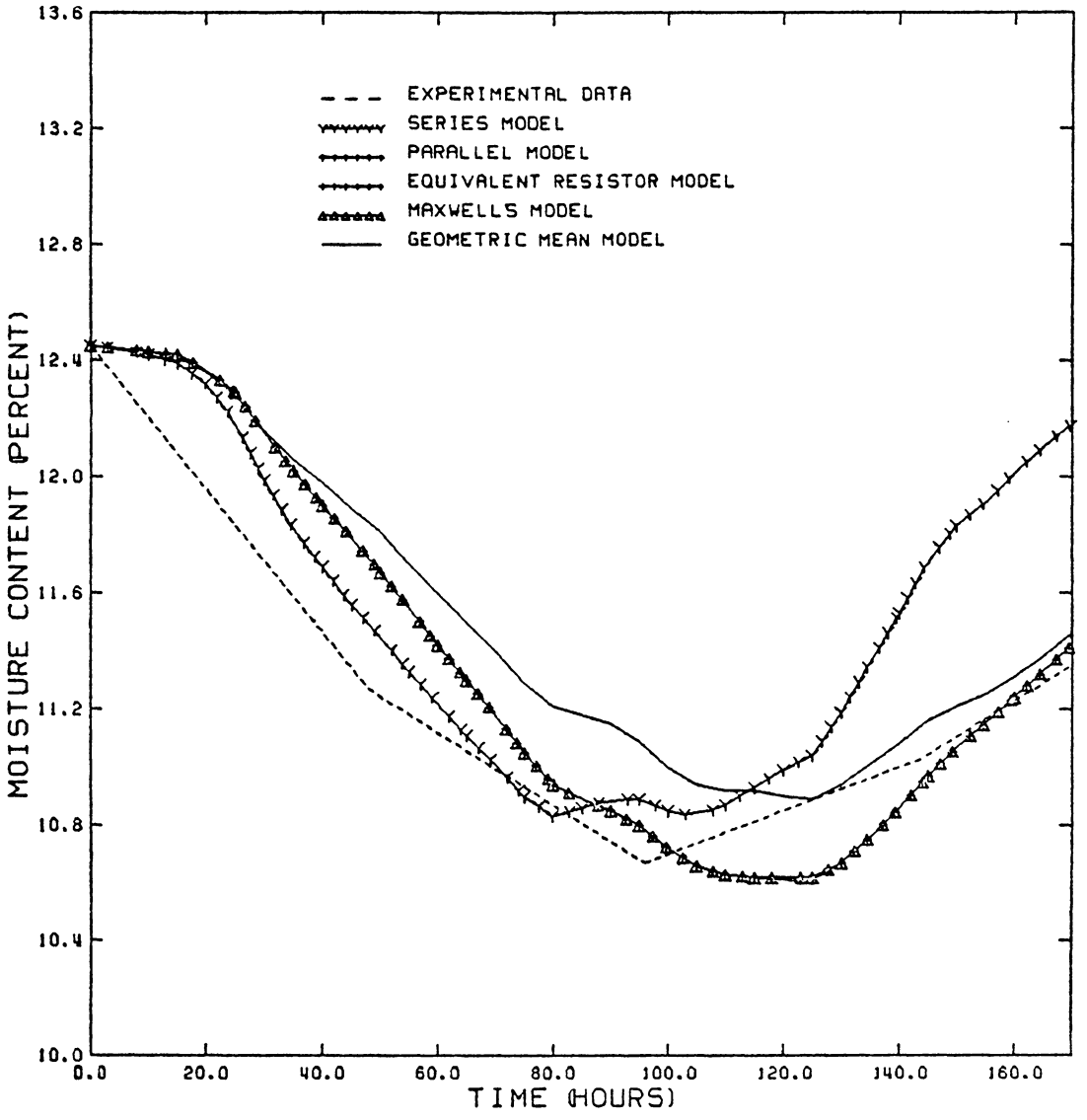

Figure 47 : Experimental and predicted moisture contents in the bottom layer at a wall distance of 8 inches using five mixing models with a phase conversion factor of 0.75. The series model has the best predicted moisture content during desorption and the geometric mean model has the best predicted values during absorption.

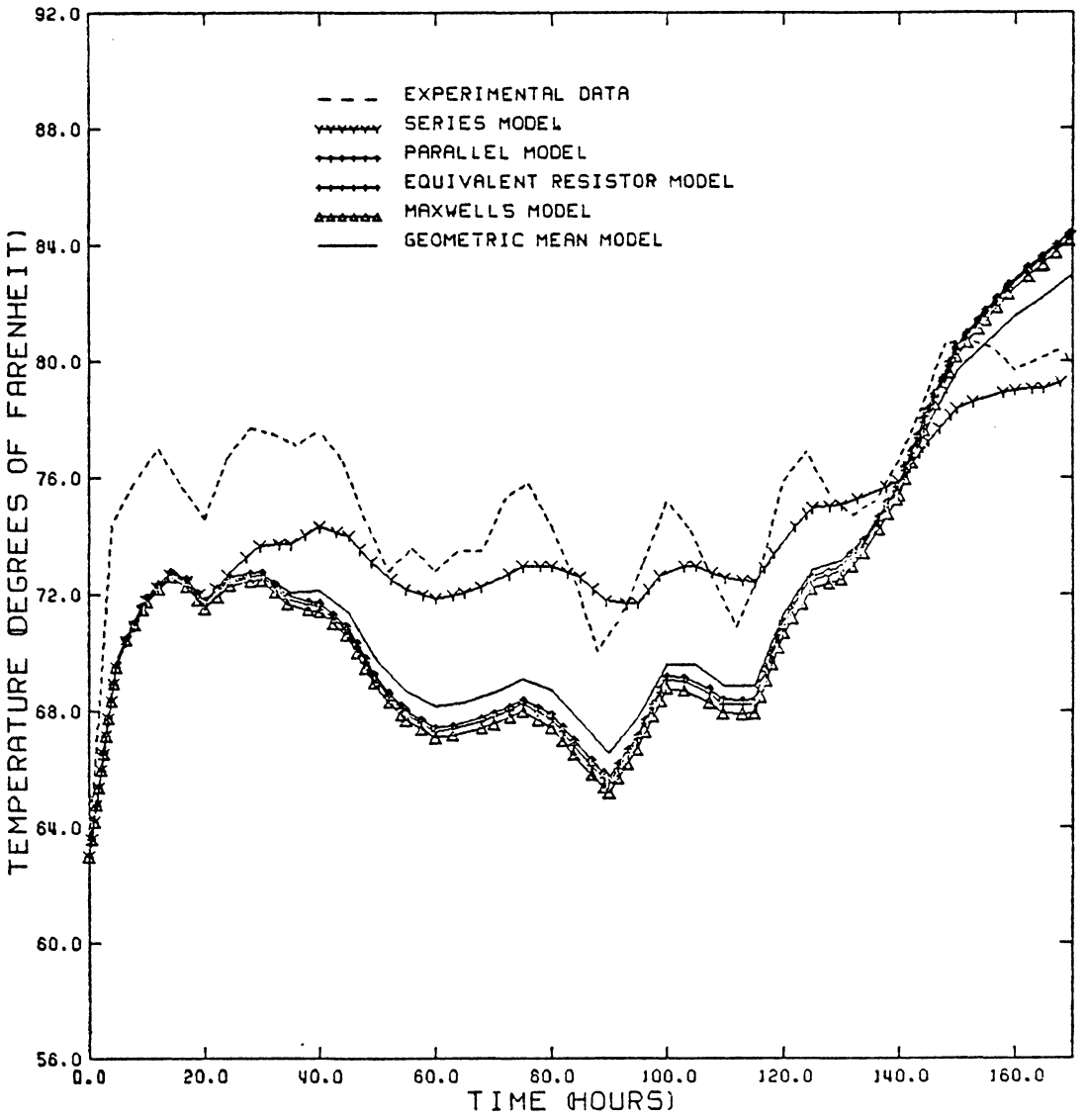

Figure 48 : Experimental and predicted temperatures in the top layer at a wall distance of 8 inches using five mixing models with a phase conversion factor of 0.75. The series model has the best predicted temperature when compared with the actual temperature.

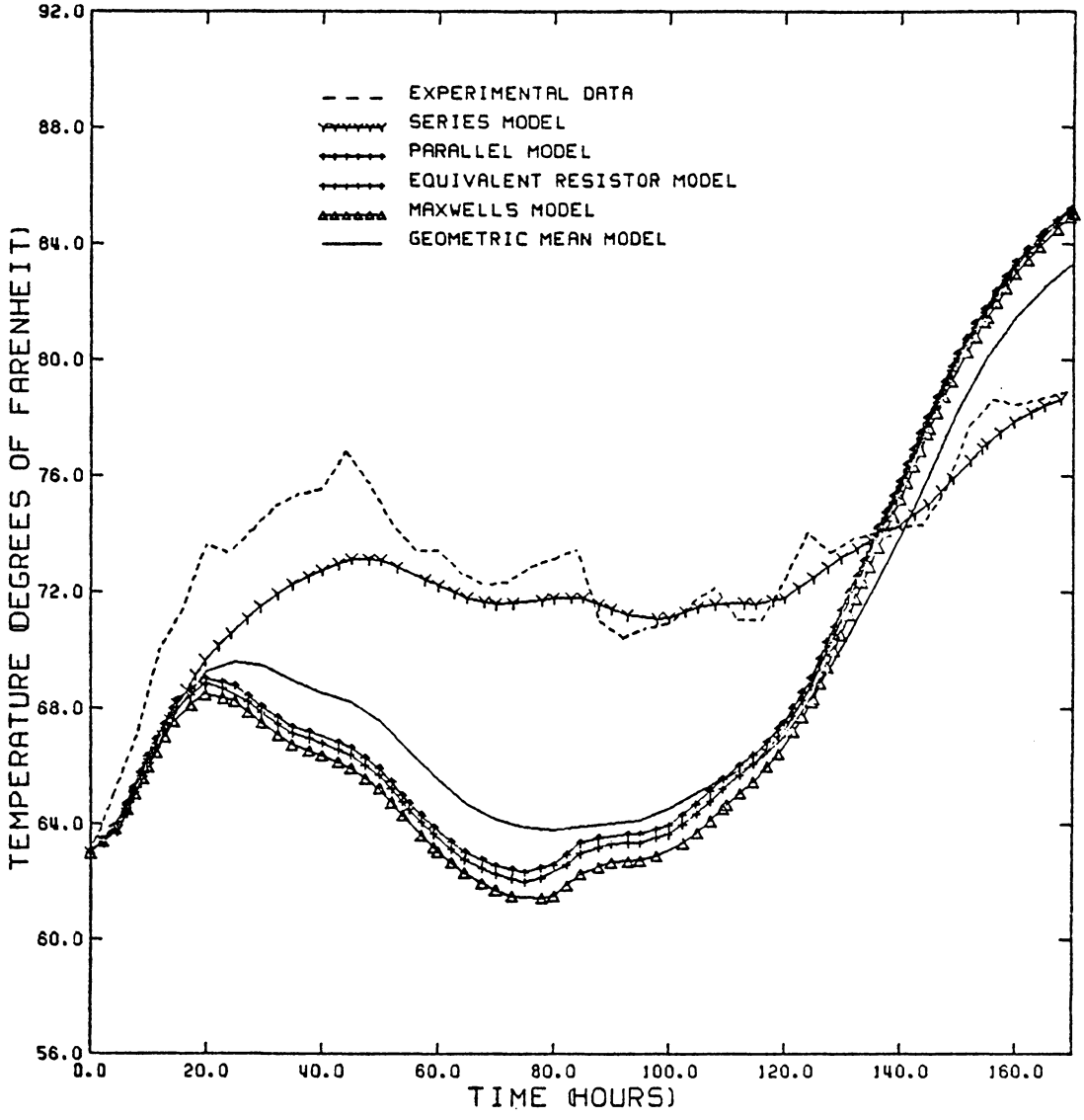

Figure 49 : Experimental and predicted temperatures in the middle layer at a wall distance of 8 inches using five mixing models with a phase conversion factor of 0.75. The series model has the best predicted temperature when compared with the actual temperature.

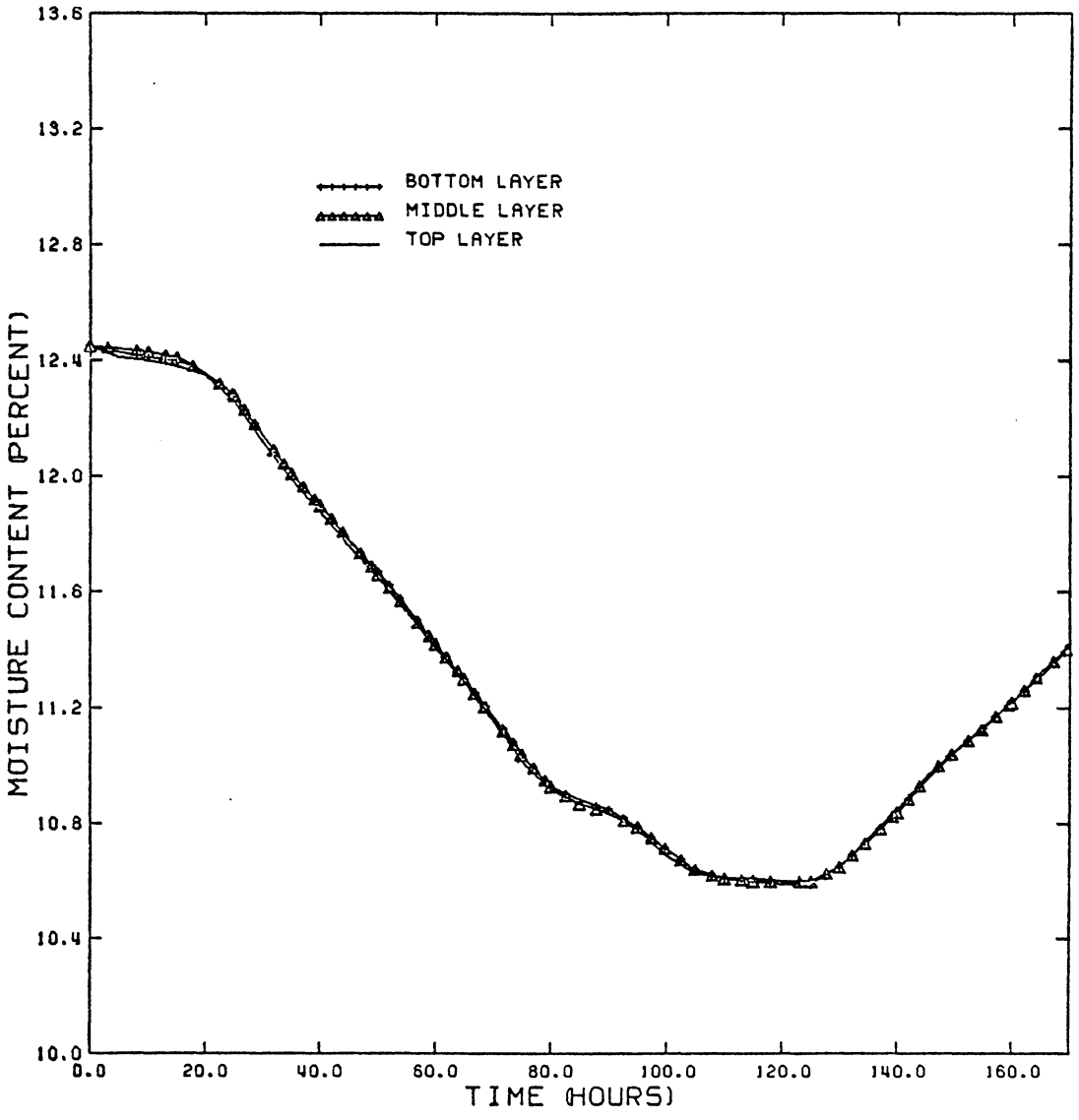

Figure 50 : The predicted moisture contents for the equivalent resistor model with a phase conversion factor of zero for a wall distance of 3 inches during Test 3. The figure indicates that the predicted moisture distributions are homogeneous throughout the bin.

and Figure 51 shows the predicted temperature distribution at the same wall distance and for a phase conversion factor of 0.25.

5.3.6 Geometric Mean Model

The bulk moisture diffusivity, calculated from the geometric mean model, is approximately 0.0027 ft^2/hr, or fifty times the moisture diffusivity of a kernel of corn and a one-hundredth of the molecular diffusivity of a vapor and air mixture. The bulk thermal diffusivity from Eqs. (51) and (52) is 0.0072ft^2/hr. A comparison of the bulk moisture diffusivity of the geometric mean model and the bulk thermal diffusivity indicates that neither can be neglected; in other words, moisture and heat trasfer must interact with each other in the storage process. As a consequence, in Figures 52 to 61 the predicted moisture and temperature curves for a phase conversion factor of 0.25 at the wall distances of 3 and 8 inches in the top, middle and bottom layers for the geometric mean model are located between the curves for the series and the parallel models. Figures 62 and 63 illustrate the existence of the internal temperature and moisture gradients for the geometric mean model using a phase conversion factor of 0.25 and a wall distance of 3 inches. A comparison of the phase conversion factors is presented in Fig-

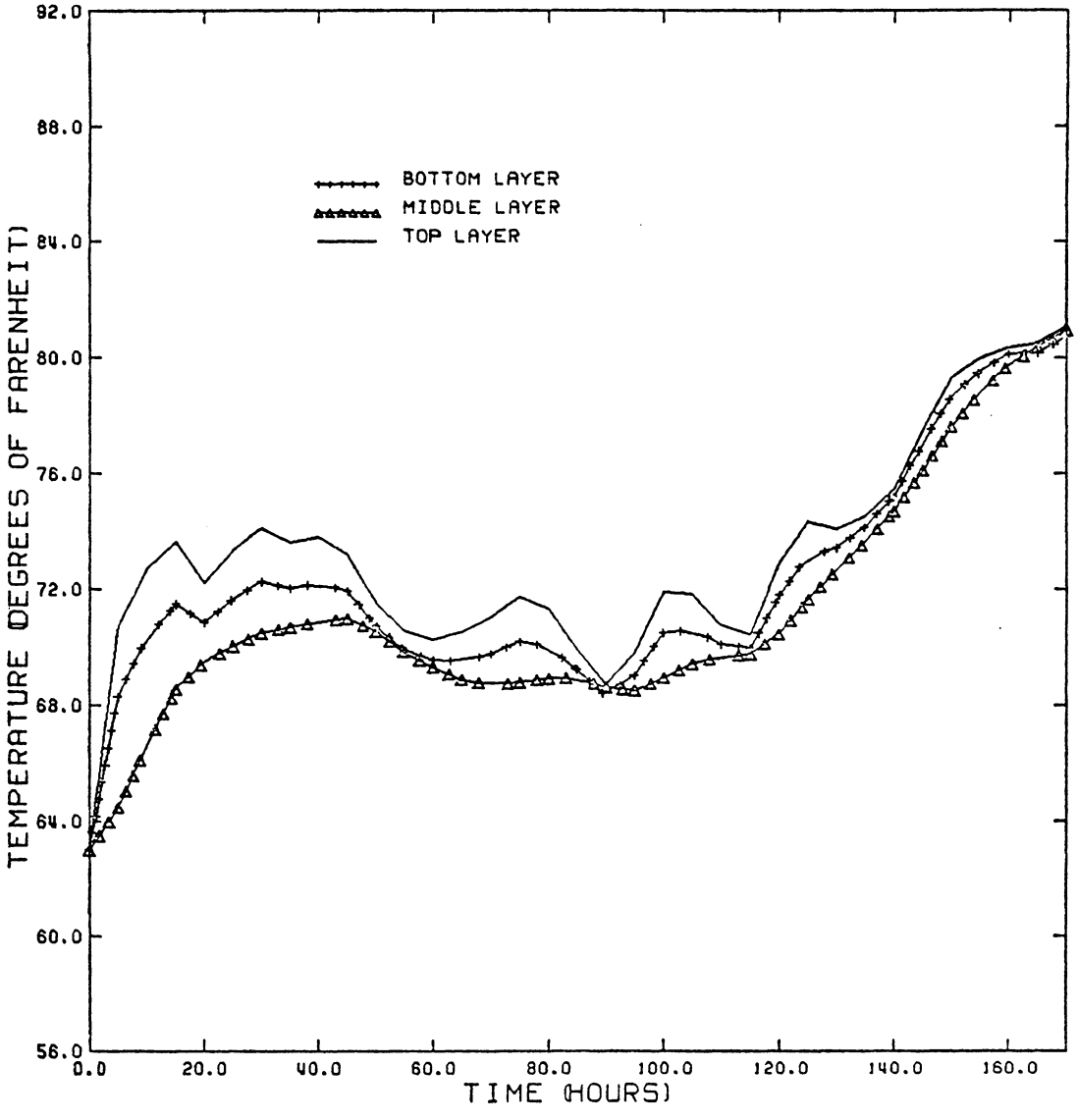

Figure 51 : The predicted temperatures at a wall distance of 3 inches using the equivalent resistor model with a phase conversion factor of 0.25 for Test 3. The figure illustrates that a internal temperature gradient exists.

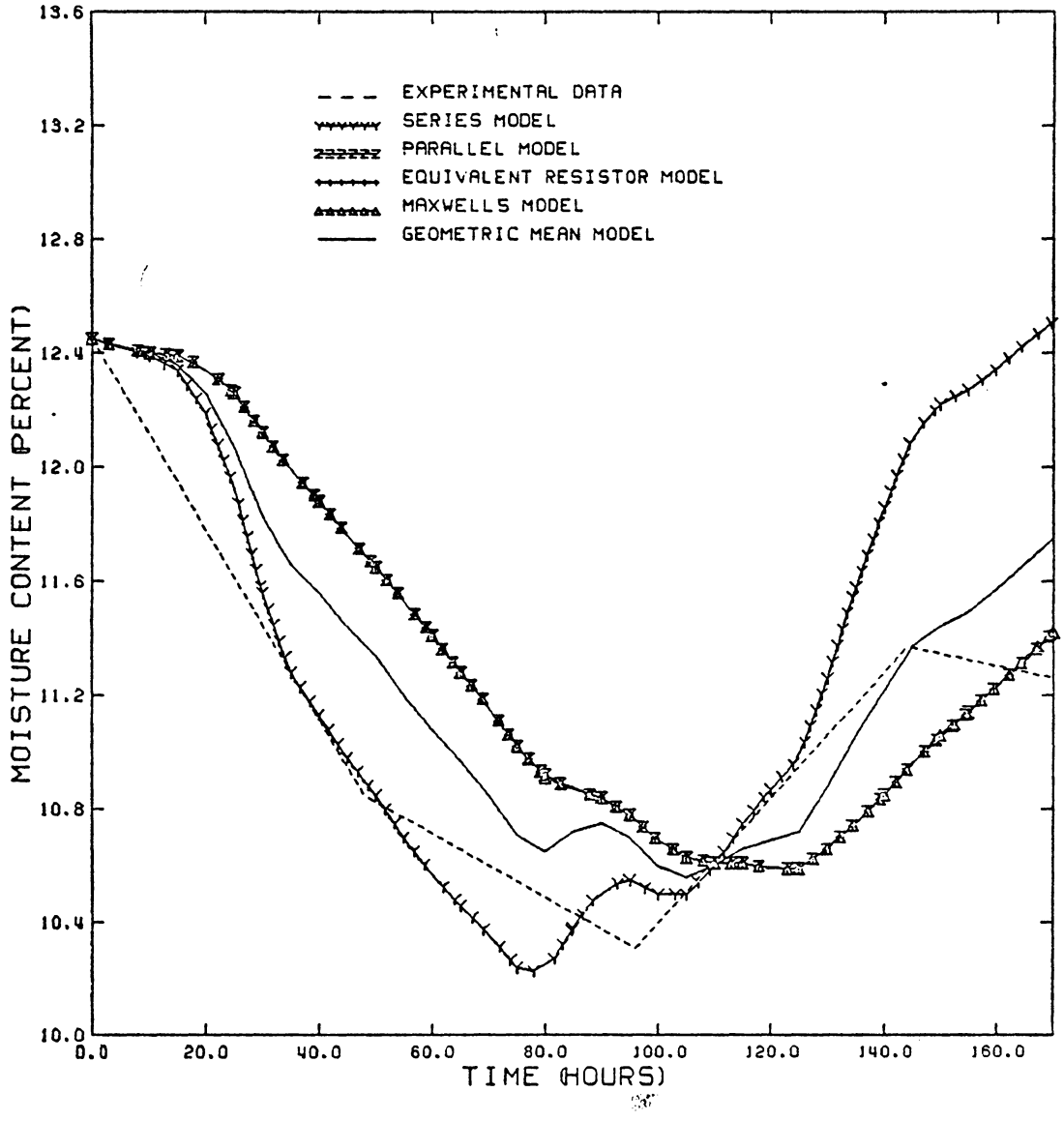

Figure 52 : Experimental and predicted moisture contents in the top layer at a wall distance of 3 inches using five mixing models with a phase conversion factor of 0.25. The geometric mean model has the best predicted moisture content when compared with the actual moisture content.

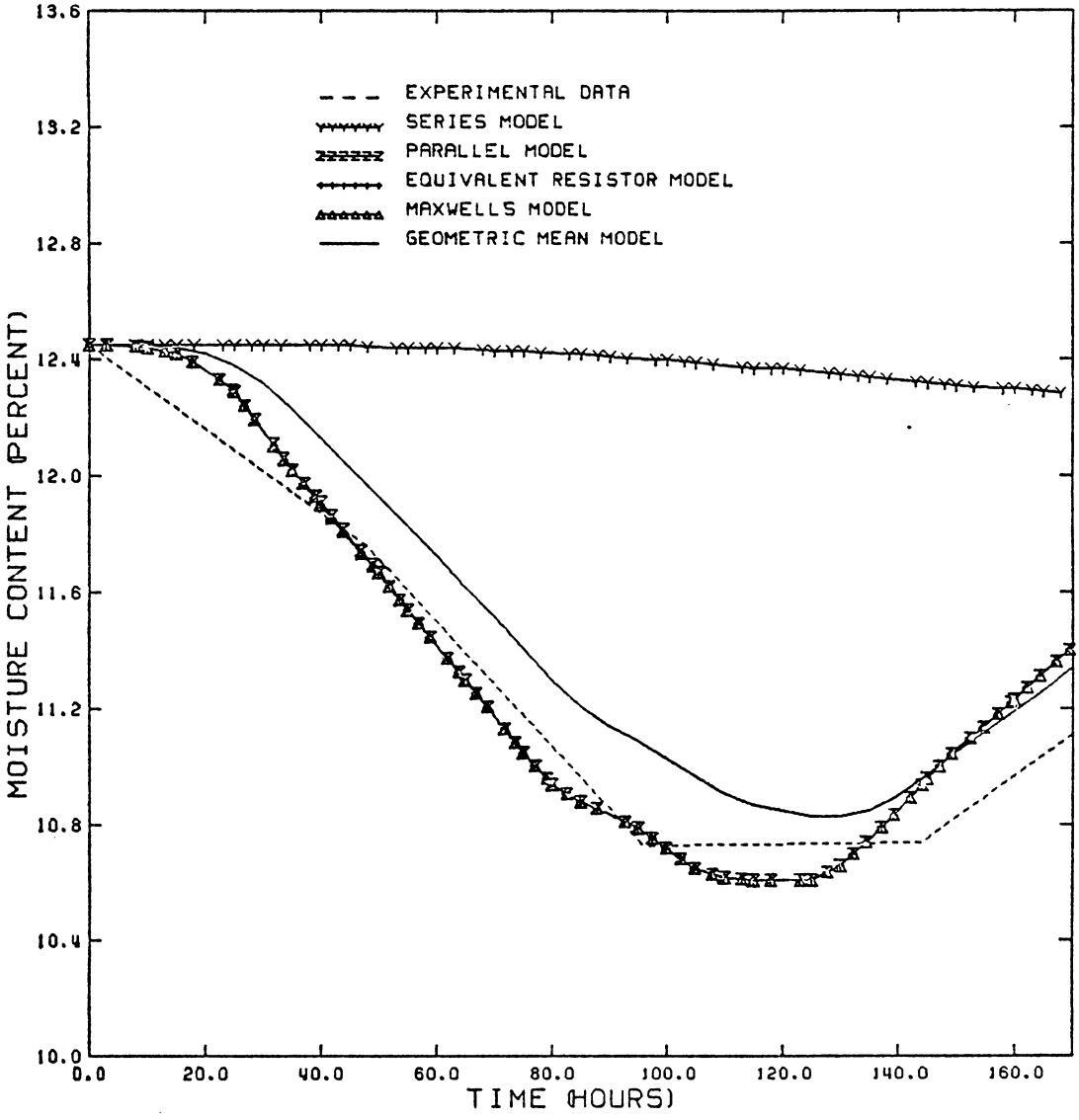

Figure 53 : Experimental and predicted moisture contents in the middle layer at a wall distance of 3 inches using five mixing models with a phase conversion factor of 0.25. The parallel model has the best predicted moisture content when compared with the actual moisture content.

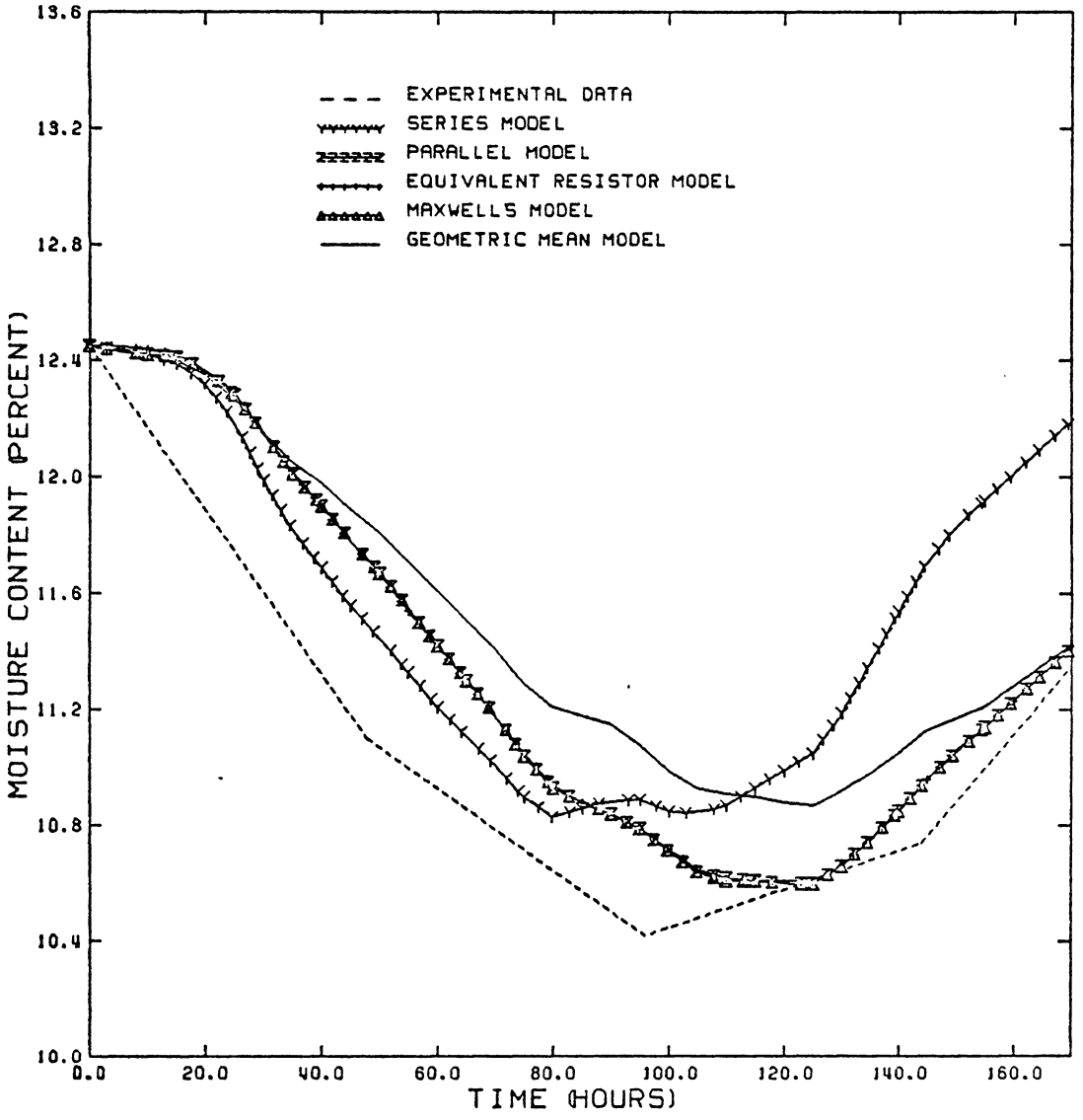

Figure 54 : Experimental and predicted moisture contents in the bottom layer at a wall distance of 3 inches using five mixing models with a phase conversion factor of 0.25. The series model has the best predicted moisture content during desorption and the parallel model has the best predicted moisture content during absorption.

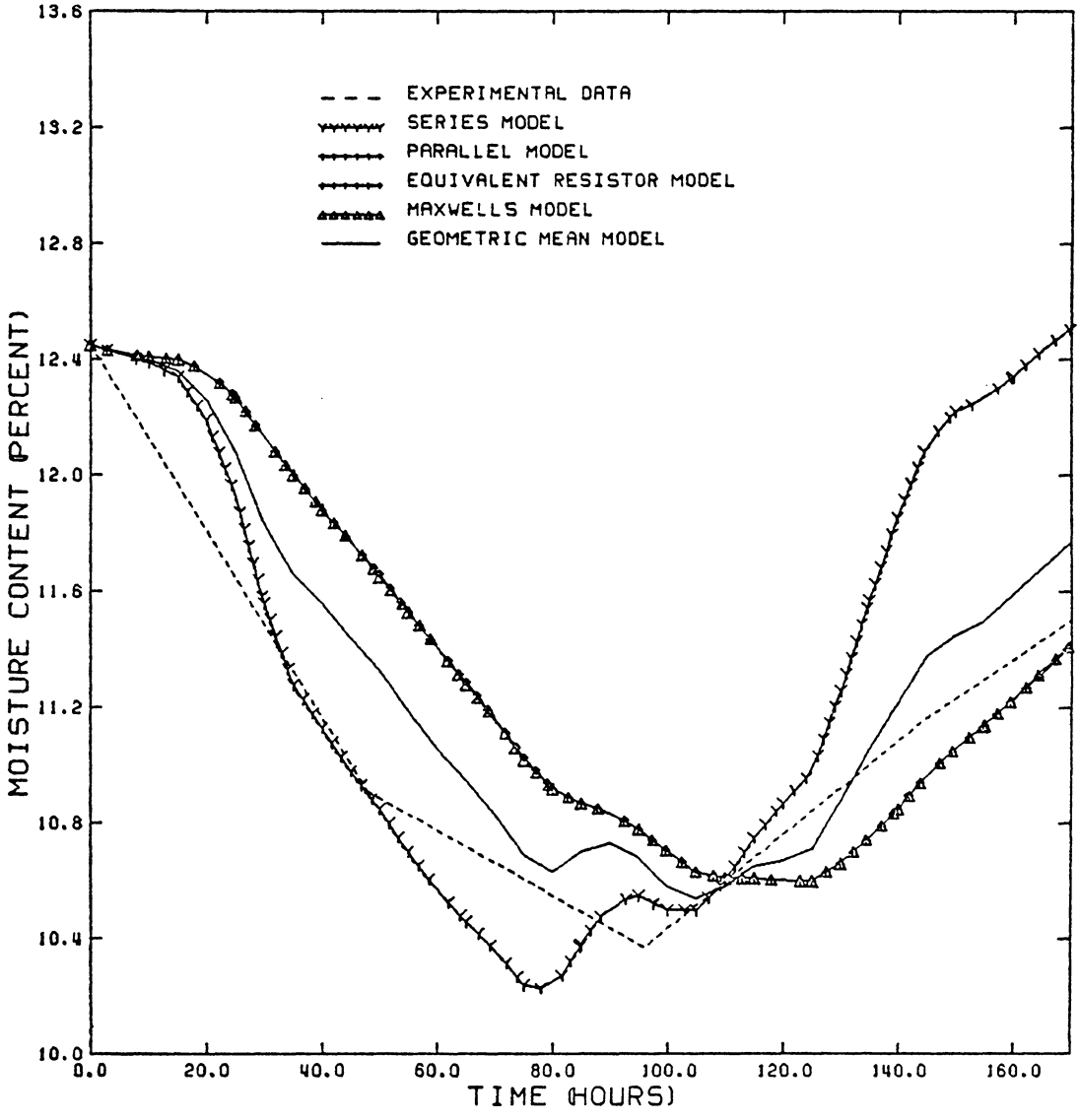

Figure 55 : Experimental and predicted moisture contents in the top layer at a wall distance of 8 inches using five mixing models with a phase conversion factor of 0.25. The geometric mean model has the best predicted moisture content when compared with the actual moisture content.

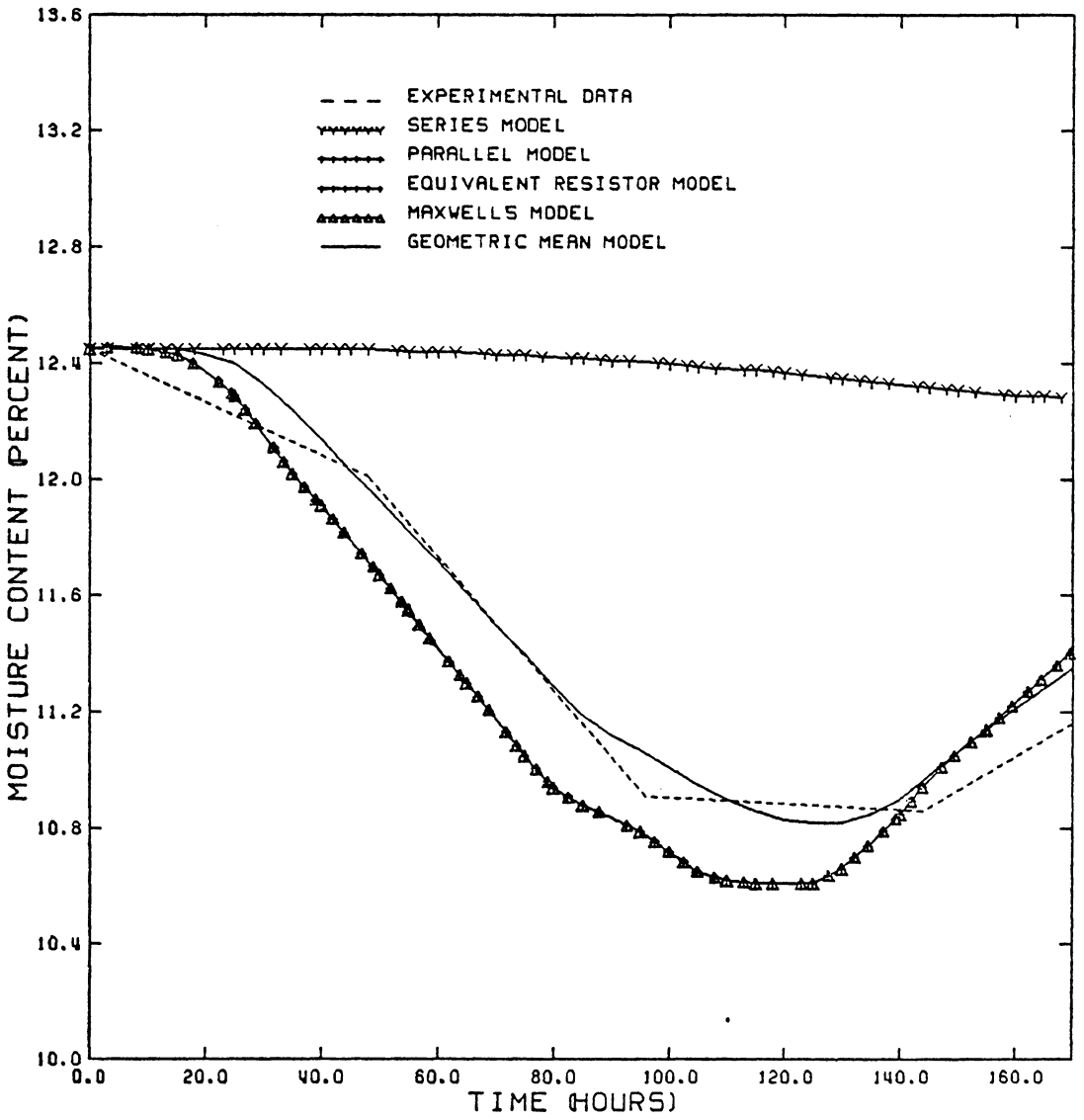

Figure 56 : Experimental and predicted moisture contents in the middle layer at a wall distance of 8 inches using five mixing models with a phase conversion factor of 0.25. The geometric mean model has the best predicted moisture content when compared with the actual moisture content.

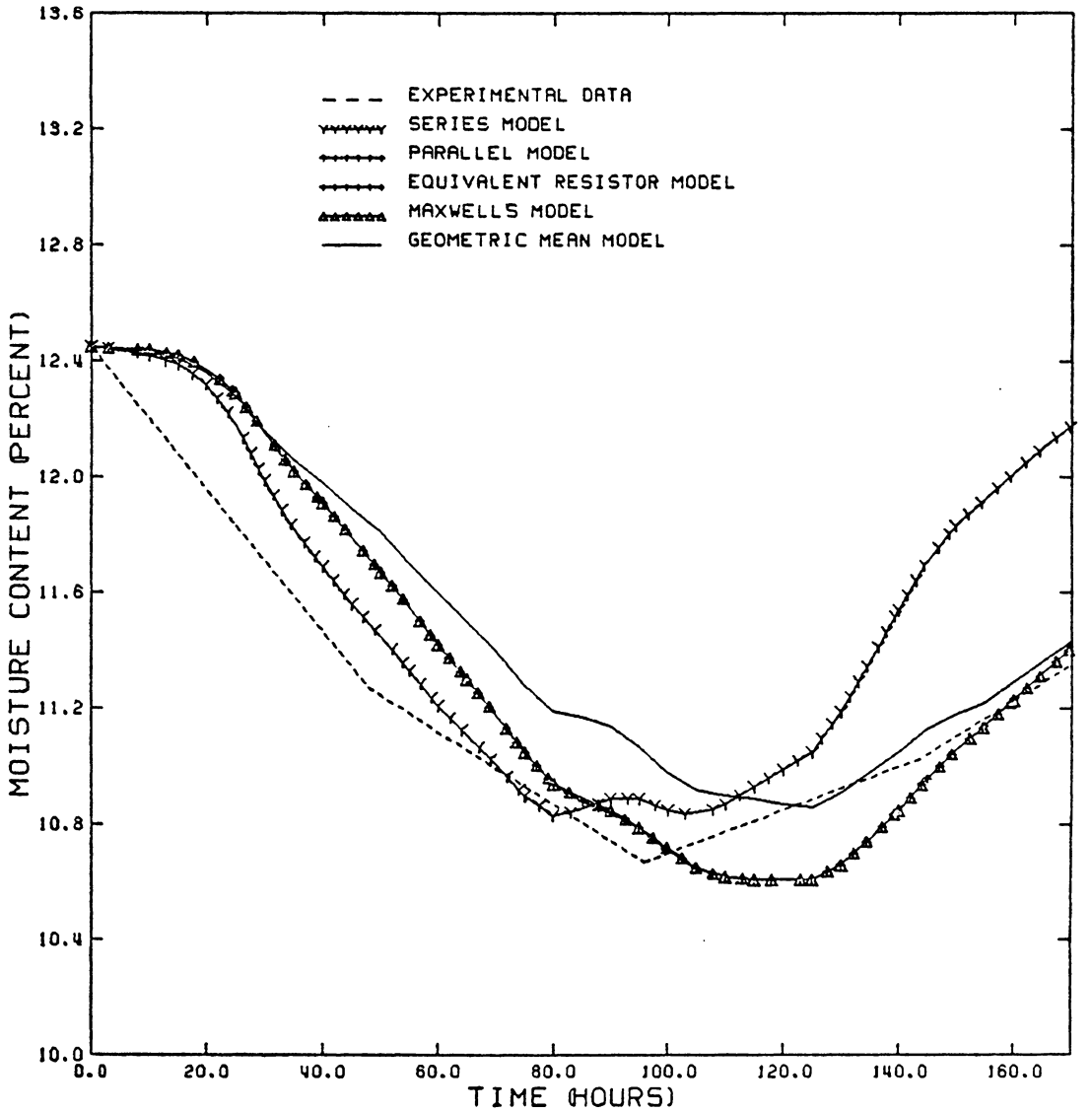

Figure 57 : Experimental and predicted moisture contents in the bottom layer at a wall distance of 8 inches using five mixing models with a phase conversion factor of 0.25. The series model has the best predicted moisture content during desorption and the geometric mean model has the best predicted values during absorption.

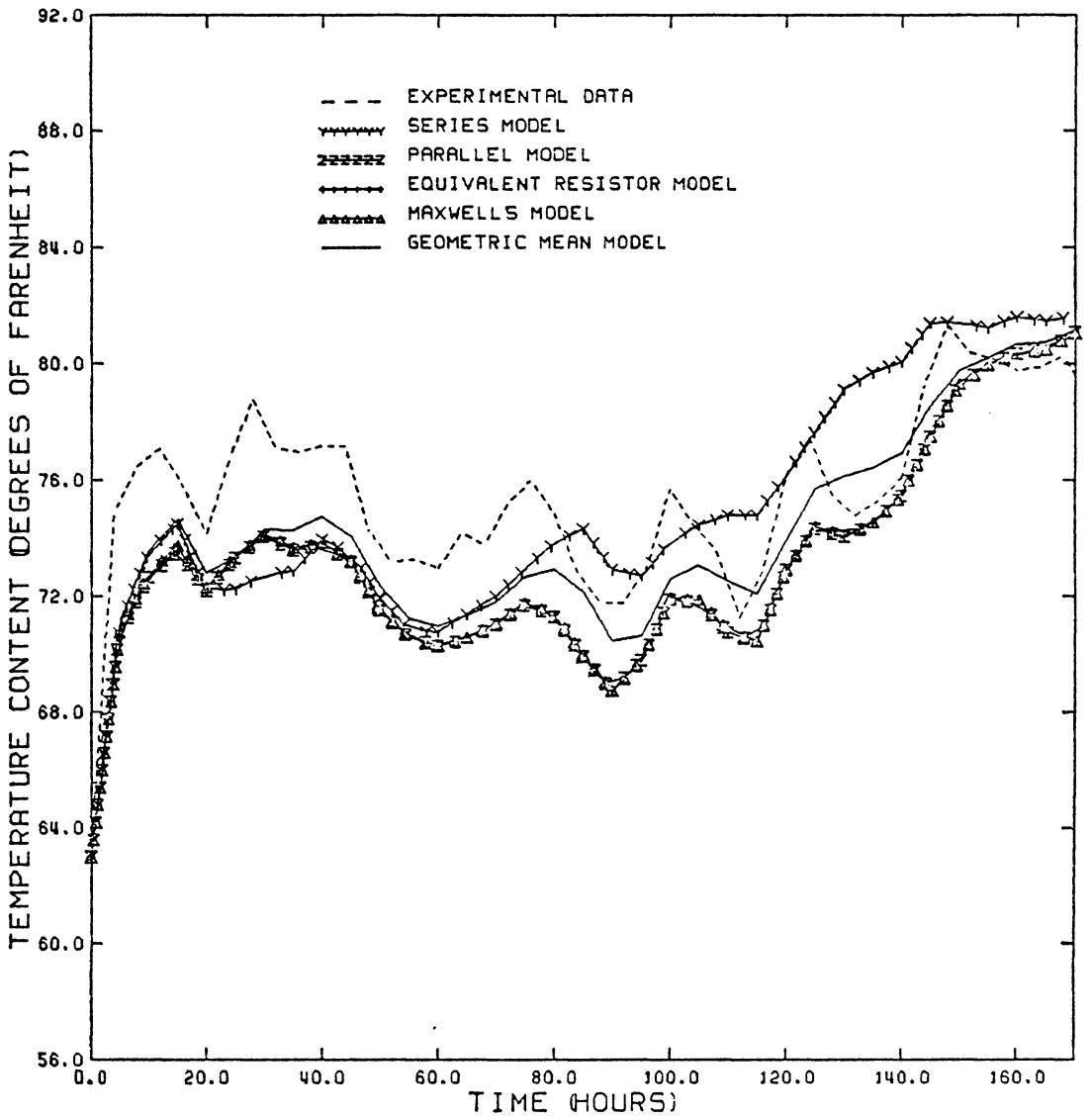

Figure 58 : Experimental and predicted temperatures in the top layer at a wall distance of 3 inches using five mixing models with a phase conversion factor of 0.25. The geometric mean model has the best predicted temperature when compared with the actual temperature.

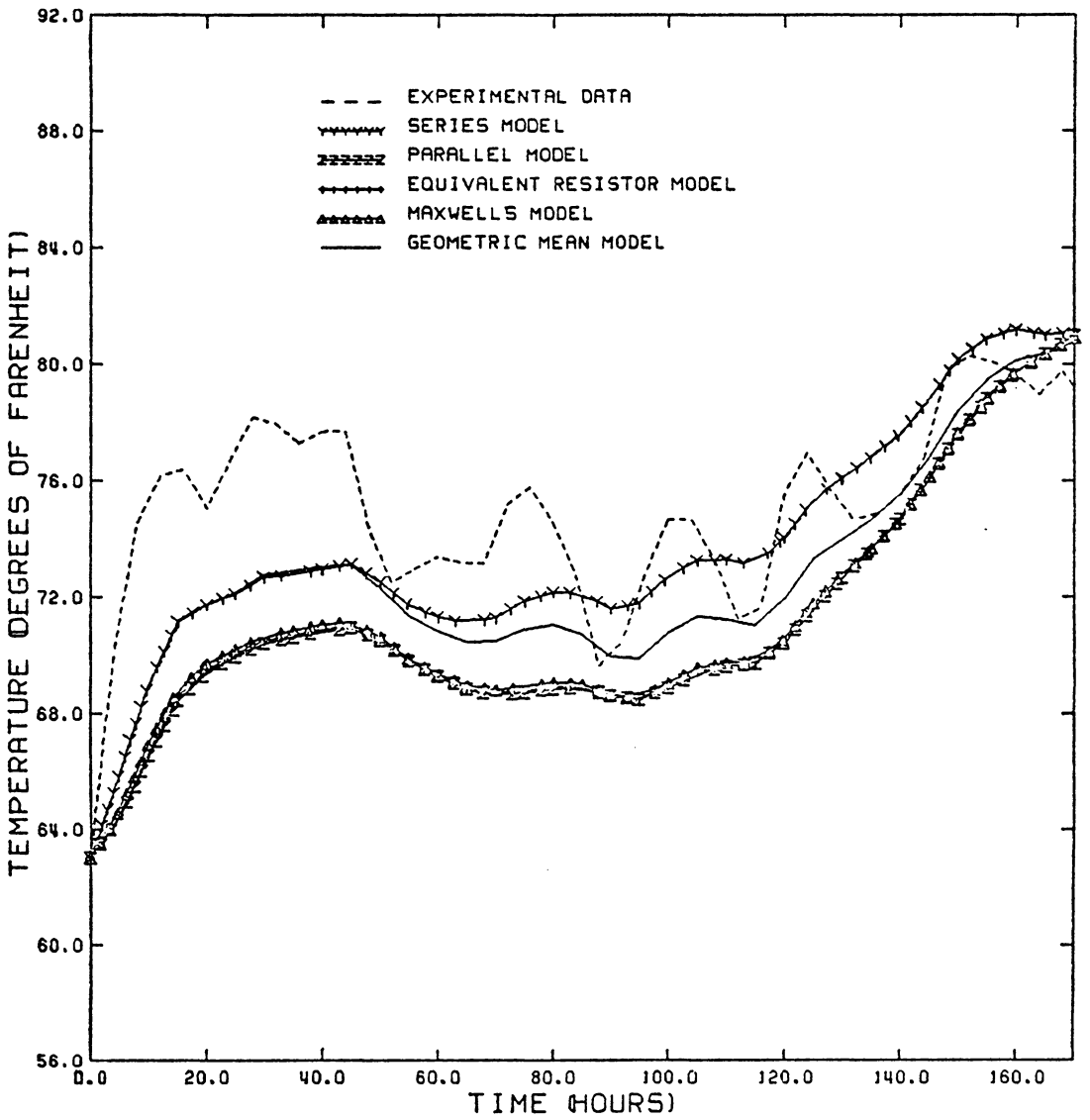

Figure 59 : Experimental and predicted temperatures in the middle layer at a wall distance of 3 inches using five mixing models with a phase conversion factor of 0.25. The geometric mean model has the best predicted temperature when compared with the actual temperature.

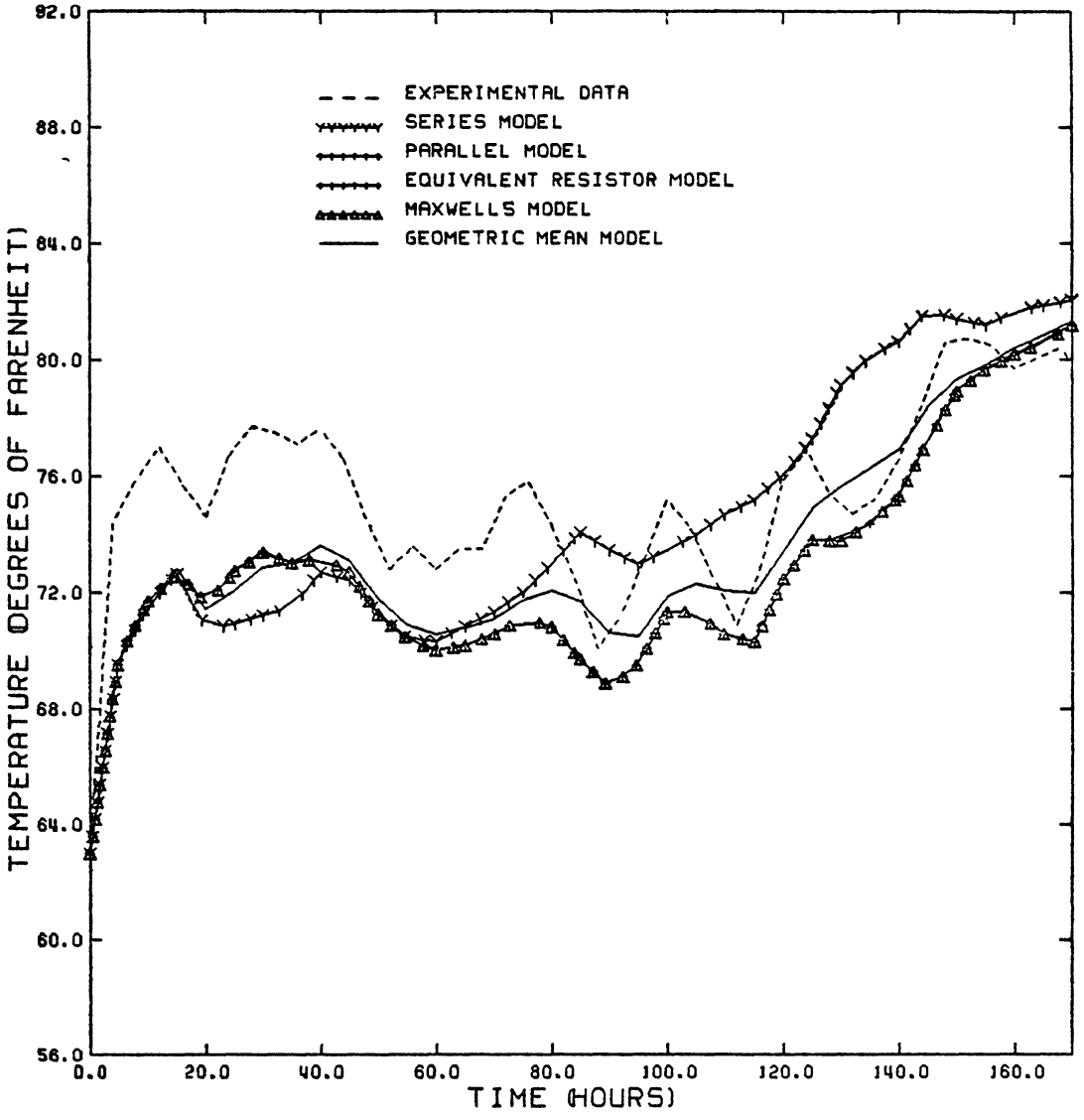

Figure 60 : Experimental and predicted temperatures in the top layer at a wall distance of 8 inches using five mixing models with a phase conversion factor of 0.25. The geometric mean model has the best predicted temperature when compared with the actual temperature.

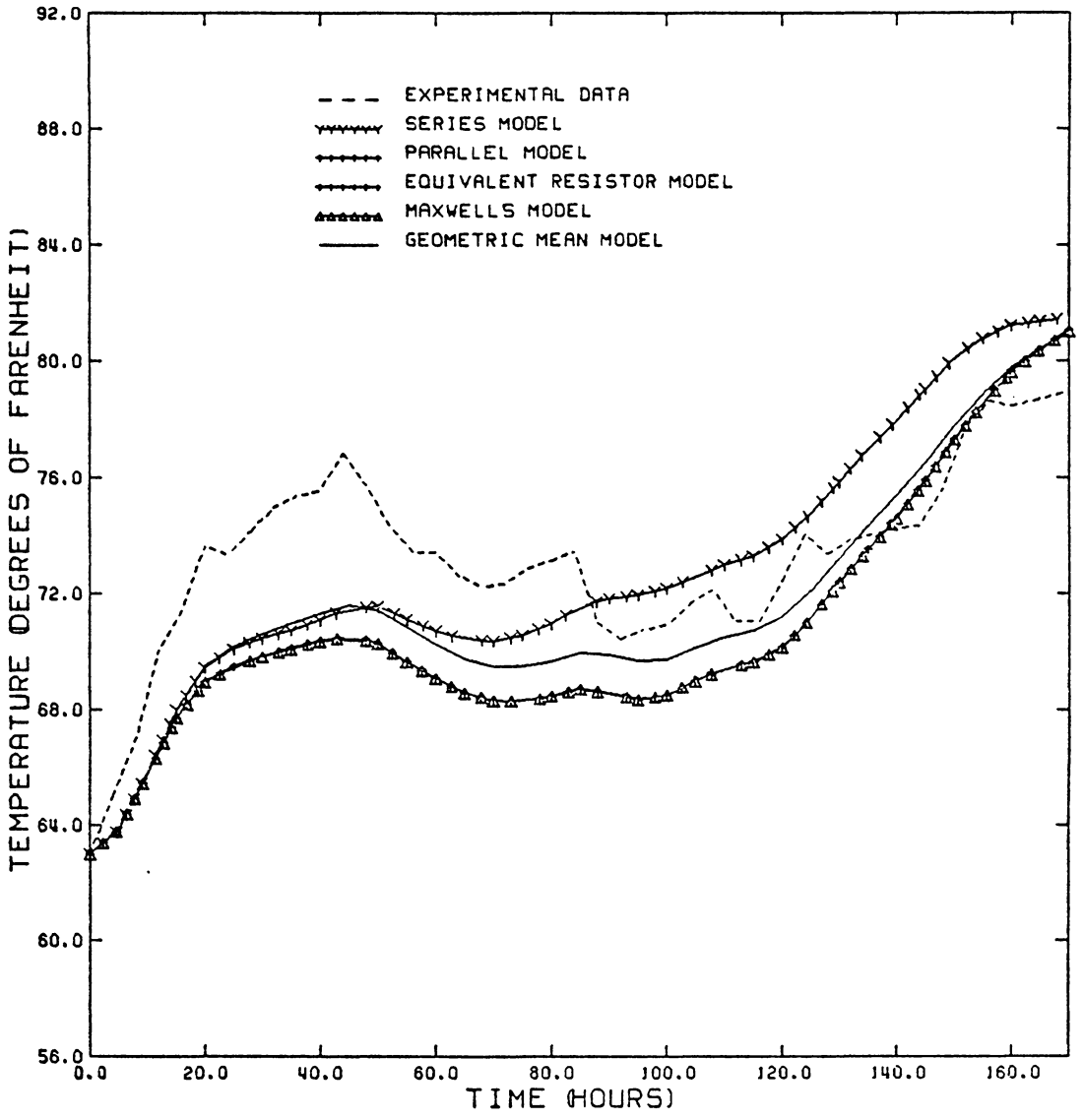

Figure 61 : Experimental and predicted temperatures in the middle layer at a wall distance of 8 inches using five mixing models with a phase conversion factor of 0.25. The geometric mean model has the best predicted temperature when compared with the actual temperature.

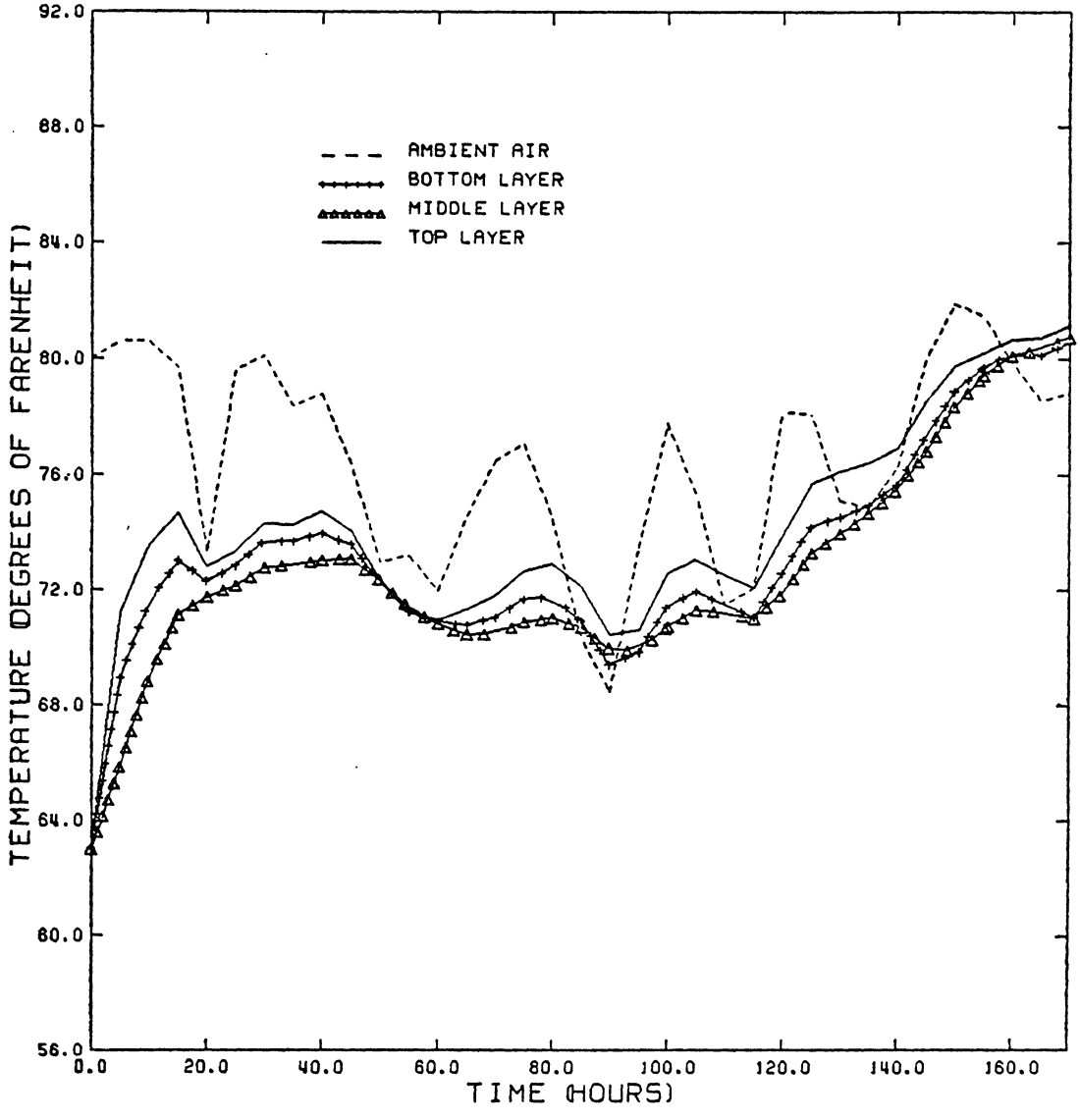

Figure 62 : Ambient and predicted temperatures at a wall distance of 3 inches using the geometric mean model with a phase conversion factor of 0.25 for Test 3. The figure indicates that the change of the predicted temperature is coincident of the change of ambient air temperature.

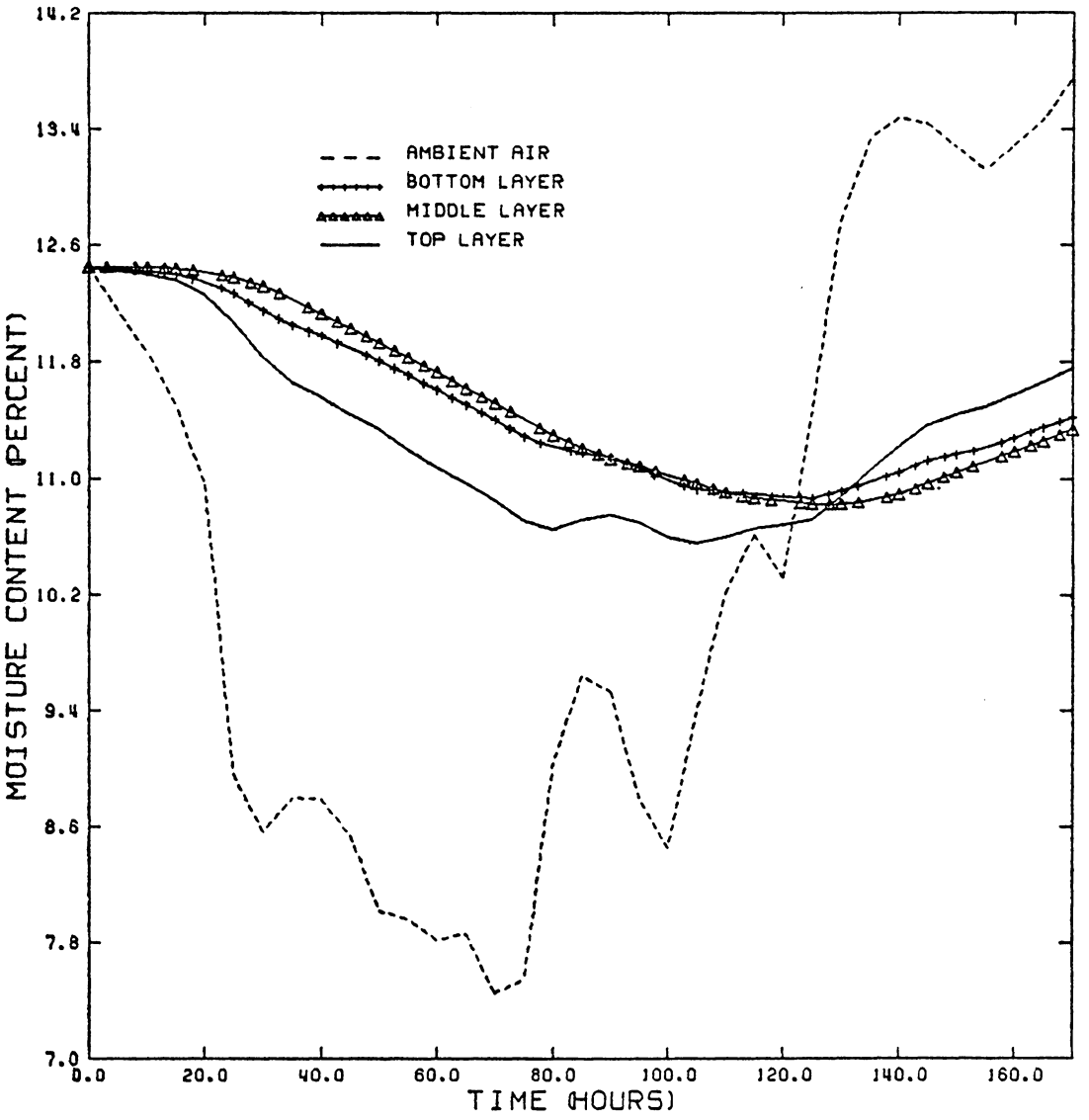

Figure 63 : Equilibrium moisture content and predicted moisture contents for the geometric mean model with a phase conversion factor of 0.25 for a wall distance of 3 inches during Test 3. The figure indicates that the predicted moisture distributions are homogeneous throughout the bin.

ures 64 and 65 for the geometric mean model. The moisture variance due to the phase conversion factor can be neglected, but the temperature changes must be considered.

Because of the fluctuations of the ambient air temperature (Fig. 9) and the equilibrium moisture content(Fig. 10), it is difficult to draw any conclusion about moisture change based on the environmental data. The entire storage process can be subdivided into two stages based on the moisture transport phenomenon.

1. Starting point to 40 hours

   The heat transported from the ambient air to the interior of the bin is used to generate a potential field for moisture migration during this stage. Due to the shortage of thermodynamic force(internal moisture gradient), the external elements lose their moisture to the surrounding air by natural convective moisture transfer only, and the internal moisture is almost uniform within the interior in the bin. The moisture changes of the system during this time interval only depend on the natural convective moisture transfer on the surface elements, thus the rates of moisture loss of the models are almost identical. The latent heat for water evaporation is much larger than the specific heat of the system; hence, a small

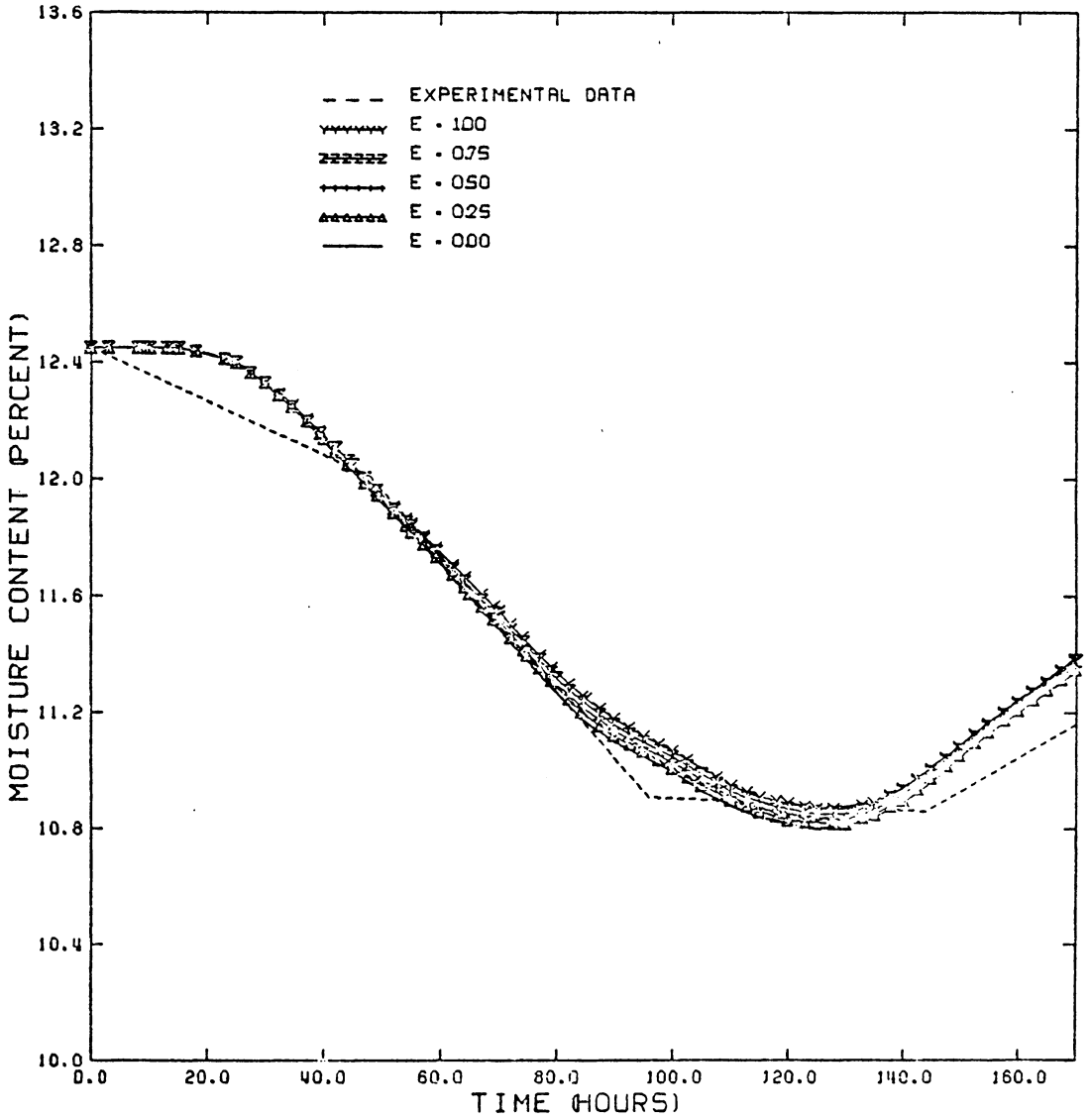

Figure 64 : Experimental and predicted moisture contents in the middle layer at a wall distance of 8 inches using the geometric mean model and five phase conversion factors for Test 3. It is obvious from this figure that moisture content is not related to the phase conversion factor.

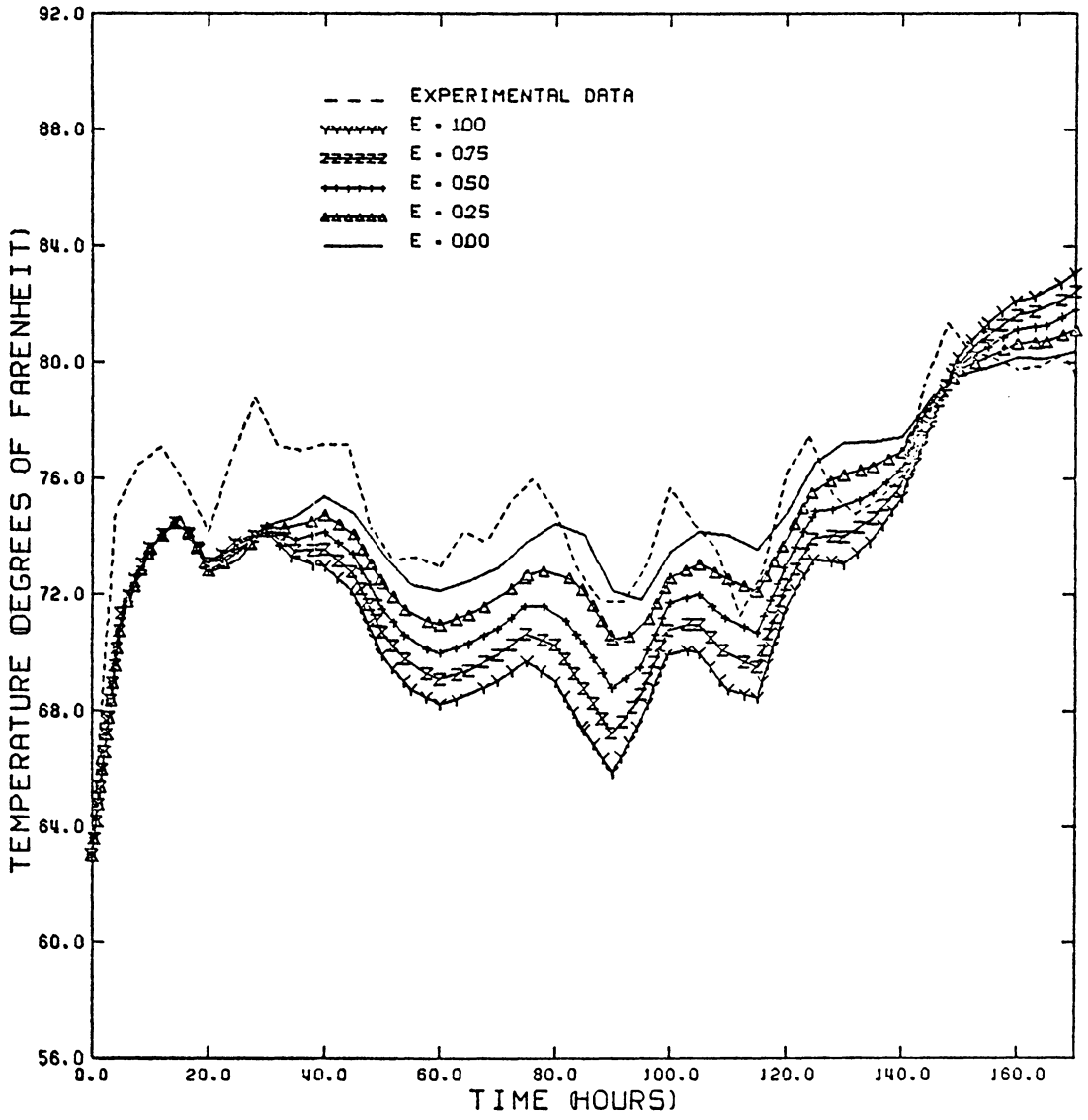

Figure 65 : Experimental and predicted temperatures in the top layer at a wall distance of 8 inches using the geometric mean model and five phase conversion factors for Test 3. It is obvious from this figure that temperature is related to the phase conversion factor.

change in moisture flow will cause a noticeable respondent change in the temperature distribution. The temperature curves of these models separate earlier than the moisture curves.

2. 40 hours to Termination

The net rate of moisture migration should include the convective moisture flow(external moisture flow) on the bin surface and the diffusive moisture flow(internal moisture flow) within the interior of the bin. The internal moisture flux is an important portion of the total moisture movement during this interval. The moisture distribution curves of the five mixing models are separated due to the different bulk moisture diffusivities. As a result of the increases in the moisture flow rates, the magnitude of the deviations in the temperature curves are enlarged.

The differences among the moisture distributions of the models are caused only due to the differences in the bulk moisture diffusivities. However, the temperature changes are relied on both the moisture diffusivity and the phase conversion factor.

5.4 PHASE CONVERSION FACTOR

The phase conversion factor is defined as the ratio of the amount of moisture flow in the vapor phase to the net amount of the moisture flux. The comparisons of the models at the factors of 0.25, 0.50 and 0.75 were presented in the preceding figures. The moisture flow is accompanied by the largest amount of heat flow at a value of one, and the amount of the accompanying heat flow is a minimum at zero. The theory of coupled transport phenomenon states that both heat and mass transfer are influenced by the temperature gradient and the moisture gradient. The effect of the temperature gradient on the moisture flow rate is influenced by both the moisture diffusivity and the thermal gradient coefficient. If the thermal gradient coefficient is too small, the moisture diffusivity is the only mechanism to control moisture removal. In 1970, Husain et al. investigated the thermal gradient coefficient of a kernel of corn and found that it was less than 0.0000767 $^{\circ}F^{-1}$. Due to the relatively low gradient coefficient, the moisture curves does not show the noticeable deviations that occur with different phase conversion factors. It is suggested that the phase conversion factor is directly determined by the temperature distribution. Figures (25, 36 and 52) indicate that the moisture distributions are independent of the phase conversion

factor. Figures (21, 39 and 58) show that the changes of temperature are highly related to the phase conversion factor. Figures 66 and 67 illustrate that the phase conversion factor, $\varepsilon = 0$, is more suitable for use in the parallel model, the modified Maxwell's model, the equivalent resistor model and the geometric mean model. Figures 68 and 69 illustrate that the phase conversion factor, $\varepsilon = 1$, is the best choice for the series model. One conclusion drawn is that a high bulk moisture diffusivity accompanies a low phase conversion factor, and a low moisture diffusivity is combined with a high phase conversion factor.

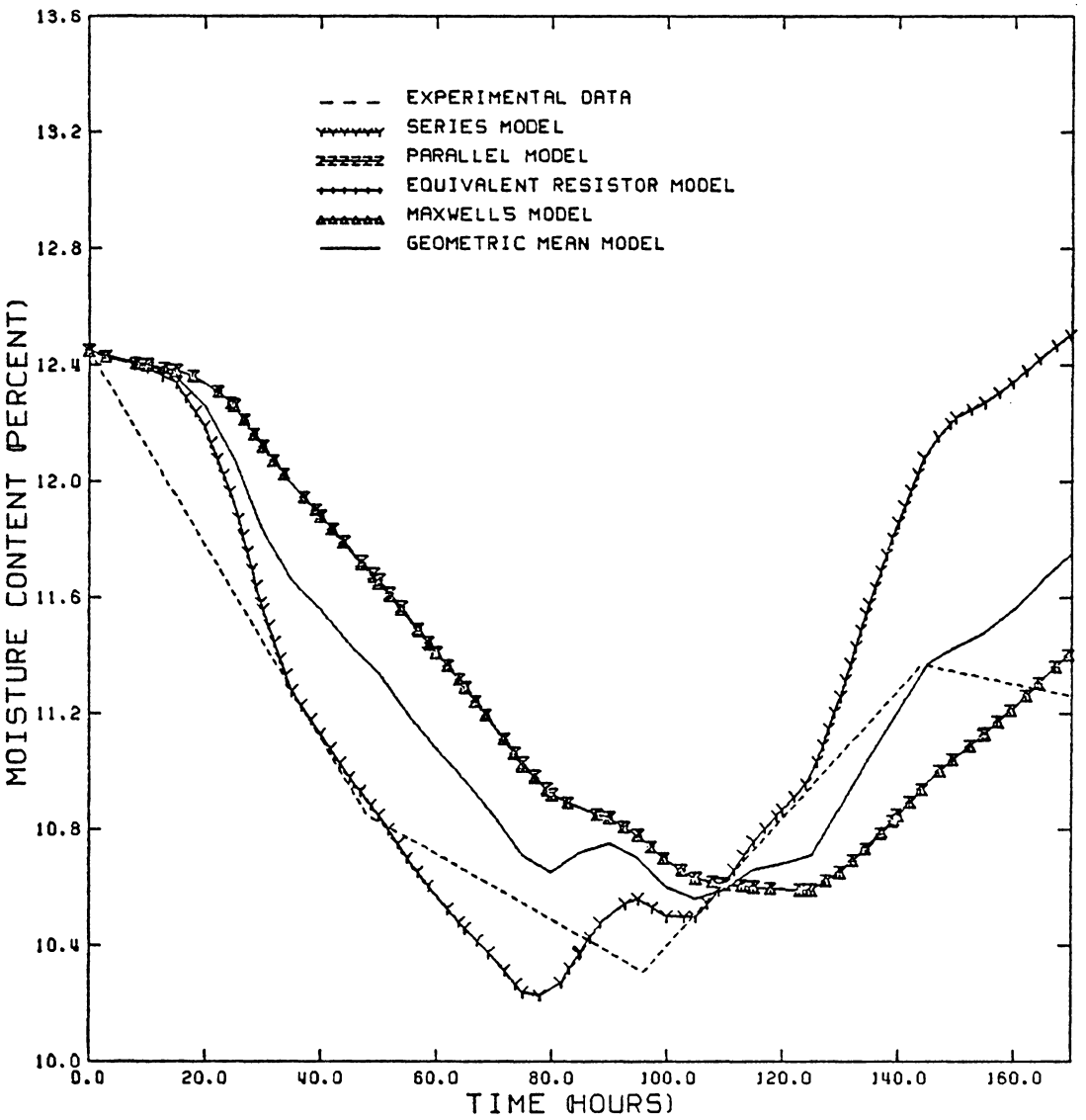

Figure 66 : Experimental and predicted moisture contents in the top layer at a wall distance of 3 inches using five mixing models with a phase conversion factor of zero. The series model has the best predicted moisture content during desorption, and the geometric mean model has the predicted moisture content during absorption.

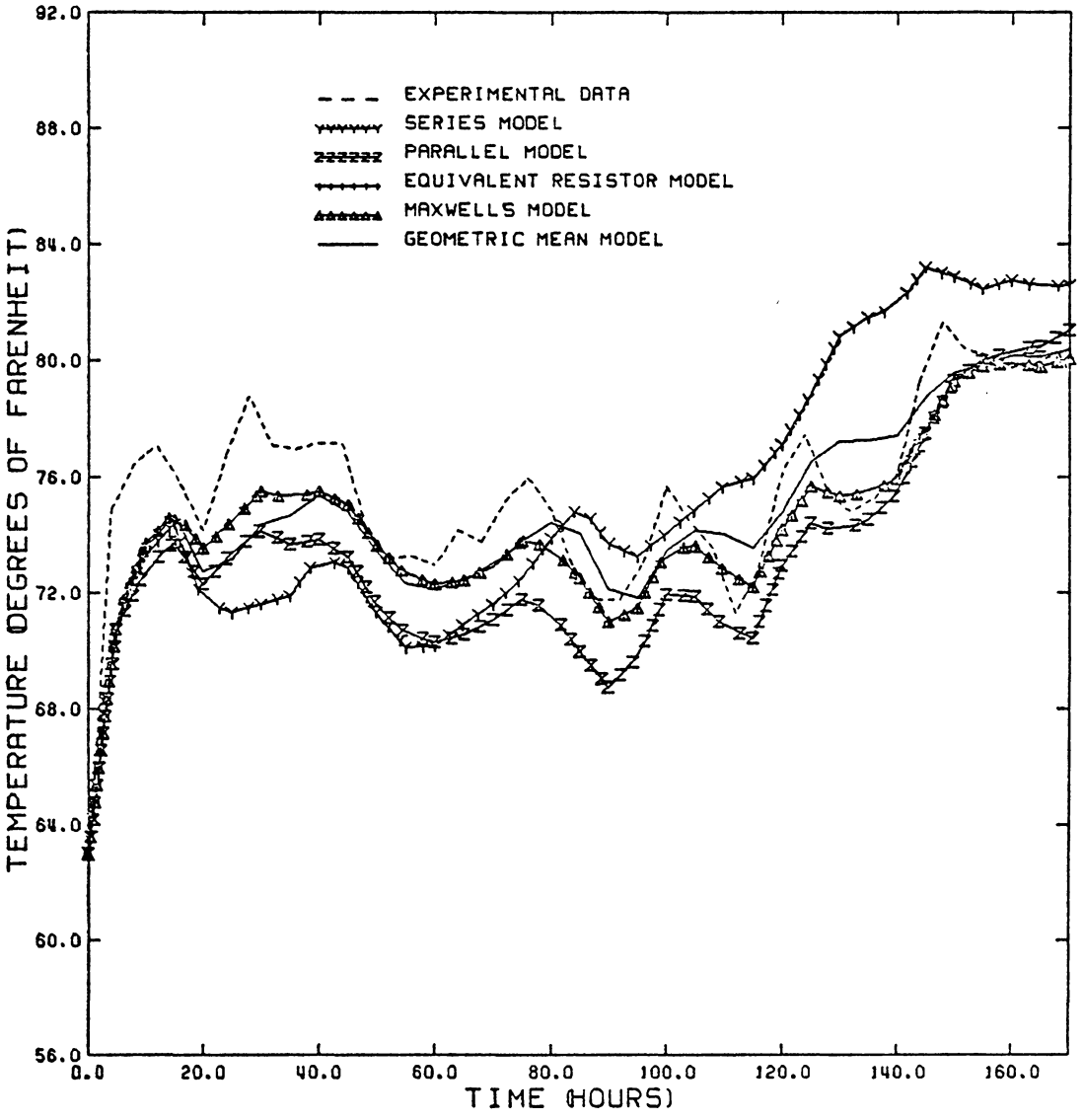

Figure 67 : Experimental and predicted temperatures in the top layer at a wall distance of 3 inches using five mixing models with a phase conversion factor of zero. The geometric mean model has the best predicted temperature when compared with the actual temperature.

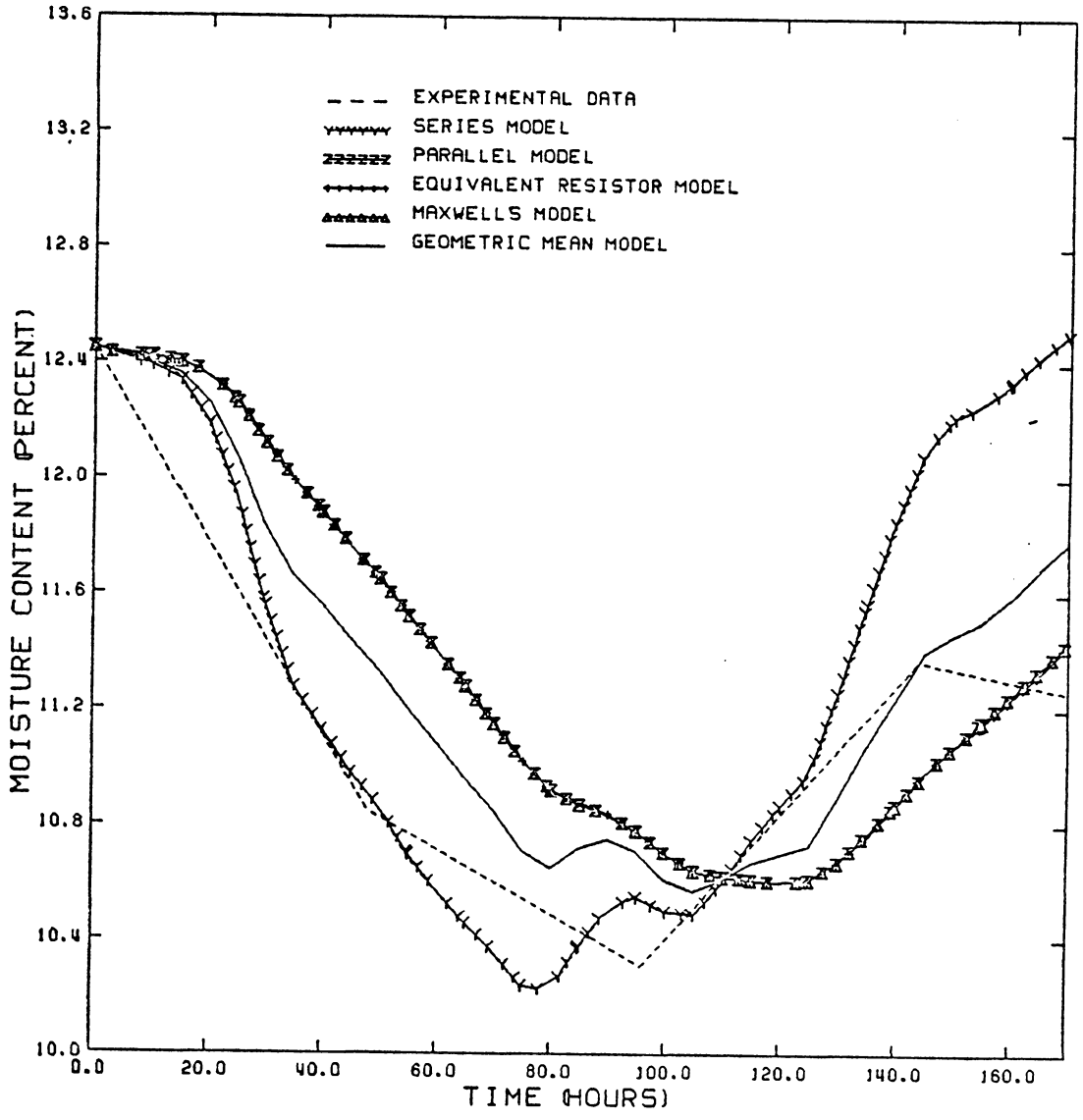

Figure 68 : Experimental and predicted moisture contents in the top layer at a wall distance of 3 inches using five mixing models with a phase conversion factor of 1.0. The series model has the best predicted moisture content during desorption and the geometirc mean model has the best predicted moisture content in absorption.

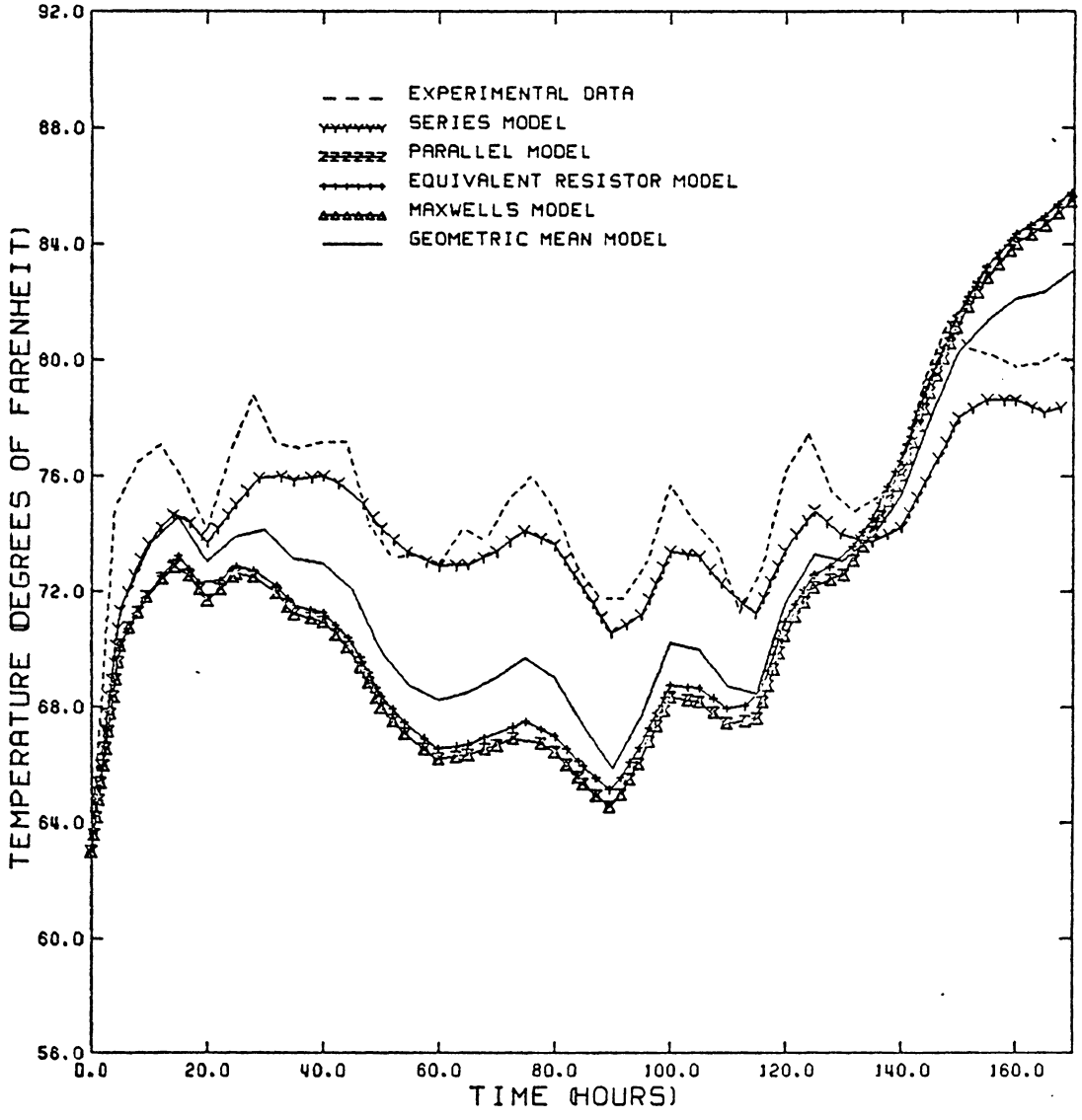

Figure 69 : Experimental and predicted temperatures in the top layer at a wall distance of 3 inches using five mixing models with a phase conversion factor of 1.0. The series model has the best predicted temperature when compared with the actual temperature.

Chapter VI

RESULTS AND DISCUSSION

The objective of this study was to develop a useful mathematical model to simulate and predict the storage behavior in a bed of corn. With only five available data points to plot each experimental moisture curve, the unknown moisture contents between any two experimental data points were determined using linear interpolation. Due to the unstable nature of the experimental environment, the linear interpolation does not seem to be a good approximation. When the predicted data are compared with the experimental results, it is hard to identify the best combination of the mixing models and the phase conversion factors.

The moisture distributions in the surface layers for the high moisture diffusivity models(parallel model, equivalent resistor model and modified Maxwell model) are matched to the experimental results, but the predicted internal moisture contents of these models were lower in a desorption process and higher in a absorption process than the experimental data. In other words, the rates of moisture migration in the high moisture diffusivity models are always larger than the actual moisture flux. Thus, the moisture distribution inside the bin is rather uniform due to the

high moisture diffusivity. It should be emphasized that a heat flux accompanies a moisture flux, and even a small moisture flow in the vapor phase can carry a lot of heat. The moisture fluxes of the models with high moisture diffusivity are exaggerated; therefore, the curves of temperature distribution are also distorted by the extra gain or loss in heat.

A low moisture diffusivity model(series model) has a better temperature prediction when the model is accompanied with a higher value of the phase conversion factor. However, the predicted internal moisture distribtion from this model is a serious drawback. The internal moisture flow rate for the series model is close to zero, and that conflicts with the experimental results. The preceding figures indicate the region of the equilibrium relative humidities of the surrounding air is from 7.5% to 13.8% dry basis, and the moisture content region of corn is from 10.2% to 12.5% dry basis in Test 3. Although the amount of moisture flow due to the equilibrium moisture gradient, the difference between the corn moisture content and the equilibrium moisture content based on the ambient air is low, the magnitude of the internal moisture flow can not be neglected as shown by reviewing the experimental results(Chapter 5 and Appendices E and F).

Making a comparison of the mixing models and the phase conversion factors, it is concluded that the change of the moisture distribution is independent of the value of the phase conversion factor, but the change of temperature distribution is very sensitive to the factor. Based on the predicted temperature distribution, the geometric mean model is better than the others at the low value of the phase conversion factor, and the series model is the best choice of the five models at the high value. Considering both temperature change and moisture change throughout the entire bin at the same time, the model based on the combination of the geometric mean model and the phase conversion factor equal to zero is the best selection.

The moisture diffusivity of the geometric mean model is still 100 times the moisture diffusivity of a kernel of corn. It is suggested that most of moisture flux flows through the porous portion of the bin due to the high moisture diffusivity of the air and vapor moisture mixture It is a well known fact that the state of moisture occupying the porous portion is vapor. One conclusion is that the phase conversion factor is equal to one, but this conclusion conflicts with the experimental result that indicates the phase conversion factor is zero. When describing the storage behavior in a bed of corn using experimental data and a mathe-

matical simulation, the possible paths for moisture flow inside the bin must be postulated.

The theory of convective heat and mass transfer inside a circular tube, which is rather complicated for a tube with regular and uniform shape, can not be used for a flow channel whose shape is irregular. Hence, three more assumptions are added to the assumptions made in Chapter 4:

1. Air cannot flow through the storage bin; i.e., there is no convective heat and mass flow inside the bin. The flows of heat and moisture diffusion are the only heat and moisture movements occurring within the interior of the bin.
2. The porous portion of the bin is separated into many independent individual spaces which are completely surrounded by corn kernels.
3. The effect of the vapor moisture gradient in the porous portion of the bin, which is dependent on the thermodynamic temperature, is much larger than the effect of the internal liquid moisture gradient in the solid portion.

6.1 A POSTULATED PATH OF MOISTURE FLOW

In 1939, Henry presented the theory of vaporization-condensation which assumed the moisture migration was in the vapor phase. A system consists of five parts: body A, body B, body C, body D and void V. The ingredients of Body A, body B, body C and body D are identical so that the bodies have the same physical and thermal properties. Void V is occupied by a mixture of air and water vapor. The molecular diffusivity of the air and water vapor mixture is significantly larger than the moisture diffusivities of the bodies. Thus, the amount of moisture migration flows through the porous portion of the bin is larger than the value through the solid portion. The gaseous mixture is assumed to be in a thermodynamic equilibrium state at any moment due to the high moisture diffusivity in comparison with the moisture diffusivities of the bodies. Because the moisture included in an individual body is in a liquid phase only, the moisture loss from the body surface to the void is evaporation and moisture gain(adsorption) from the void to the body surface is condensation. Figure 70 is a schematic illustrating the paths of moisture flows. Studies of the behavior of moisture removal indicate that a body releases or gains its moisture by the following paths.

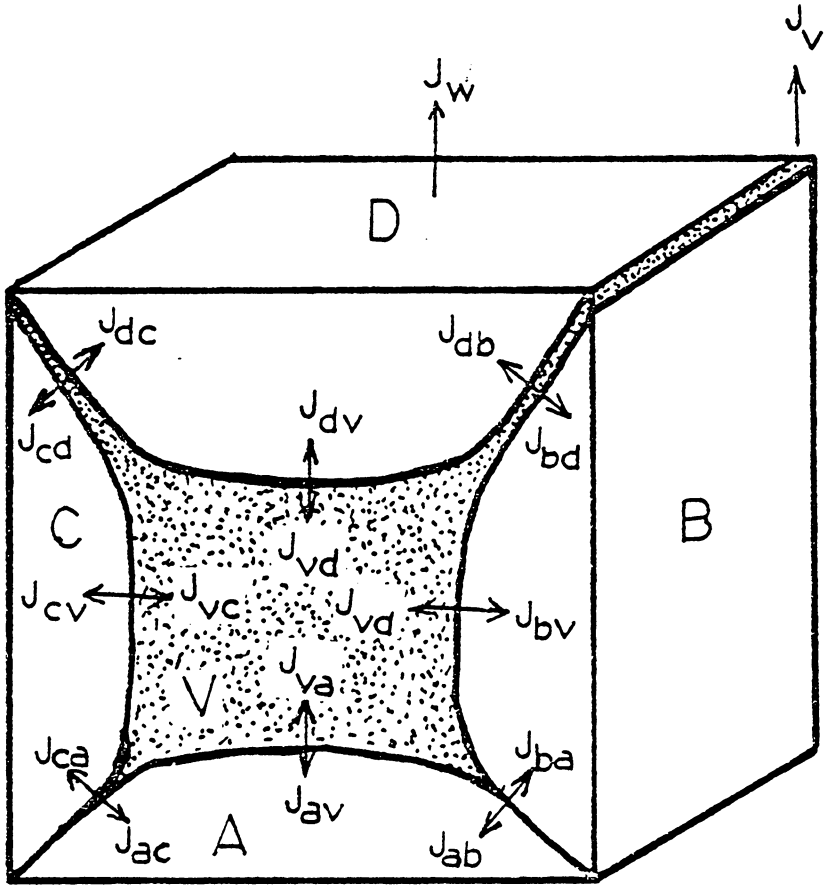

Figure 70 : A schematic model illustrating the postulated paths of moisture flow within the interior of the bin. Jw > Jv if no ventilation, and Jw < Jv if ventilation.

The behavior of the moisture migration of the five parts are

1. For body A

$$J_a = J_{av} + J_{ab} + J_{ac} \tag{75}$$

2. For body B

$$J_b = J_{bv} + J_{ba} + J_{bd} \tag{76}$$

3. For body C

$$J_c = J_{cv} + J_{ca} + J_{cd} \tag{77}$$

4. For body D

$$J_d = J_{dv} + J_{db} + J_{dc} + J_w \tag{78}$$

5. For void V

$$J' = J_{va} + J_{vb} + J_{vc} + J_{vd} + J_v \tag{79}$$

where

J_{xy} : The moisture flux from body x to body y,

$J_{xy} = -J_{yx}$

J_x : net moisture flow of body x, and

J_v : moisture flux flows out of the system in the vapor phase (A negative value indicates the direction of flow is reversed).

Due to the near equal state of equilibrium of the gaseous mixture, J' is equal to zero. Consequently, equation (79) is reduced to

$$0 = J_{va} + J_{vb} + J_{vc} + J_{vd} + J_v \qquad (80)$$

The above equations (75), (76), (77), (78) and (80), can be further rearranged to yield

$$J_a + J_b + J_c + J_d = J_w + J_v \qquad (81)$$

If Bodies B and C are also assumed to be in a thermodynamic equilibrium state,

$$J_b = 0 \qquad (82)$$

and

$$J_c = 0 \qquad (83)$$

The equation is further simplified to

$$J_a + J_d = J_w + J_v \qquad (84)$$

The phase conversion factor is now defined as

$$\varepsilon = \frac{J_v}{J_a + J_d} = \frac{J_v}{J_w + J_v} \qquad (33)$$

The individual void space is assumed to be surrounded thoroughly by the bodies; then, J_v is very small and the value of phase conversion factor, ε, is close to zero. Through this postulated path of moisture migration, the internal

moisture flow inside the element is in the vapor phase and the moisture flow through the boundary between two elements is in the phase of liquid.

Chapter VII

SUMMARY AND CONCLUSIONS

The experiments were undertaken to develop a mathematical model for the heat and mass transfer in a bulk of corn. The emphasis was primarily on measuring temperature and moisture distributions in a grain storage bin. Although the study has been confined to a single class of grain, corn, the method of analysis can be useful for other grains. Predicted and experimental data were interpreted and correlated with the existing theories.

A number of conclusions regarding the effects of moisture and temperature in a bulk of corn during the storage period are supported by these investigations:

1. The geometric mean model is the best of the five models indentified to explain and determine the bulk physical poperties in a bed of corn, based on the physical properties of individual components of air and corn.
2. Most of moisture flow within the interior of the bin is in liquid state, so that the region of the phase conversion factor is from 0.0 to 0.25.
3. The best selection of a mixing model and a phase conversion factor is the combination of the geometric mean model and a phase conversion factor of zero.

4. The annular element and the implicit finite difference approach are appropriate for solving the coupled differential equations of heat and mass transfer in storage of corn.

Many problems may occur when a experiment is conducted to validate a grain storage model based on the theory of heat and mass transfer, for example

1. Inaccurate measurements of the rates of heat flow and moisture migration.
2. Inaccurate determinations of the moisture gradients.
3. An unstable experimental environment.
4. Difficulties of measuring the physical properties, such as the moisture diffusivity, the phase conversion factor and the natural convective moisture trasfer coefficient.

RECOMMENDATIONS

Not all of the above problems are uncontrollable, but it is not easy even to deal with one of the problems. Although drawbacks to a storage model for a bulk of grain based on the theory of coupled heat and mass transfer exist, there are sufficient reasons to continue the work:

1. The moisture transfer equation for storage in a bed of grain can be simplified as Fick's second law of

mass diffusion because of small temperature fluctuation and a negligible temperature gradient coefficient during the storage period.

2. A bulk moisture diffusion equation for a bed of grain can be derived following the same mathematical analogy which was used by Fick to develop the law of mass diffusion and Fourier to develop the law of heat diffusion. The bulk moisture diffusivity must be determined with experiments.
3. Experiments similar to those used to derive the drying constants from the theory of forced convective moisture transfer can be used to measure the free convective moisture transfer coefficient for storage of a bulk of corn.

BIBLIOGRAPHY

Aldis, David F. and George H. Foster. 1980. Moisture Changes in Grain from Exposure to Ambient Air. TRANSACTIONS of the ASAE 23(3): 753-760.

Ames, William F. 1977. Numerical Methods for Partial Differential Equations. Academic Press Inc., New York.

Becker, H. A. 1959. A Study of Diffusion in Solids of Arbitrary Shape, with Application to the Drying of Wheat Kernel. Journal Applied Polymer science 1: 212-226.

Bloome, Peter D. and Gene C. Shove. 1971. Near Equilibrium Simulation of Shelled Corn Drying. TRANSACTIONS of the ASAE 14(4): 709-712.

Brailsford, A. D. and K. G. Major, 1964. The Thermal Conductivity of Aggregates of Several Phases, Including Porous Materials. British Journal Applied Science 15: 313-319.

Brooker, Donald B., Fred W. Bakker-Arkema and Carl W. Hall. 1974. Drying Cereal Grain. AVI Publishing Co., Inc., Westport, Connecticut.

Chapman, A. J. 1967. Heat Transfer, 3rd edition, Macmillan Publishing Co. Inc., New York .

Chu, Shu-Tung and Andrew Hustrulid. 1968. Numerical Solution of Diffusion Equations. TRANSACTIONS of the ASAE 11(4): 705-708.

Chu, Shu-Tung and Andrew Hustrulid. 1968. General Characteristic of Variable Diffusivity Process and the Dynamic Equilibrium Moisture Content. TRANSACTIONS of the ASAE 11(4): 709-710, 715.

Chung, Do Sup, and Harry H. Converse. 1971. Effect of Moisture Content on Some Physical Properties of Grains. TRANSACTIONS of the ASAE 14(3): 612-614, 620.

Comini, G. and R. W. Lewis. 1976. A Numerical Solution of Two-Dimensional Problems Involving Heat and Mass Transfer. International Journal of Heat and Mass Transfer 19: 1387-1392.

Crank, J. C. 1979. Mathematical of Diffusion, 2nd edition. Oxford University Press, London.

Eckert, E. R. G. and M. Faghri. 1980. A General Analysis of Moisture Migration Caused by Temperature Differences in An Unsaturated Porous Medium. International Journal of Heat and Mass Transfer 23: 1613-1623.

Flood, C. A., M. A. Sabbath, Duane Meeker and R. M. Peart. 1972. Simulation of A Natural-Air Corn Drying System. TRANSACTIONS of the ASAE 15(1): 156-169, 162.

Fortes, Mauri and Martin R. Okos. 1980. Changes in Physical Properties of Corn During Drying. TRANSACTIONS of the ASAE 23(4): 1004-1008.

Fortes, Mauri and Martin R. Okos. 1981. A Non-Equilibrium Thermodynamics Approach to Transport Phenomena in Capillary Prorous Media. TRANSACTIONS of the ASAE 24(3): 756-760.

Fortes, Mauri and Martin R. Okos. 1981. A Non-Equilibrium Thermodynamics Approach to Heat and Mass Transfer in Corn Kernels. TRANSACTIONS of the ASAE 24(3): 761-769.

Fuller, E. N., P. D. Schettler and J. C. Giddings. 1966. New Method for Prediction of Binary Gas-Phase Diffusion Coefficients. Industrial and Engineering Chemistry 58(5): 18-27.

Gorling, P. 1958. Physical Phenomena During the Drying of Foodstuffs. Fundamental Aspects of Dehydration of Foodstuffs, Society of Chemistry Industry, pp 42-53, London.

Henderson, S. M. and S. Pabis. 1961. Grain Drying Theory, Part I: Temperature Effect on Drying Coefficient. Journal Agricultural Engineering Research 6: 169-173.

Henderson, S. M. and S. Pabis. 1961. Grain Drying Theory, Part II: A Critical Analysis of the Drying Curve for Shelled Maize. Journal Agricultural Engineering Research 6: 272-277.

Henderson, S. M. and S. Pabis. 1962. Grain Drying Theory, Part III: The Air/Grain Tempeature Relationship. Journal Agricultural Engineering Research 7: 21-27.

Henderson, S. M. and R. L. Perry. 1980. Agricultural Process Engineering. AVI Publishing Co., Inc., Westport, Connecticut.

Henry, P. S. 1939. Diffusion in Absorbing Media. Proceedings of the Royal Society of London, Series A.: Mathematical and Physical Science 171: 215-241.

Hornbeck, Robert W. 1975. Numerical Methods, QPI Series. Quantum Publishers, New York.

Hougen, O. A., H. J. Cauley and W. R. Marshall. 1939. Limitation of Diffusion Equations in Drying. 1939 Meeting, American Institute of Chemical Engineers, pp 183-209.

Husain, Ashfaq., G. L. Nelson and B. L. Clary. 1970. Evaluating Thermodynamic Parameters of Moisture Transfer for Food Products(Rice, Corn and Potato). ASAE Papor No. 70-385, ASAE, St. Joseph, MI 49085.

Husain, Ashfag., C. S. Chen, J. T. Clayton and L. F. Whitney. 1972. Mathematical Simulation of Mass and Heat Transfer in High Moisture Foods. TRANSACTIONS of the ASAE 15(3): 732-736.

Husain, Ashfaq, C. S. Chen and J. T. Clayton. 1973. Simultaneous Heat and Mass Diffusion in Biological Materials. Journal of Agricultural Engineering Research 18: 343-354.

Hustrulid, A. and A. M. Flikke. 1959. Theoretical Drying Curve for Shelled Corn. TRANSACTIONS of the ASAE 2(1):112-114.

Ingram, G. W. 1979. Solution of Grain Cooling and Drying Problems by the Method of Characteristics in Comparison with Finite Difference Solutions. Journal Agricultural Engineering Research 24: 219-232.

Jakob, Max. 1949. Heat Transfer (I). John Wiley and Sons, Inc., New York.

Kass, W. and M. O'keeffe. 1966. Numerical Solution of Fick's Equation with Concentration-Dependent Diffusion Coefficients. Journal Applied Science 37: 2377-2380.

Kazarian, E. A. and C. W. Hall. 1965. Thermal Properties of Grain. TRANSACTIONS of the ASAE 8(1): 33-37, 48.

Lebedev, P. D. 1961. Heat and Mass Transfer During the Drying of Moist Materials. International Journal of Heat and Mass Transfer 1: 294-301.

Lichtenecker, Karl. 1926. The Derivation of A Logarithmic Mixing Rule by the Maxwell-Rayleigh Method. Physik 27: 115-121.

Luikov, A. V. 1961. Application of Methods of Thermodynamics of Irreversible Processes to Investigation of Heat and Mass Transfer in A Boundary Layer. International Journal of Heat and Mass Transfer 3: 167-174.

Luikov, A. V. 1964. Heat and Mass Transfer in Capillary-Porous Bodies. Advances in Heat Transfer 1: 123-185. Academic Press, Inc., New York.

Luikov, A. V. 1966. Heat and Mass Transfer in Capillary Porous Bodies. Academic Press Inc., New York.

Luikov, A. V. 1968. Analytical Heat Diffusion Theory. Academic Press Inc., New York.

Luikov, A. V. 1975. Systems of Differential Equations of Heat and Mass Transfer in Capillary-Porous Bodies. International Journal of Heat and Mass Transfer 18: 1-14.

Marshall, W. R. and S. T. Friedman. 1950. Drying, Chemical Engineers Handbook, 3rd edition. McGraw-Hill Publishing, Co., New York.

Maxwell, J. C. 1954. A Treatise on Electricity and Magnetism, Vol. 1, 3rd edition. Dover Publishing, Inc., New York.

McAdams, W. H. 1954. Heat Transmission, 3rd edition. McGraw Hill Publishing Co., New York.

McGaw, Richard. 1968. Thermal Conductivity of Compacted Sand/Ice Mixtures. Highway Research Bulletin 215: 35-47.

McGaw, Richard. 1969. Heat Conduction in Saturated Granular Materials. International Conference-Effects of Temperature and Heat on Engineering Behavior of Soils, Washington, D. C., pp 114-131.

Misra, M. K. and D. B. Brooker. 1980. Thin-Layer Drying and Rewetting Equations for Shelled Yellow Corn. TRANSACTIONS of the ASAE 23(5): 1254-1260.

Mittal, Gauri S. and Lambert Otten. 1980. Simulation of Low-Temperature Drying of Corn for Ontorio Conditions. ASAE Paper No. 80-3519, ASAE, St. Joseph, MI 49085.

Moisture Measurement-Grain and Seeds. ASAE-S352, ASAE Yearbook 1982-1983.

Nelson, Stuart O. 1980. Moisture-Dependent Kernel- and Bulk-Density Relationship for Wheat and Corn. TRANSACTIONS of the ASAE 23(1): 139-143.

Norden, P. and H. G. David. 1967. Coupled Diffusion of Moisture and Heat in Hygroscopic Textile Materials. International Journal of Heat and Mass Trasfer 10: 853-866.

Onsager, Lars. 1931. Reciprocal Relations in Irreversible Processes (I). Physics Review 38: 405-426.

Onsager, Lars. 1931. Reciprocal Relations in Irreversible Processes (II). Physics Review 38: 2265-2279.

Philip, J. R. and D. A. De Veries. 1957. Moisture Movement in Porous Materials Under Temperature Gradients. TRANSACTIONS of American Geophysical Union 38: 222-231.

Sabbath, M. A., H. M. Keener and G. E. Meyer. 1979. Simulation of Solar Drying of Shelled Corn Using the Logarithmic Model. TRANSACTIONS of the ASAE 22(3): 637-643.

Sherwood, T. K. 1936. The Air Drying of Solids. TRANSACTIONS of American Institution of Chemical Engineers 32: 150-168.

Sherwood, T. K. and R. L. Pigford. 1952. Adsorption and Extraction, 2nd edition, McGraw-Hill Publishing, Co., New York.

Strohman, R. D. and R. R. Yoerger. 1967. A Non-Equilibrium Moisture Content Equation. TRANSACTIONS of the ASAE 10(3): 675-677.

Thompson, T. L., R. M. Peart and G. H. Foster. 1968. Mathematical Simulation of Corn Drying-A New Model. TRANSACTIONS of the ASAE 11(3): 582-586.

Troeger, J. M. and W. V. Hukill. 1971. Mathematical Description of the Drying Rate of Fully Exposed Corn. TRANSACTIONSS of the ASAE 14(5): 1153-1156, 1162.

Van Ea, G. R. and G. L. Kline. 1979. FALDRY- A Model for Low Temperature Corn Drying Systems. ASAE Paper No. 79-3524, ASAE, St. Joseph, MI 49085.

Van Arsdel, W. B. 1947. Approximate Diffusion Calculations for the Falling-Rate Phase of Drying. TRANSACTION of American Institute of Chemical Engineers 43: 13-24.

Van Arsdel, B. Wallace, Michael J. Copley and Arthur I. Morgan. 1980. Food Dehydration. AVI Publishing Co., Inc., Westport, Connecticut.

Van Rooyen, M. and H. F. Winterkorn. 1957. Theoretical and Practical Aspects of the Thermal Conductivity of Soils and Similar Granular System. Highway Research Bulletin 168: 143-205.

Vemuganti, Gangadhar Rao. and Harry B. Pfost. 1980. Physical Properties Related to Drying 20 Grains. ASAE Papor No. 80-3539, ASAE, St. Joseph, MI 49085.

Wang, J. K. and C. W. Hall. 1961. Moisture Movement in Hygroscopic Materials-A Mathematical Analysis. TRANSACTIONS of the ASAE 4(1): 33-36.

Whitaker, T., H. J. Barre and M. Y. Hamdy. 1969. Theoretical and Experimental studies of Diffusion in Spherical Bodies with A Variable Diffusion Coefficients. TRANSACTIONS of the ASAE 12(2): 668-672.

Whitney, J. D. and J. G. Poterfield. 1968. Moisture Movement in A Porous Hygroscopic Solid. TRANSACTIONS of the ASAE 11(4): 716-719, 723.

Willie, M. R. J. and S. L. Southwick. 1954. An Experimental Investigation of the Self Potential and Resistivity Phenomena in Dirty Sands. Journal Petroleum Technology 6(2): 44-57.

Woodside, W. and J. H. Messmer. 1961. Thermal Conductivity of Porous Media, Part (I): Unconsolidated Sands. Journal of Applied Physics 32: 1688-1699.

Young, James H. 1969. Simultaneous Heat and Mass Transfer in A Porous Hygroscopic Solid. TRANSACTIONS of the ASAE 12(4): 720-725.

Young, James H. and J. B. Whitaker. 1971. Numerical Analysis of Vapor Diffusion in A Porous Composite Sphere with Concentric Shells. TRANSACTIONS of the ASAE 14(5): 1051-1057.

Appendix A

NOMENCLATURE

Letter Symbols

A^{o} -Lennard-John's force constant, Angstron

A -area normal to the direction of heat or mass flow, ft^2

C -concentration of water vapor, lb/ft^3

C'_w -concentration of water vapor in an absorbed state, lb/ft^3

C_{vc} -concentration of water vapor in air filling the interfibre void space, lb/ft^3

C_i -collision integral

C_d -specific heat of solid, $Btu/lb-^{o}F$

C_w -specific heat for the liquid moisture, $Btu/lb-^{o}F$

C_p -bulk specific heat of corn, $Btu/lb-^{o}F$

C_m -moisture capacity, lb/lb-moistness

D -molecular diffusivity, ft^2/hr

D_m -moisture diffusivity, ft^2/hr

D_p -total filtration coefficient, ft^2/hr

D_v -diffusivity for vapor moisture, ft^2/hr

F -thermodynamic force

f -porosity in a bed of corn, decimal

H_m -molecular diffusivity coefficient of water vapor in air, m/s^2

h -latent heat for water vaporization in moist corn, Btu/lb

h_m -free convective mass transfer coefficient, $lb/hr-ft^2$

h_q -free convective heat transfer coefficient, Btu/hr-ft^2-^oF

h_w -latent heat for water vaporization from a free surface, Btu/lb

h'_w -specific differential heat of adsorption, Btu/lb

I_m -mass source or sink, lb/hr-ft^3

I_q -heat source or sink, Btu/hr-ft^3

J_m -moisture flux, lb/hr-ft^2

J_p -moisture flux caused by the difference of vapor pressure, lb/hr-ft^2

J_q -heat flux, Btu/hr-ft^2

J_v -vapor moisture flux, lb/hr-ft^2

J_w -liquid moisture flux, lb/hr-ft^2

K -bulk thermal conductivity, Btu/hr-ft-^oF

K_d -thermal conductivity of solid skeleton, Btu/hr-ft-^oF

K_f -thermal conductivity for porous portion, Btu/hr-ft-^oF

L -coupled coefficient for Onsager's equation

L_{em} -modified Lewis number

M -moisture content, decimal (dry basis)

M_e -equilibrium moisture content, decimal (dry basis)

M_i -initial moisture content, decimal (dry basis)

M_s -moisture content at the surface of the bin, decimal (dry basis) (dry basis)

$M\rho$ -molecular weight, gm/mole

P -atmospheric pressure, atm; vapor pressure, moles/ft^3

P_{bm} -logarithmic mean of pressure at surface and at medium, N/m^2

P_{vd} -partial vapor pressure of solid skeleton, N/m^2

P_{va} -partial vapor pressure of air, N/m^2

Q -internal generated heat, Btu/hr-ft^3

Q_d -heat flow through the solid component only, Btu/hr

Q_f -heat flow through the fluid component only, Btu/hr

R -radium, ft

Re -Renold's number

RH -relative humidity of ambient air, decimal

R_v -universal gas constant

Sc -Schmidt's number

T -temperature, ^oF

T_a -ambient air temperature, ^oF

T_s -surface temperature, ^oF

T' -thermodynamic temperature, ^oR

t -time, hr

U -chemical potential

V -velocity, ft/hr

W -moisture potential, moistness

W_d -weight of an evaporation disk, lb

W_i -initial weight including moist corn and an evaporation disk, lb

W_f -final weight including total dried corn and an evaporation disk, lb

Greek Symbols

α -thermal diffusivity, ft^2/hr

ε -phase conversion factor, decimal

δ -thermal gradient coefficient, $^oF^{-1}$

ν -kinematic viscosity, m^2/hr

ρ -bulk density, lb/ft^3

Subscripts

a -ambient air

d -solid skeleton(total dried corn)

f -porous portion of the bin

m -mass

q -heat

s -the surface of the bin

T -temperature

w -liquid moisture

v -vapor moisture

1 -body 1

2 -body 2

Appendix B

AN ANALYTICAL SOLUTION OF COUPLED HEAT AND MASS TRANSFER EQUATIONS FOR A ONE-DIMENSION PLATE

The system of simultaneous differential equations of heat and mass transfer for a one-dimensional infinite plate are

$$\frac{\partial M}{\partial t} = D_m \frac{\partial^2 M}{\partial x^2} + D_m \delta \frac{\partial^2 T}{\partial x^2}$$

and

$$\frac{\partial T}{\partial t} = \frac{h \varepsilon D_m}{C_p} \frac{\partial^2 M}{\partial x^2} + (\alpha + \frac{h \varepsilon D_m \delta}{C_p}) \frac{\partial^2 T}{\partial x^2}$$

Before solving the equations, the following terms are defined as:

1. Biot's Number for Heat Transfer

$$Bi_q = \frac{h_q R}{\alpha}$$

2. Biot's Number for Mass Transfer

$$Bi_m = \frac{h_m R}{D_m}$$

3. Fedorov's Number

$$Fe = \frac{\varepsilon \delta \rho}{C_p}$$

4. Posnov's Number

$$Pn = \frac{\delta \Delta T}{\Delta M}$$

5. Kossovich's Number

$$Ko = \frac{\rho \Delta M}{C_p \Delta T}$$

6. Fourier's Number

$$Fo = \frac{\alpha t}{R^2}$$

7. Lu's Number

$$Lu = \frac{D_m}{\alpha}$$

and the nomenclatures are

R: half thickness of the plate

ε: phase conversion factor

α: thermal diffusivity

δ: thermal gradient coefficient

ρ: density

C_p: specific heat capacity

D_m: mass diffusivity

h: latent heat of water vaporization

h_m: convective mass transfer coefficient

h_q: convective heat transfer coefficient

M: moisture concentration

T: temperature

The symmetric heat and mass transfer of an infinite plate of thickness 2R is identical with the heat and mass transfer of an infinite plate of thickness R, one surface of which is insulated from heat and mass. The solutions of the differential equations are written as:

$$\frac{T(x,t) - T_o}{T_a - T_o} = 1 - \sum_{n=1}^{\infty} (C_{n2} \cos \nu_1 \mu_n \frac{x}{R} - C_{n1} \cos \nu_2 \mu_n \frac{x}{R}) \cdot e^{-\mu_n^2 Fo}$$

and

$$\frac{M_o - M(x,t)}{M_o - M_e} = 1 - \sum_{n=1}^{\infty} (C^*_{n1}(1 - \nu_2^2)\cos \nu_2 \mu_n \frac{x}{R} - C^*_{n2}(1 - \nu_1^2)\cos \nu_1 \mu_n \frac{x}{R}) \, e^{-\mu_n^2 Fo}$$

where

$$\nu_i^2 = \frac{1}{2} \left((1 + Fe + \frac{1}{Lu}) + (-1)^i \left((1 + Fe + \frac{1}{Lu})^2 - \frac{4}{Lu}\right)^{1/2}\right), \quad (i = 1,2)$$

$$C_{ni} = \frac{2 P_{ni} + Ko (Q_{ni} - K_1 P_{ni})}{\mu_n \psi_n}, \quad (i = 1,2)$$

$$C^*_{ni} = \frac{C_{ni}}{\varepsilon Ko}$$

$$K_1 = \frac{1 - \varepsilon}{\varepsilon} Lu \frac{Bi_q}{Bi_m}$$

$$\psi_n = \nu_1 A_{ni} P_{n2} + \nu_2 B_{n2} Q_{n1} - \nu_2 A_{n2} P_{n1} - \nu_1 B_{n1} Q_{n2}$$

$$A_{ni} = (1 + \frac{1}{Bi_q} + (1 - \nu_i^2) K_1) \sin\nu_i\mu_n + \frac{\nu_i \mu_n}{Bi_q} \cos\nu_i\mu_n$$

$$B_{ni} = (1 - \nu_i^2)\sin\nu_i\mu_n + \frac{(1-\nu_i^2)+Fe}{Bi_m}(\sin\nu_i\mu_n+\nu_i\mu_n\cos\nu_i\mu_n)$$

$$Q_{ni} = (1 + (1 - \nu_i^2)K_1) \cos\nu_i\mu_n - \frac{\nu_i \mu_n}{Bi_m} \sin\nu_i\mu_n$$

$$P_{ni} = (1 - \nu_i)^2\cos\nu_i\mu_n + ((1 - \nu_i^2) + Fe) \frac{\nu_i \mu_n}{Bi_m} \sin\nu_i\mu_n$$

μ_n : characteristics values

Appendix C

REFERENCE OF TABLES

Table C.1 : Thermal gradient coefficient for shelled corn.

Temp. (°F)	M.C. % (d.b.)	Thermal Gradient Coefficient 1/°F
86	4.17	0.00007697
86	8.70	0.00007685
86	11.11	0.00007673
86	13.64	0.00007655
86	19.05	0.00007577
86	25.00	0.00007375
122	4.17	0.00007057
122	8.60	0.00006787
122	11.11	0.00006519
122	13.64	0.00006087
122	19.05	0.00004274
122	25.00	0.00000422
140	4.17	0.00006761
140	8.70	0.00006365
140	11.11	0.00005986
140	13.62	0.00005341
140	19.05	0.00002686
140	25.00	0.00004193

Table C.2 : Natural convective heat transfer coefficient of air.

Configuration	h in Btu/hr-ft^2-°F L and D in feet T in °F Laminar flow $10^9 > Gr\ Pr > 10^4$
Horizontal cylinders D = diameter	$h = 0.27 \left(\frac{Ts - Ta}{D} \right)^{1/4}$
Vertical plates and cylinders L = vertical dimension	$h = 0.29 \left(\frac{Ts - Ta}{L} \right)^{1/4}$
Horizontal plates Heated plates, up Cooled plates, down	$h = 0.27 \left(\frac{Ts - Ta}{L} \right)^{1/4}$
Heated plates, down Cooled plates, up L = side dimension	$h = 0.12 \left(\frac{Ts - Ta}{L} \right)^{1/4}$

Ts : the surface temperature
Ta : the surrounding air temperature
Pr : the Prandtal number
Gr : the Grashof number

(From Heat Transmission, 3rd edition, by W. H. McAdams. 1954)

Table C.3 : Geometric dimensions of corn kernels.

Major axis (inch)	Medium axis (inch)	Short axis (inch)	Source
0.5236	0.3425	0.1850	Fortes and Okos (1980)
0.4567	0.3425	0.1732	Henderson and Pabis (1961)
0.4958	0.3156	0.1711	Nelson (1980)
0.4920	0.3335	0.1765	Average Values

Appendix D

THE COEFFICIENTS OF COUPLED HEAT AND MASS TRANSFER EQUATIONS IN NUMERICAL FORM

Set $a_1 = \frac{\Delta t}{\Delta r^2}$, and

$a_2 = \frac{\Delta t}{\Delta z^2}$

$b_1 = (\alpha + \frac{D_m h \delta}{C_p})$, and

$b_2 = \frac{D_m h}{C_p}$

1. for mass transfer

$C_{i+1jk} = -a_1 D_m (1 + \frac{1}{2i})$

$C_{ijk} = 1 + 2 D_m (a_1 + a_2)$

$C_{i-1jk} = -a_1 D_m (1 - \frac{1}{2i})$

$C_{ij+1k} = -a_1 D_m$

$C_{ij-1k} = -a_2 D_m$

$C'_{i+1jk} = -a_1 D_m \delta (1 + \frac{1}{2i})$

$C'_{ijk} = 2 D_m \delta (a_1 + a_2)$

$C'_{i-1jk} = -a_1 D_m \delta (1 + \frac{1}{2i})$

$$C'_{ij+1k} = -a_2 \, D_m \, \delta$$

$$C'_{ij-1k} = -a_2 \, D_m \, \delta$$

$$B_{ijk} = M_{ijk}$$

2. for heat transfer

$$C_{i+1jk} = -a_1 \, b_2 \, (1 + \frac{1}{2i})$$

$$C_{ijk} = 2 \, b_2 \, (a_1 + a_2)$$

$$C_{i-1jk} = -a_1 \, b_2 \, (1 - \frac{1}{2i})$$

$$C_{ij+1k} = -a_2 \, b_2$$

$$C_{ij-1k} = -a_2 \, b_2$$

$$C'_{i+1jk} = -a_1 \, b_1 \, (1 + \frac{1}{2i})$$

$$C'_{ijk} = 1 + 2 \, b_1 \, (a_1 + a_2)$$

$$C'_{i-1jk} = -a_1 \, b_1 \, (1 - \frac{1}{2i})$$

$$C'_{ij+1k} = -a_2 \, b_1$$

$$C'_{ij-1k} = -a_2 \, b_1$$

$$B_{ijk} = T_{ijk}$$

Appendix E

MEASUREMENT DATA FOR EXPERIMENT 1

Table E.1 : Misture contents in five layers at wall distance of 2 and 6 inches for Test 1.

Time (hr)	M.C. (top)	M.C. (n.t.)	M.C. (mid)	M.C. (n.b.)	M.C. (bot)
R=2.0					
0	13.58	13.58	13.58	13.58	13.58
96	12.01	12.79	13.00	12.78	12.20
192	11.15	11.40	11.69	11.41	11.17
264	10.94	11.21	11.61	11.32	10.76
330	10.41	10.93	11.15	10.99	10.45
R=6.0					
0	13.58	13.58	13.58	13.58	13.58
96	10.26	11.79	12.45	12.48	12.10
192	9.87	11.04	12.01	11.45	11.49
264	10.31	10.92	11.61	11.32	11.07
330	10.31	10.23	10.64	10.35	10.37

top : layer at the top surface
n.t. : layer next to the top layer
mid : layer at the middle
n.b. : layer next to the bottom layer
bot. : layer at the bottom surface
R : the interval from the wall

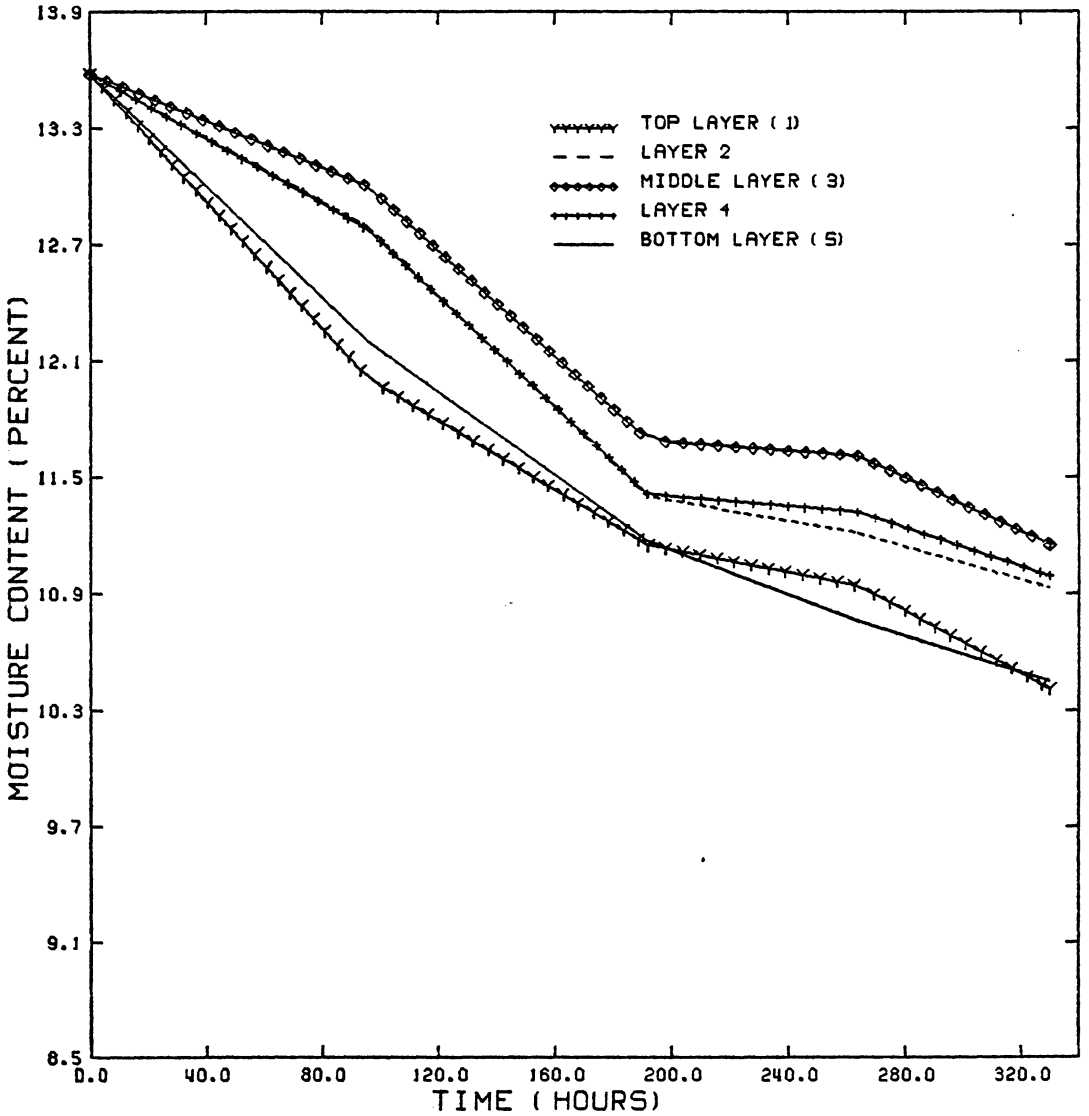

Figure E.1 : Experimental moisture contents in the five layers during Test 1 at a wall distance of 2 inches.

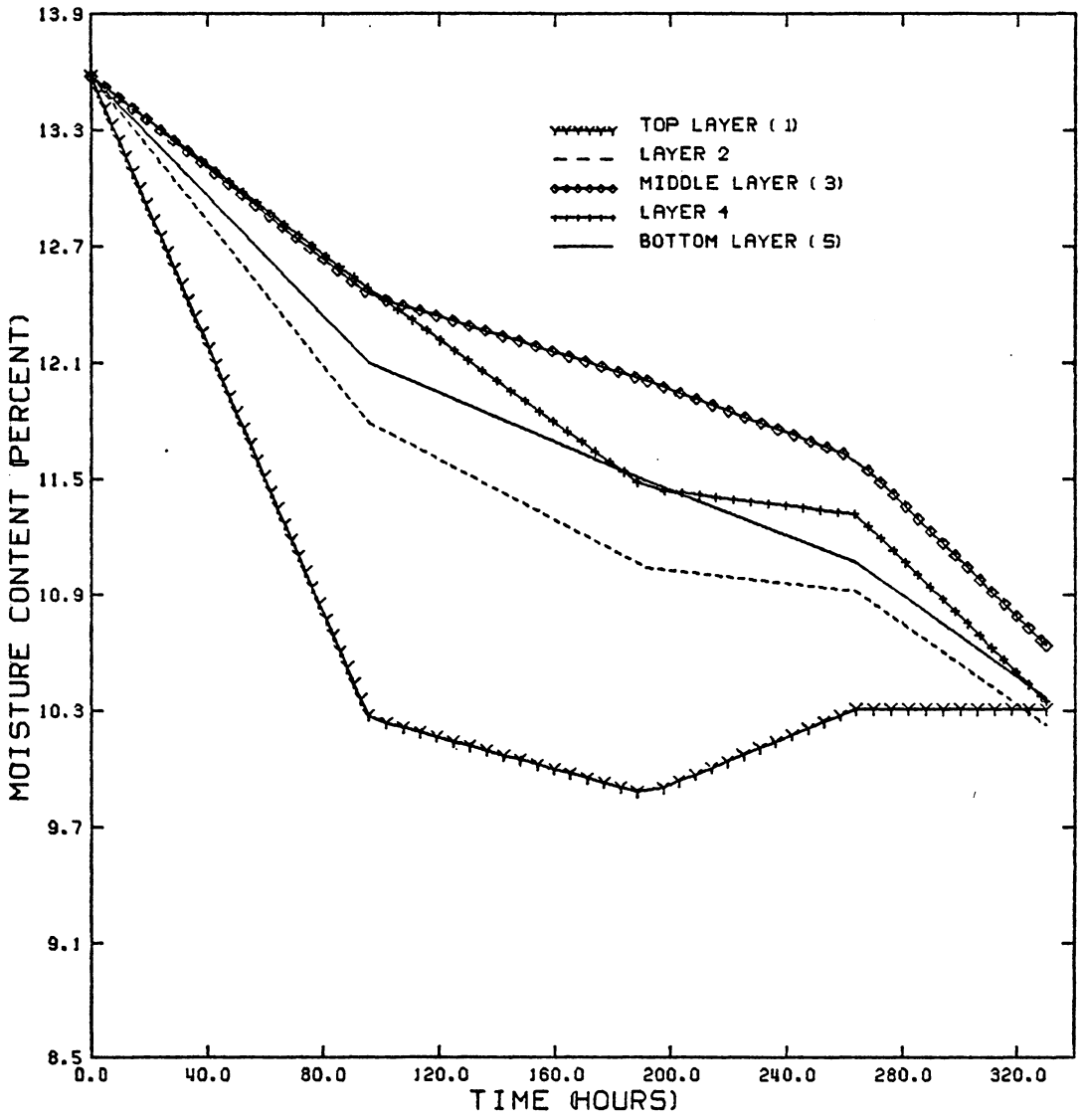

Figure E.2 : Experimental moisture contents in the five layers during Test 1 at a wall distance of 6 inches.

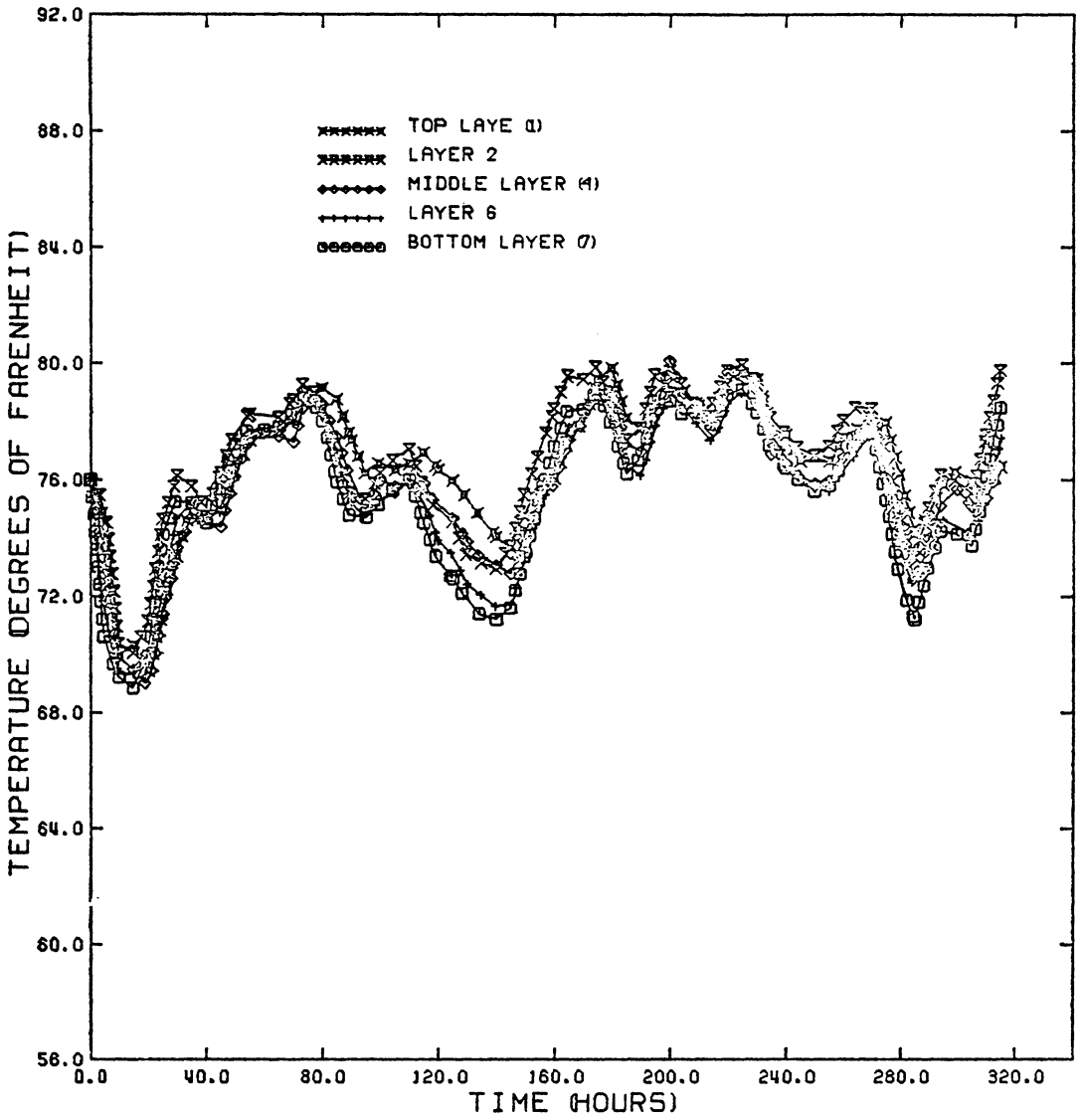

Figure E.3 : Experimental temperatures in the five layers during Test 1 at a wall distance of 2 inches.

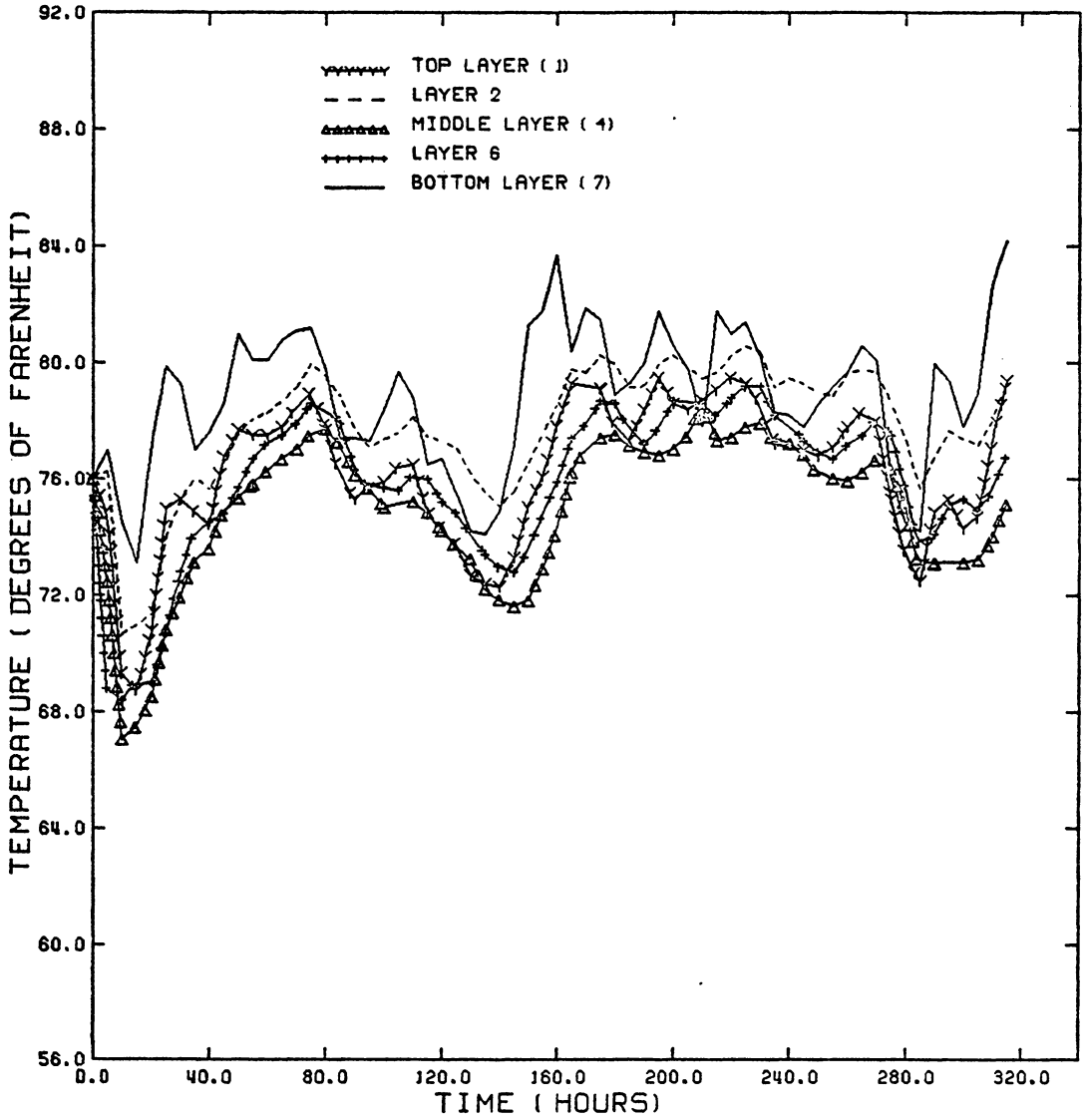

Figure E.4 : Experimental temperatures in the five layers during Test 1 at a wall distance of 6 inches.

Appendix F

MEASUREMENT DATA FOR EXPERIMENT 2

Table F.1 : Misture contents in five layers at wall distance of 3 and 8 inches for Test 1.

Time (hr)	M.C. (top)	M.C. (n.t.)	M.C. (mid)	M.C. (n.b.)	M.C. (bot)
R=3.0					
0	12.85	12.85	12.85	12.85	12.85
84	11.50	12.07	12.36	12.22	12.12
180	10.12	10.52	11.29	11.02	10.54
252	10.11	10.48	10.61	10.35	10.24
333	9.78	10.10	10.46	10.31	10.11
R=8.0					
0	12.85	12.85	12.85	12.85	12.85
84	11.55	12.16	12.34	12.26	11.87
180	10.01	10.78	11.11	11.03	10.37
252	10.09	10.21	10.45	10.53	10.15
333	9.94	10.06	10.26	10.31	10.14

top : layer at the top surface
n.t. : layer next to the top layer
mid : layer at the middle
n.b. : layer next to the bottom layer
bot. : layer at the bottom surface
R : the interval from the wall

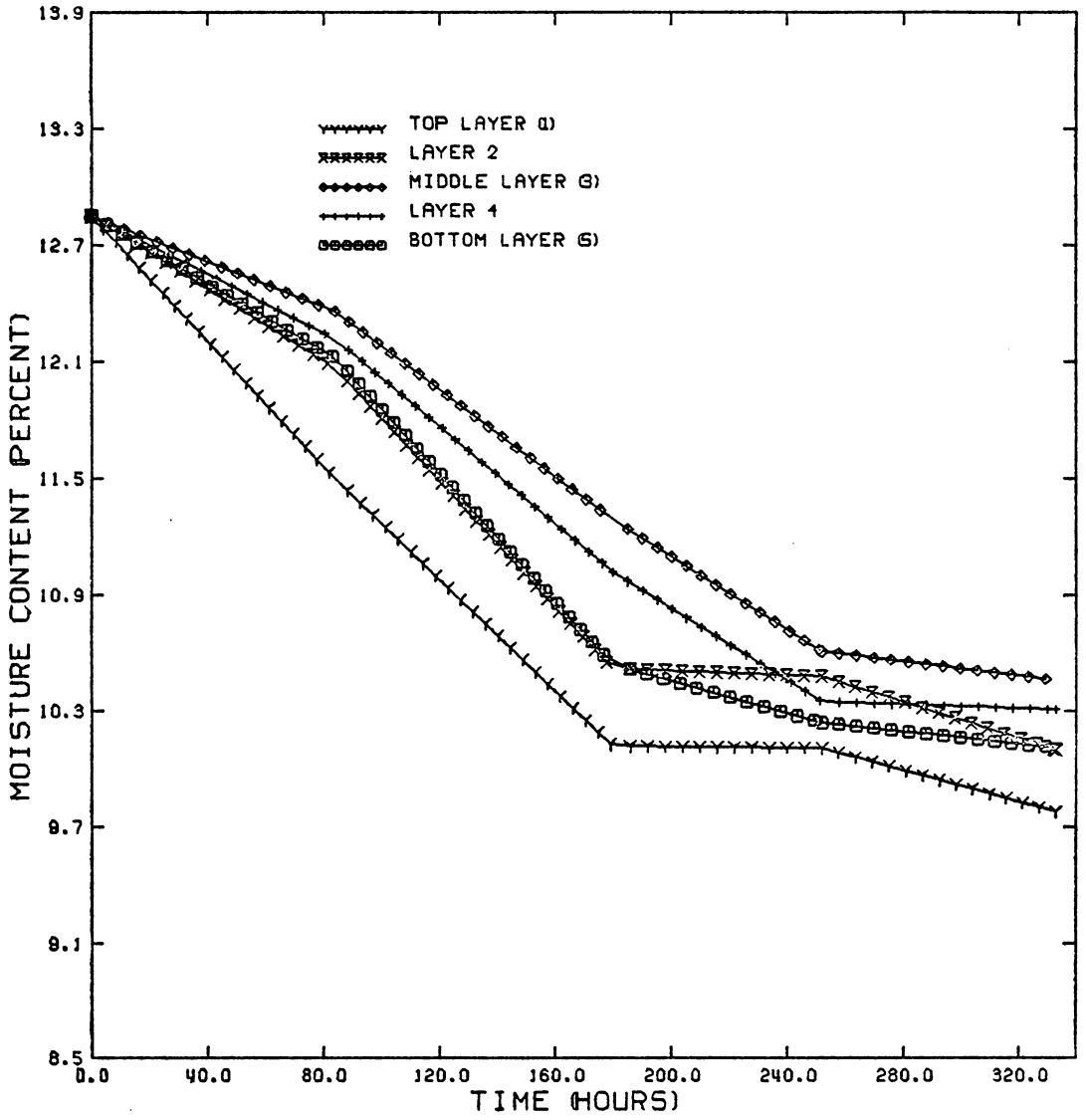

Figure F.1 : Experimental moisture contents in the five layers during Test 2 at a wall distance of 3 inches.

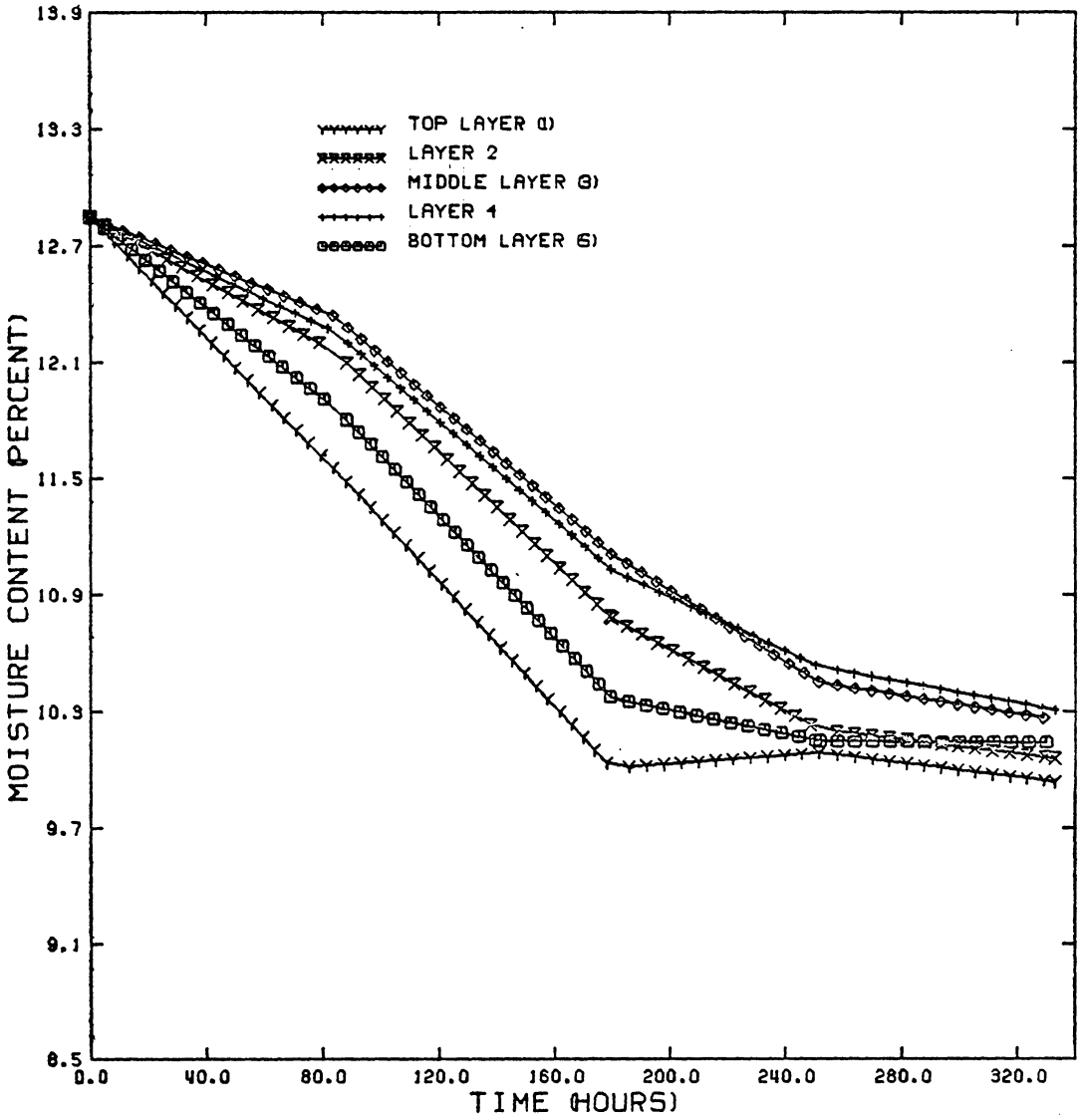

Figure F.2 : Experimental moisture contents in the five layers during Test 2 at a wall distance of 8 inches.

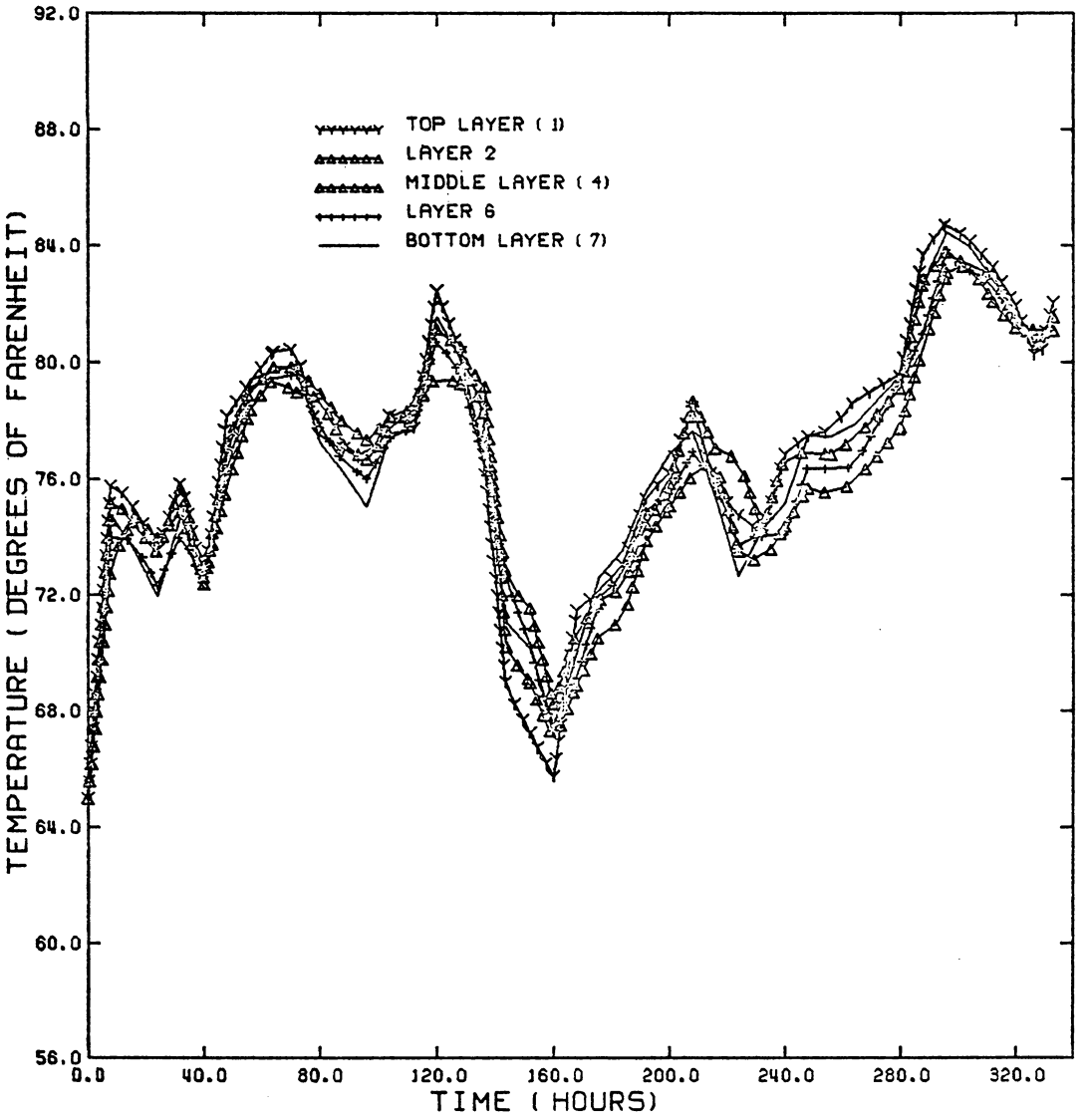

Figure F.3 : Experimental temperatures in the five layers during Test 2 at a wall distance of 3 inches.

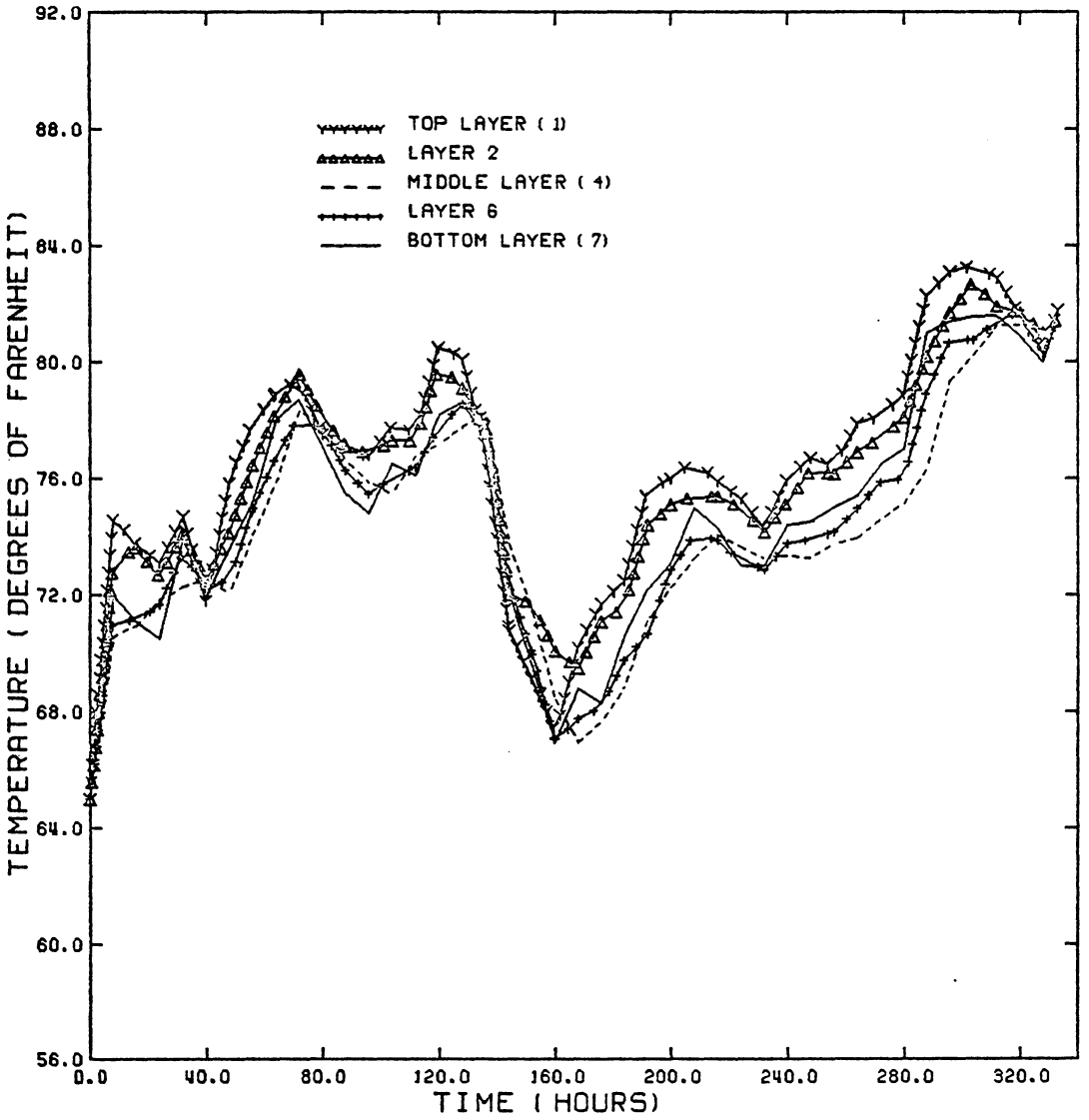

Figure F.4 : Experimental temperatures in the five layers during Test 2 at a wall distance of 8 inches.

Appendix G

FLOW CHART AND FORTRAN PROGRAM LISTING

This program is written to solve the coupled heat and mass transfer equations for a bed of corn. The implicit finite difference method is applied in this problem. The numerical method is based on the concept that the coefficients are assumed as constant within a time increment, one hour, then the terminal conditions are calculated for the 1-hour period. The conditions at the end of each 1-hour period serve as initial conditions for the next 1-hour period, and the values of the coefficients are updated for every 1-hour period.

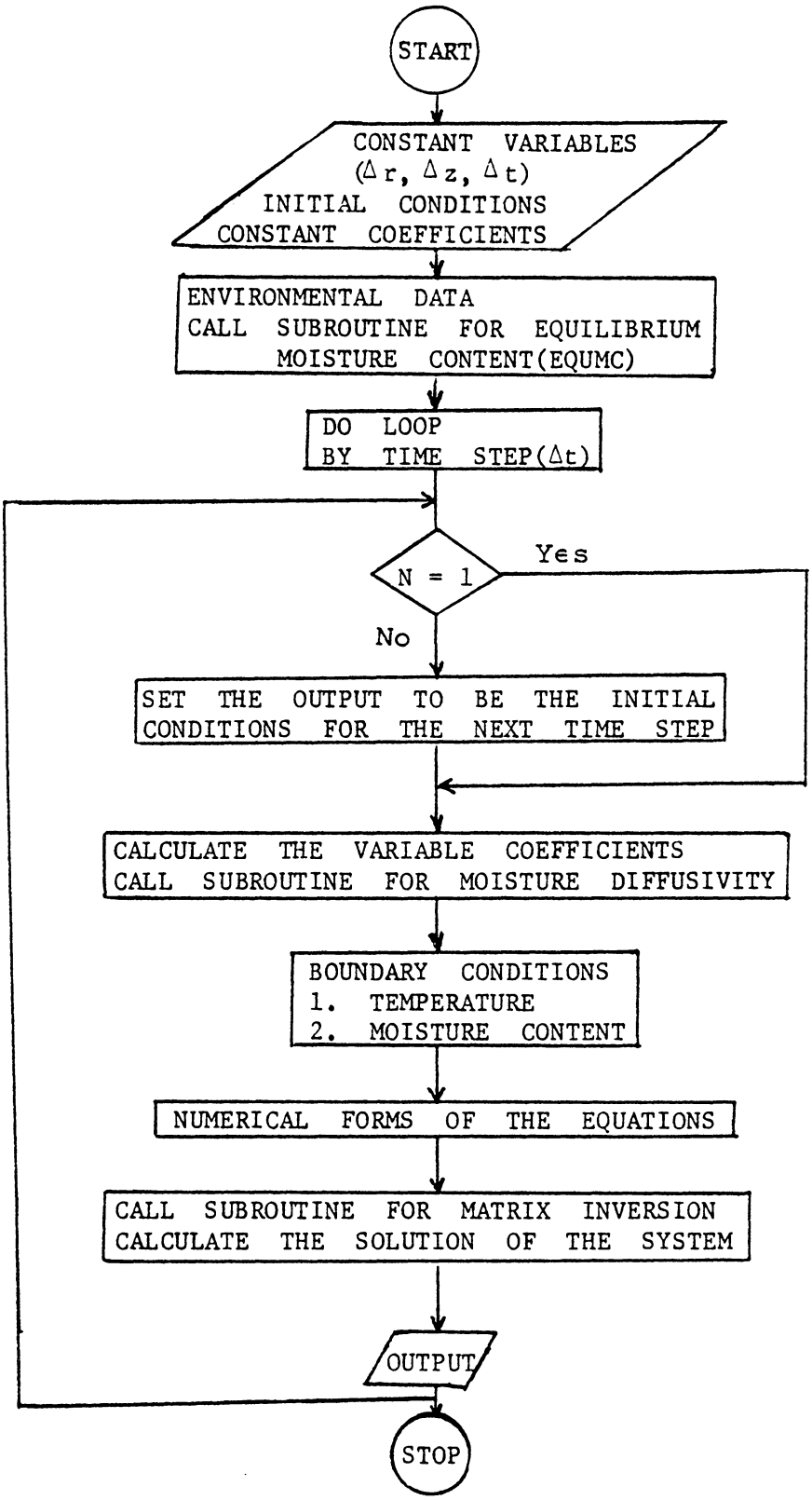
START
CONSTANT VARIABLES
(Δr, Δz, Δt)
INITIAL CONDITIONS
CONSTANT COEFFICIENTS
ENVIRONMENTAL DATA
CALL SUBROUTINE FOR EQUILIBRIUM
MOISTURE CONTENT(EQUMC)
DO LOOP
BY TIME STEP(Δt)
N = 1
Yes
No
SET THE OUTPUT TO BE THE INITIAL
CONDITIONS FOR THE NEXT TIME STEP
CALCULATE THE VARIABLE COEFFICIENTS
CALL SUBROUTINE FOR MOISTURE DIFFUSIVITY
BOUNDARY CONDITIONS
1. TEMPERATURE
2. MOISTURE CONTENT
NUMERICAL FORMS OF THE EQUATIONS
CALL SUBROUTINE FOR MATRIX INVERSION
CALCULATE THE SOLUTION OF THE SYSTEM
OUTPUT
STOP

FORTRAN VARIABLES

AA, A1, A2, A3, A4, TA, TA1, TA2,
- area, ft^2

COVHH - convective heat transfer coefficient on a horizontal plane, $Btu/hr\text{-}ft^2\text{-}^oF$

COVHV - convective heat transfer coefficient on a vertical plane, $Btu/hr\text{-}ft^2\text{-}^oF$

DAIR - moisture diffusivity, ft^2/hr

DCORN - moisture diffusivity of a kernel of corn, ft^2/hr

DELR - a spatial increment in radial direction, ft

DELT - a time increment, hr

DELZ - a spatial increment in axial direction, ft

DIFF - moisture diffusivity for a bed of corn, ft^2/hr

E - phase conversion factor, decimal

KAIR - thermal conductivity of air, $Btu/hr\text{-}ft\text{-}^oF$

KCORN - thermal conductivity of a kernel of eorn, ft^2/hr

LHEAT - latent heat for moisture vaporization inside a kernel of corn, Btu/lb

MC - moisture content(the bin is split into six layers in axial direction), decimal d.b.

MCI - initial moisture content, decimal d.b.

MCS - surface moisture content, decimal d.b.

R - radius, ft

RH - relative humidity of ambient air, decimal

RMC - moisture content(the bin is split into five layers in axial direction), decimal d.b.

ROOMT - temperature of ambient air, ^{o}F

Rtemp - temperature(the bin is split into five layers in axial direction), ^{o}F

RVOL - porosity, decimal

SDENS - bulk density of corn, lb/ft^3

SHEAT - specific heat for a bed of corn, $Btu/lb-^{o}F$

TCOND - bulk thermal conductivity, $Btu/hr-ft-^{o}F$

TDIFF - bulk thermal diffusivity, ft^2/hr

TEMP - temperature(the bin is split into six layers in axial direction), ^{o}F

TEMPI - initial temperature, ^{o}F

TGC - thermal gradient coefficient, $^{o}F^{-1}$

THMCE - equilibrium moisture content corresponding to ambient air, decimal d.b.

VOL, CVOL, CTVOL, EVOL, TTVOL

- volume, ft^3

SUBROUTINES

EQUMC - equilibrium moisture content corresponding to ambient air

INMAT - matrix inversion

CDRY - drying equation of corn

MDIFF - moisture diffusivity of a kernel of corn

THCON - bulk thermal conductivity

MIXED - bulk moisture diffusivity of corn using equivalent-resistor model

MIXED2 - bulk moisture diffusivity of corn using modified Maxwell model

MAXMIX - bulk moisture diffusivity of corn using parallel model

MINMIX - bulk moisture diffusivity of corn using series model

GEOMIX - bulk moisture diffusivity of corn using geometric mean model

```
      IMPLICIT REAL*8(A-H,Q-Z)
      DIMENSION  DIFF(6,6),  MCS(6,2), TEMP(6,6,170),  RH(254),
     1SHEAT(6,6), LHEAT(6,6), RST(6,6), THMCE(170), ROOMT(254),
     2TDIFF(6,6),  TCOND(6,6),  X(170), DELRR(6),  MC(6,6,170),
     3COVHV(1,6),   COVHH(6,6),  TA1(6),  TA2(6),   DCORN(6,6),
     4AA1(6,6),  AA2(6,6),   AA3(6,6),  AA4(6,6),   KCORN(6,6),
     5AA5(6,6),  AA6(6,6), B1(6,6),  B2(6,6), B3(6,6), B4(6,6),
     6B5(6,6), B6(6,6),  C(72,72),  D(72), TCAL(72),  MCAL(72),
     7TA(6), RMC(6,5,170), RTEMP(6,5,170), TTVOL(6)
      COMMON NR,NA,TEMP,MC,RVOL,DIFF,TCOND,DCORN,KCORN
      INTEGER  O, P
      REAL*8 MC, LHEAT, MCAL, MCS, KAIR, KCORN, MCI
      NA=6
      NR=6
      NT=170
C  BULK DENSITY OF CORN
      SDENS = 46.8D0
C  POROSITY IN A BED OF CORN
      RVOL  = 0.425D0
C  THERMAL GRADIENT COEFFICIENT
      TGC = 75.56D-06
C  PHASE CONVERSION FACTOR
      READ(5,402) E
      WRITE(6,2020) E
 2020 FORMAT(/,' PAHSE CONVERSION FACTOR ',9X,D12.6)
C  R = 11 INCHES (=0.916665 FT) RADIUM
      READ(5,402) R
C  DELR : THE RADIAL LENGTH FOR NUMERICAL CALCULATION ELEMENT
      READ(5,402) DELR
      DDELR=0.75D0*DELR
      DLR  =1.5D0*DELR
C  Z = 10 INCHES (=0.833332 FT) AXIAL LENGTH
      READ(5,402) Z
C  DELZ : THE AXIAL LENGTH FOR NUMERICAL CALCULATION ELEMENT
      READ(5,402) DELZ
      DDELZ=0.75D0*DELZ
C  DELT : TIME INCREMENT FOR NUMERICAL CALCULATION
      READ(5,402) DELT
      WRITE(6,2026) DELT
 2026 FORMAT(/,' DELT : TIME INCREMENT   ',9X,D12.6)
      PI    =3.1416D0
      READ(5,402) KAIR
      READ(5,402) DAIR
  402 FORMAT(6X,D10.4)
      WRITE(6,2027) KAIR
 2027 FORMAT(/,' CONDUCTIVITY OF AIR     ',9X,D12.6)
      WRITE(6,2028) DAIR
 2028 FORMAT(/,' DIFFISIVITY OF AIR      ',9X,D12.6)
C              ****************************************
```

```
C* THE AREAS AND VOLUMES OF THE ELEMENTS
      AA    =PI*DELR*DELZ
      A1    =PI*5.5D0*DELR*DELZ
      A2    =PI*5.0D0*DELR*DELZ
      A3    =PI*(5.5D0*5.5D0-5.0D0*5.0D0)*DELR*DELR
      A4    =PI*DELR*DELR
      VOL   =A3*DELZ
      CVOL  =A4*DELZ
      CTVOL=A4*DELZ/2.0D0
      EVOL  =A3*DELZ/2.0D0
      DO 28 N=1,4
      TA(N)    =PI*((6.0D0-DFLOAT(N))**2.0D0-(5.0D0-DFLOAT(N))
     $**2.0D0)*DELR*DELR
      TA1(N)   =PI*2.0D0*(6.0D0-DFLOAT(N))*DELR*DELZ/2.0D0
      TA2(N)   =PI*2.0D0*(5.0D0-DFLOAT(N))*DELR*DELZ/2.0D0
      TTVOL(N)=TA(N)*DELZ/2.0D0
   28 CONTINUE
C  ******************************************************************
C* TEMPERATURES AND RELATIVE HUMIDITIES OF THE SURROUNDING AIR
      READ(5,405) (ROOMT(N),N=1,3)
      DO 406 I=1,41
      READ(5,401) (ROOMT(I*6+N-3),N=1,6)
  406 CONTINUE
      READ(5,403) (ROOMT(N+249),N=1,5)
      READ(5,405) (RH(N),N=1,3)
      DO 407 I=1,41
      READ(5,401) (RH(I*6+N-3),N=1,6)
  407 CONTINUE
      READ(5,403) (RH(N+249),N=1,5)
  401 FORMAT(6X,6(D10.4,1X))
  403 FORMAT(6X,5(D10.4,1X))
  405 FORMAT(39X,3(D10.4,1X))
C  ******************************************************************
C
C* SUBROUTINE OF THE EQUILIBRIUM MOISTURE CONTENT
      CALL EQUMC(NT,ROOMT,RH,THMCE)
C
C  ******************************************************************
C
C  **********              INITIAL CONDITIONS             **********
      READ(5,402) TEMPI
      READ(5,402) MCI
      DO 1 N=1,6
      DO 1 O=1,6
      TEMP(N,O,1)=TEMPI
      MC(N,O,1)  =MCI
    1 CONTINUE
C  ******************************************************************
C  *****                                                       *****
C  *****                   THE MAIN DO-LOOP (9)                *****
C  *****                                                       *****
C  ******************************************************************
```

```
      DO 9    P=1,169
      DO 131  I=1,72
      MCAL(I) =0.0D0


      TCAL(I) =0.0D0
      D(I)    =0.0D0
      DO 131 J=1,72
      C(I,J)  =0.0D0
  131 CONTINUE
C*   THE CALCUATION FOR COEFFICIENTS
      DO 10 N=1,6
      DO 10 O=1,6
C   SPECIFIC HEAT
      SHEAT(N,O)=0.35D0+0.00851D0*(MC(N,O,P)
     &           /(1.D0+MC(N,O,P)))*100.D0
C   LATENT HEAT FROM THOMPSON MODEL
      LHEAT(N,O)=(1094.D0-0.57D0*TEMP(N,O,P))*(1.0D0
     &           +4.35D0*DEXP(-28.5D0*MC(N,O,P)))
   10 CONTINUE
C   ***************************************************************
C
C   THE SUBROUTINE FOR THE BULK THERMAL CONDUCTIVITY
      CALL THCON(P)
C
C   ***************************************************************
C
C   THE SUBROUTINE OF MOISTURE DIFFUSIVITY FOR A KERNEL OF CORN
C
      CALL MDIFF(P)
C
C   THE SUBROUTINE FOR THE BULK MOISTURE DIFFUSIVITY
C
C     CALL MAXMIX(P,DAIR)
C
C     CALL MINMIX(P,DAIR)
C
C     CALL MIXED(P,DAIR)
C
C     CALL MIXED2(P,DAIR)
C
      CALL GEOMIX(P,DAIR)
C
C   ***************************************************************
C   THERMAL DIFFUSIVITY
      DO 49 N=1,6
      DO 49 O=1,6
      TCOND(N,O)= KCORN(N,O)
      TDIFF(N,O)=KCORN(N,O)/(SDENS*SHEAT(N,O))
   49 CONTINUE
C   ***************************************************************
```

```
C
C* SUBROUTINE FOR THE TRANSIENT MOISTURE CONTENTS USING SABBAH'S
C     DRYING EQUATION
C
      CALL CDRY(DELT,NT,ROOMT,RH,X)
C
C  ****************************************************************
      DO 2 M=1,2
      DO 2 N=1,6


      MCS(N,M)=X(P)*(MC(N,(M-1)*5+1,P)-THMCE(P))+THMCE(P)
    2 CONTINUE
C  ****************************************************************
C  *****                BOUNDARY   CONDITIONS                 *****
C  ********                                                 ********
C  ************          FOR MOISTURE CONTENT           ************
C  **************                                     **************
C*  THE TOP SURFACE
      DO 24 N=1,4
      I=6*(N+1)
      J=6*(N+1)
      C(I,J-1) =(C(I,J-1)-DIFF(N+1,6)*TA(N)/DDELZ)
      C(I,J+35)=(C(I,J+35)-DIFF(N+1,6)*TGC*TA(N)/DDELZ)
      IF(N.EQ.1) GO TO 25
      IF(N.EQ.4) GO TO 26
      C(I,J)   =(TTVOL(N)/DELT+DIFF(N+1,6)*(TA(N)/DDELZ
     &          +TA1(N)/DELR+TA2(N)/DELR)+C(I,J))
      C(I,J-6) =(C(I,J-6)-DIFF(N+1,6)*TA1(N)/DELR)
      C(I,J+6) =(C(I,J+6)-DIFF(N+1,6)*TA2(N)/DELR)
      C(I,J+36)=(DIFF(N+1,6)*TGC*(TA(N)/DDELZ+TA1(N)/DELR
     &          +TA2(N)/DELR)+C(I,J+36))
      C(I,J+30)=(C(I,J+30)-DIFF(N+1,6)*TGC*TA1(N)/DELR)
      C(I,J+42)=(C(I,J+42)-DIFF(N+1,6)*TGC*TA2(N)/DELR)
      GO TO 27
   25 C(I,J)   =(TTVOL(N)/DELT+DIFF(N+1,6)*(TA(N)/DDELZ
     &          +TA1(N)/DDELR+TA2(N)/DELR)+C(I,J))
      C(I,J-6) =(C(I,J-6)-DIFF(N+1,6)*TA1(N)/DDELR)
      C(I,J+6) =(C(I,J+6)-DIFF(N+1,6)*TA2(N)/DELR)
      C(I,J+36)=(DIFF(N+1,6)*TGC*(TA(N)/DDELZ+TA1(N)/DDELR
     &          +TA2(N)/DELR)+C(I,J+36))
      C(I,J+30)=(C(I,J+30)-DIFF(N+1,6)*TGC*TA1(N)/DDELR)
      C(I,J+42)=(C(I,J+42)-DIFF(N+1,6)*TGC*TA2(N)/DELR)
      GO TO 27
   26 C(I,J)   =(TTVOL(N)/DELT+DIFF(N+1,6)*(TA(N)/DDELZ
     &          +TA1(N)/DELR+TA2(N)/DLR)+C(I,J))
      C(I,J-6) =(C(I,J-6)-DIFF(N+1,6)*TA1(N)/DELR)
      C(I,J+6) =(C(I,J+6)-DIFF(N+1,6)*TA2(N)/DLR)
      C(I,J+36)=(DIFF(N+1,6)*TGC*(TA(N)/DDELZ+TA1(N)/DELR
     &          +TA2(N)/DLR)+C(I,J+36))
```

```
      C(I,J+30)=(C(I,J+30)-DIFF(N+1,6)*TGC*TA1(N)/DELR)
      C(I,J+42)=(C(I,J+42)-DIFF(N+1,6)*TGC*TA2(N)/DLR)
   27 CONTINUE
      D(I)      =(TTVOL(N)*MC(N+1,6,P)/DELT-TTVOL(N)*(MC(N+1,6,P)
     &           -MCS(N+1,2))/5.00D0+D(I))
   24 CONTINUE
C*  THE BOTTOM SURFACE
      DO 61 N=1,4
      I=N*6+1
      J=N*6+1
      C(I,J+1) =(C(I,J+1)-DIFF(N+1,1)*TA(N)/DDELZ)
      C(I,J+37)=(C(I,J+37)-DIFF(N+1,1)*TGC*TA(N)/DDELZ)
      IF(N.EQ.1) GO TO 62
      IF(N.EQ.4) GO TO 63
      C(I,J)    =(TTVOL(N)/DELT+DIFF(N+1,1)*(TA(N)/DDELZ
     &           +TA1(N)/DELR+TA2(N)/DELR)+C(I,J))



      C(I,J-6) =(C(I,J-6)-DIFF(N+1,1)*TA1(N)/DELR)
      C(I,J+6) =(C(I,J+6)-DIFF(N+1,1)*TA2(N)/DELR)
      C(I,J+36)=(DIFF(N+1,1)*TGC*(TA(N)/DDELZ+TA1(N)/DELR
     &          +TA2(N)/DELR)+C(I,J+36))
      C(I,J+30)=(C(I,J+30)-DIFF(N+1,1)*TGC*TA1(N)/DELR)
      C(I,J+42)=(C(I,J+42)-DIFF(N+1,1)*TGC*TA2(N)/DELR)
      GO TO 64
   62 C(I,J)    =(TTVOL(N)/DELT+DIFF(N+1,1)*(TA(N)/DDELZ
     &           +TA1(N)/DDELR+TA2(N)/DELR)+C(I,J))
      C(I,J-6) =(C(I,J-6)-DIFF(N+1,1)*TA1(N)/DDELR)
      C(I,J+6) =(C(I,J+6)-DIFF(N+1,1)*TA2(N)/DELR)
      C(I,J+36)=(DIFF(N+1,1)*TGC*(TA(N)/DDELZ+TA1(N)/DDELR
     &          +TA2(N)/DELR)+C(I,J+36))
      C(I,J+30)=(C(I,J+30)-DIFF(N+1,1)*TGC*TA1(N)/DDELR)
      C(I,J+42)=(C(I,J+42)-DIFF(N+1,1)*TGC*TA2(N)/DELR)
      GO TO 64
   63 C(I,J)    =(TTVOL(N)/DELT+DIFF(N+1,1)*(TA(N)/DDELZ
     &           +TA1(N)/DELR+TA2(N)/DLR)+C(I,J))
      C(I,J-6) =(C(I,J-6)-DIFF(N+1,1)*TA1(N)/DELR)
      C(I,J+6) =(C(I,J+6)-DIFF(N+1,1)*TA2(N)/DLR)
      C(I,J+36)=(DIFF(N+1,1)*TGC*(TA(N)/DDELZ+TA1(N)/DELR
     &          +TA2(N)/DLR)+C(I,J+36))
      C(I,J+30)=(C(I,J+30)-DIFF(N+1,1)*TGC*TA1(N)/DELR)
      C(I,J+42)=(C(I,J+42)-DIFF(N+1,1)*TGC*TA2(N)/DLR)
   64 CONTINUE
      D(I)      =(TTVOL(N)*MC(N+1,1,P)/DELT-TTVOL(N)*(MC(N+1,1,P)
     &           -MCS(N+1,1))/12.0D0+D(I))
   61 CONTINUE
C*  THE EDGES AT THE TOP AND BOTTOM SURFACES
      C(6,6) =(C(6,6)+EVOL/DELT+DIFF(1,6)*(A2/DDELR+A3/DDELZ))
      C(6,12)=(C(6,12)-A2*DIFF(1,6)/DDELR)
      C(6,5) =(C(6,5)-A3*DIFF(1,6)/DDELZ)
```

```
      C(6,42)=(C(6,42)+DIFF(1,6)*TGC*(A2/DDELR+A3/DDELZ))
      C(6,48)=(C(6,48)-DIFF(1,6)*TGC*A2/DDELR)
      C(6,41)=(C(6,41)-DIFF(1,6)*TGC*A3/DDELZ)
      D(6)   =(EVOL*MC(1,6,P)/DELT-EVOL*(MC(1,6,P)-MCS(1,2))
     &        /5.00D0+D(6))
      C(1,1) =(C(1,1)+EVOL/DELT+DIFF(1,1)*(A2/DDELR+A3/DDELZ))
      C(1,7) =(C(1,7)-A2*DIFF(1,1)/DDELR)
      C(1,2) =(C(1,2)-A3*DIFF(1,1)/DDELZ)
      C(1,37)=(C(1,37)+DIFF(1,1)*TGC*(A2/DDELR+A3/DDELZ))
      C(1,43)=(C(1,43)-DIFF(1,1)*TGC*A2/DDELR)
      C(1,38)=(C(1,38)-DIFF(1,1)*TGC*A3/DDELZ)
      D(1)   =(EVOL*MC(1,1,P)/DELT-EVOL*(MC(1,1,P)-MCS(1,1))
     &        /12.0D0+D(1))
C  THE CENTERS ON THE TOP AND BOTTOM SURFACES
      C(36,36)=(C(36,36)+CTVOL/DELT+DIFF(6,6)*(A4/DDELZ+AA/DLR))
      C(36,30)=(C(36,30)-AA*DIFF(6,6)/DLR)
      C(36,35)=(C(36,35)-A4*DIFF(6,6)/DDELZ)
      C(36,72)=(C(36,72)+DIFF(6,6)*TGC*(A4/DDELZ+AA/DLR))
      C(36,66)=(C(36,66)-AA*DIFF(6,6)*TGC/DLR)
      C(36,71)=(C(36,71)-A4*DIFF(6,6)*TGC/DDELZ)
      D(36)   =(CTVOL*MC(6,6,P)/DELT-CTVOL*(MC(6,6,P)-MCS(6,2))
     &         /5.00D0+D(36))
      C(31,31)=(C(31,31)+CTVOL/DELT+DIFF(6,1)*(A4/DDELZ+AA/DLR))



      C(31,25)=(C(31,25)-AA*DIFF(6,1)/DLR)
      C(31,32)=(C(31,32)-A4*DIFF(6,1)/DDELZ)
      C(31,67)=(C(31,67)+DIFF(6,1)*TGC*(A4/DDELZ+AA/DLR))
      C(31,61)=(C(31,61)-AA*DIFF(6,1)*TGC/DLR)
      C(31,68)=(C(31,68)-A4*DIFF(6,1)*TGC/DDELZ)
      D(31)   =(CTVOL*MC(6,1,P)/DELT-CTVOL*(MC(6,1,P)-MCS(6,1))/
     &         12.0D0+D(31))
C*  SIDE SURFACE(WALL) OF THE BIN
      DO 11   O=1,4
      I        =O+1
      J        =O+1
      C(I,J+6) =C(I,J+6)-DIFF(1,O+1)*2.0D0*A2/DDELR
      C(I,J+42)=C(I,J+42)-DIFF(1,O+1)*2.0D0*A2*TGC/DDELR
      IF(O.EQ.1) GO TO 35
      IF(O.EQ.4) GO TO 36
      C(I,J)   =(C(I,J)+VOL/DELT+DIFF(1,O+1)*(2.D0*A2/DDELR
     &          +A3/DELZ+A3/DELZ))
      C(I,J+1) =(C(I,J+1)-DIFF(1,O+1)*A3/DELZ)
      C(I,J-1) =(C(I,J-1)-DIFF(1,O+1)*A3/DELZ)
      C(I,J+36)=(C(I,J+36)+DIFF(1,O+1)*TGC*(2.D0*A2/DDELR+A3
     &          /DELZ+A3/DELZ))
      C(I,J+37)=(C(I,J+37)-DIFF(1,O+1)*TGC*A3/DELZ)
      C(I,J+35)=(C(I,J+35)-DIFF(1,O+1)*TGC*A3/DELZ)
      GO TO 37
   35 C(I,J)   =(C(I,J)+VOL/DELT+DIFF(1,O+1)*(2.0D0*A2/DDELR
```

```
     &           +A3/DDELZ+A3/DELZ))
      C(I,J+1) =(C(I,J+1)-DIFF(1,O+1)*A3/DELZ)
      C(I,J-1) =(C(I,J-1)-DIFF(1,O+1)*A3/DDELZ)
      C(I,J+36)=(C(I,J+36)+DIFF(1,O+1)*TGC*(2.0D0*A2/DDELR+A3
     &           /DELZ+A3/DDELZ))
      C(I,J+37)=(C(I,J+37)-DIFF(1,O+1)*TGC*A3/DELZ)
      C(I,J+35)=(C(I,J+35)-DIFF(1,O+1)*TGC*A3/DDELZ)
      GO TO 37
   36 C(I,J)   =(C(I,J)+VOL/DELT+DIFF(1,O+1)*(2.D0*A2/DDELR
     &           +A3/DELZ+A3/DDELZ))
      C(I,J+1) =(C(I,J+1)-DIFF(1,O+1)*A3/DDELZ)
      C(I,J-1) =(C(I,J-1)-DIFF(1,O+1)*A3/DELZ)
      C(I,J+36)=(C(I,J+36)+DIFF(1,O+1)*TGC*(2.0D0*A2/DDELR
     &           +A3/DDELZ+A3/DELZ))
      C(I,J+37)=(C(I,J+37)-DIFF(1,O+1)*TGC*A3/DDELZ)
      C(I,J+35)=(C(I,J+35)-DIFF(1,O+1)*TGC*A3/DELZ)
   37 CONTINUE
      D(I)     =(D(I)+VOL*MC(1,O+1,P)/DELT)
   11 CONTINUE
C*  FOR THE CORE OF THE BIN
      DO 13 O=1,4
      I=31+O
      J=I
      C(I,J-6) =(C(I,J-6)-DIFF(6,O+1)*2.0D0*AA/DLR)
      C(I,J+30)=(C(I,J+30)-DIFF(6,O+1)*TGC*2.0D0*AA/DLR)
      IF(O.EQ.1) GO TO 31
      IF(O.EQ.4) GO TO 32
      C(I,J)   =(C(I,J)+CVOL/DELT+DIFF(6,O+1)*(A4/DELZ
     &           +2.0D0*AA/DLR+A4/DELZ))
      C(I,J+1) =(C(I,J+1)-DIFF(6,O+1)*A4/DELZ)



      C(I,J-1) =(C(I,J-1)-DIFF(6,O+1)*A4/DELZ)
      C(I,J+36)=(C(I,J+36)+DIFF(6,O+1)*TGC*(A4/DELZ
     &           +2.0D0*AA/DLR+A4/DELZ))
      C(I,J+37)=(C(I,J+37)-DIFF(6,O+1)*TGC*A4/DELZ)
      C(I,J+35)=(C(I,J+35)-DIFF(6,O+1)*TGC*A4/DELZ)
      GO TO 33
   31 C(I,J)   =(C(I,J)+CVOL/DELT+DIFF(6,O+1)*(A4/DELZ
     &           +2.D0*AA/DLR+A4/DDELZ))
      C(I,J+1) =(C(I,J+1)-DIFF(6,O+1)*A4/DELZ)
      C(I,J-1) =(C(I,J-1)-DIFF(6,O+1)*A4/DDELZ)
      C(I,J+36)=(C(I,J+36)+DIFF(6,O+1)*TGC*(A4/DELZ
     &           +2.0D0*AA/DLR+A4/DDELZ))
      C(I,J+37)=(C(I,J+37)-DIFF(6,O+1)*TGC*A4/DELZ)
      C(I,J+35)=(C(I,J+35)-DIFF(6,O+1)*TGC*A4/DDELZ)
      GO TO 33
   32 C(I,J)   =(C(I,J)+CVOL/DELT+DIFF(6,O+1)*(A4/DDELZ
     &           +2.0D0*AA/DLR+A4/DELZ))
      C(I,J+1) =(C(I,J+1)-DIFF(6,O+1)*A4/DDELZ)
```

```
      C(I,J-1) =(C(I,J-1)-DIFF(6,O+1)*A4/DELZ)
      C(I,J+36)=(C(I,J+36)+DIFF(6,O+1)*TGC*(A4/DDELZ
     &          +2.0DO*AA/DLR+A4/DELZ))
      C(I,J+37)=(C(I,J+37)-DIFF(6,O+1)*TGC*A4/DDELZ)
      C(I,J+35)=(C(I,J+35)-DIFF(6,O+1)*TGC*A4/DELZ)
   33 CONTINUE
      D(I)     =(D(I)+CVOL*MC(6,O+1,P)/DELT)
   13 CONTINUE
C  *********                                          ************
C  ************          FOR TEMPERATURE            ***************
C  ***************                                ******************
C
C*  NATURAL CONVECTIVE HEAT TRANSFER COEFFICIENT
      DO   12  O=1,6
      RST(1,O)  =DABS(ROOMT(P+1)-TEMP(1,O,P))
   12 CONTINUE
      DO   51  N=1,6
      RST(N,1)  =DABS(ROOMT(P+1)-TEMP(N,1,P))
      RST(N,6)  =DABS(ROOMT(P+1)-TEMP(N,6,P))
   51 CONTINUE
      DO   14  O=1,6
      COVHV(1,O)=0.29DO*((RST(1,O)/Z)**0.25DO)
   14 CONTINUE
      DO   15  N=1,6
C*  CONECTIVE HEAT TRANSFER COEFFICIENTS FOR THE TOP SURFACE
      IF(TEMP(N,6,P).GT.ROOMT(P+1)) GO TO 16
      COVHH(N,6)=1.5DO*0.27DO*((RST(N,6)/(1.772DO*R))**0.25DO)
      GO TO 15
   16 COVHH(N,6)=1.5DO*0.12DO*((RST(N,6)/(1.772DO*R))**0.25DO)
   15 CONTINUE
      DO 101 N=1,6
C*  CONVECTIVE HEAT TRANSFER COEFFICIENTS FOR THE BOTTOM SURFACE
      IF(TEMP(N,1,P).GT.ROOMT(P+1)) GO TO 102
      COVHH(N,1)=1.5DO*0.12DO*((RST(N,1)/(1.772DO*R))**0.25DO)
      GO TO 101
  102 COVHH(N,1)=1.5DO*0.27DO*((RST(N,1)/(1.772DO*R))**0.25DO)
  101 CONTINUE


C  ***************************************************************
C* SIDE SURFACE(WALL) OF THE BIN
      DO 103 O=1,4
      I         =37+O
      J         =37+O
      C(I,J-36)=(C(I,J-36)-E*VOL*LHEAT(1,O+1)*SDENS/DELT)
      C(I,J+6) =(C(I,J+6)-2.0DO*A2*TCOND(1,O+1)/DDELR)
      IF(O.EQ.1) GO TO 45
      IF(O.EQ.4) GO TO 46
      C(I,J)   =(C(I,J)+VOL*SHEAT(1,O+1)*SDENS/DELT+2.0DO*A1
     &          *COVHV(1,O+1)+2.0DO*A2*TCOND(1,O+1)/DDELR+A3
```

```
     &           *TCOND(1,O+1)/DELZ+A3*TCOND(1,O+1)/DELZ)
      C(I,J+1) =(C(I,J+1)-A3*TCOND(1,O+1)/DELZ)
      C(I,J-1) =(C(I,J-1)-A3*TCOND(1,O+1)/DELZ)
      GO TO 47
   45 C(I,J)   =(C(I,J)+VOL*SHEAT(1,O+1)*SDENS/DELT+2.0D0
     &           *A1*COVHV(1,O+1)+2.0D0*A2*TCOND(1,O+1)/DDELR+A3
     &           *TCOND(1,O+1)*(1.0D0/DELZ+1.0D0/DDELZ))
      C(I,J+1) =(C(I,J+1)-A3*TCOND(1,O+1)/DELZ)
      C(I,J-1) =(C(I,J-1)-A3*TCOND(1,O+1)/DDELZ)
      GO TO 47
   46 C(I,J)   =(C(I,J)+VOL*SHEAT(1,O+1)*SDENS/DELT+2.0D0*A1
     &           *COVHV(1,O+1)+2.0D0*A2*TCOND(1,O+1)/DDELR+A3
     &           *TCOND(1,O+1)*(1.0D0/DELZ+1.0D0/DDELZ))
      C(I,J+1) =(C(I,J+1)-A3*TCOND(1,O+1)/DDELZ)
      C(I,J-1) =(C(I,J-1)-A3*TCOND(1,O+1)/DELZ)
   47 CONTINUE
      D(I)     =(D(I)+TEMP(1,O+1,P)*VOL*SHEAT(1,O+1)*SDENS/DELT
     &           +2.0D0*A1*COVHV(1,O+1)*ROOMT(P+1)-E*MC(1,O+1,P)
     &           *VOL*LHEAT(1,O+1)*SDENS/DELT)
  103 CONTINUE
C*   FOR THE TOP SURFACE
      DO 18 N=1,4
      I=42+6*N
      J=I
      C(I,J-36)=(C(I,J-36)-(1.0D0-E)*TTVOL(N)*LHEAT(N+1,6)
     &           *SDENS/DELT)
      C(I,J-1) =(C(I,J-1)-TA(N)*TCOND(N+1,6)/DDELZ)
      IF(N.EQ.1) GO TO 41
      IF(N.EQ.4) GO TO 42
      C(I,J)   =(C(I,J)+TTVOL(N)*SHEAT(N+1,6)*SDENS/DELT+TA(N)
     &           *COVHH(N+1,6)+TA1(N)*TCOND(N+1,6)/DELR+TA2(N)
     &           *TCOND(N+1,6)/DELR+TA(N)*TCOND(N+1,6)/DDELZ)
      C(I,J+6) =(C(I,J+6)-TA2(N)*TCOND(N+1,6)/DELR)
      C(I,J-6) =(C(I,J-6)-TA1(N)*TCOND(N+1,6)/DELR)
      GO TO 43
   41 C(I,J)   =(C(I,J)+TTVOL(N)*SHEAT(N+1,6)*SDENS/DELT+TA(N)
     &           *COVHH(N+1,6)+TA1(N)*TCOND(N+1,6)/DDELR+TA2(N)
     &           *TCOND(N+1,6)/DELR+TA(N)*TCOND(N+1,6)/DDELZ)
      C(I,J+6) =(C(I,J+6)-TA2(N)*TCOND(N+1,6)/DDELR)
      C(I,J-6) =(C(I,J-6)-TA1(N)*TCOND(N+1,6)/DDELR)
      GO TO 43
   42 C(I,J)   =(C(I,J)+TTVOL(N)*SHEAT(N+1,6)*SDENS/DELT+TA(N)
     &           *COVHH(N+1,6)+TA1(N)*TCOND(N+1,6)/DELR+TA2(N)
     &           *TCOND(N+1,6)/DLR+TA(N)*TCOND(N+1,6)/DDELZ)


      C(I,J-6) =(C(I,J-6)-TA1(N)*TCOND(N+1,6)/DELR)
      C(I,J+6) =(C(I,J+6)-TA2(N)*TCOND(N+1,6)/DLR)
   43 CONTINUE
      D(I)     =(D(I)+TEMP(N+1,6,P)*TTVOL(N)*SHEAT(N+1,6)*SDENS
```

```
C*  THE EDGES ON THE TOP AND BOTTOM SURFACES
      C(37,1) =(C(37,1)-(1.0D0-E)*EVOL*SDENS*LHEAT(1,1)/DELT)
      C(37,37)=(C(37,37)+EVOL*SDENS*SHEAT(1,1)/DELT+A1*
     &          COVHV(1,1)+A2*TCOND(1,1)/DDELR+A3
     &          *COVHH(1,1)+A3*TCOND(1,1)/DDELZ)
      C(37,43)=(C(37,43)-A2*TCOND(1,1)/DDELR)
      C(37,38)=(C(37,38)-A3*TCOND(1,1)/DDELZ)
      D(37)   =(D(37)+ROOMT(P+1)*COVHV(1,1)*A1+ROOMT(P+1)*A3
     &          *COVHH(1,1)+TEMP(1,1,P)*EVOL*SDENS*SHEAT(1,1)/DELT
     &          -(1.0D0-E)*MC(1,1,P)*EVOL*SDENS*LHEAT(1,1)/DELT)
      C(42,6) =(C(42,6)-(1.0D0-E)*EVOL*SDENS*LHEAT(1,6)/DELT)
      C(42,42)=(EVOL*SDENS*SHEAT(1,6)/DELT+A1*COVHV(1,6)+A2
     &          *TCOND(1,6)/DDELR+A3*COVHH(1,6)+A3*TCOND(1,6)
     &          /DDELZ+C(42,42))
      C(42,48)=(C(42,48)-A2*TCOND(1,6)/DDELR)
      C(42,41)=(C(42,41)-A3*TCOND(1,6)/DDELZ)
      D(42)   =(D(42)+ROOMT(P+1)*(A1*COVHV(1,6)+A3*COVHH(1,6))-
     &          (1.0D0-E)*MC(1,6,P)*EVOL*SDENS*LHEAT(1,6)/DELT
     &          +TEMP(1,6,P)*EVOL*SDENS*SHEAT(1,6)/DELT)
C*  THE CORE OF THE BIN
      DO 113 N=1,4
      O=N+1
      I=67+N
      J=I
      C(I,J-6) =(C(I,J-6)-2.0D0*AA*TCOND(6,O)/DLR)
      C(I,J-36)=(C(I,J-36)-E*SDENS*LHEAT(6,O)*CVOL/DELT)
      IF(O.EQ.1) GO TO 110
      IF(O.EQ.4) GO TO 111
      C(I,J)   =(SDENS*SHEAT(6,O)*CVOL/DELT+A4*TCOND(6,O)/DELZ+
     &           2.D0*AA*TCOND(6,O)/DLR+A4*TCOND(6,O)/DELZ+C(I,J))
      C(I,J+1) =(C(I,J+1)-A4*TCOND(6,O)/DELZ)
      C(I,J-1) =(C(I,J-1)-A4*TCOND(6,O)/DELZ)
      GO TO 112
  110 C(I,J)   =(SDENS*SHEAT(6,O)*CVOL/DELT+A4*TCOND(6,O)/DELZ+AA
     &           *2.0D0*TCOND(6,O)/DLR+A4*TCOND(6,O)/DDELZ+C(I,J))
      C(I,J+1) =(C(I,J+1)-A4*TCOND(6,O)/DELZ)
      C(I,J-1) =(C(I,J-1)-A4*TCOND(6,O)/DDELZ)
      GO TO 112
  111 C(I,J)   =(SDENS*SHEAT(6,O)*CVOL/DELT+A4*TCOND(6,O)/DELZ+AA
     &           *2.0D0*TCOND(6,O)/DLR+A4*TCOND(6,O)/DDELZ+C(I,J))
      C(I,J+1) =(C(I,J+1)-A4*TCOND(6,O)/DDELZ)
      C(I,J-1) =(C(I,J-1)-A4*TCOND(6,O)/DELZ)
  112 CONTINUE
      D(I)     =(D(I)-E*MC(6,O,P)*SDENS*LHEAT(6,O)*CVOL/DELT
     &          +TEMP(6,O,P)*SDENS*SHEAT(6,O)*CVOL/DELT)
  113 CONTINUE
C  **********  THE END OF THE BOUNDARY CONDITIONS     **********
C
C  *****************                                *****************
```

```
C  **************    THE INTERIOR OF THE BIN      ****************
C  ************                                     *************
C*  COEFFICIENTS FOR LUIKOV'S EQUATIONS
      C1=1.0D0/(DELR*DELR)
      DO 115 N=1,4
      DELRR(N+1)=(5.5D0-DFLOAT(N))*DELR*(2.0D0*DELR)


      DO 115 O=1,4
      I=N+1
      J=O+1
      AA1(I,J)=DIFF(I,J)/(DELZ*DELZ)
      AA2(I,J)=DIFF(I,J)*C1
      AA3(I,J)=DIFF(I,J)/DELRR(I)
      AA4(I,J)=DIFF(I,J)*TGC*C1
      AA5(I,J)=AA4(I,J)
      AA6(I,J)=DIFF(I,J)*TGC/DELRR(I)
      B1(I,J) =(TDIFF(I,J)+E*LHEAT(I,J)*DIFF(I,J)*TGC
     &          /SHEAT(I,J))/(DELZ*DELZ)
      B2(I,J) =B1(I,J)
      B3(I,J) =B1(I,J)*DELZ*DELZ/DELRR(I)
      B4(I,J) =(DIFF(I,J)*E*LHEAT(I,J)/SHEAT(I,J))*C1
      B5(I,J) =B4(I,J)
      B6(I,J) =(DIFF(I,J)*E*LHEAT(I,J)/SHEAT(I,J))/DELRR(I)
  115 CONTINUE
C*  NUMERICAL IMPLICIT FORMS OF INTERIOR ELEMENTS
      DO 121 O=1,4
      L       =O+1
      DO 121 N=1,4
      K       =N+1
      I       =6*N+O+1
      J       =6*N+O+1
      C(I,J)  =C(I,J)+(1.0D0/DELT+2.0D0*AA1(K,L)+2.0D0*AA2(K,L))
      C(I,J+1)=(C(I,J+1)-AA1(K,L))
      C(I,J-1)=(C(I,J-1)-AA1(K,L))
      C(I,J+6)=(C(I,J+6)-AA2(K,L)-AA3(K,L))
      C(I,J-6)=(C(I,J-6)-AA2(K,L)+AA3(K,L))
      D(I)    =(D(I)+MC(K,L,P)/DELT)
  121 CONTINUE
C                  ******************************
      DO 122 O=1,4
      L       =O+1
      DO 122 N=1,4
      K       =N+1
      I       =6*N+O+1
      J       =37+6*N+O
      C(I,J)  =(C(I,J)+2.0D0*AA4(K,L)+2.0D0*AA5(K,L))
      C(I,J+1)=(C(I,J+1)-AA4(K,L))
      C(I,J-1)=(C(I,J-1)-AA4(K,L))
      C(I,J+6)=(C(I,J+6)-AA5(K,L)-AA6(K,L))
```

```
      C(I,J-6)=(C(I,J-6)-AA5(K,L)+AA6(K,L))
  122 CONTINUE
C                     ********************************
      DO 123 O=1,4
      L       =O+1
      DO 123 N=1,4
      K       =N+1
      I       =37+6*N+O
      J       =6*N+O+1
      C(I,J)  =(C(I,J)+2.0D0*B4(K,L)+2.0D0*B5(K,L))
      C(I,J-1)=(C(I,J-1)-B4(K,L))
      C(I,J+1)=(C(I,J+1)-B4(K,L))
      C(I,J-6)=(C(I,J-6)-B5(K,L)-B6(K,L))



      C(I,J+6)=(C(I,J+6)-B5(K,L)+B6(K,L))
      D(I)    =(D(I)+TEMP(K,L,P)/DELT)
  123 CONTINUE
C                     ********************************
      DO 124 O=1,4
      L       =O+1
      DO 124 N=1,4
      K       =N+1
      I       =37+6*N+O
      J       =37+6*N+O
      C(I,J)  =(C(I,J)+1.0D0/DELT+2.0D0*B1(K,L)+2.0D0*B2(K,L))
      C(I,J+1)=(C(I,J+1)-B1(K,L))
      C(I,J-1)=(C(I,J-1)-B1(K,L))
      C(I,J+6)=(C(I,J+6)-B2(K,L)-B3(K,L))
      C(I,J-6)=(C(I,J-6)-B2(K,L)+B3(K,L))
  124 CONTINUE
C  ****************************************************************
C
C  THE SUBROUTINE FOR MATRIX INVERSION
      N=72
      CALL INMAT(C,N,DETM)
C
C  ****************************************************************
C*   THE SIMULATION RESULTS AFTER A TIME INCREMENT
      DO 141 I=1,36
      DO 141 J=1,72
      MCAL(I) =MCAL(I)+C(I,J)*D(J)
  141 CONTINUE
      DO 143 N=1,36
      I       =36+N
      DO 143 J=1,72
      TCAL(I) =TCAL(I)+C(I,J)*D(J)
  143 CONTINUE
      DO 144 I=1,6
      DO 144 J=1,6
```

```
     &           /DELT-(1.0D0-E)*MC(N+1,6,P)*TTVOL(N)*LHEAT(N+1,6)
     &           *SDENS/DELT+ROOMT(P+1)*TA(N)*COVHH(N+1,6))
   18 CONTINUE
C*  FOR THE BOTTOM SURFACE
      DO 19 N=1,4
      I=37+6*N
      J=I
      C(I,J-36)=C(I,J-36)-(1.0D0-E)*TTVOL(N)*LHEAT(N+1,1)
     &          *SDENS/DELT
      C(I,J+1) =(C(I,J+1)-TA(N)*TCOND(N+1,1)/DDELZ)
      IF(N.EQ.1) GO TO 56
      IF(N.EQ.4) GO TO 57
      C(I,J)   =(C(I,J)+TTVOL(N)*SHEAT(N+1,1)*SDENS/DELT+TA(N)
     &          *COVHH(N+1,1)+TA2(N)*TCOND(N+1,1)/DELR+TA1(N)
     &          *TCOND(N+1,1)/DELR+TA(N)*TCOND(N+1,1)/DDELZ)
      C(I,J-6) =(C(I,J-6)-TA1(N)*TCOND(N+1,1)/DELR)
      C(I,J+6) =(C(I,J+6)-TA2(N)*TCOND(N+1,1)/DELR)
      GO TO 58
   56 C(I,J)   =(C(I,J)+TTVOL(N)*SHEAT(N+1,1)*SDENS/DELT+TA(N)
     &          *COVHH(N+1,1)+TA2(N)*TCOND(N+1,1)/DELR+TA1(N)
     &          *TCOND(N+1,1)/DDELR+TA(N)*TCOND(N+1,1)/DDELZ)
      C(I,J-6) =(C(I,J-6)-TA1(N)*TCOND(N+1,1)/DDELR)
      C(I,J+6) =(C(I,J+6)-TA2(N)*TCOND(N+1,1)/DELR)
      GO TO 58
   57 C(I,J)   =(C(I,J)+TTVOL(N)*SHEAT(N+1,1)*SDENS/DELT+TA(N)
     &          *COVHH(N+1,1)+TA2(N)*TCOND(N+1,1)/DLR+TA1(N)
     &          *TCOND(N+1,1)/DELR+TA(N)*TCOND(N+1,1)/DDELZ)
      C(I,J-6) =(C(I,J-6)-TA1(N)*TCOND(N+1,1)/DELR)
      C(I,J+6) =(C(I,J+6)-TA2(N)*TCOND(N+1,1)/DLR)
   58 CONTINUE
      D(I)     =(D(I)-(1.0D0-E)*TTVOL(N)*MC(N+1,1,P)*LHEAT(N+1,1)
     &          *SDENS/DELT+TEMP(N+1,1,P)*TTVOL(N)*SHEAT(N+1,1)
     &          *SDENS/DELT+ROOMT(P+1)*TA(N)*COVHH(N+1,1))
   19 CONTINUE
C*  THE CENTER ON THE TOP AND BOTTOM SURFACES
      C(67,31)=(C(67,31)-(1.0D0-E)*CTVOL*SDENS*LHEAT(6,1)/DELT)
      C(67,67)=(CTVOL*SDENS*SHEAT(6,1)/DELT+A4*COVHH(6,1)+A4
     &         *TCOND(6,1)/DDELZ+AA*TCOND(6,1)/DLR+C(67,67))
      C(67,68)=(C(67,68)-A4*TCOND(6,1)/DDELZ)
      C(67,61)=(C(67,61)-AA*TCOND(6,1)/DLR)
      D(67)   =(D(67)+ROOMT(P+1)*A4*COVHH(6,1)-(1.0D0-E)
     &         *MC(6,1,P)*CTVOL*LHEAT(6,1)*SDENS/DELT
     &         +TEMP(6,1,P)*CTVOL*SHEAT(6,1)*SDENS/DELT)
      C(72,36)=(C(72,36)-(1.0D0-E)*CTVOL*SDENS*LHEAT(6,6)/DELT)
      C(72,72)=(C(72,72)+CTVOL*SDENS*SHEAT(6,6)/DELT+COVHH(6,6)
     &         *A4+A4*TCOND(6,6)/DDELZ+AA*TCOND(6,6)/DLR)
      C(72,71)=(C(72,71)-A4*TCOND(6,6)/DDELZ)
      C(72,66)=(C(72,66)-AA*TCOND(6,6)/DLR)
      D(72)   =(D(72)+ROOMT(P+1)*A4*COVHH(6,6)-(1.0D0-E)
     &         *MC(6,6,P)*CTVOL*SDENS*LHEAT(6,6)/DELT
     &         +TEMP(6,6,P)*CTVOL*SDENS*SHEAT(6,6)/DELT)
```

```
      MC(I,J,P+1)    =MCAL((I-1)*6+J)
      TEMP(I,J,P+1) =TCAL(36+(I-1)*6+J)
  144 CONTINUE
      DO 146 I=1,6
      DO 146 J=1,5
      RMC(I,J,P+1)   =(MC(I,J,P+1)+MC(I,J+1,P+1))/2.0D0
      RTEMP(I,J,P+1)=(TEMP(I,J,P+1)+TEMP(I,J+1,P+1))/2.0D0
  146 CONTINUE
    9 CONTINUE
C   ****************************************************************
C   *****                                                      *****
C   *****            THE END OF THE MAIN DO-LOOP (9)           *****
C   *****                                                      *****
C   ****************************************************************
C   *****                       THE OUTPUT                     *****
C   ****************************************************************
      DO 421 P=1,34
      N        =5*P
      WRITE(6,412) N, (TEMP(2,J,N),J=1,6), ROOMT(N)
  421 CONTINUE



      DO 422 P=1,34
      N        =5*P
      WRITE(6,410) N, (TEMP(5,J,N),J=1,6)
  422 CONTINUE
      DO 423 P=1,34
      N        =5*P
      WRITE(6,410) N, (RMC(2,J,N),J=1,5), THMCE(N)
  423 CONTINUE
      DO 424 P=1,34
      N        =5*P
      WRITE(6,411) N, (RMC(5,J,N),J=1,5)
  424 CONTINUE
      DO 425 P=1,34
      N        =5*P
      WRITE(6,410) N, (MC(I,3,N),I=1,6)
  425 CONTINUE
      DO 426 P=1,34
      N        =5*P
      WRITE(6,410) N, (TEMP(I,3,N),I=1,6)
  426 CONTINUE
  410 FORMAT(2X,I4,6(2X,F10.4))
  411 FORMAT(2X,I4,5(2X,F10.4))
  412 FORMAT(2X,I4,7(2X,F8.4))
  501 FORMAT(10(1X,D10.4))
  503 FORMAT(6(4X,D10.4))
      STOP
      END
C   ****************************************************************
C
C*  THE SUBROUTINE FOR THE EQUILIBRIUM MOISTURE CONTENT
```

```
      SUBROUTINE EQUMC(NT,ROOMT,RH,THMCE)
      IMPLICIT REAL*8(A-H,Q-Z)
      DIMENSION A(170), B(170)
      DIMENSION ROOMT(254), RH(254), THMCE(170)
      C       =-3.82D-05
      DO 71  N=1,NT
      A(N)    =DLOG(1.0D0-RH(N))
      B(N)    =A(N)/(C*(ROOMT(N)+50D0))
      THMCE(N)=DSQRT(B(N))/1.0D2
   71 CONTINUE
      RETURN
      END
C  ****************************************************************
C
C*  THE SUBROUTINE FOR THE MATRIX INVERSION
      SUBROUTINE INMAT(C,N,DETM)
      IMPLICIT REAL*8(A-H,Q-Z)
      DIMENSION C(72,72), J(125)
      DETM    =1.0D0
      DO 225 L=1,N
  225 J(L+20) =L
      DO 244 L=1,N
      CC      =0.0D0
      M       =L
      DO 235 K=L,N


      IF((DABS(CC)-DABS(C(L,K))).GE.0.0D0) GO TO 235
  226 M       =K
      CC      =C(L,K)
  235 CONTINUE
  227 IF(L.EQ.M) GO TO 238
  228 K       =J(M+20)
      J(M+20) =J(L+20)
      J(L+20) =K
      DO 237 K=1,N
      S       =C(K,L)
      C(K,L)  =C(K,M)
  237 C(K,M)  =S
  238 C(L,L)  =1.0D0
      DETM    =DETM*CC
      DO 239 M=1,N
  239 C(L,M)  =C(L,M)/CC
      DO 242 M=1,N
      IF (L.EQ.M) GO TO 242
  229 CC      =C(M,L)
      IF(CC.EQ.0.0D0) GO TO 242
  230 C(M,L)  =0.0D0
      DO 241 K=1,N
  241 C(M,K)  =C(M,K)-CC*C(L,K)
```

```
  242 CONTINUE
  244 CONTINUE
      DO 243 L=1,N
      IF(J(L+20).EQ.L) GO TO 243
  231 M        =L
  232 M        =M+1
      IF(J(M+20).EQ.L) GO TO 233
  236 IF(N.GT.M) GO TO 232
  233 J(M+20) =J(L+20)
      DO 263 K=1,N
      CC       =C(L,K)
      C(L,K)   =C(M,K)
  263 C(M,K)   =CC
      J(L+20) =L
  243 CONTINUE
      DETM     =DABS(DETM)
      RETURN
      END
C  ***********************************************************************
C
C  THE SUBROUTINE FOR THE DRYING EQUATION
      SUBROUTINE CDRY(DELT,NT,T,R,X)
      IMPLICIT REAL*8(A-H,Q-Z)
      DIMENSION  T(254), X(170), R(254)
      DO 11 K=1,NT
      A        =DSQRT(6.0142D0+1.43D0*R(K)*R(K))-1.0D-2*T(K)
     &          *DSQRT(3.353D0+3.0D0*R(K)*R(K))
      B        =0.1245D0-2.2D-3*R(K)+2.3D-5*R(K)*T(K)-5.8D-5*T(K)
      C        =DEXP(-A*(DELT**B))
      X(K)     =DEXP(-C*(DELT**0.664D0))
   11 CONTINUE
      RETURN


      END
C  ***********************************************************************
C
C  THE SUBROUTINE FOR THE MASS DIFFUSIVITY OF CORN
      SUBROUTINE MDIFF(K)
      IMPLICIT REAL*8(A-H,Q-Z)
      DIMENSION AT(6,6)
      COMMON NR,NA,T(6,6,170),M(6,6,170),D,DD(6,6,2),A(6,6),
     &DDD(6,6)
      REAL*8 M
      DO 99 I =1,NR
      DO 99 J =1,NA
      DUMMY    =DUMMY+(T(I,J,K)-114.8D0)*1.95253D-2
      A(I,J)   =1.092193D-4*DEXP(DUMMY)
   99 CONTINUE
      RETURN
```

```
      END
C  ****************************************************************
C
C  THE SUBROUTINE FOR THERMAL CONDUCTIVITY OF CORN
      SUBROUTINE THCON(N)
      IMPLICIT REAL*8(A-H,Q-Z)
      DIMENSION  CT(6,6)
      COMMON NR,NA,T(6,6,170),M(6,6,170),D,DD(6,6,3),TC(6,6)
      REAL*8 M
      DO 1 I  =1,NR
      DO 1 J  =1,NA
      CT(I,J) =(T(I,J,N)-32.0D0)*5.0D0/9.0D0
      DUMMY   =-1.738D0-3.696D0*M(I,J,N)+4.725D-2*CT(I,J)
     &          +6.843D0*M(I,J,N)*M(I,J,N)-1.499D-4*CT(I,J)
     &          *CT(I,J)+6.272D-4*M(I,J,N)*CT(I,J)
      TC(I,J) =DEXP(DUMMY)/1.738D0
    1 CONTINUE
      RETURN
      END
C  ****************************************************************
C
C*  THE SUBROUTINE FOR THE MIXED PROPERTIES
      SUBROUTINE MIXED(N,AIR)
      IMPLICIT REAL*8(A-H, Q-Z)
      COMMON NR,NA,D(6,6,340),V,R(6,6),DD(6,6),
     &CORN(6,6),DDD(6,6)
      DO 100 I=1,NR
      DO 100 J=1,NA
      C       =V-0.03D0
      A       =1.0D0-C
      DUMMY   =(1.0D0-V)/A
      R(I,J)  =A*CORN(I,J)*AIR/(CORN(I,J)*(1.0D0-DUMMY)+DUMMY
     &         *AIR)+C*AIR
  100 CONTINUE
      RETURN
      END
C  ****************************************************************
C
C*  THE SUBROUTINE OF THE MIXED PROPERTIES FROM JACOB'S TEXTBOOK


C*  ----- THE MODIFIED MAXWELL'S MIXING MODEL
      SUBROUTINE MIXED2(I,AIR)
      IMPLICIT REAL*8(A-H,Q-Z)
      DIMENSION A1(6,6), A2(6,6), A3(6,6)
      COMMON NR,NA,D(6,6,340),V,R(6,6),DD(6,6),
     &CORN(6,6),DDD(6,6)
      DO 10 J =1,NR
      DO 10 N =1,NA
      A1(J,N) =3.0D0*AIR/(2.0D0*AIR+CORN(J,N))
```

```
      A2(J,N) =1.0D0-(1.0D0-A1(J,N)*CORN(J,N)/AIR)*(1.0D0-V)
      A3(J,N) =1.0D0+(A1(J,N)-1.0D0)*(1.0D0-V)
      R(J,N)  =AIR*A2(J,N)/A3(J,N)
   10 CONTINUE
      RETURN
      END
C  ****************************************************************
C
C    THE SUBROUTINE FOR THE PARALLEL MIXING MODEL
      SUBROUTINE MAXMIX(N,AIR)
      IMPLICIT REAL*8(A-H,Q-Z)
      COMMON NR,NA,D(6,6,340),V,R(6,6),DD(6,6),CORN(6,6),DDD(6,6)
      DO 98 I=1,NR
      DO 98 J=1,NA
      R(I,J) =V*AIR+(1.0D0-V)*CORN(I,J)
   98 CONTINUE
      RETURN
      END
C ****************************************************************
C
C* THE SUBROUTINE FOR THE SERIES MIXING PROPERTIES
      SUBROUTINE MINMIX(N,AIR)
      IMPLICIT REAL*8(A-H,Q-Z)
      DIMENSION  A(6,6)
      COMMON NR,NA,D(6,6,340),V,R(6,6),DD(6,6),
     &CORN(6,6),DDD(6,6)
      DO 97 I =1,NR
      DO 97 J =1,NA
      A(I,J)  =V*CORN(I,J)+(1.0D0-V)*AIR
      R(I,J)  =AIR*CORN(I,J)/A(I,J)
   97 CONTINUE
      RETURN
      END
C  ****************************************************************
C
C*  THE SUBROUTINE FOR THE MIXING MODEL OF GEOMETRIC MEAN
C     SUBROUTINE GEOMIX(N,NR,NA,AIR,CORN,V,R)
      SUBROUTINE GEOMIX(N,AIR)
      IMPLICIT REAL*8(A-H,Q-Z)
      DIMENSION  A(6,6), B(6,6)
      COMMON NR,NA,D(6,6,340),V,R(6,6),DD(6,6),
     &CORN(6,6),DDD(6,6)
      DO 96 I  =1,NR
      DO 96 J  =1,NA
      A(I,J)   =AIR**V
      B(I,J)   =CORN(I,J)**(1.0D0-V)


      R(I,J)   =A(I,J)*B(I,J)
   96 CONTINUE

      RETURN
      END
```

Appendix H

EXPERIMENTAL AND PREDICTED DATA DURING TEST 3 USING THE GEOMETRIC MEAN MODEL WITH A PHASE CONVERION FACTOR OF ZERO

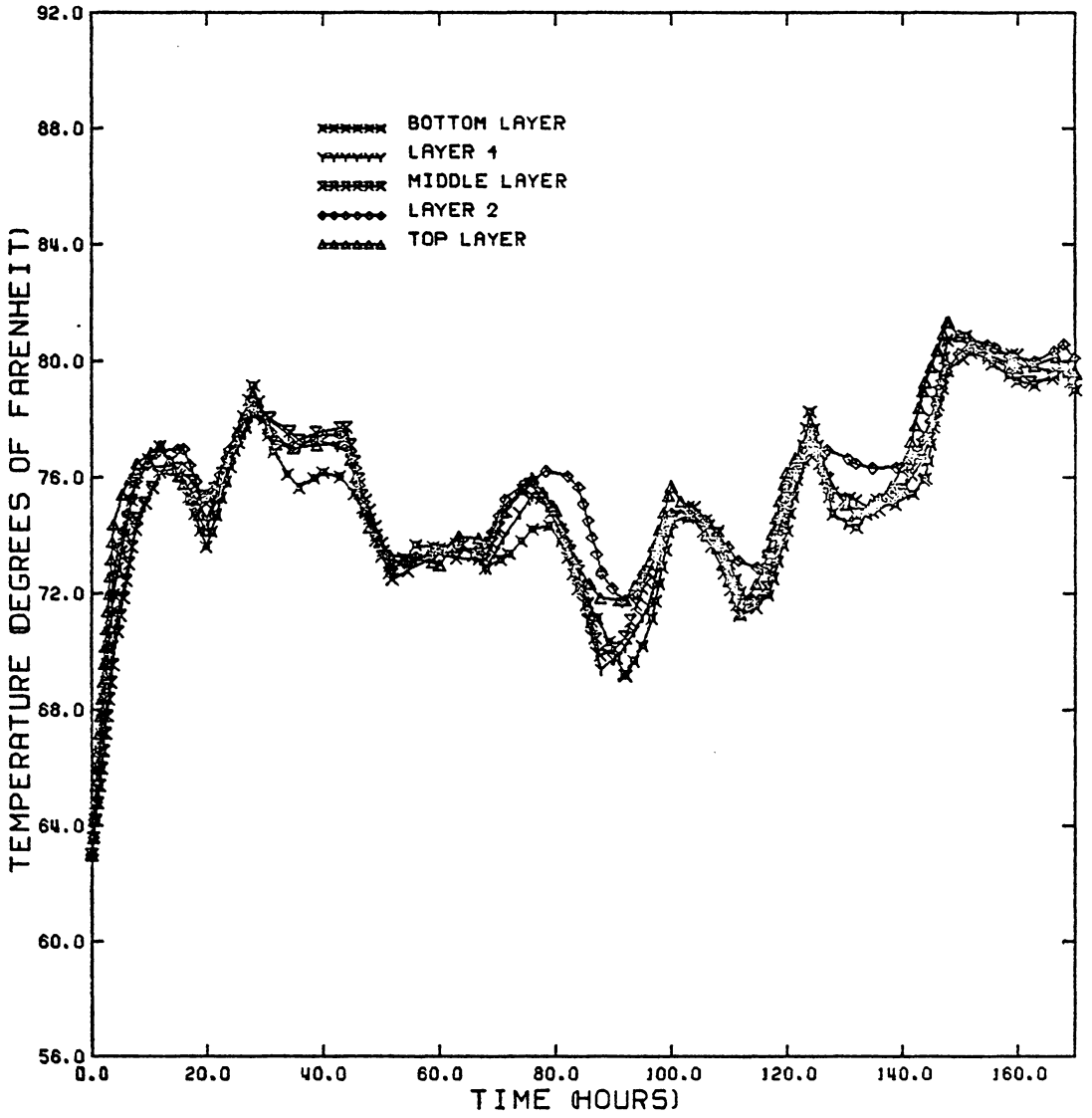

Figure H.1 : Experimental temperatures in the five layers during Test 3 at a wall distance of 3 inches.

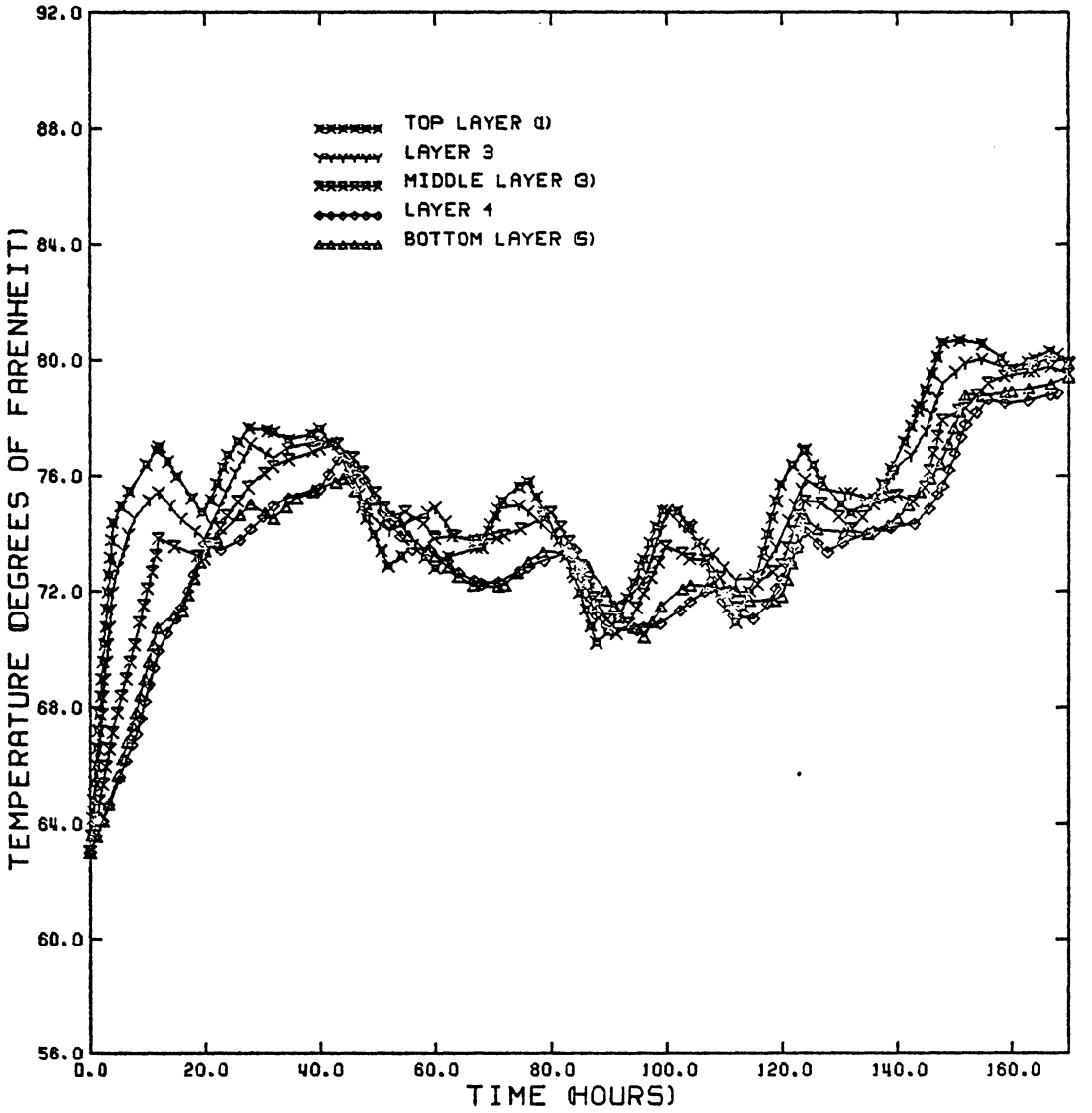

Figure H.2 : Experimental temperatures in the five layers during Test 3 at a wall distance of 8 inches.

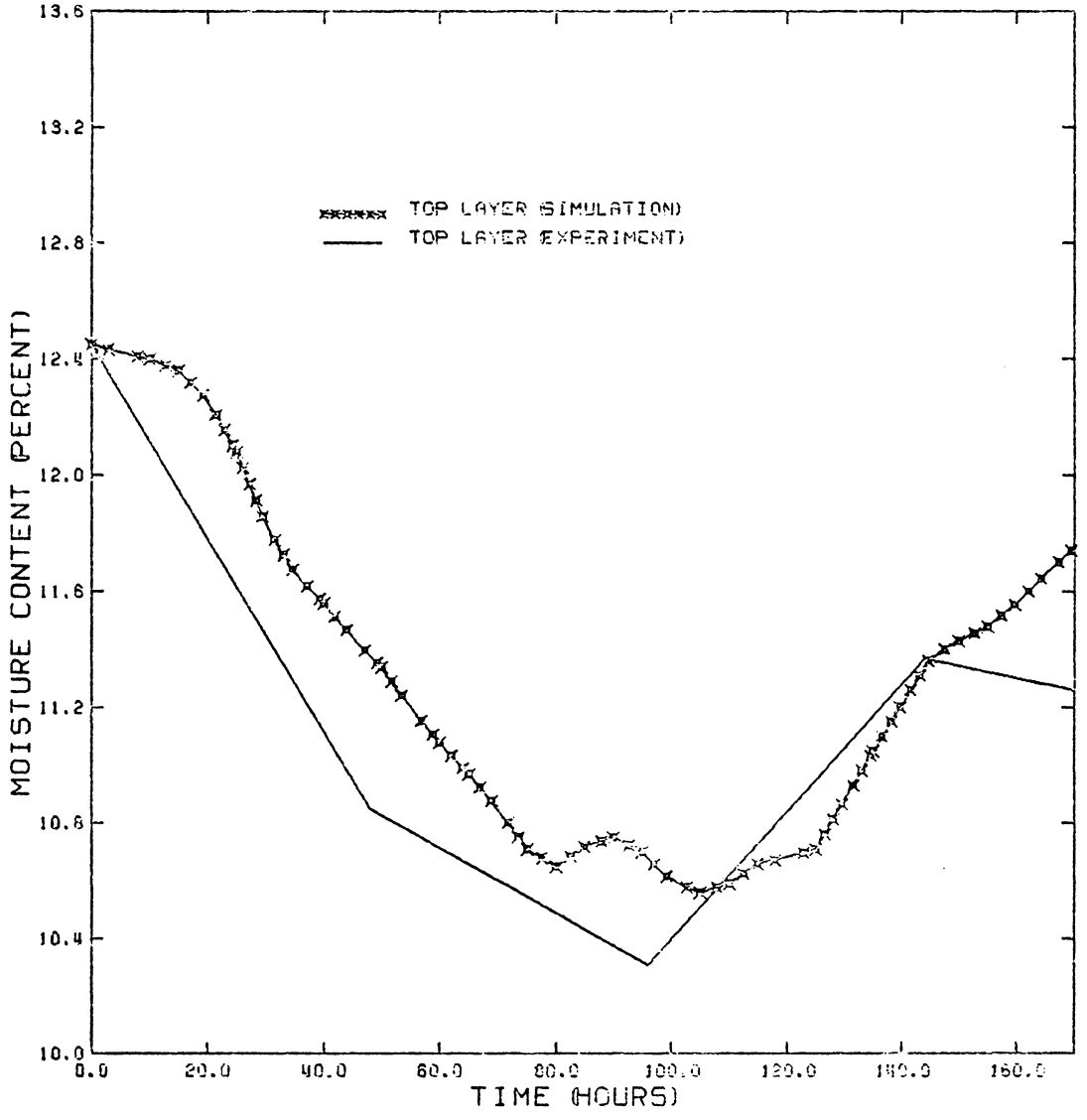

Figure H.3 : Experimental and predicted moisture contents in the top layer during Test 3 at a wall distance of 3 inches using the geometric mean model with a phase conversion factor of zero.

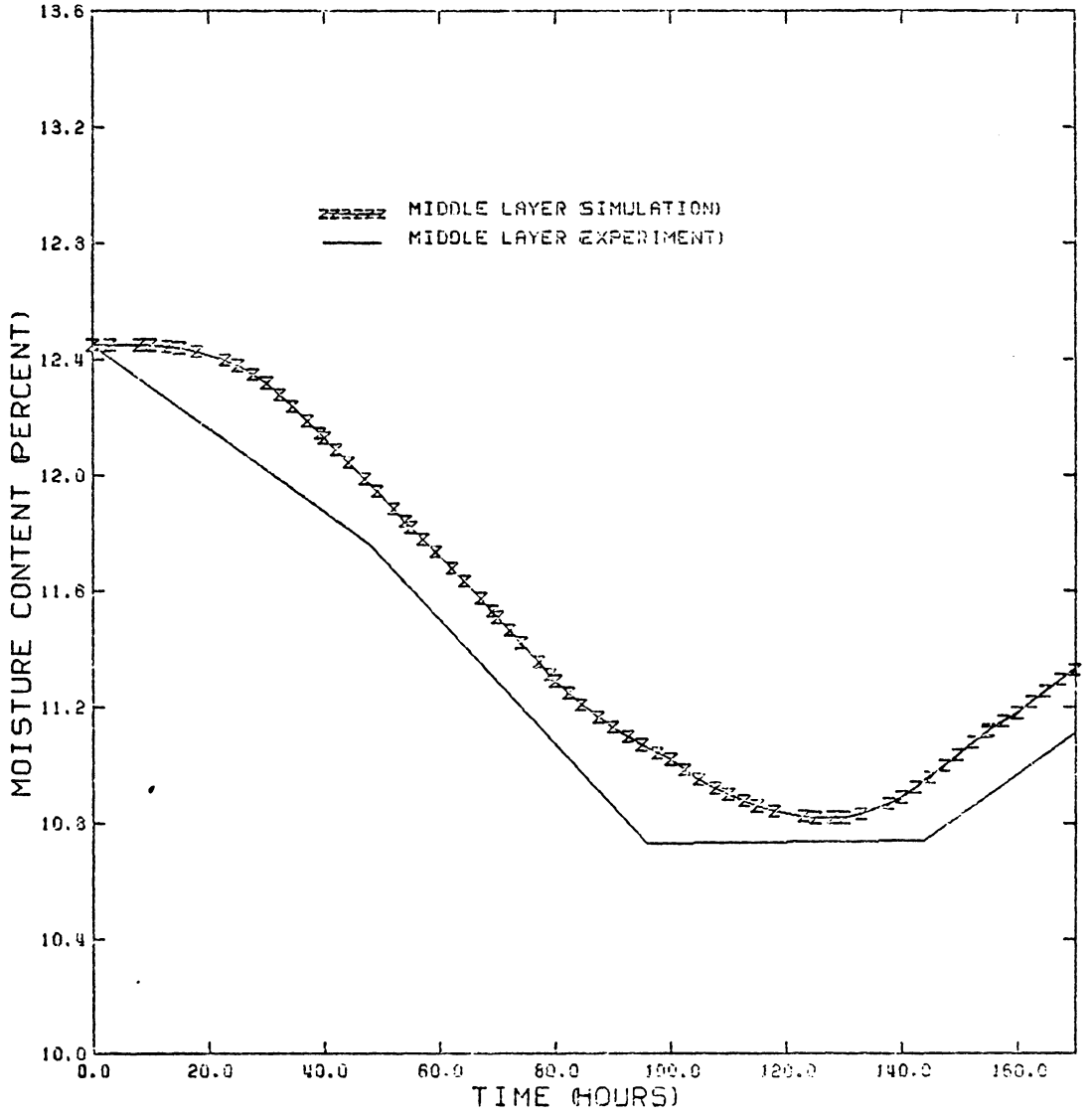

Figure H.4 : Experimental and predicted moisture contents in the middle layer during Test 3 at a wall distance of 3 inches using the geometric mean model with a phase conversion factor of zero.

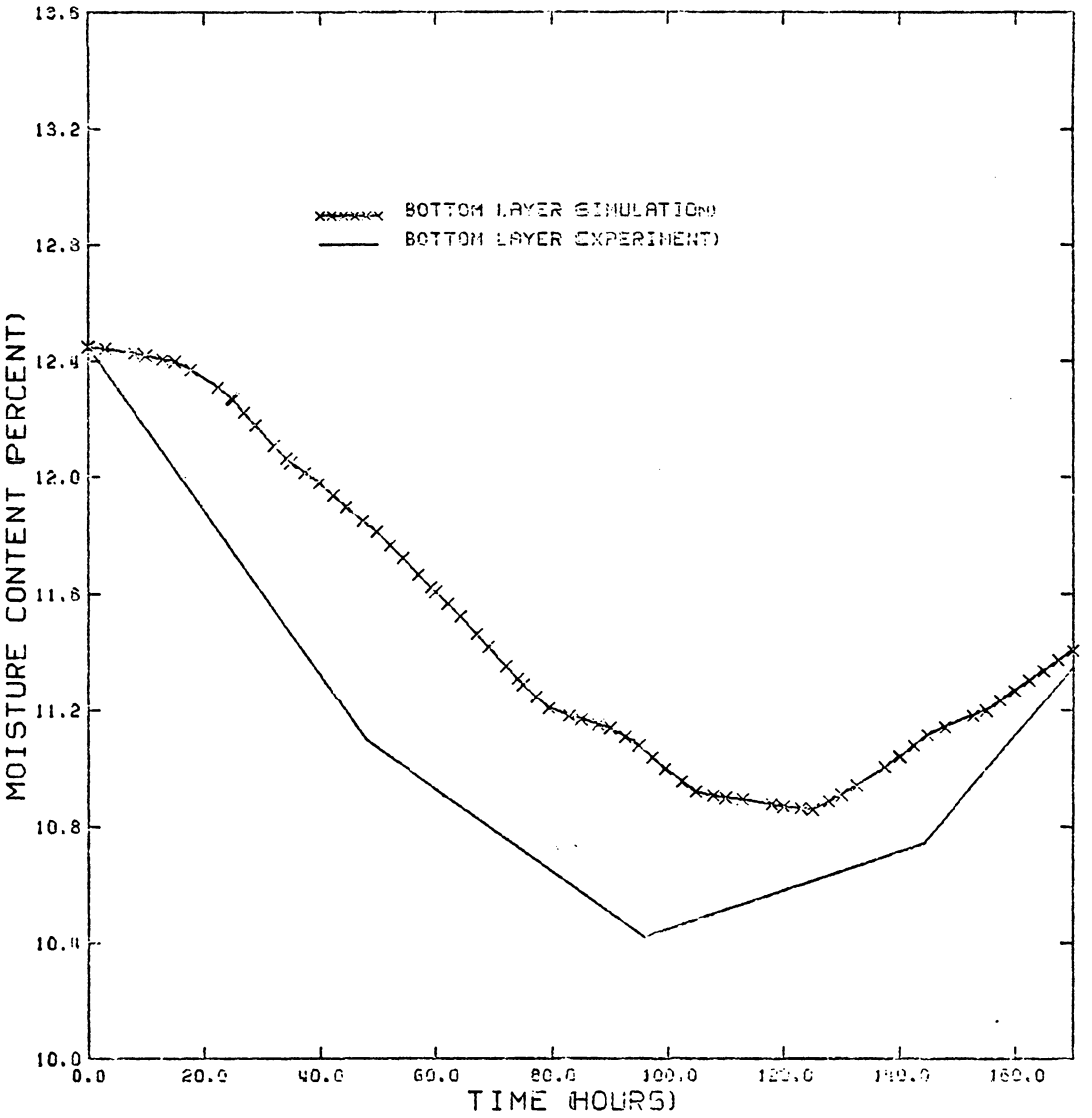

Figure H.5 : Experimental and predicted moisture contents in the bottom layer during Test 3 at a wall distance of 3 inches using the geometric mean model with a phase conversion factor of zero.

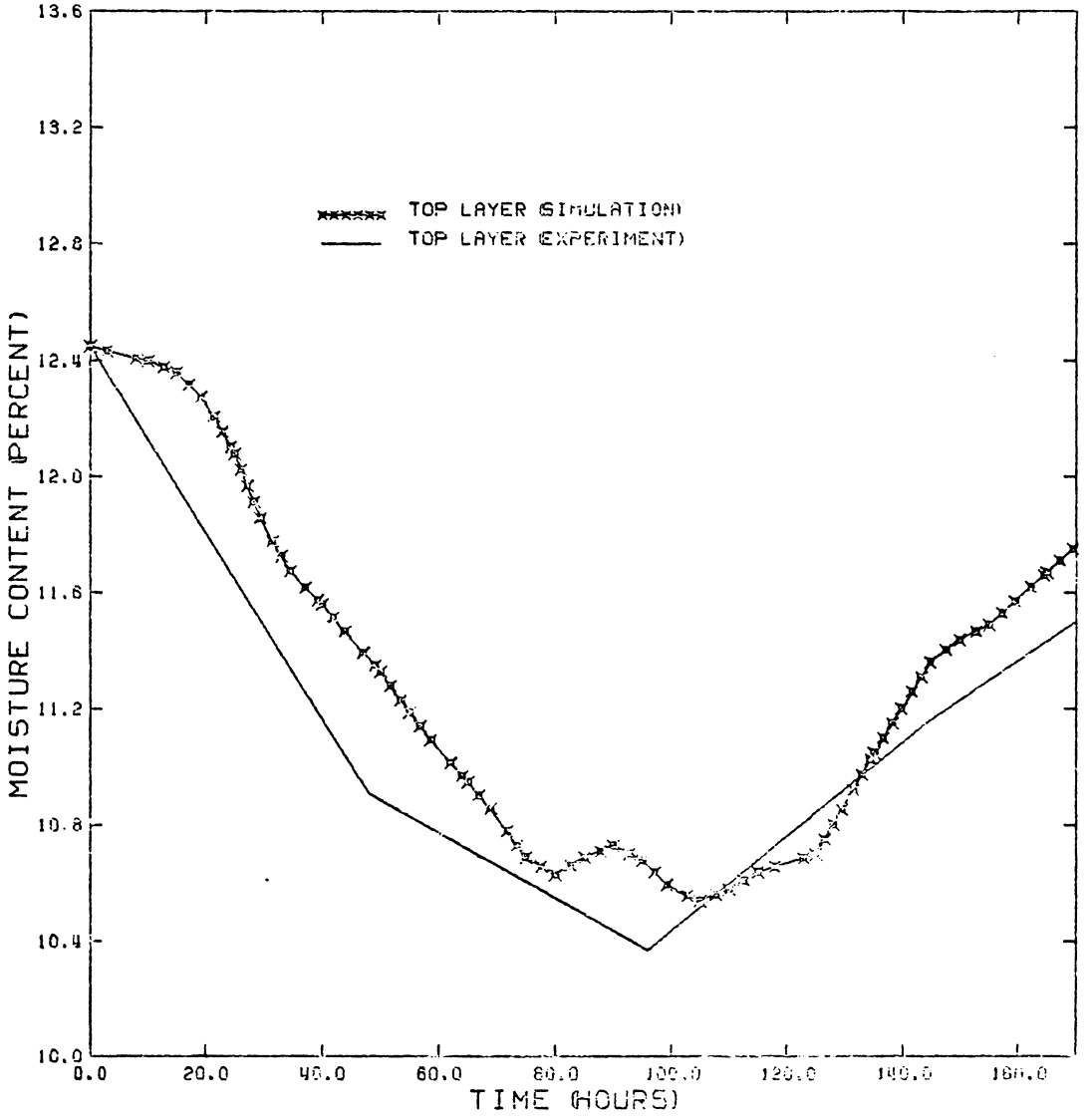

Figure H.6 : Experimental and predicted moisture contents in the top layer during Test 3 at a wall distance of 8 inches using the geometric mean model with a phase conversion factor of zero.

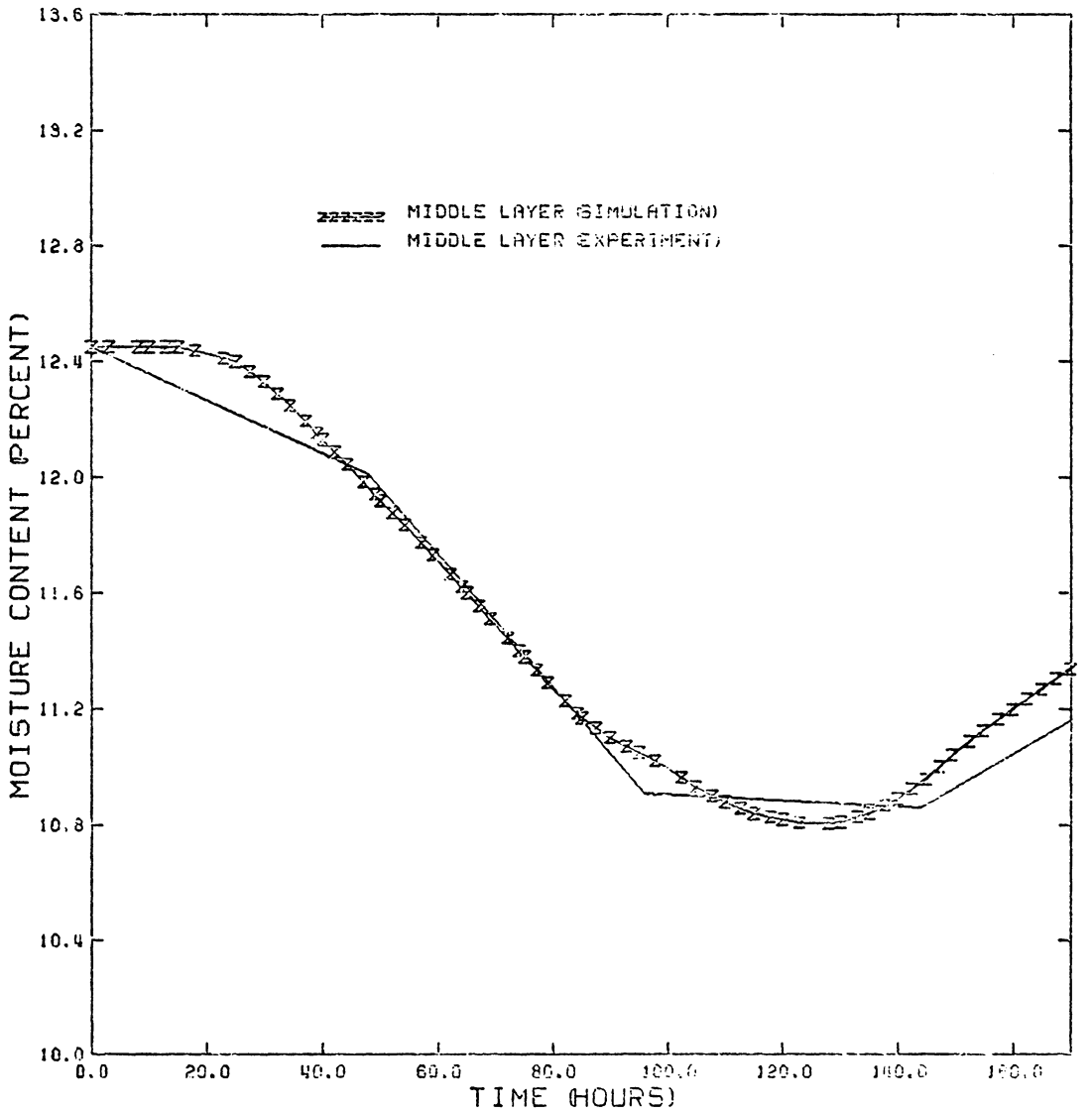

Figure H.7 : Experimental and predicted moisture contents in the middle layer during Test 3 at a wall distance of 8 inches using the geometric mean model with a phase conversion factor of zero.

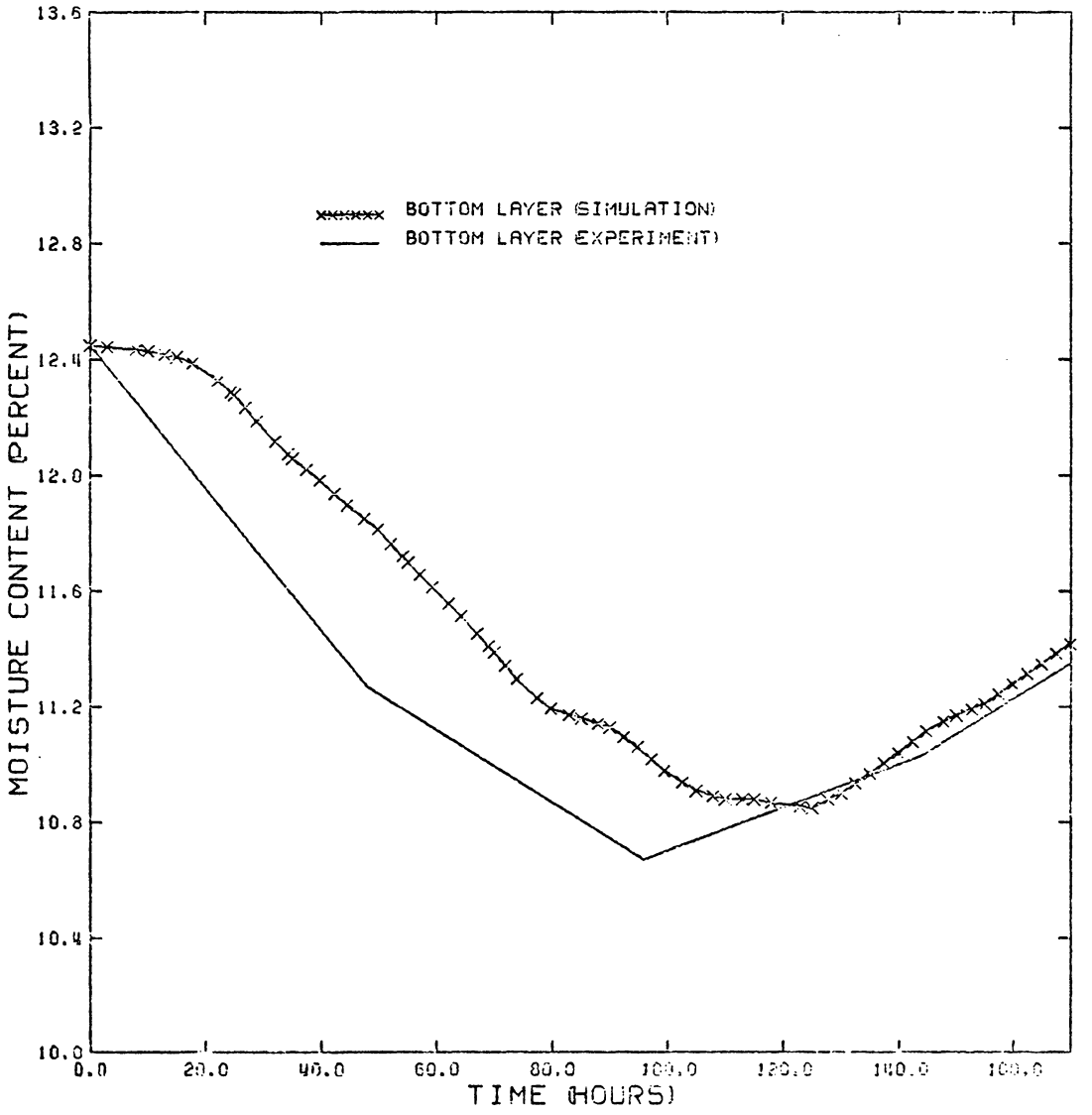

Figure H.8 : Experimental and predicted moisture contents in the bottom layer during Test 3 at a wall distance of 8 inches using the geometric mean model with a phase conversion factor of zero.

The vita has been removed from the scanned document

A THERMODYNAMIC SIMULATION MODEL FOR STORAGE OF CORN

by

Chung-Teh Sheng

(ABSTRACT)

A mathematical simulation model based on the theories of transport phenomena and thermodynamics was developed to predict the storage behavior in a bed of corn. Coupled heat and mass transfer equations for a porous-capillary hygroscopic body were utilized in this study. The boundary conditions of heat and moisture were determined using the law of conservation, the law of heat and mass diffusion, and the law of convective heat and mass transfer. The system was solved using the implicit finite difference method with matrix inversion for and axisymmetric body eith 36 annular elements. The bulk moisture diffusivities were determined using five mixing models(parallel, series, equivalent-resistor, modified Maxwell, and geometric mean). Five phase conversion factors(0.0, 0.25, 0.50, 0.75, and 1.0) were utilized to evaluate the five mixing models.

Three laboratory storage bins, and eight grain sample columns were designed and constructed. Three experiments were conducted to enable the determinations of temperature and moisture content within the interior of the storage bin. The simulation model was verified by comparing the predicted results with the experimental the values. Results indicate that geometric mean model with a phase conversion factor of zero was the best selection. A postulated path for internal moisture flow was suggested.